



## Pilkington Library

Author/Filing Title ..... H. O. D. E. M. A. N. .....

Vol. No. .... Class Mark ..... T .....

**Please note that fines are charged on ALL  
overdue items.**

**FOR PREFERENCE ONLY**

0402390369





BRANCHED CHAINS IN POLY(METHYL  
METHACRYLATE) POLYMERISATIONS  
INCORPORATING A POLYMERIC CHAIN  
TRANSFER AGENT

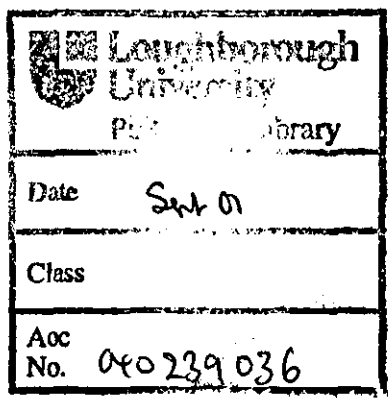
by

Jon Houseman

Supervisors: Professor John V. Dawkins  
Dr. Andrew Slark

A Doctorial Thesis submitted in partial fulfilment of the  
requirements for the award of Doctor of Philosophy of  
Loughborough University

July 2000



Dedicated to my  
Mum and Dad

## ACKNOWLEDGEMENTS

I wish to thank Prof. John Dawkins for his support and understanding over the years at Loughborough, both as an undergraduate and postgraduate. I am forever grateful to him for my achievements and wish him all the best in future endeavours. I wish to thank my industrial supervisor Dr. Andrew Slark for his support and encouragement. I would like to thank the EPSRC and ICI Acrylics for funding.

I would also like to thank Alan Titterton at ICI Acrylics for his assistance in characterising branched samples using TDSEC. Thanks also to the technical staff at Loughborough, notably Dave Wilson.

A special thanks to my expanding family for their constant support, my fantastic mum and dad, my favourite twin Marky for being there and sharing many adventures, big bro Andy, Alison and Laura, stuntman Stevie and Ali.

A special thanks to my fellow Yorkshireman and friend Mat, for which my time at Loughborough and Westfield Drive wouldn't have been quite the same – tea and SB? A thanks goes to Dave for putting up with the mess.

I would like thank my colleagues and friends in Polymer Research: Dave Price, Helen, Claire, Dave 'gin' Maton, Ian, Luke, Mark and last but not least Ben – the ambassador for Britain in Europe.

I would also like to thank my good friend Phil and all the Loughborough lads, blonde Jo and Buddy Sean for many mellow moments underwater. Also Orange, Pulau Weh and La Tarentaise for inspirational moments.

## ABSTRACT

Branching in poly(methyl methacrylate) (PMMA) is produced by incorporating a pre-prepared polymeric chain transfer agent (PCTA) into a single stage radical polymerisation. Samples of PCTA having a range of transfer functionalities and molar masses were synthesised by modifying a methacrylate-based copolymer. Control of branching in PMMA has been studied as a function of transfer functionality and molar mass in the PCTA and a function of MMA and initiator concentrations in the MMA polymerisation. The branched samples of PMMA have been characterised by size exclusion chromatography (SEC) with multi-detectors to determine Mark-Houwink and other parameters to assess levels of branching. Some PCTA samples have been prepared with a UV chromophore to facilitate characterisation by SEC-UV.

# CONTENTS

<b>1</b>	<b>INTRODUCTION.....</b>	<b>1</b>
<b>2</b>	<b>BACKGROUND AND THEORY.....</b>	<b>6</b>
2.1	<b>RADICAL POLYMERISATION.....</b>	<b>6</b>
2.1.1	<i>Radical Polymerisation of MMA .....</i>	7
2.1.1.1	Initiation .....	7
2.1.1.2	Propagation.....	7
2.1.1.3	Termination .....	8
2.1.2	<i>Steady-State Kinetics .....</i>	9
2.1.3	<i>Kinetic Chain Length.....</i>	12
2.1.4	<i>Chain Transfer.....</i>	13
2.1.4.1	Chain Transfer to Monomer, Initiator and Solvent.....	15
2.1.4.2	Chain Transfer to Polymer.....	16
2.1.4.3	Chain Transfer to Modifier.....	16
2.1.5	<i>Mechanism of Termination of MMA and Gel Effect.....</i>	17
2.2	<b>COPOLYMERISATION.....</b>	<b>19</b>
2.2.1	<i>Kinetics of Copolymerisation.....</i>	19
2.2.2	<i>Monomer Reactivity Ratios and Copolymer Composition.....</i>	21
2.2.2.1	Estimation of Monomer Reactivity Ratios .....	23
2.3	<b>MOLAR MASS DEFINITION .....</b>	<b>24</b>
2.4	<b>POLYMER SOLUTIONS .....</b>	<b>25</b>
2.4.1	<i>Polymer Solubility .....</i>	25
2.4.2	<i>Properties of Dilute Solutions.....</i>	26
2.4.3	<i>Solution Viscosity.....</i>	27
2.4.4	<i>Effects of Branching .....</i>	29
2.5	<b>SIZE EXCLUSION CHROMATOGRAPHY (SEC) .....</b>	<b>30</b>
2.5.1	<i>Background.....</i>	30
2.5.2	<i>Calibration.....</i>	31
2.5.3	<i>Detectors for SEC.....</i>	33
2.5.3.1	Concentration Detectors .....	33
2.5.3.1.1	Refractive Index (RI) Detectors .....	33
2.5.3.2	Structure-Selective Detectors .....	33
2.5.3.2.1	Ultraviolet (UV) Detectors.....	33
2.5.3.3	Molar Mass Detectors.....	34
2.5.3.3.1	Differential Viscosity (VISC) Detector.....	34
2.5.3.3.2	Light Scattering (LS) Detector .....	35
2.5.4	<i>Triple Detector SEC (TDSEC).....</i>	39
2.6	<b>BRANCHED POLYMERS .....</b>	<b>41</b>
2.6.1	<i>Star Polymers.....</i>	41

2.6.1.1 Preparation .....	41
2.6.1.2 Solution Behaviour.....	45
2.6.1.2.1 Regular Star Polymers.....	45
2.6.1.2.2 Asymmetric Star Polymers.....	46
2.6.2 <i>Comb Polymers and Graft Copolymers</i> .....	48
2.6.2.1 Preparation .....	48
2.6.2.2 Solution Behaviour.....	54
2.6.3 <i>Statistically Branched Polymers</i> .....	58
2.6.3.1 Preparation .....	58
2.6.3.2 Solution Behaviour.....	58
2.6.4 <i>Hyperbranched Polymers</i> .....	60
2.6.4.1 Preparation .....	60
2.6.4.2 Solution Behaviour.....	61
<b>3. EXPERIMENTAL.....</b>	<b>64</b>
3.1 LIST OF CHEMICALS WITH ABBREVIATIONS .....	64
3.2 MONOMER DESTABILISATION AND STORAGE .....	66
3.3 DEVELOPMENT AND PREPARATION OF PCTA .....	67
3.3.1 <i>Synthesis of MMA</i> .....	67
3.3.1.1 Absence of CTA.....	67
3.3.1.2 Presence of CTA.....	67
3.3.2 <i>Synthesis of MMA-co-HEMA Copolymers</i> .....	68
3.3.3 <i>Synthesis of BzMA-co-HEMA Copolymers</i> .....	68
3.3.4 <i>Functionalisation of Copolymers</i> .....	69
3.3.4.1 Esterification Method Provided by ICI Acrylics .....	69
3.3.4.2 Developed Method for Esterification .....	69
3.3.5 <i>Analysis of Residual SH Functionality</i> .....	70
3.4 NOMENCLATURE OF PCTA SAMPLES .....	71
3.5 SYNTHESIS OF BRANCHED/REFERENCE POLYMERS .....	72
3.5.1 <i>Preparation with PETM</i> .....	72
3.5.2 <i>Preparation with PCTA</i> .....	72
3.5.3 <i>Reference Samples</i> .....	73
3.5.4 <i>Conversion Reactions with PCTA</i> .....	73
3.5.5 <i>Solubility Experiments</i> .....	73
3.6 CHARACTERISATION TECHNIQUES .....	74
3.6.1 <i>Nuclear Magnetic Resonance (NMR) Spectroscopy</i> .....	74
3.6.2 <i>Size Exclusion Chromatography (SEC)</i> .....	75
3.6.2.1 SEC with RI Detector.....	75
3.6.2.1.1 Apparatus .....	75
3.6.2.1.2 Molar Mass Determination and Calibration .....	76
3.6.2.2 SEC with UV / RI Detectors.....	78
3.6.2.2.1 Apparatus .....	78

3.6.2.2.2 Characterisation.....	78
3.6.2.3 SEC with LS / RI / VISC Detectors (TDSEC).....	79
3.6.2.3.1 Apparatus .....	79
3.6.2.3.2 Set-up.....	80
3.6.2.3.3 Sample Preparation .....	80
<b>4 RESULTS .....</b>	<b>81</b>
<b>4.1 PREPARATION OF PMMA.....</b>	<b>81</b>
4.1.1 <i>Preparation without CTA</i> .....	81
4.1.2 <i>Preparation with CTA</i> .....	82
4.1.2.1 Calculation of Chain Transfer Constant .....	82
<b>4.2 STATISTICAL COPOLYMERS .....</b>	<b>84</b>
4.2.1 <i>MMA-co-HEMA Copolymers</i> .....	84
4.2.1.1 Determination of HEMA Concentration and Functionality.....	88
4.2.1.2 Estimation of Reactivity Ratios .....	89
4.2.2 <i>BzMA-co-HEMA Copolymers</i> .....	92
4.2.2.1 Determination of HEMA Concentration and Functionality.....	96
4.2.2.1.1 Proton NMR Spectroscopy.....	96
<b>4.3 PREPARATION OF PCTA.....</b>	<b>97</b>
4.3.1 <i>Method Development of Functionalisation Reaction</i> .....	98
4.3.1.1 Initial Investigations .....	98
4.3.1.2 PCTA Insolubility and Implications .....	99
4.3.1.3 Reaction Parameters .....	102
4.3.1.3.1 Copolymer Phase Separation.....	102
4.3.1.3.2 Esterification Temperature .....	102
4.3.1.3.3 Esterification Reaction Time.....	103
4.3.1.3.4 Sequential Addition of TGA .....	103
4.3.2 <i>Characterisation of MMA-co-HEMA PCTA</i> .....	104
4.3.2.1 Conversion of Copolymer to PCTA .....	107
4.3.2.2 Estimation of SH Concentration in PCTA.....	107
4.3.2.3 Calculation of SH Concentration in PCTA.....	113
4.3.3 <i>Characterisation of BzMA-co-HEMA PCTA</i> .....	114
4.3.3.1 Conversion of Copolymer to PCTA .....	117
4.3.3.2 Estimation of SH Concentration in PCTA.....	117
4.3.3.3 Calculation of SH Concentration in PCTA.....	121
<b>4.4 COPOLYMER AND PCTA SUMMARY TABLES.....</b>	<b>122</b>
<b>4.5 BRANCHING INVESTIGATIONS WITH PETM .....</b>	<b>124</b>
<b>4.6 BRANCHING INVESTIGATIONS WITH PCTA.....</b>	<b>127</b>
4.6.1 <i>Initial Investigations with MMA-co-HEMA PCTA</i> .....	127
4.6.2 <i>Investigations with BzMA-co-HEMA PCTA</i> .....	129
4.6.2.1 Reaction Variables.....	129
4.6.2.2 Phase Separation of PCTA .....	132
4.6.2.3 Phase Separation during Polymerisation with PCTA .....	133

4.7	CHARACTERISATION OF SAMPLES BY TDSEC .....	134
4.7.1	<i>Series ONE</i> .....	135
4.7.1.1	Linear Samples .....	135
4.7.1.2	Samples Prepared with MMA-co-HEMA PCTA .....	137
4.7.1.3	Samples Prepared with BzMA-co-HEMA PCTA.....	141
4.7.2	<i>Series TWO</i> .....	144
4.7.2.1	Linear/Reference Samples.....	144
4.7.2.2	Samples Prepared with MMA-co-HEMA PCTA .....	147
5	DISCUSSION OF BRANCHING .....	167
5.1	ROLE OF PCTA .....	167
5.1.1	<i>Activation</i> .....	167
5.1.2	<i>Branched Polymer Formation Containing Single PCTA Molecules</i> .....	168
5.1.3	<i>Branched Polymer Formation Containing Coupled PCTA Molecules</i> .....	170
5.1.3.1	Coupling during Preparation of PCTA .....	170
5.1.3.2	Combination Reactions .....	171
5.1.3.3	Branching through Terminal Unsaturation .....	171
5.2	CHARACTERISATION OF BRANCHED POLYMERS .....	172
5.2.1	<i>Molar Mass Determination</i> .....	172
5.2.2	<i>Solution Behaviour</i> .....	173
5.3	PREDICTION OF BRANCHED POLYMER MOLAR MASS .....	174
5.4	IMPLICATIONS OF UTILISING PCTA .....	177
5.4.1	<i>Polymerisation Media and Kinetics</i> .....	177
5.4.2	<i>Nature of PCTA</i> .....	178
5.4.3	<i>PCTA Partial Phase Separation</i> .....	179
5.4.4	<i>Concentration of Free SH</i> .....	179
5.5	BRANCHED POLYMER FORMATION WITH PCTA .....	180
5.5.1	<i>Conversion with 6 kg/mol PCTA</i> .....	180
5.5.2	<i>Conversion with 16 kg/mol PCTA</i> .....	181
5.6	REACTION VARIABLES .....	184
5.6.1	<i>Concentration of MMA</i> .....	184
5.6.1.1	PCTA 6H-M426 .....	184
5.6.1.2	PCTA 16H-M427 .....	185
5.6.2	<i>Concentration of AIBN</i> .....	186
5.7	PCTA VARIABLES .....	188
5.7.1	<i>Molar Mass of PCTA</i> .....	188
5.7.2	<i>Influence of PCTA Concentration at Fixed SH Concentration</i> .....	190
5.7.2.1	PCTA 6H-M426 .....	191
5.7.2.2	PCTA 16L-M403 .....	191
5.7.2.3	PCTA 16H-M427 .....	192
5.7.2.4	Summary .....	192
5.7.3	<i>Influence of SH Concentration in PCTA</i> .....	193

5.7.3.1	Influence of SH Concentration at Fixed PCTA Molar Mass and PCTA Concentration .....	193
5.7.3.2	Distribution of SH on PCTA .....	194
5.7.3.2.1	PCTA 6H-M426 vs PCTA 6L-M402 .....	195
5.7.3.2.2	PCTA 16H-M427 vs PCTA 16L-M403 .....	196
5.7.3.3	Influence of SH Concentration and PCTA Molar Mass .....	198
5.7.3.3.1	PCTA 6H-M426 vs PCTA 16L-M403 .....	198
5.7.3.3.2	PCTA 16H-M427 vs PCTA 6L-M402 .....	200
<b>6</b>	<b>SUMMARY AND CONCLUSIONS.....</b>	<b>201</b>
<b>7</b>	<b>PROPOSALS FOR FURTHER WORK.....</b>	<b>203</b>
<b>8</b>	<b>REFERENCES.....</b>	<b>205</b>

## **APPENDIX**

## Common Abbreviations and Symbols

$v$	kinetic chain length
$\Theta$	theta conditions
$\alpha$	expansion coefficient
[ ]	concentration
$[\eta]$	intrinsic viscosity
$a$	exponent of Mark-Houwink relationship
$A_2$	second virial coefficient
AIBN	$\alpha, \alpha'$ -azobis(isobutyronitrile)
BzBr	benzyl bromide
BzMA	benzyl methacrylate
BzMA-co-HEMA	benzyl methacrylate-co-2-hydroxyethyl methacrylate copolymer
CTA	chain transfer agent
$C_x$	chain transfer constant of species x
D	polydispersity
DP	degree of polymerisation
EVA	ethylene-co-vinyl acetate copolymer
$f$	initiator efficiency
$g$	the ratio of the radius of gyration of branched/linear polymer at the same molar mass
$g'$	the ratio of the intrinsic viscosity of branched/linear polymer at the same molar mass
HEMA	2-hydroxyethyl methacrylate
IR	infra-red
K	Mark-Houwink constant
$k_x$	rate constant of step x
LS	light scattering
M	monomer unit
M-H	Mark-Houwink
MMA	methyl methacrylate
MMA-co-HEMA	methyl methacrylate-co-2-hydroxyethyl methacrylate copolymer

MMD	molar mass distribution
$M_n$	number average molar mass
$M_w$	weight average molar mass
NMR	nuclear magnetic resonance
PCTA	polymeric chain transfer agent
PETM	pentaerythritol tetrakis(3-mercaptopropionate)
PMMA	poly(methyl methacrylate)
PS	poly(styrene)
$r_1 r_2$	monomer reactivity ratios of monomer 1 and monomer 2
RI	refractive index
$R_x$	rate of step x
SEC	size exclusion chromatography
SEC-UV	size exclusion chromatography coupled with a UV detector
STY	styrene
TDSEC	triple detector size exclusion chromatography
TEA	triethylamine
TGA	thioglycolic acid
THF	tetrahydrofuran
UV	ultra-violet
VISC	viscosity

# 1 INTRODUCTION

Polymer coatings play an invaluable role in everyday life. They are utilised in the packaging, printing and automotive industries to give enhance product performance. With a growing concern over environmental issues, there is a drive in industry to reduce the concentration of organic solvents in such polymer coatings. A reduction in the concentration of solvent requires enhanced resin solubility or a lower solution viscosity at a higher solids content.

The solution viscosity of a polymer is a measure of the size or extension of the polymer molecule in solution. The size of a dissolved polymer molecule is dependent on a number of factors that include molar mass, chain structure, solvent and temperature. The presence of even a small fraction of branching can result in solution properties considerably different from those of the corresponding linear polymer of the same molar mass, as a branched polymer molecule is generally smaller in size.<sup>1,2</sup> Therefore, incorporation of branching on a polymer molecule can reduce the solution viscosity compared with the linear molar mass equivalent.<sup>3</sup>

With the advent of modern synthetic techniques, there has been an explosion in the development of both controlled and statistical polymer structures. A selection of structures is presented in Figure 1-1(a-h). Chain architectures with a single polyfunctional branch point are classified as star polymers; within this classification there exists a multitude of configurations. Regular star chains have compositional and arm molar mass homogeneity (a).<sup>4</sup> Asymmetric star polymers have arms of unequal molar mass (b), topological asymmetry or chemical asymmetry (miktoarm stars) (c). Chain structures with branch points distributed statistically or uniformly along a backbone are classified as comb polymers (d). A densely branched comb polymer may take a star or a brush configuration if the backbone length is small compared with the branch chain length and frequency (e). If the composition of a branch chain is different from the backbone chain, the species is termed a graft copolymer (f). High levels of structural symmetry and density can be introduced into polymers through repeated polymerisation steps to produce molecules such as dendrimers (g).<sup>5,6</sup>

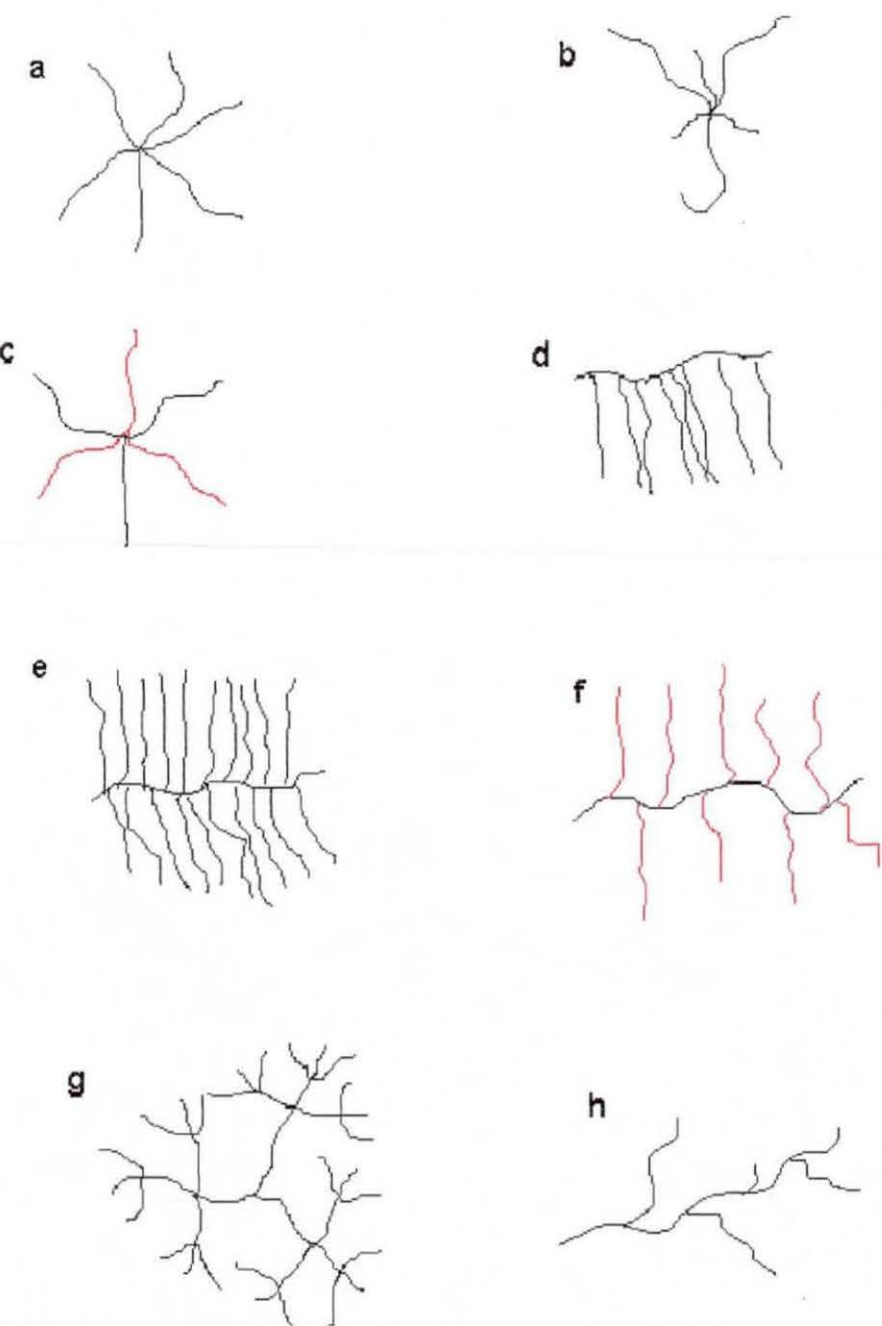


Figure 1-1 Representations of (a) regular star polymer, (b) star polymer with molar mass asymmetry, (c) miktoarm star copolymer, (d) comb polymer, (e) brush polymer, (f) graft copolymer, (g) dendrimer and (h) statistically branched polymer.

Dense polymer molecules can be also be prepared in one-step reactions using  $A_xB$  monomers (hyperbranched polymers). Statistically branched polymers have a statistical distribution of branch chain lengths and branch points ( $h$ ). The properties of all these polymeric structures can be quite different from those of their linear molar mass equivalents.

The synthesis of branched polymers with a controlled structure generally involves 'living' polymerisation techniques (i.e. anionic and cationic polymerisations). These techniques allow excellent control on branch chain length and structure. The disadvantage of these techniques is the demanding conditions typically required. The need for high purity monomers and solvents, reactive initiators and anhydrous conditions has dramatically limited the industrial application of many of these techniques.

Radical polymerisation is robust and is adaptable to many types of monomer under mild conditions using simple equipment. Monomer purification is not necessarily required to a high extent and the initiator residues need not be removed from the polymer because they have little or no affect on the polymer properties. Radical polymerisation processes can be readily and economically performed, an advantage that has made the process the preferred route for many commercial polymers.

As early as 1933, an inactive polymer chain in the presence of growing polymer chains was observed to increase in molecular size.<sup>7</sup> In 1937, Flory suggested that branched vinyl polymers could result from chain transfer reactions involving polymer molecules and growing polymer chains.<sup>8</sup> In 1943, Mayo also proposed that the growing polymer chains could undergo chain transfer reactions with inactive polymer molecules.<sup>9</sup> In a chain transfer reaction the activity of a growing chain is transferred to another species, producing an inactive chain and a new species carrying the active centre. If the new species is sufficiently active to initiate monomer, propagation can commence and another chain will emanate from the new centre. Transfer reactions can occur with monomer, initiator, polymer, solvent or an added modifier.

Incorporating specific functional groups on a polymer backbone can increase susceptibility of a polymer chain to a chain transfer reaction. It is well known that SH

groups have a high chain transfer activity with a variety of monomers in the presence of radicals.<sup>10</sup> Moares et al.<sup>11</sup> prepared a branched polymer in the presence of a SH functionalised poly(ethylene-co-vinyl acetate) (EVA) backbone, which was utilised as a polymeric chain transfer agent (PCTA). However, the SH groups on the backbone suffered from poor accessibility due to natural coiling of the backbone chain. Fox et al.<sup>12,13</sup> prepared graft poly(styrene) (PS) in the presence of a PCTA based on a poly(methyl methacrylate-co-glycidal methacrylate) (MMA-co-GMA) copolymer; however, the graft copolymers were not subjected to detailed characterisation.

The work performed here centred on the preparation of branched PMMA in the presence of a PCTA based on a poly(methyl methacrylate-co-2-hydroxyethyl methacrylate) (MMA-co-HEMA) copolymer and a poly(benzyl methacrylate-co-2-hydroxyethyl methacrylate) (BzMA-co-HEMA) copolymer.<sup>14</sup> The SH groups were located away from the backbone to minimise any steric effects that might be encountered with a smaller, multi-functional molecule. The influence of PCTA in radical polymerisation was explored by investigating several reaction parameters. A selection of samples was characterised using triple detector size exclusion chromatography (TDSEC). With TDSEC the absolute molar mass, the intrinsic viscosity and the extent of branching could be determined. A literature survey revealed no work had been reported utilising this PCTA system or characterising samples prepared in the presence of PCTA using TDSEC. The research programme was co-sponsored by ICI Acrylics and had a potential industrial application.

## Main Aims of the Project

- 1) The development of a method for the preparation and characterisation of a PCTA.
- 2) Identification of PCTA incorporation in a polymerisation with MMA.
- 3) Preparation and characterisation of a series of PMMA samples prepared in the presence of a PCTA exploring the following reaction variables:
  - PCTA concentration.
  - Molar mass of PCTA.
  - Functionality of PCTA.
  - MMA concentration.
  - AIBN concentration.
- 4) Interpretation of the branching data obtained from TDSEC and identification of the variables that influence the solution properties of samples prepared in the presence of a PCTA.

## 2 BACKGROUND AND THEORY

### 2.1 Radical Polymerisation

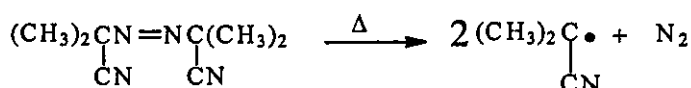
The concept and practice of radical polymerisation date back over 60 years. It is a diverse process and is encountered in numerous forms that can be classified by homogeneous processes (bulk and solution polymerisations) and heterogeneous processes (emulsion and suspension polymerisations).

A radical is an atomic or molecular species whose normal bonding has been modified such that an unpaired electron remains associated with the new structure. Radicals can be generated from the decomposition of specific molecules (termed initiators) susceptible to radical formation. Heat or light is employed to enhance decomposition of the initiator molecules, usually with the loss of a small molecule. In a radical polymerisation of a vinyl monomer, the initiator radical attacks the unsaturated bond to produce a species bearing a radical at one end and an initiator fragment at the other. This species is capable of propagating with additional monomer units, retaining the terminal radical with each unit addition. Propagation ceases when the active chain carrier is terminated. Termination of the active chain carrier can occur via an abstraction mechanism or via combination of two active radicals. Other mechanisms may interfere in the polymerisation, namely chain transfer, inhibition and retardation. These mechanisms are addressed in Section 2.1.4.

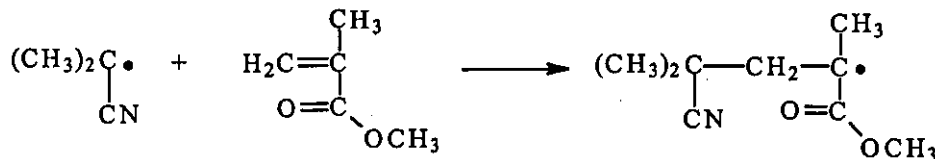
## 2.1.1 Radical Polymerisation of MMA

### 2.1.1.1 Initiation

The thermal decomposition of AIBN is one method of generating radicals in a polymerisation of MMA. The AIBN molecule decomposes to produce 2 radical species with the loss of nitrogen. The radical species reacts with the unsaturated bond in MMA.



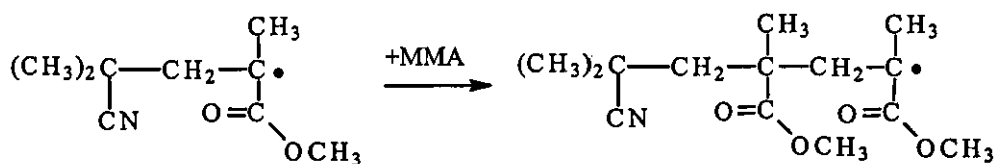
Eqn 2-1



Eqn 2-2

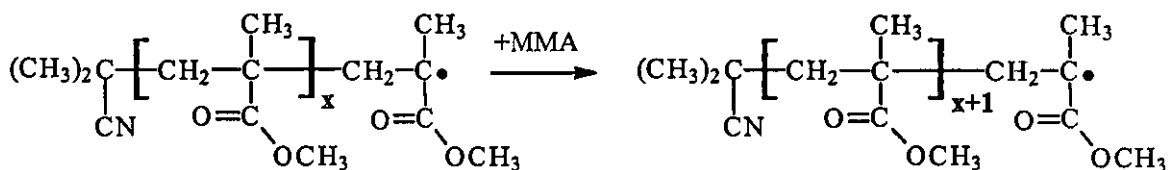
### 2.1.1.2 Propagation

A monomer unit is added in each propagation step, retaining the active centre.



Eqn 2-3

The propagation process can be represented by the general step:

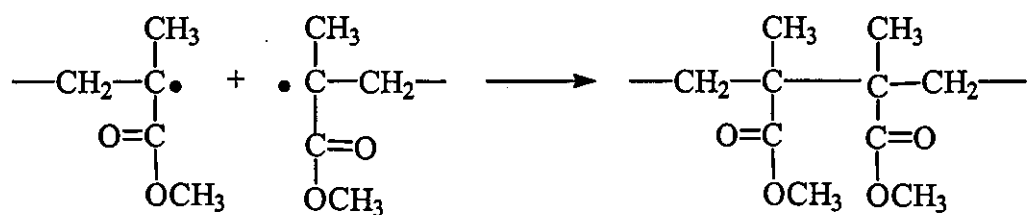


Eqn 2-4

### 2.1.1.3 Termination

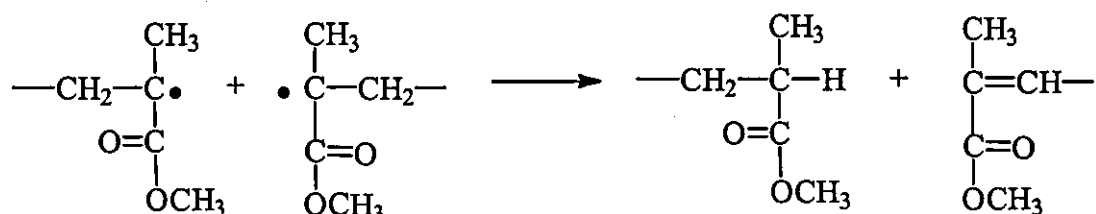
Termination can occur via the bimolecular combination of two radicals or the abstraction of a small molecule; these mechanisms are termed combination and disproportionation respectively.

#### Combination



Eqn 2-5

#### Disproportionation



Eqn 2-6

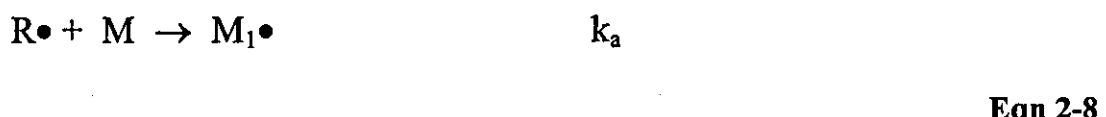
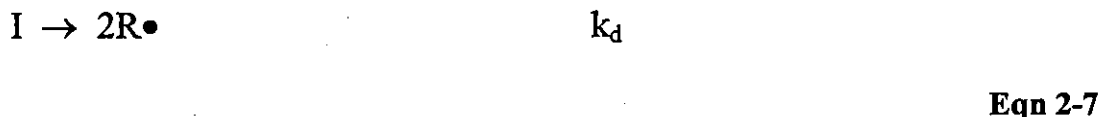
Termination via combination produces one polymer molecule and termination via disproportionation produces two polymer molecules.

## 2.1.2 Steady-State Kinetics

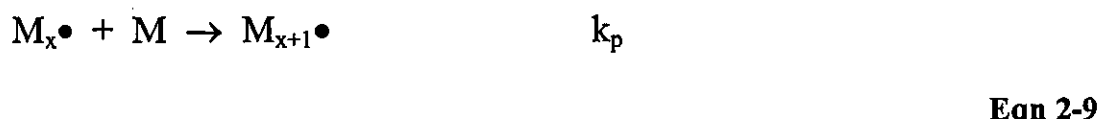
The kinetics of a radical polymerisation can be equated to the kinetics of a simple chain reaction. Neglecting the presence of primary radical termination, inhibition and chain transfer, three fundamental component reactions can be considered: initiation, propagation and termination. They can be represented by the following equations (the rate constant for each reaction is included).

### Rate Constants

#### Initiation

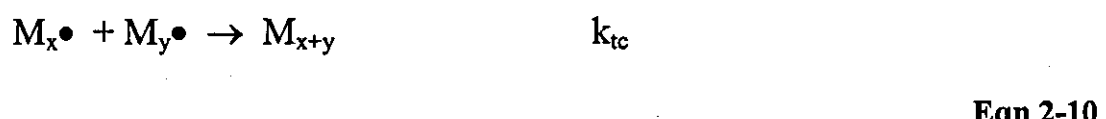


#### Propagation

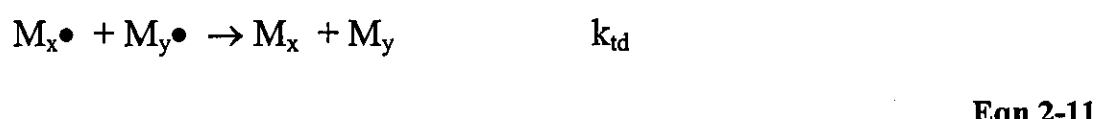


#### Termination

##### Combination



##### Disproportionation



In deriving these kinetic expressions for a radical polymerisation, four simplifying assumptions are made:

- The length of the propagating chain is large, so that the total rate of monomer consumption may be equated to the rate of consumption in the propagation reactions alone.
- The rate coefficients of propagation and termination are independent of chain length. In the case of long chains, the radical activity is determined by the molecular structure near the radical.
- A stationary state in radical concentration is established, allowing the rate of change of concentration of any radical intermediate to be equated to zero. A more serious limitation on this assumption is that as the reaction proceeds the reactants are consumed and the rate of initiation varies with time (batch polymerisation).
- Termination involving primary radicals is negligible. This assumption is valid for most systems under conditions of long chain length, since the primary radical concentration is small compared to the total radical concentration.

The rates of the three component reactions can be written in terms of the concentrations of the species involved and the rate constants. The rate of initiation,  $R_i$ , can be defined as:

$$R_i = \left( \frac{d[M\bullet]}{dt} \right)_i = 2fk_d[I]$$

Eqn 2-12

where  $f$  represents the initiator efficiency (the fraction of radicals formed that are successful in initiating chains), and  $[M\bullet]$  and  $[I]$  are the monomer radical and initiator concentration respectively. In many cases, the primary radicals are not 100% efficient in chain initiation due to the recombination of primary radicals. If radicals are generated by the loss of a small molecule in the initiator, recombination of the primary radicals may produce a stable species that may not yield a radical.

The rate of termination,  $R_t$ , is given by Eqn 2-13.

$$R_t = - \left( \frac{d[M \bullet]}{dt} \right)_t = 2k_t [M \bullet]^2$$

Eqn 2-13

In many cases  $[M \bullet]$  becomes essentially constant very early in the reaction as radicals are formed and destroyed at similar rates. The steady-state condition  $R_i = R_t$  can be applied to simplify and solve for  $[M \bullet]$ :

$$[M \bullet] = \left( \frac{f k_d [I]}{k_t} \right)^{1/2}$$

Eqn 2-14

The rate of propagation,  $R_p$ , is essentially the same as the overall rate of disappearance of the monomer since the number of monomers used in chain activation must be small compared to those used in propagation if polymer is obtained.

$$R_p = - \left( \frac{d[M]}{dt} \right) = k_p [M] [M \bullet]$$

Eqn 2-15

Or, with substitution for  $[M \bullet]$

$$R_p = k_p \left( \frac{f k_d [I]}{k_t} \right)^{1/2} [M]$$

Eqn 2-16

In the early stages of polymerisation, the overall rate should be proportional to the square root of the initiator concentration and to the first power of the monomer concentration, if the initiator efficiency is high and independent of the monomer concentration.

### 2.1.3 Kinetic Chain Length

The kinetic chain length,  $\nu$ , is defined as the number of monomer units consumed per active radical centre and is given by Eqn 2-17 (where  $R_p/R_t = R_p/R_t$ ).

$$\nu = \frac{k_p[M]}{2k_t[M\bullet]}$$

**Eqn 2-17**

Eliminating the radical concentration by the substitution of Eqn 2-15 into Eqn 2-17 leads to the expression:

$$\nu = \frac{k_p^2 [M]^2}{2k_t R_p}$$

**Eqn 2-18**

For initiated polymerisation, substitution of Eqn 2-16 with Eqn 2-18 leads to:

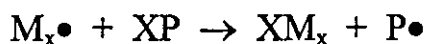
$$\nu = \frac{k_p[M]}{2(fk_d k_t)^{0.5} [I]^{0.5}}$$

**Eqn 2-19**

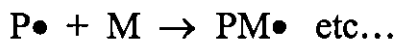
The kinetic chain length should be related to the degree of polymerisation, DP. For termination reactions by combination  $DP = 2\nu$  and for disproportionation  $DP = \nu$ . Since termination can occur at all stages of chain growth, individual radicals continue to grow for different periods of time and the resultant polymer contains a distribution of molecular sizes.

## 2.1.4 Chain Transfer

In a simple chain transfer reaction the activity of a growing chain is transferred, typically by abstraction of a hydrogen atom, to another species yielding an inactive chain and a new species capable of initiating further chain growth. The chain transfer process is represented by Eqn 2-20 and Eqn 2-21.



Eqn 2-20



Eqn 2-21

where XP is a chain transfer agent (CTA) and  $P \cdot$  is a radical species produced from the transfer reaction. The distinguishing characteristic of a chain transfer process is the interruption to normal chain growth by the transfer of the active centre. The effect of chain transfer reactions on the molar mass and structure of the polymer is summarised in Table 2-1. The consequence of a chain transfer reaction is dependent on the type/activity of the newly formed species.

**Table 2-1 The effect of a chain transfer reaction in a polymerisation.**

Chain Transfer Reaction To:	$R_p$	$M_n$	$M_w$	Structural Consequences
A small molecule, giving an active radical	None	Decreases	Decreases	None
A small molecule, with retardation or inhibition	Decreases	May increase or decrease	May increase or decrease	None
A polymer chain via an intermolecular process	None	None	Increases	Produces long branch
A polymer chain via an intramolecular process	None	None	Increases	Produces short branch

Several kinetic expressions are affected as a consequence of chain transfer. The predominant influence is on the polymer molar mass. The degree of polymerisation can be re-written in terms of the rate of growth divided by all the reactions leading to a dead polymer chain (assuming termination via a disproportionation mechanism).

$$DP = \frac{R_p}{2f k_d [I] + k_{tr,M} [M][M \cdot] + k_{tr,S} [S][M \cdot] + k_{tr,I} [I][M \cdot] + k_{tr,X} [X][M \cdot]}$$

**Eqn 2-22**

The denominator represents termination by disproportionation and chain transfer to monomer, solvent, initiator and modifier respectively. If termination is via bimolecular combination, the first term becomes  $f k_d [I]$ . A kinetic parameter that describes the magnitude of chain transfer reactions is called a chain transfer constant. This constant is the ratio of the rate coefficient for a particular chain transfer process against the rate of propagation. Chain transfer constants for monomer, solvent, initiator and modifier can be defined by Eqn 2-23, Eqn 2-24, Eqn 2-25 and Eqn 2-26 respectively.

$$C_M = k_{tr,M} / k_p$$

**Eqn 2-23**

$$C_S = k_{tr,S} / k_p$$

**Eqn 2-24**

$$C_I = k_{tr,I} / k_p$$

**Eqn 2-25**

$$C_X = k_{tr,X} / k_p$$

**Eqn 2-26**

Then, assuming termination via disproportionation, Eqn 2-22 can be simplified to:

$$\frac{1}{DP} = \frac{2k_t}{k_p^2 [M]^2} \frac{R_p}{f k_d} + C_M + C_S \frac{[S]}{[M]} + C_I \frac{k_t}{f k_p^2 k_d} \frac{R_p^2}{[M]^3} + C_X \frac{[X]}{[M]}$$

**Eqn 2-27**

This assumes that the radical produced in a chain transfer reaction has a similar reactivity to the original chain radical. The derivations assume that chain transfer radicals play no part in termination reactions. This assumption is usually valid due to the low concentration of chain transfer radicals present compared to propagating radicals. The kinetic scheme can be complicated by the introduction of a high concentration of chain transfer radicals, chain transfer to initiator or chain transfer to polymer.

Chain transfer constants are important when attempting to predict the effect of an added modifier on a polymerisation. An agent with a chain transfer constant near unity indicates that it is consumed at the same rate as the monomer, so that  $[X]/[M]$  remains constant throughout the entirety of the polymerisation. An agent with a chain transfer constant  $>5$  is consumed quickly in a polymerisation. When the chain transfer constant is very low, the newly formed radical may react slowly or not at all; this is retardation and inhibition respectively.

#### **2.1.4.1 Chain Transfer to Monomer, Initiator and Solvent**

Chain transfer reactions with monomer can occur by two mechanisms; both involve competitive hydrogen abstractions. Monomers containing  $\alpha$ -methyl groups are potentially susceptible to chain transfer by abstraction of a hydrogen atom.

Chain transfer reactions with an initiator molecule can result in complications that are dependent on the mechanism of the transfer reaction. A chain transfer reaction can destroy the activity of an initiator or it can abstract an atom from the initiator, preserving the reactive linkage that produces the radical species.

Chain transfer reactions with solvent are dependent on the solvent concentration, the strength of the bond involved in the abstraction step and the stability of the solvent radical produced.

#### 2.1.4.2 Chain Transfer to Polymer

A chain transfer reaction to a polymer molecule during a radical polymerisation can lead to the formation of a branched species. A primary radical or a chain radical abstraction on a polymer molecule can produce a branch site capable of propagating monomer. The length of the branch chain is dependent on the mechanism of termination. Bimolecular termination of the branch chain via disproportionation yields a simple branched species, bimolecular termination via combination with a linear molecule produces a long branch chain and combination with another branched species produces a cross-link. The importance of chain transfer to polymer increases as the concentration of polymer increases; hence, monomer conversion and concentration are important factors in determining the extent of branching. Chain transfer to polymer increases the  $M_w$  of the resultant dead polymer and broadens the molar mass distribution (MMD).<sup>15</sup>

#### 2.1.4.3 Chain Transfer to Modifier

Specific compounds and functional groups are more susceptible to transfer reactions with radicals because of the strength of the bond involved in the abstraction. Sulphur and sulphur-based compounds are generally effective chain transfer agents. Alkyl mercaptans are susceptible to chain transfer through abstraction of the labile hydrogen atom.<sup>16</sup> Disulphide-based compounds, especially polysulphides,<sup>17</sup> are involved in chain transfer reactions through attack of the S-S bond. Polymerisations performed in the presence of chain transfer agents are known to modify the limiting conversion of the polymerisation (with respect to those found in their absence).<sup>18</sup> The chain transfer activities of numerous compounds have been reported.<sup>10</sup>

Eqn 2-27 defining the DP can be simplified if chain transfer reactions of other species are negligible compared with the modifier (termination via disproportionation).

$$\frac{1}{DP} = \frac{k_t}{k_p^2} \frac{R_p}{[M]^2} + C_X \frac{[X]}{[M]}$$

Eqn 2-28

## 2.1.5 Mechanism of Termination of MMA and Gel Effect

It is generally agreed that in the polymerisation of MMA the proportion of termination by disproportionation increases with temperature.<sup>19</sup> The termination mechanism appears to be related to both steric factors and the availability of hydrogen for abstraction. The disproportionation mechanism appears to be linked with the availability of transferable hydrogen atoms. The introduction of a  $\alpha$ -methyl group on the radical enhances termination by a disproportionation mechanism. Studies into the kinetics of radical polymerisation of MMA have concluded that termination proceeds by both disproportionation and combination mechanisms. Szesztay et al.<sup>20</sup> concluded that there were no significant chain transfer reactions to PMMA chains and disproportionation was the dominant mechanism of termination. Recent work by Zammit et al.<sup>21</sup> on the mode of termination for the thermally initiated radical polymerisation of MMA yielded the same conclusion. Primary radical termination as a chain stopping mechanism was shown to contribute significantly at a high concentration of initiator; at a lower concentration of initiator it was not significant (disproportionation =  $4.37 \pm 1.1$ ).

The termination reaction of propagating radicals requires the close approach of large macromolecular entities and inevitably involves complex diffusive processes, often through viscous media. The first indications that restricted diffusion was important in such termination reactions came from the studies of Norrish and Smith,<sup>22</sup> and subsequently of Tromsdorff et al.<sup>23</sup> These authors observed that in some polymerisations, the rate of reaction increased rapidly after some critical conversion was reached, instead of continuing to decrease with time due to the consumption of reactants. It was postulated that the increased reaction rate was a consequence of a decrease in the rate of termination. This resulted in an increase in the concentration of reactive species due to the significant increase in macroscopic viscosity restricting diffusion of the macro-radicals. Auto-acceleration is a feature of some polymerisations, and is well known as the gel-effect. During the period of auto-acceleration extremely high rates of polymerisation may be observed.

The explanation of the gel effect is not completely answered. O'Neil et al.<sup>24,25</sup> recently investigated the gel effect and termination mechanisms. They concluded that chain entanglements play an identifiable role in some termination reactions but this was the exception rather than the rule. Diffusion data of species and experimental data were used to draw their conclusions. Their investigations supported the idea that the shortest chains present in the polymerisation preferentially dominated termination, as they were the fastest diffusing species.

Tsukahara et al.<sup>26</sup> investigated the homopolymerisation behaviour of macromonomers. In contrast to the polymerisation of small monomers (where a large increase in molar mass is observed with an increase in conversion at high monomer concentration) the gel effect was demonstrated to appear from the beginning of the polymerisation reaction because of the high viscosity of the polymerisation media. Hence, the extent of the gel effect was shown to be a function of the macromonomer concentration. The study of the polymerisation kinetics revealed that  $R_p$  was not first order with respect to monomer concentration (Eqn 2-16), but was higher and increased as the macromonomer concentration increased. The deviation was attributed to the high viscosity of the polymerisation media.

A reduction in the initiator efficiency was also observed at high macromonomer concentration due to decreased mobility of the primary radicals; this reduced the polymerisation rate. Electron spin resonance (ESR) spectroscopy was utilised to obtain direct information on the propagating radical.<sup>27</sup> It was demonstrated that the concentration of propagating radicals of macromonomers was considerably higher than those of conventional monomers in solution polymerisation of the same range of monomer concentration. The rate constants  $k_p$  and  $k_t$  of macromonomers were much smaller than those of corresponding small monomers due to the diffusion control effect as a result of the viscous polymerisation media.

## 2.2 Copolymerisation

The ability to copolymerise two monomers yields a powerful method for the variation and control of polymer structure and properties. Some monomers, such as maleic anhydride, homopolymerise with great difficulty but copolymerise readily. Copolymer structures include alternating copolymers (monomers alternating regularly along the chain), statistical copolymers (monomers are statistically located in the chain) and block copolymers (numerous units of one monomer type in succession). The type of copolymer structure produced is dependent on the reactivity of the comonomers toward each other. The copolymerisation of MMA and HEMA has been documented.<sup>28</sup>

### 2.2.1 Kinetics of Copolymerisation

The copolymerisation of two monomers ( $M_1$  and  $M_2$ ) can be defined by four elementary kinetic steps (Eqn 2-29 to Eqn 2-32).

Reaction

Rate



Eqn 2-29



Eqn 2-30



Eqn 2-31



Eqn 2-32

where  $k_{11}$  and  $k_{22}$  are the rate constants for the self-propagating reactions and  $k_{12}$  and  $k_{21}$  are the corresponding cross-propagation rate constants. It is assumed that the reactivity of the chain ends is dependent only on the last unit added to the chain end.

The rate of consumption of monomers can be defined by:

$$-\frac{d[M_1]}{dt} = k_{11} [M_1^\bullet][M_1] + k_{21} [M_2^\bullet][M_1]$$

**Eqn 2-33**

$$-\frac{d[M_2]}{dt} = k_{22} [M_2^\bullet][M_2] + k_{12} [M_1^\bullet][M_2]$$

**Eqn 2-34**

To simplify the calculations, the ratio of the rate constants for the two monomers adding to the same active site can be utilised. These are defined by  $r_1$  (Eqn 2-35) and  $r_2$  (Eqn 2-36).

$$r_1 = k_{11} / k_{12}$$

**Eqn 2-35**

$$r_2 = k_{22} / k_{21}$$

**Eqn 2-36**

These terms are known as monomer reactivity ratios for monomers  $M_1$  and  $M_2$  respectively. The copolymer equation can be obtained by dividing Eqn 2-33 by Eqn 2-34, and substituting the monomer reactivity ratios for the rate constants, leading to Eqn 2-37.

$$\frac{d[M_1]}{d[M_2]} = \frac{[M_1]}{[M_2]} \left( \frac{r_1[M_1] + [M_2]}{[M_1] + r_2[M_2]} \right)$$

**Eqn 2-37**

where  $d[M_1]/d[M_2]$  corresponds to the concentration ratio of the monomer units in the copolymer. The copolymer equation is general for all chain reaction polymerisations regardless of whether the mechanism involves anionic, cationic, radical, or organometallic reactive chain species; it is independent of the mode of termination of chain growth.

The copolymer equation provides a means of calculating the concentration of comonomer units incorporated in a chain from a given reaction mixture or feed (when the monomer reactivity ratios are known).

Let  $F_1$  and  $F_2$  be the mole fractions of the monomer units 1 and 2 in the copolymer being formed at any instant. Similarly, if  $f_1$  and  $f_2$  represent the mole fractions of monomers in the feed, the copolymer equation can be written:

$$F_1 = 1 - F_2 = \frac{r_1 f_1^2 + f_1 f_2}{r_1 f_1^2 + 2f_1 f_2 + r_2 f_2^2}$$

Eqn 2-38

This equation can be used to calculate curves for instantaneous copolymer composition versus monomer feed compositions. The equation predicts the average composition of the copolymer formed at any instant during the copolymerisation; however, there may be statistical deviations and deviations due to the monomer feed. The equation can be used to calculate curves of monomer feed versus instantaneous copolymer composition for various monomer reactivity ratios.

## 2.2.2 Monomer Reactivity Ratios and Copolymer Composition

The reactivities of both monomer and radical are determined by the nature of the substituents on the double bond. The effect of a second substituent on the same carbon is usually additive. The order of reactivity of a radical depends on the resonance stabilisation of the radical formed after addition. Resonance stabilisation depresses the reactivity of radicals so that their order of reactivity is reverse to that of their monomer. The effect of a substituent in depressing the activity of a radical is much greater than its effect in enhancing the activity of the monomer. Steric hindrance on the radical caused by substituents can result in reactivity changes; 1,1-substituted species are far more reactive than 1,2-substituted species.

The monomer reactivity ratios, described by Eqn 2-35 and Eqn 2-36, can be used to estimate the copolymer composition. The behaviour of a monomer in a copolymerisation can be predicted from the value of the monomer reactivity ratio.

$r_1 < 1$   $M_1\bullet$  prefers to add  $M_2$ .

$r_1 = 1$   $M_1\bullet$  has an equal probability of adding  $M_1$  or  $M_2$ .

$r_1 > 1$   $M_1\bullet$  prefers to add  $M_1$ .

The monomer reactivity ratio determined for each comonomer in a copolymerisation can be utilised to predict the resultant copolymer composition.

$r_1 = r_2 = 0$  Tendency towards alternating copolymer – monomers alternate regardless of the feed composition.

$0 < r_1 r_2 < 1$  Tendency towards alternating copolymer formation (common case).

$r_1 r_2 = 1$

$r_1 = r_2 = 1$  Tendency towards statistical ideal copolymer formation.

$r_1 < 1$  and  $r_2 > 1$  Tendency to obtain composition drift. The more reactive  $M_2$  will be depleted until only  $M_1$  remains.

$r_1 r_2 \gg 1$  Tendency to obtain block copolymer.

In some cases it is desirable to prepare a copolymer that has a homogeneous composition rather than one having compositional drift. This can be achieved by stopping the copolymerisation before the maximum conversion has been attained or by maintaining a specific feed composition by adding monomers to the copolymerisation.

### 2.2.2.1 Estimation of Monomer Reactivity Ratios

Kelen and Tudos developed a method to determine the monomer reactivity ratios in a copolymerisation based on Eqn 2-37.<sup>29</sup> The method removed some of the weaknesses associated with previous methods. Eqn 2-37 was substituted with the following parameters:

$$G = x(y-1)/y \quad F_{KT} = x^2/y.$$

where

$$x = (M_1/M_2) \quad y = (d[M_1]/d[M_2])$$

Eqn 2-39 was then developed:

$$\sigma = r_1 \xi - \frac{r_2}{\beta} (1 - \xi)$$

Eqn 2-39

where  $\sigma = (G/\beta + F_{KT})$  and  $\xi = (F_{KT}/\beta + F_{KT})$ .

The constant  $\beta$  has a value defined by the square root of the product of the highest and the lowest values for  $F_{KT}$  (Eqn 2-40).

$$\beta = \sqrt{F_{KT-LOW} \times F_{KT-HIGH}}$$

Eqn 2-40

Thus, a plot of  $\sigma$  calculated from the experimental data can be plotted against the values obtained for  $\xi$  to obtain a straight line, which extrapolated to  $\xi = 0$  gives  $(-r_2/\beta)$  and extrapolated to  $\xi = 1$  gives  $r_1$  (both as intercepts).

## 2.3 Molar Mass Definition

Small molecules have a discrete and well-defined molar mass. However, most polymers are composed of hundreds to thousands of chains of different molar mass that result in a characteristic molar mass distribution (MMD). Every polymer will have a MMD, and its shape and breadth will depend on the polymerisation mechanism, kinetics and conditions. Average molar masses are used because of this distribution. An average based on the number of molecules present is the number average molar mass,  $M_n$ , defined by (Eqn 2-41), which is the sum of the masses of all the molecules divided by the number of molecules.

$$M_n = \frac{\sum N_i M_i}{\sum N_i}$$

Eqn 2-41

where  $N_i$  is the number of molecules of species  $i$  of molar mass  $M_i$

An average based on mass of the molecules is the weight average molar mass,  $M_w$ , (Eqn 2-42) which is the sum of the mass multiplied by the molar mass of all the molecules divided by the total mass of the mixture.

$$M_w = \frac{\sum N_i M_i^2}{\sum N_i M_i}$$

Eqn 2-42

$M_w$  is always greater than  $M_n$  because heavier molecules contribute more to  $M_w$ .

The ratio of  $M_w / M_n$  is a measure of the width of the MMD in a polymer sample – termed polydispersity (D). If D is unity the polymer sample is monodisperse.  $M_p$  is another parameter utilised to define the peak molar mass.

## 2.4 Polymer Solutions

### 2.4.1 Polymer Solubility

When a polymer is mixed with a solvent it can produce a homogeneous solution, partially dissolve, swell or be completely insoluble. Cross-linking generally eliminates solubility and crystallinity generally acts like cross-linking. In the absence of these conditions, the sign of the Gibbs free energy component in Eqn 2-43 determines polymer dissolution.

$$\Delta G = \Delta H - T\Delta S$$

Eqn 2-43

where  $\Delta G$  is the change in Gibbs free energy,  $\Delta H$  is the change in enthalpy,  $T$  is the absolute temperature and  $\Delta S$  is the change in entropy. Consider the process of mixing at constant pressure and temperature where pure polymer and pure solvent (state 1) mix to produce a solution (state 2). Only if  $\Delta G$  is negative will the solution process be thermodynamically feasible. The value of  $T$  must be positive and  $\Delta S$  is generally positive, as the molecules are in a more statistical state in solution than in a solid (the term  $-T\Delta S$  favours solubility). The  $\Delta H$  term can be positive or negative; a negative enthalpy change indicates the solution is the lower energy state compared with the energy states of the individual components. A negative  $\Delta H$  usually arises where specific interactions, such as hydrogen bonds, are formed between the solvent and polymer molecules. If the enthalpy change is positive the polymer will be soluble when  $T\Delta S > \Delta H$ .

A special feature of polymers is the smaller value of  $\Delta S$  in forming a solution compared with an equivalent mass of a low molar mass solute. This is related to a reduction in the number of possible conformations because each chain segment is attached to the next chain segment. The entropy change of dissolution will therefore increase with lower molar mass polymer. In the absence of specific interactions, predicting polymer solubility is dependent on minimising  $\Delta H$ . Solubility parameters can be utilised to predict polymer dissolution in a specific solvent system.<sup>30</sup>

## 2.4.2 Properties of Dilute Solutions

When a polymer is mixed with a suitable solvent, the polymer disperses in the solvent and behaves as a statistically coiling mass. The dimensional functions used to describe the conformation of a polymer chain in solution are the mean square end-to-end distance,  $\langle R \rangle^2$ , and the mean square radius of gyration,  $\langle R_g \rangle^2$ . An average value is required due to the large array of possible conformations.

Long-range interactions are intramolecular interactions between segments or groups of one and the same polymer molecule that are separated by many chemical bonds along the chain; they are remote in sequence but adjacent in space. Short-range interactions are interactions between chain groups that are near to each other in sequence. They are determined by the length of the chain bonds, the valence angles between chain atoms, and the hindrance to rotation around chain bonds.

In a thermodynamically 'good' solvent the polymer molecule will tend to expand. This behaviour is related to the energy of interaction between a polymer segment and a solvent molecule adjacent to it. If this interaction exceeds the interaction between the polymer-polymer and solvent-solvent pairs, the molecule will tend to expand to reduce the frequency of contacts between pairs of polymer segments. In a thermodynamically 'poor' solvent, the attractive forces between the segments of the polymer chain will be greater than those between the chain segments and the solvent, the molecule will tend to contract to minimise these interactions. Hence, perturbed dimensions differ from the unperturbed dimensions due to long range effects. The extent of this difference between states is measured by the average expansion of a molecule, defined by  $\alpha$ .

Phase separation sets the limit on how poor a solvent can be. The theta ( $\Theta$ ) temperature represents the lowest temperature for complete miscibility in the given poor solvent at the limit of infinite molar mass. In a theta solvent the polymer-solvent interactions are just balanced by polymer-polymer and solvent-solvent interactions (the second virial coefficient  $A_2 = 0$ ). The long-range interactions disappear and the polymer molecule can assume its unperturbed dimensions. The second virial coefficient is a measure of the interaction between two bodies, which depends on the chemical structure

and the molar mass of the polymer, the solvent structure and the temperature. For a given polymer, the  $\Theta$  state can be obtained at a fixed temperature by adjusting the solvent or by adjusting the temperature with a particular solvent to reach the  $\Theta$  temperature.  $\Theta$  conditions for PMMA have been reported.<sup>10</sup>

### 2.4.3 Solution Viscosity

Dissolved polymers, even at very low concentrations, increase the solution viscosity of the solvent in which they are dissolved. This phenomenon is attributed to the large size difference between the polymer and solvent molecules. Solution viscosity measurements yield information about chain dimensions, molar mass and branching.

Intrinsic viscosity,  $[\eta]$ , is a parameter derived from the solution viscosity of a polymer using either the relative viscosity,  $\eta_{rel}$ , (where  $\eta_{rel} = \eta_{solution}/\eta_{solvent}$ ) or the specific viscosity,  $\eta_{sp}$  (where  $\eta_{sp} = \eta_{rel} - 1$ ). Intrinsic viscosity is the limiting case extrapolated to infinite dilution and is independent of the mass concentration,  $c$ , of the polymer. Intrinsic viscosity is defined by Eqn 2-44 and Eqn 2-45.

$$[\eta] = \lim_{c \rightarrow 0} \frac{\eta_{sp}}{c}$$

Eqn 2-44

$$[\eta] = \lim_{c \rightarrow 0} \frac{\ln \eta_{rel}}{c}$$

Eqn 2-45

The intrinsic viscosity can be considered to be proportional to the ratio of the effective volume of the molecule in solution divided by the molar mass.<sup>15</sup> The intrinsic viscosity should depend on the molar mass and the expansion factor. The simple relationship between intrinsic viscosity and molar mass can be expressed by the Mark-Houwink (M-H) equation (Eqn 2-46).

$$[\eta] = KM^a$$

Eqn 2-46

where the constant  $K$  and the exponent  $a$  are determined by the intercept and the slope of the plot of  $\log[\eta]$  against  $\log(\text{molar mass})$ . The values for  $K$  and  $a$  vary with the solvent, polymer and temperature. The exponent  $a$  generally lies within the range 0.5 - 0.8.

The influence of expansion resulting from intramolecular interactions can be removed by careful choice of solvent and temperature. In the  $\Theta$  state the expansion factor is 1 and the following relationship holds for a linear, flexible polymer.

$$[\eta]_{\Theta} = K_{\Theta} M^{0.5}$$

Eqn 2-47

The intrinsic viscosity in the  $\Theta$  state should be proportional to the square root of molar mass, assuming the contribution of a polymer molecule to the solution viscosity is proportional to the cube of its linear dimension. Intrinsic viscosity changes rapidly with temperature in the vicinity of the  $\Theta$  point; hence accurate control is required. Experiments performed in the  $\Theta$  state confirm the linear relationship (slope  $a_{\Theta} = 0.5$ ) for linear polymers with molar mass  $> 10,000$  g/mol. Deviations from 0.5 are related to solvent-polymer interactions and polymer expansion. Polymer molecules with long side chains have been shown to deviate from the  $a_{\Theta} = 0.5$  condition.<sup>31</sup>

## 2.4.4 Effects of Branching

The introduction of chain branching changes the relationship between hydrodynamic volume and molar mass. A branched molecule occupies a smaller volume than an equivalent linear molecule of the same molar mass. The decrease in the size of a molecule as a consequence of branching can be described by the parameter  $g$ , which is the ratio of the mean square radius of gyration of a branched molecule to that of a linear molecule with identical molar mass.<sup>3</sup>

$$g = \left[ \frac{\langle R_g \rangle_{br}^2}{\langle R_g \rangle_{lin}^2} \right]_M$$

Eqn 2-48

The decrease in hydrodynamic volume as a consequence of branching is described by the parameter  $g'$ , which is the ratio of the intrinsic viscosity of a branched molecule to a linear molecule of equivalent molar mass (Eqn 2-49).

$$g' = \left[ \frac{[\eta]_{br}}{[\eta]_{lin}} \right]_M$$

Eqn 2-49

A relationship exists between the values of  $g'$  and  $g$  that is dependent on the structure of the branched molecule (Eqn 2-50).<sup>32</sup>

$$g' = g^\epsilon$$

Eqn 2-50

The value of  $\epsilon$  is found to vary experimentally between 0.5 and 1.5 depending on the type/extent of branching present. Zimm and Kilb found  $\epsilon = 0.5$  for star chain molecules.<sup>32</sup> For comb polymers with short branch chains  $\epsilon = 1.5$ <sup>33</sup> and for comb shaped polymers with longer side chains,  $\epsilon$  ranged between 0.5 and 1.5.<sup>32</sup> For H-polymers  $\epsilon$  was 0.70<sup>34</sup> and for star chains with molar mass asymmetry it is in the range 0.70 - 0.85.<sup>35</sup>

## 2.5 Size Exclusion Chromatography (SEC)

### 2.5.1 Background

SEC is a liquid column chromatographic technique that discriminates between molecules according to their molecular size (or hydrodynamic volume). Size separation is achieved by repeated exchange of the solute molecules between the bulk solvent of the mobile phase and the stagnant liquid phase within the pores of the packing. As the polymer elutes through the column, molecules that are too large to penetrate the pores of the packing elute in the interstitial volume of the column. As the molecular size of the polymer decreases, the molecules penetrate into the pores and access greater pore volume. The larger solute molecules elute at a faster rate because they penetrate the packing pores to a lower extent.

Modern SEC systems consist of a constant flow pump, injection system, column(s), detector(s) and a data recording system connected to a personal computer with appropriate software. A high purity mobile phase is required to carry the sample through the SEC system. For precise and accurate data a high quality pump is required to minimise fluctuations in the flow rate as the molar mass data is based on elution time.

The core of a SEC system is the column that contains a packing of swollen polymer beads or silica that separates the polymer molecules according to their hydrodynamic size. A packing material must have mechanical/chemical/thermal stability, a high-resolution separation and a low backpressure when packed in a column. Chemical inertness with the mobile phase and solute is paramount. In order to maintain a high-resolution separation (high efficiency) the particle size of the packing should be low and the size distribution narrow. However, there is a lower limit to the particle size in the column packing due to the high backpressure created by pumping the mobile phase through the column. The solute molecules should be separated solely by size exclusion without any secondary interaction with the gel. Column selection is largely based on the molar mass range of separation. Attention to the pore size of packed gels is important as this determines the range of molar mass separation (measured by exclusion limits). Other important operating variables are sample concentration, injection volume, flow rate and temperature.

## 2.5.2 Calibration

In the absence of an absolute molar mass detector the SEC system must be calibrated as the calculations to determine molar mass are based on elution time or elution volume. The calibration curve should cover the molar mass range of the polymer samples of interest. Calibration can be performed by various methods, the most common being a series of narrow MMD calibrants of known molar mass.<sup>36</sup> A calibration curve can be generated by plotting  $\log(\text{molar mass})$  against elution volume/time at the peak maximum for a series of calibrants of narrow MMD (Figure 2-1). For linear polymers there is a linear relationship between molar mass and elution volume or elution time. Hence, the molar mass of a sample can be determined from its elution time or elution volume on a calibrated SEC system. The gradient of the calibration and the extent of the range of selective permeation reveal information about the separation capabilities of the system. A shallow gradient improves resolution of similar sized species.

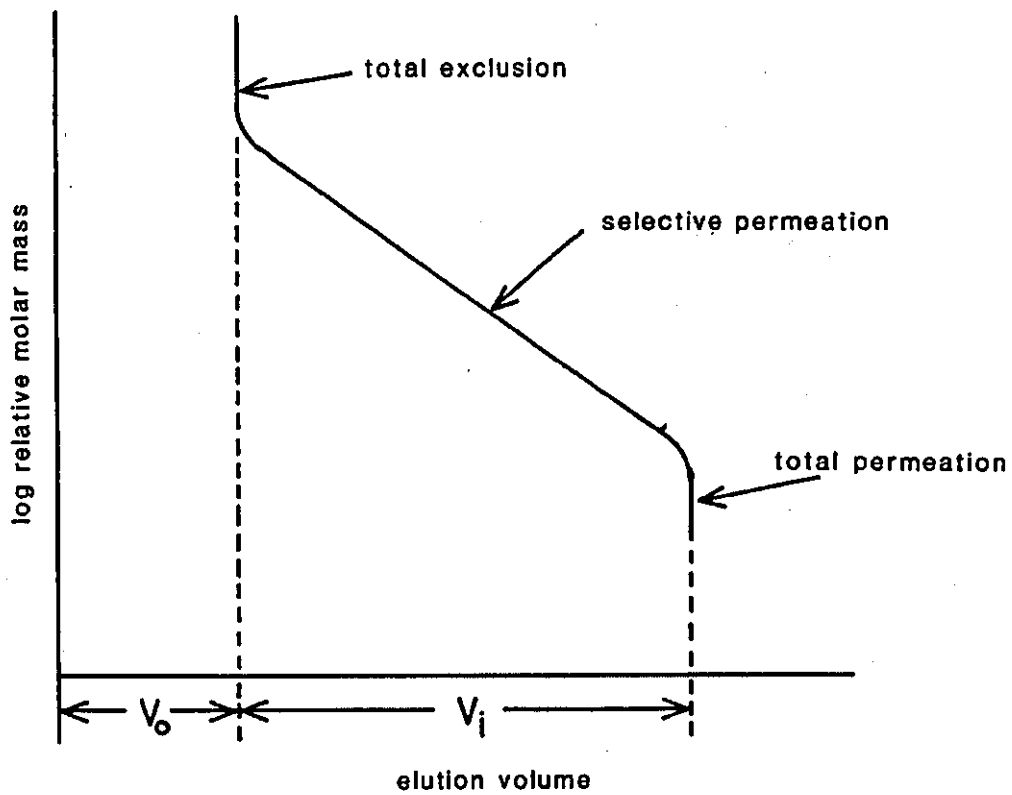


**Figure 2-1** Representation of the separating efficiency of a SEC system determined using narrow MMD calibrants of known molar mass. Total permeation or total exclusion determines the limits of size separation.

The peak position calibration curve varies according to the polymer type, which is attributed to the molecular size of different polymers in solution. Unfortunately, there are only a limited number of monodisperse standards available. The relationship between hydrodynamic volume and molar mass can be used as another method of calibration, which for flexible statistical coils at infinite dilution is proportional to  $[\eta]M$ . A universal calibration is then obtained by plotting  $\log([\eta]M)$  against elution volume/time. A knowledge of the M-H constant  $K$  and exponent  $a$  is required to correct for different expansions between the standard polymer and the unknown. If the universal calibration curve is valid then at a given elution volume/time:

$$\log[\eta]_s M_s = \log[\eta]_u M_u$$

**Eqn 2-51**

and

$$\log K_s M_s^{(a_s+1)} = \log K_u M_u^{(a_u+1)}$$

**Eqn 2-52**

where subscript  $s$  denotes the standard calibration and  $u$  the polymer to be calibrated. The molar mass  $M_u$  can be obtained from:

$$\log M_u = \frac{1}{1+a_u} \times \log \left[ \frac{K_s}{K_u} \right] + \frac{1+a_s}{1+a_u} \times \log M_s$$

**Eqn 2-53**

In order for the universal calibration concept to be valid, there should be no secondary interactions between the stationary phase and the sample molecules and the separation should be solely by size exclusion. The selection of the values  $K$  and  $a$  are important.

## 2.5.3 Detectors for SEC

### 2.5.3.1 Concentration Detectors

#### 2.5.3.1.1 Refractive Index (RI) Detectors

A dissolved solute in the mobile phase will change the RI of pure mobile phase. The detector continually measures the difference in RI between the reference cell (containing pure mobile phase) and the mobile phase eluted from the column. The difference in RI is proportional to the solute concentration. A RI detector is a common detector in a SEC system. The detector is universal as many solutes have a different RI compared to the solvent (the sensitivity of the detector being proportional to the difference). RI detectors are simple and robust instruments but temperature variations can cause problems.

### 2.5.3.2 Structure-Selective Detectors

#### 2.5.3.2.1 Ultraviolet (UV) Detectors

UV detectors are solute specific, as an active chromophore at the wavelength of detection is required to yield a response. The solvent requires a high transmittance at the operating wavelength, which limits the range of solvents available. The detectors are sensitive, stable and robust to environmental conditions. A variable wavelength detector increases versatility.

### 2.5.3.3 Molar Mass Detectors

#### 2.5.3.3.1 Differential Viscosity (VISC) Detector

The specific viscosity of the eluent from the column can be measured directly and utilised to calculate the intrinsic viscosity of a polymer in solution. The absolute molar mass data can be calculated using the 'universal calibration' procedure with an on-line viscosity detector when coupled with a concentration detector.<sup>37</sup>

The differential viscometer utilised in this project was a 'Viscotek' differential viscosity detector.<sup>38</sup> The specific viscosity is measured using four capillaries ( $R_1$ - $R_4$ ) in a Wheatstone bridge configuration (Figure 2-2).

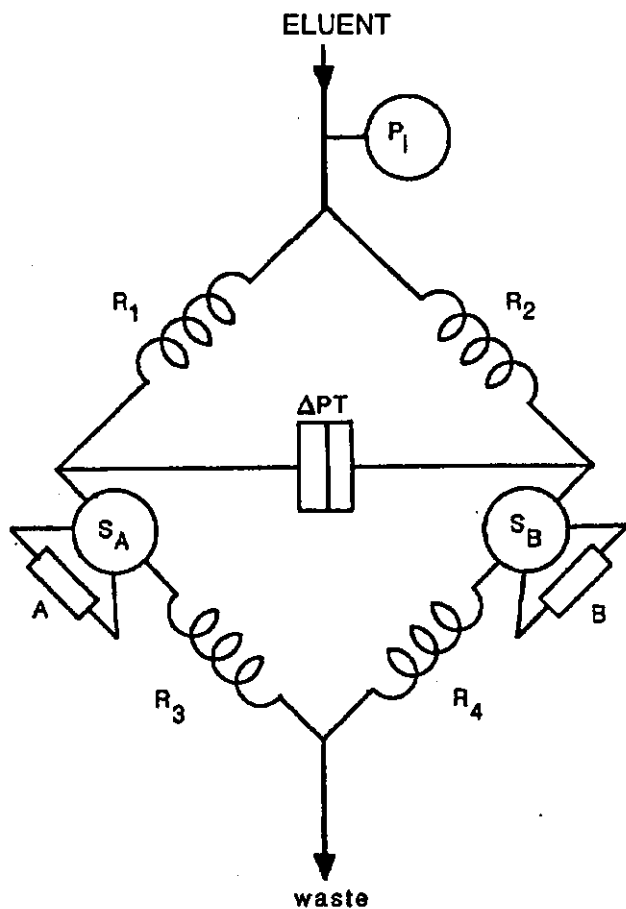


Figure 2-2 Schematic of a Wheatstone bridge configuration to measure the specific viscosity in a 'Viscotek' differential viscosity detector.

The pressure gauge  $P_1$  monitors the inlet pressure (should be constant).  $\Delta P$  is a differential pressure transducer, and  $S_A$  and  $S_B$  are tandem switching valves that enable the reservoirs A and B to be switched in or out of the bridge circuit. Reservoir A compensates for any volume changes due to variations in temperature, whilst reservoir B holds eluent from the column and prevents it entering capillary  $R_4$ . Initially, the reservoirs are switched out of the circuit and filled with mobile phase via a separate pumping system. When the valves are switched to inject, the eluent from the chromatograph flows into reservoir B (displacing solvent) as well as into capillaries  $R_1 - R_3$ . At any time during the elution of the sample, polymer solution will be present in capillaries  $R_1 - R_3$  and pure solvent in  $R_4$ . The volume of reservoirs A and B must be enough to hold sufficient solvent so that reservoir B is not completely displaced until after the sample is eluted. From the measured inlet pressure  $P_1$  and differential pressure  $\Delta P$  the specific viscosity at any instant can be calculated (Eqn 2-54):

$$\eta_{sp} = \frac{4\Delta P}{P_1 - 2\Delta P}$$

Eqn 2-54

A RI detector is connected in parallel with the viscosity detector using a stream splitter, and the data from both devices enable the intrinsic viscosity to be determined. This can be related to the molar mass via the M-H relationship.

#### 2.5.3.3.2 Light Scattering (LS) Detector

The addition of a LS detector in combination with a concentration detector allows the absolute weight average molar mass to be calculated and the presence of branching to be assessed. The molar mass of the polymer, its concentration, and the differential RI for the polymer-solvent combination determine the response of the detector. When combined with SEC, the LS intensity of scattering is measured only at a single concentration for each molar mass fraction in the elution stream. Optically clean solutions must be carefully prepared for LS measurements to avoid particulate contamination.

When light passes through an inhomogeneous medium, the species in the medium scatters a fraction of the beam in all directions. The perturbed electrons oscillate about their equilibrium positions with the same frequency as the exciting beam. This action induces transient dipoles in the molecules that act as secondary scattering centres by re-emitting the absorbed energy in all directions. The wavelength of the scattered radiation is almost the same as that of the incident radiation (Rayleigh scattering).

Complications arise with polymer molecules due to their large size. If the dimensions of the molecule are greater than  $\lambda'/20$  (where  $\lambda' = \lambda/RI_{\text{solvent}}$ ), intraparticle interference causes scattered light from two or more centres to arrive out of phase at the detector. The scatter pattern becomes dependent on the shape of the molecule. This attenuation, as a consequence of destructive interference, is zero in the direction of the incident beam, but increases as  $\theta$  increases because the path length difference in the forward direction is less than the backward direction (Figure 2-3). The difference in path length can be measured from disymmetry.

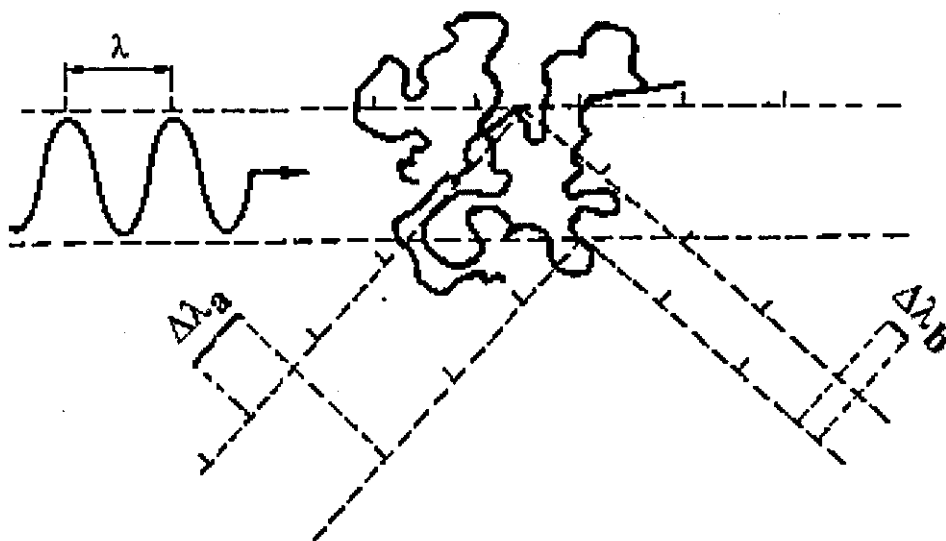


Figure 2-3 Destructive interference of light scattered by large particles leads to scattered light out of phase.

In LS measurements, the reduced scattering intensity at a scattering angle  $\theta$  is measured ( $R_\theta$ ), which is denoted as the Rayleigh ratio:

$$R_\theta = \frac{(I_\theta r^2)}{(I_0 V)}$$

Eqn 2-55

where  $I_0$  is the intensity of the incident radiation,  $I_\theta$  the intensity of the scattered radiation at a scattering angle  $\theta$ ,  $r$  the distance from the scattering centre to the detector, and  $V$  is the scattering volume of the sample solution. The excess Rayleigh ratio is defined as:

$$R(\theta) = R_\theta - R_0$$

Eqn 2-56

where  $R_0$  is the Rayleigh ratio of the solvent.

For a dilute solution of a monodisperse polymer with molar mass  $M_w$ ,  $R(\theta)$  is expressed as:

$$\frac{K^* c}{R(\theta)} = \frac{1}{M_w P(\theta)} + 2A_2 c + 3A_3 c^2 + \dots$$

Eqn 2-57

where  $c$  is the concentration of the polymer in the solution (g/ml), and  $A_2$  and  $A_3$  are the second and third virial coefficients respectively.  $P(\theta)$  is the particle scattering constant defined by the ratio  $R_\theta/R_0$ .  $K^*$  is the optical constant and for unpolarised incident light is given by:

$$K^* = \frac{(2\pi^2 n_0^2 (dn/dc)^2)}{(N_A \lambda_0^4)} (1 + \cos^2 \theta)$$

Eqn 2-58

where  $n_0$  is the refractive index of the solvent,  $dn/dc$  is the specific refractive index increment for a polymer in the SEC eluent,  $\lambda_0$  is the wavelength of light in vacuum, and  $N_A$  is Avogadro's number. The optical constant for vertically polarised incident light is

$$K^* = \frac{4\pi^2 n_0^2 (dn/dc)^2}{(N_A \lambda_0^4)}$$

Eqn 2-59

For a solution of a polymer with polydispersity, Eqn 2-57 is modified to Eqn 2-60:

$$\frac{K^* c}{R(\theta)} = \frac{1}{M_w} \left[ 1 + \left( 16\pi^2 n_0^2 / 3\lambda_0^2 \right) (R_g^2)_z \sin^2 \frac{\theta}{2} \right] + 2A_2 c + 3A_3 c^2 + \dots$$

Eqn 2-60

where  $(R_g^2)$  is the squared radius of gyration. In order to estimate the values of  $M_w$ ,  $(R_g^2)$ , and  $A_2$  by LS, values of  $K^*c/R(\theta)$  at various scattering angles and concentrations at constant temperature are plotted against  $\sin^2(\theta/2) + K'c$ , where  $K'$  is an arbitrary constant chosen to produce a reasonable spread of data points. A value of  $K' = 1/c_{max}$ , where  $c_{max}$  is the maximum concentration used, is usually employed. This plot is called a Zimm plot. The value of the limiting slope of the Zimm plot at  $c = 0$  is proportional to the square of the radius of gyration (z-average), and the intercept is  $1/M_w$ .

## 2.5.4 Triple Detector SEC (TDSEC)

The combination of molar mass sensitive detectors with SEC increases the quantity of information that can be obtained from a polymer sample compared to conventional SEC. The combination of a LS / VISC / RI detector system allows direct measurement of both molar mass and intrinsic viscosity.<sup>39,40,41</sup> This can be applied to the investigation of polymer conformation and branching because of the special relationship between molar mass and hydrodynamic volume. The additional information obtained using multiple detectors is offset against the complexity of the instrumentation and data handling.<sup>42</sup>

When three detectors are used together the responses from the detectors are initially misaligned because the detectors are located at different positions in the elution stream. The volume between the detectors must be known before the data can be analysed. Inaccuracies in determining the interdetector volume can lead to gross errors in the molar mass calculation.

By their nature, instruments measuring different polymer properties will have different sensitivities and measurement ranges. These differences need to be considered when evaluating results, especially at the extremes of the MMD where the signal-to-noise ratio is poor. Branching generally increases the molar mass of the polymer, which will increase the intensity of scattered light and produce a large response from the LS detector. A low concentration of high molar mass material is detected by the LS detector but the concentration is too low to register on the RI detector. At the low molar mass end of the distribution, the situation is reversed. These effects result in an underestimation of the breadth of the MMD.

The LS and VISC peaks appear at lower elution volumes than the RI peak because these detectors have increased sensitivity to higher molar mass species. The corresponding shift in peaks depends on the polydispersity of the sample. As the polydispersity increases, the peaks from the molar mass sensitive detectors shift to lower elution volumes (Figure 2-4). The VISC detector response peak is shifted to a lesser extent than LS detector response because intrinsic viscosity is proportional to the molar mass raised to the power

of the exponent  $\alpha$  in the M-H equation. For a statistical coil,  $\alpha$  is less than unity so the peak is shifted by a volume increment related to  $\alpha$ .<sup>43</sup> The extent of the shift in the LS signal is a measure of the sample polydispersity.

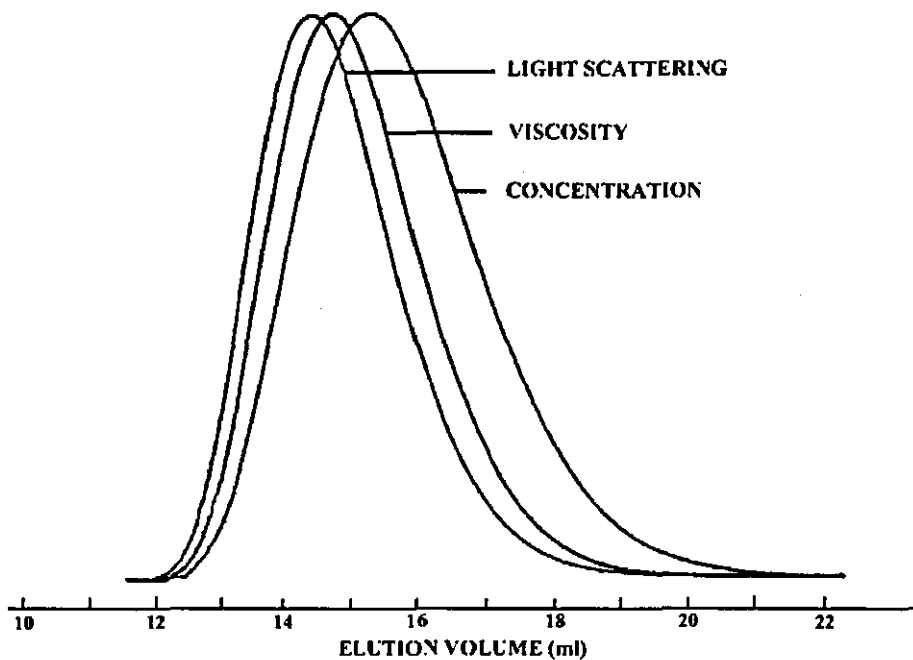


**Figure 2-4** Representation of a chromatogram for a polydisperse sample obtained with multi-detection SEC (LS, VISC, RI).

Although molar mass-sensitive detectors avoid some of the accuracy problems associated with column calibration, a number of other calibration procedures become necessary. When a molar mass sensitive detector is added, the absolute concentration of the eluting polymer is needed. To measure this absolute concentration, the concentration detector must be calibrated and the sample property used to measure concentration (RI or absorbance) must also be known. For LS analysis, the specific RI of the polymer in the mobile phase is needed (usually the second virial coefficient is taken as zero, which does not introduce significant error). For viscometry, the universal calibration curve is required to derive molar mass data.

## 2.6 Branched Polymers

### 2.6.1 Star Polymers

#### 2.6.1.1 Preparation

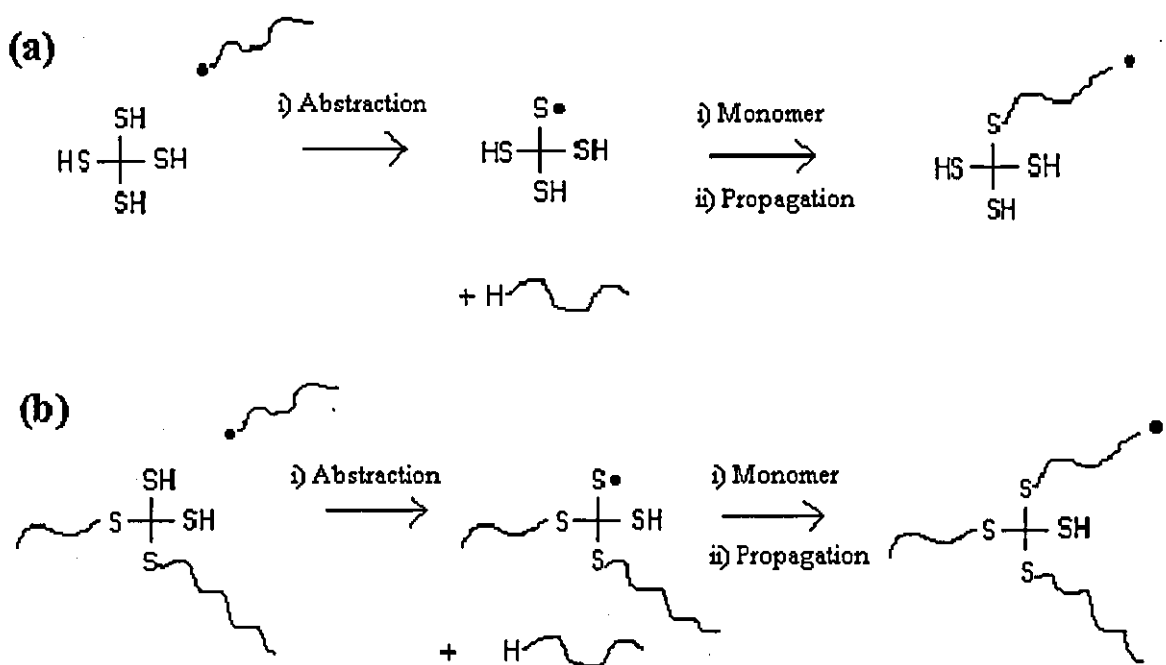
Chain architectures with a single polyfunctional branch point are classified as star polymers. Within this classification there exists a multitude of configurations. Regular star polymers have compositional and arm molar mass homogeneity. Asymmetric star polymers have molar mass asymmetry, topological asymmetry or chemical asymmetry (miktoarm star copolymers).<sup>44</sup> The preparation of asymmetric star polymers has been recently reviewed.<sup>45</sup> Recent reviews for the preparation of star polymers using cationic polymerisation and macromonomers have been reported.<sup>46,47</sup>

Three methodologies can be applied to the preparation of star polymers: 'core-first' techniques, 'core-last' techniques, and mixed techniques. The are dependent on the target structure and on the availability of initiators and linking agents.

In a 'core-first' approach a di-functional monomer is polymerised to produce a core with living active sites or a multi-functional initiator can be utilised. Branch arms can be subsequently grown from the core by the addition of a monomer. Di-functional monomers, such as divinyl benzene or ethylene glycol dimethacrylate, have been used to prepare a branch point in the form of a microgel core.<sup>48,49</sup> Maier et al.<sup>50</sup> prepared poly(methyl acrylate) star structures via atom transfer radical polymerisation (ATRP) with a macro-initiator.

Ullisch and Burchard studied the effect of a tetra-functional CTA in a radical polymerisation both theoretically and experimentally.<sup>51,52</sup> The proposed mechanism of a chain transfer reaction with a tetra-functional agent is outlined in Scheme 2-1. The initial step is the abstraction of a hydrogen atom from the CTA to yield a thio radical and an inactive chain as a consequence of the chain transfer process (part (a)). The thio radical can propagate with monomer units and produce a chain that has the tetra-functional species

at one end and an active radical at the other end. The radical can terminate via bimolecular combination, disproportionation or be involved in a further chain transfer reaction. This sequence of events is typical of the early stages of the polymerisation where chain formation is predominantly by chain transfer to CTA. An increase in conversion increases the probability that a CTA bearing one or two polymeric chains will participate in further chain transfer reactions as a consequence of the diminishing concentration of SH, producing a branched polymer (part (b)). During the course of the polymerisation the number of functional groups on a tetra-functional CTA is gradually exhausted. Under these conditions chain coupling via bimolecular combination increasingly gains importance. Chain coupling at higher monomer conversion now has a decisive effect on the structure of the branched polymer. The star-like polymers may become multiple-branched species through coupling processes, producing high molar mass polymer; in the extreme case a gel.



**Scheme 2-1** (a) A chain transfer reaction with a CTA to yield a thio radical, which can propagate with monomer to produce a chain bearing the CTA molecule. (b) The latter stages of the polymerisation where a CTA bearing 2 chains participates in further chain transfer reactions to produce a branched molecule.

Styrene was polymerised in the presence of the tetra-functional CTA neopentanetetrayl tetrakis(2-mercaptoproacetate), the mono-functional CTA 2-ethylhexyl 2-mercaptoproacetate, and no CTA at 333K.<sup>52</sup> Polymerisations were performed up to a conversion of 25%. Styrene polymerised in the absence of a CTA yielded a relatively high molar mass polymer. The mono-functional CTA had a dramatic effect on the molar mass, causing a sharp reduction in the chain length. The behaviour of a tetra-functional CTA was complex in comparison to a mono-functional CTA. At very low conversion, the effect of a tetra-functional CTA was similar to the mono-functional CTA, probably as only one of the SH groups had been involved in a transfer reaction. As conversion increased, star-shaped polymers were produced and eventually, due to chain coupling, large molecules were formed. The apparent number of branch arms was estimated to increase sharply at very low conversion.

A low concentration of tetra-functional CTA had less impact on the molar mass than a high concentration because of a reduction in the number of possible transfer reactions. At a low concentration of CTA the propagating chains from a tetra-functional agent had a comparatively larger length, as they were less likely to be involved in a chain transfer related termination reaction. Transfer reactions were expected to proceed without any impediment for the first and second transfer groups in the tetra-functional CTA. The remaining groups became hindered because the CTA was situated in the midst of coiled chains from previous chain transfer reactions. At a high concentration of CTA the molar mass was reduced, which was attributed to more frequent chain transfer reactions. The shorter branch chains were not predicted to interfere in the hindrance of the remaining transfer group; however, some effect was operating. It was postulated that a positive substitution increased the susceptibility of the remaining SH groups to a chain transfer reaction, which was counterbalanced by the kinetically controlled decrease in rate of propagation due to lower monomer concentration within the coil domain.

Farina et al.<sup>53,54,55</sup> also investigated theoretical and experimental polymerisations incorporating a tetra-functional CTA. Two problems were identified from the work by Ullisch and Buchard, namely the high  $C_{tr}$  of the tetra-functional CTA in the system and the occurrence of termination by bimolecular combination (with PS). The authors modified the polymerisation to eliminate these problems by using a large concentration of CTA with  $C_{tr} < 1$  and MMA as the monomer. The theoretical treatment derived equations for number

average and weight average degree of polymerisations and the MMD. The most favourable condition for producing a narrow MMD star polymer by radical polymerisation was a CTA with a value of  $C_{tr}$  near to/or equal to unity.

MMA was polymerised in the presence of a various CTA with SH groups = 1, 2, 3 and 4 per molecule. The  $C_{tr}$  for MMA with mercaptoacetate at 333K is 0.64, which was applied to each CTA.<sup>56</sup> The monomer conversion reached 100% within 24 hours. Evidence of branching was obtained from exposure of the resultant PMMA to UV light. The MMD of the polymer broadened from 1.29 to 2.02 after 15 hours of exposure. The transfer reaction of each thiol group on the tetra-functional CTA was shown to occur at different stages in the polymerisation. The molar mass data for polymers prepared in the presence of tri-functional and tetra-functional CTA was obtained using SEC in the absence of a mass detector.

Tobita et al.<sup>57,58</sup> have recently investigated a tetra-functional CTA system using a Monte Carlo simulation based on a statistical sampling technique and compared the predictions with experimental data. The Monte Carlo simulation proposed is fundamentally simple. At a given reaction time, a large number of polymer molecules were statistically sampled. The size and structure of each polymer molecule was determined on the basis of chain connection probabilities and kinetics. The mean square radius of gyration for each molecule was then determined. An equal reactivity model was applied to all the SH groups on the CTA. Styrene was polymerised with CTA bearing SH groups = 1, 2, 3, and 4. The experimental results were compared against predicted molar masses. Good agreement was observed for samples prepared with CTA having SH groups = 1, 2 and 3. However, with PS prepared with tetra-functional CTA the predicted molar mass was larger than the experimental value. It was proposed the final SH group in the tetra-functional CTA had reduced reactivity and the equal reactivity model was invalid, as the simulation for SH = 3 gave good agreement with experimental data. It was postulated that substitution effects from reacted SH groups altered the reactivity of the remaining groups both chemically and physically. The reactivity of the final SH group was set to 0.2 relative to the other groups. The modification improved the fit of data, which suggested reactivity of the final group in the tetra-functional CTA had reduced reactivity.

Star polymers have been prepared in a ‘core-last’ approach, where the arm chains are grown first and then linked together. A di-functional monomer can be utilised to link the arms together.<sup>59,60,61,62,63</sup> Star-shaped poly(t-butyl acrylate) was prepared using copper-mediated ATRP and coupled with divinylbenzene and 1,4-butanediol diacrylate.<sup>64</sup> Star polymers with controlled architecture have been prepared by the reaction of living polymeric chains with multi-functional electrophilic/nucleophilic linking species. Linking agents, such as tetrachlorosilane, have functional groups that react with the living chain ends to produce a branch point. Linking reactions have been utilised to prepare regular star polymers<sup>65,66</sup> and hetero-arm star polymers.<sup>67,68,69</sup> Poly(macromonomers) with a limited number of arms have been shown to behave like star polymers.

Mixed techniques have been utilised to prepare star polymers with molar mass asymmetry by adding additional monomer to tethered chains linked with di-functional monomer, as active sites are still present in the core which can further propagate monomer.<sup>35,70</sup>

### 2.6.1.2 Solution Behaviour

#### 2.6.1.2.1 Regular Star Polymers

The overall structure of regular star polymers results in considerable deviations in solution viscosity from that of linear chains of an equivalent molar mass. The number and length of the arms tethered to a branch centre determine the extent of the deviation. The behaviour is evident from the M-H plot included in Figure 2-5. The profiles for a star polymer are observed to be parallel to the corresponding molar mass dependence for linear chains, the extent of the deviation corresponding to the arm number reflected in the value of the constant K. The relationship is found in both  $\Theta$  and thermodynamically good solvents for regular star polymers with 4-arms,<sup>71</sup> 6-arms,<sup>72</sup> 18-arms,<sup>73</sup> 32-arms,<sup>74</sup> 64-arms<sup>75</sup> and 128-arms.<sup>75</sup> Stars with 200-arms<sup>76</sup> and 270-arms have been prepared that exhibit similar behaviour. The effect of arm number on the solution behaviour of the star polymer decreases as the number of arms increases; adding 2 arms to a 64-arm star will not enhance solution properties substantially. Significant changes in dimensions are detectable when the number of arms in a star polymer changes from 2 and 6. Star polymers with a high

number of arms behave as compact structures in solution with low intrinsic viscosities compared with linear chains of comparable molar mass.

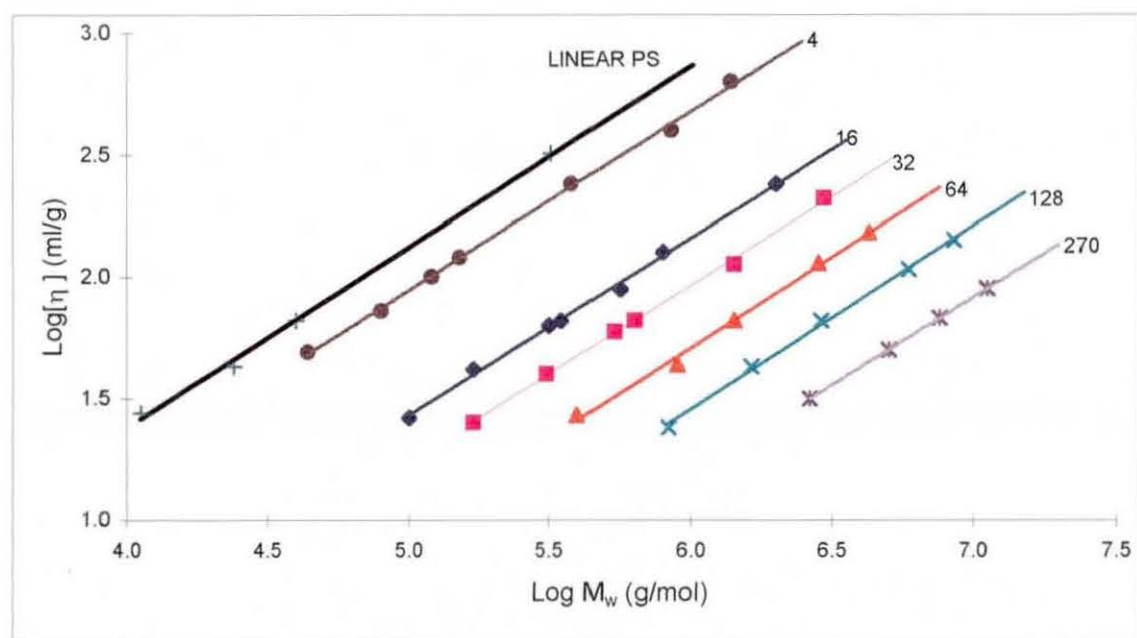


**Figure 2-5** The M-H plot for a series of star polymers. The number at the top of each plot corresponds to the star arm number. A linear PS is included for comparison.

#### 2.6.1.2.2 Asymmetric Star Polymers

Six-arm PS star polymers with molar mass asymmetry have been prepared and characterised by Jackson et al.<sup>35</sup> Star polymers were prepared with arm lengths of 23 kg/mol and 123 kg/mol in varying mole fractions. It was shown that in a 50:50 mol fraction of arm lengths there were more short arms than expected on the star polymers. This was explained by the faster diffusion coefficient of smaller chains. The M-H plot for a star polymer prepared in the presence of a 50:50 mol fraction of long and short arms is included in Figure 2-6a. The profile of the M-H plot is attributed to a decrease in branch chain polydispersity on the star molecule with an increase in molar mass. The number and functionality of branch points is the same in each molecule. The variation in the branching factors  $g'$  and  $g$  with number of long arms per star is illustrated in Figure 2-6b. The values of the branching factors increase initially when one long arm replaces a short arm; then both factors decrease as the number of long arms increases because the long branch arms

dominate the size of the molecule. A six-arm star with one or two long arms has a radius of gyration and hydrodynamic size that is closer to that of a linear molecule of the same molar mass than that of a uniform six-arm star with the same molar mass.

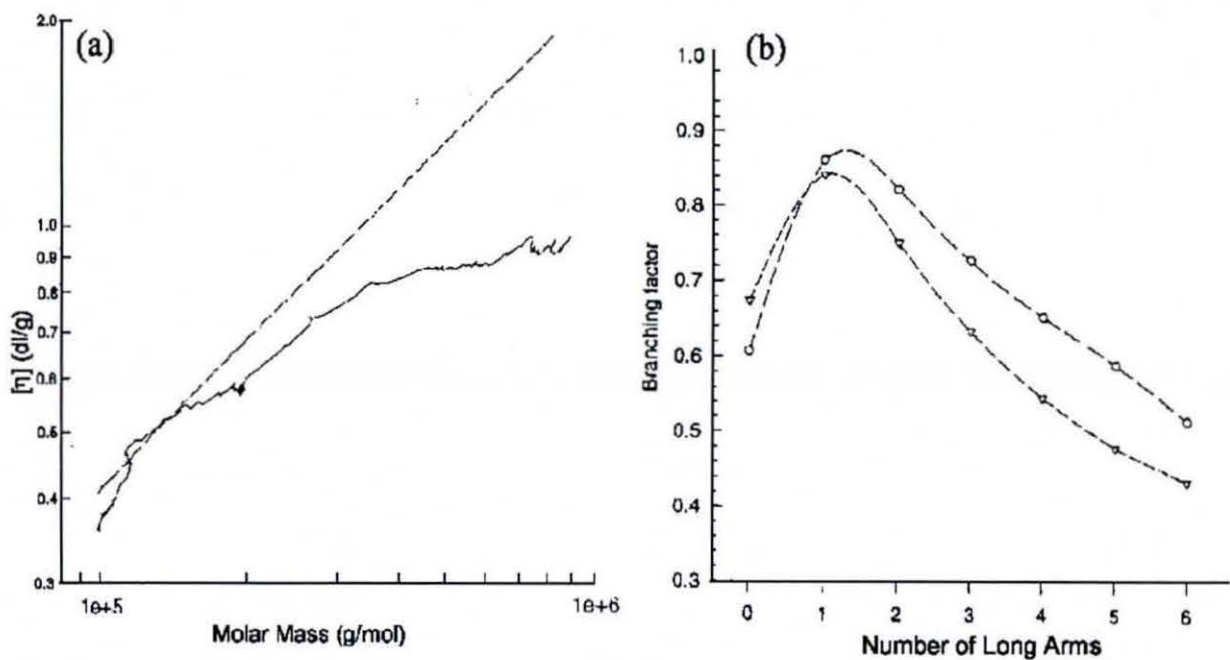


Figure 2-6 Asymmetric 6-arm star with 50:50 short:long arms (a) the  $[\eta]$  vs molar mass plot (b) the influence of long arm number on  $g$  and  $g'$  ( $g'$ -open circles).

## 2.6.2 Comb Polymers and Graft Copolymers

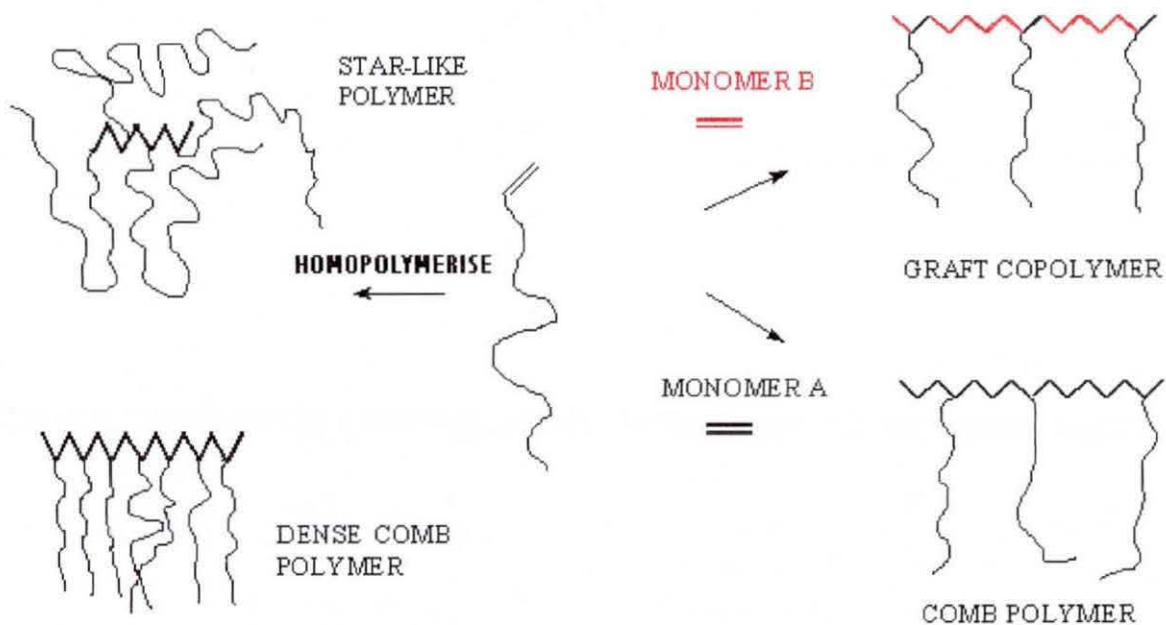
### 2.6.2.1 Preparation

Structures with branch points distributed statistically or uniformly along a backbone are classified as comb polymers. If the branch chains are of a different composition from the backbone, the structure is termed a graft copolymer. Three strategies are presented for the preparation of comb polymers and graft copolymers. These are termed ‘grafting-through’, ‘grafting-onto’ and ‘grafting-from’ techniques.

Macromonomers can be utilised to prepare both graft copolymers and comb polymers by a ‘grafting-through’ strategy (Scheme 2-2). A macromonomer is a polymer or an oligomer with polymerisable functionality as an end group. The polymerisation of a macromonomer with a conventional monomer yields a graft copolymer or comb polymer, depending on whether the monomer is of the same composition as the macromonomer.<sup>77</sup> Macromonomers can be homopolymerised to produce a poly(macromonomer). The structure of this poly(macromonomer) is dependent on steric factors resulting from the macromonomer chain length and the backbone chain length. One can envisage a star-type structure if the backbone chain is small relative to the branch chain length and a dense comb-shaped or brush-like polymer if the backbone is large relative to the branch chain. Ito et al.<sup>78</sup> studied the solution properties of a regular comb polymer prepared by the polymerisation of a PEO macromonomer.

Radical and living polymerisation can be utilised to prepare macromonomers. The advantage of using living polymerisation (anionic and cationic) to prepare the macromonomer is accurate control of the branch chain length. The treatment of hydroxy-ended PMMA with methacryloyl chloride or isocyanatoethyl methacrylate yields a PMMA macromonomer, when polymerised with MMA results in well-defined branched polymers containing nearly monodisperse branch chains of controlled molar mass.<sup>79,80</sup> Radke et al.<sup>81</sup> utilised pre-formed  $\omega$ -methacryloyl-PMMA macromonomer in a radical polymerisation with MMA to produce a well-defined comb PMMA. Comb polymers have been prepared by the radical polymerisation of macromonomers prepared by anionic polymerisation.<sup>26,82</sup> A comprehensive review exploring the design and characterisation of branched polymers

prepared with macromonomers has been reported.<sup>46</sup> The synthetic procedures for the preparation of over 100 macromonomers have also been recently reviewed.<sup>83</sup>



**Scheme 2-2 The homopolymerisation and polymerisation of macromonomers in the presence of an additional monomer to yield comb polymers or graft copolymers.**

Branched polymers have been prepared by a radical copolymerisation of a chain transfer monomer with a conventional monomer. A chain transfer monomer is a monomer that is susceptible to a chain transfer reaction, such as vinyl benzenethiol or vinyl benzenebromide. These monomers have been copolymerised with styrene.<sup>84,85</sup> A chain transfer reaction to a monomer unit yields a species capable of monomer propagation with a polymerisable double bond at one end. Alternatively, propagation through the double bond produces a transfer site on the polymer chain that may participate in a chain transfer reaction, potentially leading to a branch chain. The theoretical treatment for these systems has been investigated.<sup>2,86</sup>

Comb polymers and graft copolymers can be prepared by the reaction of a macromonomer with a polymeric backbone bearing pendant functional groups (termed a 'grafting-onto' process). Comb PS has been prepared by the reaction of a chloromethylated PS backbone with an acid ended PS macromonomer.<sup>87</sup> The PS backbone and PS macromonomers were prepared by anionic polymerisation to produce well-defined

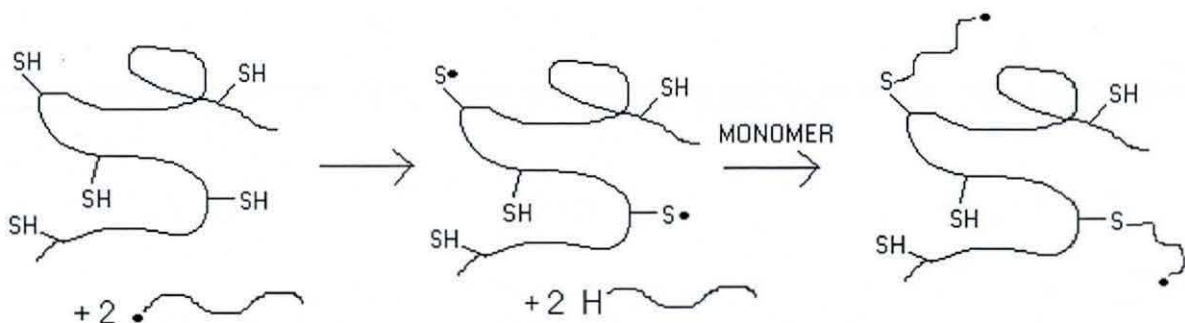
structures. Other backbone functionalities that have been incorporated onto a backbone include esters, anhydrides, nitriles and epoxides.

Comb polymers and graft copolymers can be prepared by the initiation of a polymer bearing pendant functional groups with a second monomer in a 'grafting-from' process to yield branch chains. The polymeric precursor can be envisaged as a macromolecular multi-functional initiator. Functional groups can be introduced on a polymer by organolithium compounds, such as 1,1-diphenylethylene derivatives,<sup>88,89</sup> which allow an excellent scheme for general functionalisation. The derivatives have been utilised for the preparation of phenol, amino, and carboxyl functionalised polymers.<sup>90</sup> Peroxide and hydroperoxide sites have been generated on EVA backbones through ozonolysis.<sup>91</sup> Subsequent radical polymerisation in the presence of styrene yielded a graft copolymer. Metalation grafting involves the generation of carbanionic initiator sites on the backbone of a polymer molecule, monomer is then added and anionic polymerisation proceeds to yield graft branch chains. The initiation sites can be obtained by a number of techniques that include metalation of the C-H bonds using an organometallic compound,<sup>92,93</sup> metal-halogen exchange reactions with carbon-halogen bonds using an organometallic compound<sup>94</sup> or an alkali metal and the addition of an organometallic compound to a reactive vinyl group on the polymer.<sup>95</sup> Radical sites can be generated on a polymer in the presence metal ions such as ceric (IV), vanadium (V) and manganese (III) to prepare branched polymers.<sup>96,97</sup>

Chain transfer reactions with a polymeric backbone can yield a branched polymer. Examples of polymers that undergo chain transfer are poly(vinyl acetate),<sup>98,99</sup> poly(n-butyl acrylate)<sup>100</sup> and poly(ethylene).<sup>101</sup> Incorporation of a dead polymer (susceptible to chain transfer) in a polymerisation with another monomer can yield a branched polymer with grafted branch chains. High density poly(ethylene-g-butyl acrylate) has been prepared using this method.<sup>102</sup> Graft copolymers have been prepared with poly(butadiene) in the presence of styrene, acrylate and methacrylate monomers activated by the radical initiators AIBN and benzoyl peroxide.<sup>103,104,105,106</sup> The branching in these species resembles a comb-type structure.

The transfer activity of a polymer can be enhanced by inclusion of functional groups susceptible to chain transfer reactions. Work by Fox et al.<sup>12,13</sup> dating back to the

late 1950's, investigated the preparation of graft copolymers in the presence of a pre-formed polymer containing pendant mercaptan groups. The pre-formed polymer was capable of acting as a multi-functional polymeric CTA (PCTA) in the presence of radicals (Scheme 2-3). Theoretical and experimental work investigated the effect of a PCTA on the polymerisation. A kinetic analysis was devised to predict the grafting efficiency (defined as the mass ratio of polymer attached to the backbone against the total mass of new polymer produced) and  $M_n$ . A high grafting efficiency was postulated to occur with a low initial rate of polymerisation and a high initial concentration of SH.



**Scheme 2-3** A representation of the effect of a PCTA in a radical polymerisation leading to the formation of branched polymer through chain transfer reactions.

A series of polymerisations was performed using styrene, ethyl acrylate, butyl methacrylate and lauryl methacrylate in the presence of a PCTA based on a MMA-co-GMA copolymer.<sup>13</sup> The nature of the monomer was varied in an attempt to obtain high grafting efficiencies. Of the graft systems reported, only PS systems were successfully separated and analysed through solvent extraction. The growing PS chains were assumed to terminate via bimolecular combination. The bulk polymerisation of styrene in the presence of PCTA produced a turbid solution before the polymerisation was complete. A grafting efficiency of 58% from the extraction results was obtained, which was lower than the predicted 99%. It was suspected that phase separation of the grafted PMMA caused the turbidity, which reduced the effective concentration of mercaptan groups in the system. This was suspected to lower the grafting efficiency and increase the concentration of PS linear polymer.

Barbosa et al.<sup>107</sup> reported a method for the preparation of branched PS using a PCTA based on a partially hydrolysed EVA copolymer modified with TGA. Styrene

polymerised in the presence of PCTA with a high concentration of SH yielded gel products under all conditions, even when extra solvent was added. Cross-linking was attributed to the high concentration of SH in the PCTA. Polymers prepared in the presence of a PCTA with a lower concentration of SH yielded products that were soluble in hot toluene. Evidence of grafting was obtained from gravimetric analysis, SEC and IR spectroscopy.

Research by the same group was extended to the polymerisation of MMA in the presence of a PCTA.<sup>11</sup> The branched polymer was isolated by solvent extraction. The effect of polymerisation time on the conversion to linear polymer and grafted polymer was studied. It was observed that linear polymer was produced up to a conversion of 50%. As the conversion exceeded 50% however, the proportion of grafted polymer gradually increased. At 80% conversion the grafted polymer and linear polymer were present at similar mass fractions. Above 80% conversion, grafted polymer was predominantly produced. The average molar mass of linear PMMA and grafted polymer decreased as the polymerisation proceeded. This was attributed to a low  $C_{tr}$  estimated at 0.1 as a consequence of the natural coiling of the EVA-SH chains in the toluene/MMA solution leading to poor SH accessibility. The poor SH accessibility produced an increase in the molar mass of grafted PMMA at the beginning of the polymerisation. As the extent of grafting increased, the backbone became more soluble in the polymerisation mixture, which increased the SH accessibility and improved grafting efficiency. SEC performed on branched PMMA indicated the presence of low molar mass polymer. This was attributed to an increased SH accessibility toward the end of the polymerisation that produced a flurry of transfer reactions.

A series of graft copolymers was prepared exploring experimental parameters. At a fixed concentration of AIBN and MMA, a high concentration of SH increased the overall MMA conversion and grafting efficiency. This resulted in a decrease in the molar mass of the graft copolymer. Samples prepared in the presence of PCTA with a higher concentration of SH had lower grafting efficiencies. SEC revealed that a uniform MMD of branched PMMA was obtained with samples prepared at a lower concentration of AIBN. At a higher concentration of AIBN the SEC profiles became bimodal.

### Preparation of PCTA

PCTA based on a MMA-co-GMA copolymer was prepared by Fox et al.<sup>12,13</sup> in refluxing toluene for 48 hours with an excess of TGA. The reaction produced two pendant thiol groups for each original epoxide. Barbosa et al.<sup>107</sup> used a similar method to prepare PCTA based on a partially hydrolysed EVA copolymer with isolated OH groups. An alternative preparation involved reaction of the copolymer with hydrogen sulphide in an autoclave for several days.<sup>13</sup> To avoid the problems of oxidation of mercaptan groups, methods to protect SH groups have been developed.<sup>108</sup> The disadvantage of utilising a protecting group is the extra step of deprotection. Several authors have demonstrated the rapid oxidation of mercaptans after deprotection to afford disulphide.<sup>109,110</sup>

### 2.6.2.2 Solution Behaviour

The solution behaviour of a comb polymer is determined by the molar mass of the branch chain, the number of branch chains and the molar mass of the backbone polymer to which the chains are attached. Evidence suggests that comb polymers behave like highly compact molecules with relatively low levels of intramolecular entanglements.<sup>80</sup> Regular comb polymers can exhibit solution behaviour similar to star polymer structures when the branch chains are long relative to a short backbone.<sup>111</sup>

Roovers investigated the effect of backbone functionality, backbone molar mass and branch chain molar mass on the solution behaviour of well-defined PS comb polymers.<sup>87</sup> In some cases, the intrinsic viscosity of the comb polymers was less than the backbone polymer itself. The M-H profiles are presented in Figure 2-7. The first number in the legend corresponds to the backbone molar mass (kg/mol) and the second number corresponds to the backbone functionality (the number of branch chains per molecule).

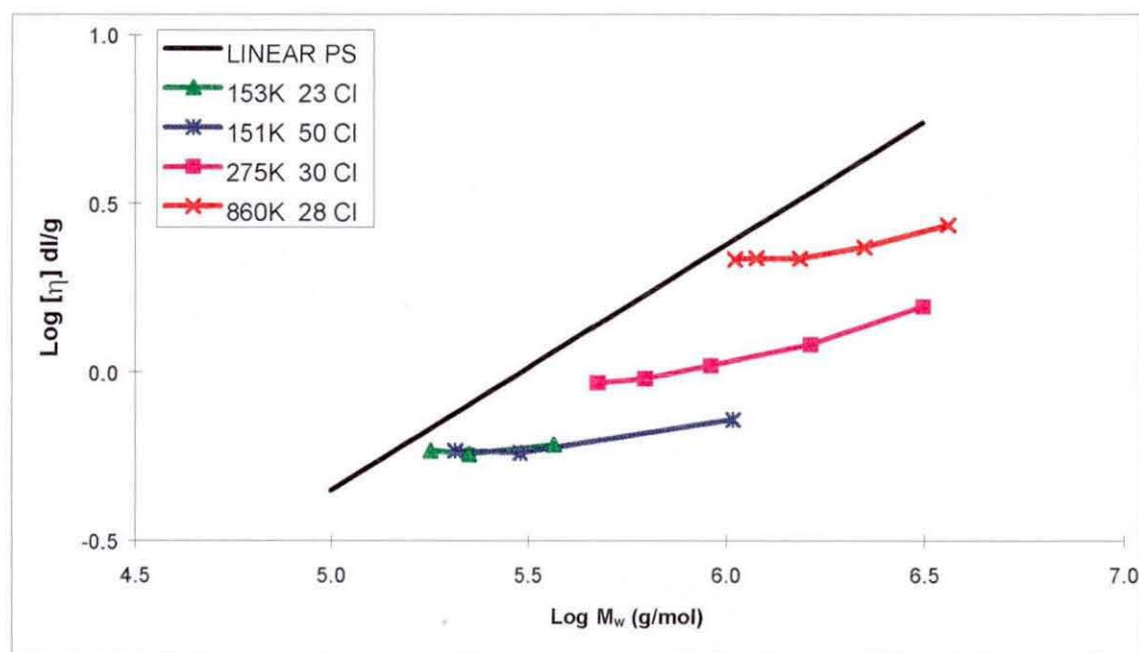


**Figure 2-7** Mark-Houwink plot for PS comb polymers prepared in the presence of backbone polymers of different molar mass and functionality (first term corresponds to backbone molar mass (kg/mol) and the second term is the branch chain number).

At a fixed backbone and branch chain molar mass (153k vs 151k series) an increase in backbone functionality increased the molar mass of the final polymer but the intrinsic viscosity remained the same. When the branch chain molar mass was increased, the backbone of higher functionality exhibited a lower intrinsic viscosity as a result of a more compact structure.

The influence of the backbone molar mass can be compared as the 275k and 860k series both have a similar number of branch chains per molecule. The molar mass of the branch chains was the same in each point of the series. The 275k series exhibited a lower intrinsic viscosity at a comparable molar mass. A comb polymer with a 275k backbone and 47k branch chains had a lower intrinsic viscosity than a comb polymer with a 860k backbone and 25.7k branch chains, of similar overall molar mass and branch number. This indicated that a polymer with a small backbone and long branch chains exhibited a lower intrinsic viscosity than a longer backbone with shorter branch chains of similar functionality.

When macromonomers are homopolymerised, they produce dense comb structures (brush-like polymers) because of the high number of branch chains. The solution behaviour of polymers prepared from the homopolymerisation of PS macromonomers have been reported by Tsukahara et al.<sup>77</sup> The authors studied the molar mass of the macromonomer (2,900 to 27,000 g/mol) and number per molecule (6 to 448). The M-H plot is included in Figure 2-8 (results obtained in toluene at 298K). The 2,900 series had 6 to 448 macromonomers per molecule. The slope up to 81 macromonomers per molecule remained relatively shallow, which indicated the molecule did not change in hydrodynamic size but increased in density. An increase in macromonomer number (81/171/448) changed the relationship between intrinsic viscosity and molar mass, probably attributed to an expansion of the molecular size due to steric crowding. A value of  $\alpha$  (near zero) for the 12,400 series suggested the molecules behaved like rigid spheres with a polymer chain segment density almost independent of the molar mass (6 to 33 branches). As the macromonomer number increased to 415 the rigid sphere behaviour diminished, probably due to steric crowding. The 27,000 series became denser as the macromonomer number increased but remained relatively unchanged in hydrodynamic size.

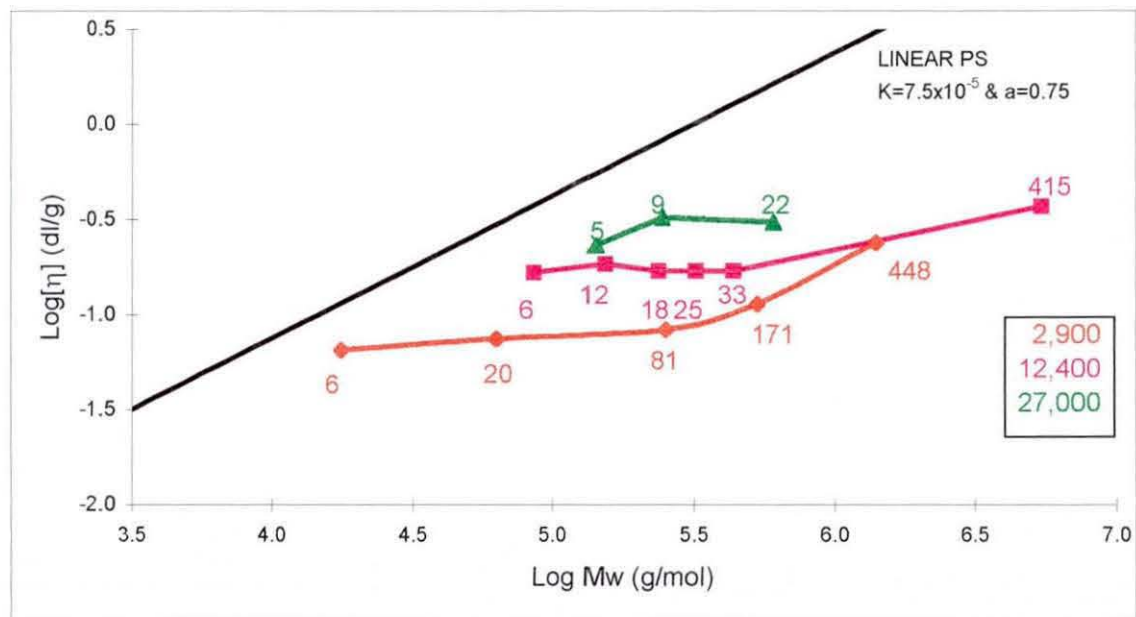


**Figure 2-8** The M-H plot for poly(macromonomers) with changes in molar mass and number per molecule. The number in the legend refers to the molar mass of the macromonomer in the series and the individual labels refer to the number of macromonomers per molecule.

Ito et al.<sup>78</sup> studied the solution properties of regular comb polymers with a PS main chain and poly(ethylene oxide) (PEO) side chains prepared by radical polymerisation using macromonomers. The branch chain length was varied by changing the number of repeat units,  $n$ , in the macromonomer ( $n = 3, 22, 44, 103$ ). The average number of branch chains per molecule was calculated from LS data.

The M-H plot for the comb polymers prepared with a different branch chain length are included in Figure 2-9. The M-H exponent  $\alpha$  is included in the brackets. The values of  $\alpha$  around 0.6 to 0.7 were observed for the comb polymers with short branch chains ( $n=3$  and  $n=22$ ). Each isolated polymer chain in solution appeared to behave like an expanded-coil linear polymer chain, but with a more contracted dimension because of the geometric requirement for a comb structure. The comb polymers with longer branch chains ( $n=44$  and  $n=103$ ) exhibited very low values of  $\alpha$  within the experimental molar mass range. The intrinsic viscosity results suggested a densely filled, very compact sphere-like structure.

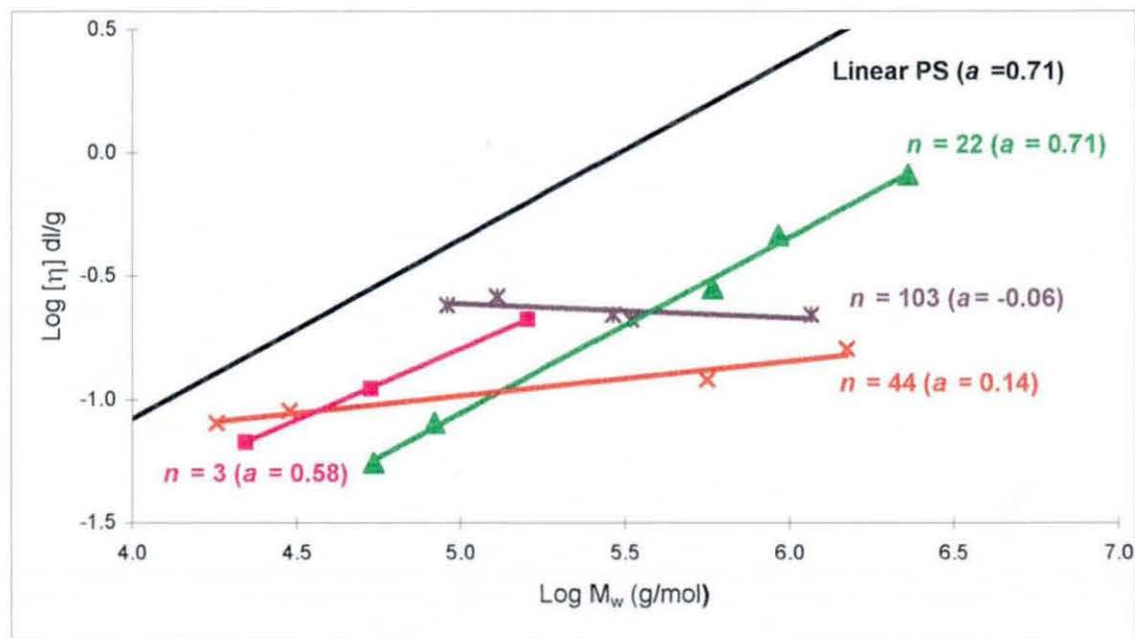


**Figure 2-9** The M-H plot for comb polymers prepared with PEO macromonomer. The term  $n$  corresponds to the number of units in the macromonomer. The M-H exponent  $a$  is given in brackets. Measured in THF at 298K.

## 2.6.3 Statistically Branched Polymers

### 2.6.3.1 Preparation

Statistically branched polymers have been prepared in the copolymerisation of a di-functional monomer and a regular monomer. Statistically branched PS has been prepared in the radical copolymerisation of styrene and 1,4-divinyl-2-3-5-6-tetrachlorobenzene.<sup>112</sup> The concentration of di-functional monomer must be minimised to avoid gel formation. Statistically branched PMMA has been prepared by the radical copolymerisation of MMA and ethylene glycol dimethacrylate.<sup>113</sup>

### 2.6.3.2 Solution Behaviour

The number of branch chains in a statistically branched polymer may be expected to increase as the molar mass increases.<sup>41</sup> The slope of the M-H plot for a statistically branched polymer deviates increasingly from linearity as the molar mass increases and yields a curve because branching is not evenly distributed across the MMD. The behaviour is primarily attributed to the probability that a high molar mass chain will have more branches than a low molar mass chain. The branching factor  $g'$  as a function of molar mass is unity at the lowest molar masses, reflecting the presence of predominantly linear polymer. As the molar mass increases the curve rapidly decreases reflecting an increase in branching at high molar mass.

The solution behaviour of statistically branched PS prepared in a copolymerisation with a di-functional monomer has been reported.<sup>112</sup> The effects of branching on the intrinsic viscosity were measured for fractions of copolymer. The M-H plot is included in Figure 2-10. The results indicate an increase in the deviation from linearity as the molar mass increases as expected with statistically branched polymers.

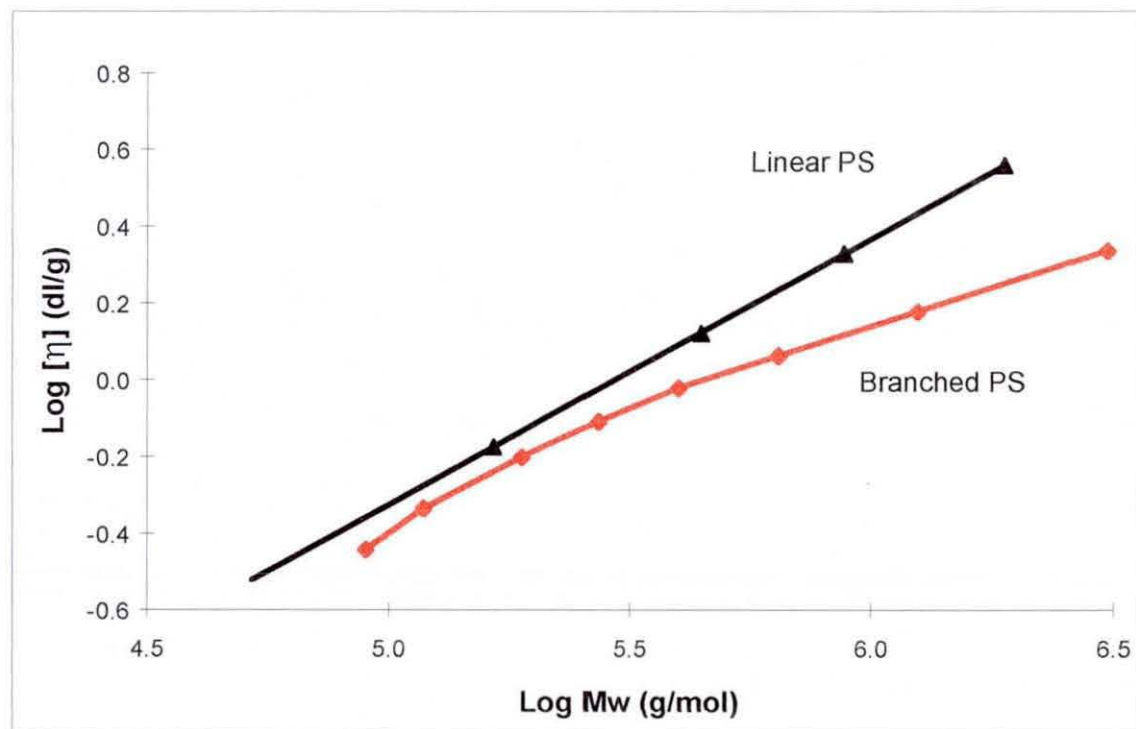


Figure 2-10 The M-H plot of a linear PS and branched PS fractions obtained in toluene at 303K.

## 2.6.4 Hyperbranched Polymers

### 2.6.4.1 Preparation

The synthesis of hyperbranched polymers can often be simplified compared with that of dendrimers. The most common synthetic route follows a one-pot procedure where  $A_xB$  monomers are condensed in the presence of a catalyst, typically an acid or transesterification reagent. A representation of the polymerisation of an  $A_2B$  monomer is included in Figure 2-11. Another method using a core molecule and an  $A_xB$  monomer has been utilised. To accomplish a satisfactory conversion the low molar mass condensation product formed during the polymerisation has to be removed. Recent reviews on the preparation of a wide variety of hyperbranched polymers have been reported.<sup>114,115</sup>

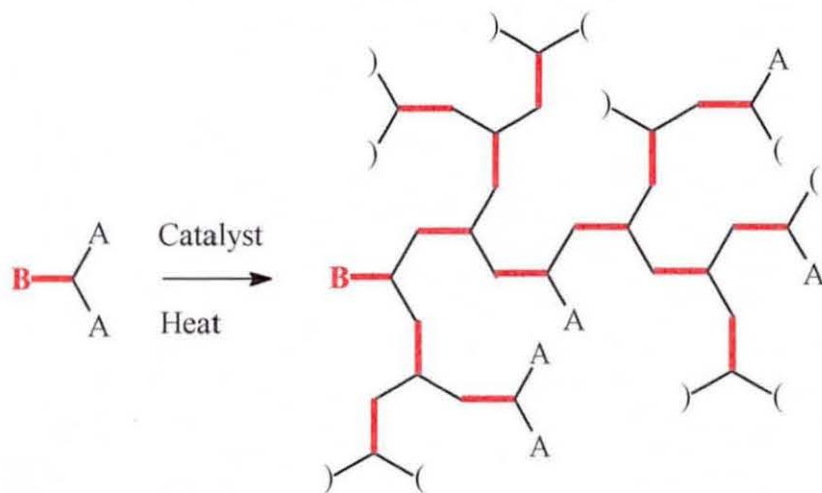


Figure 2-11 The representation of the polymerisation of a  $A_2B$  monomer.

Turner et al.<sup>116,117</sup> prepared hyperbranched aromatic polyesters derived from 3,5-bis(trimethylsiloxy)benzoyl chloride and 3,5-diacetoxybenzoic acid by melt condensation. Hyperbranched polyamides have been prepared by thermal polymerisation and direct polycondensation using condensing agents.<sup>118</sup>

Arborescent polymers have a dendritic structure but rely on successive grafting reactions using polymer chains rather than on small molecules as the building blocks.<sup>119</sup>

Gauthier et al.<sup>120</sup> grafted linear polystyryl anions onto a partially chloromethylated linear PS chain to yield a comb polymer (G=0). Repetition of the chloromethylation and anionic grafting procedures led to arborescent polymers with increased branching functionalities, identified as generations G=1, G=2 and so on. The functionalisation process resulted in a statistical distribution of grafting sites throughout the molecule. The high branching functionalities used (10-15 branches per backbone chain) produced a very rapid increase in molar mass of the polymers.

#### 2.6.4.2 Solution Behaviour

The solution behaviour of hyperbranched aromatic polyesters has been reported.<sup>116</sup> The polymers were characterised in THF at 298K. The M-H plot obtained by SEC and viscometry is included in Figure 2-12. The slope of the polyester polymer P2 deviated from the linear PS as the molar mass increased. The exponent  $\alpha$  was estimated at 0.35. The M-H plot passed through a minimum, which was shown to be a consequence of the ratio of the mass to volume for each successive generation.

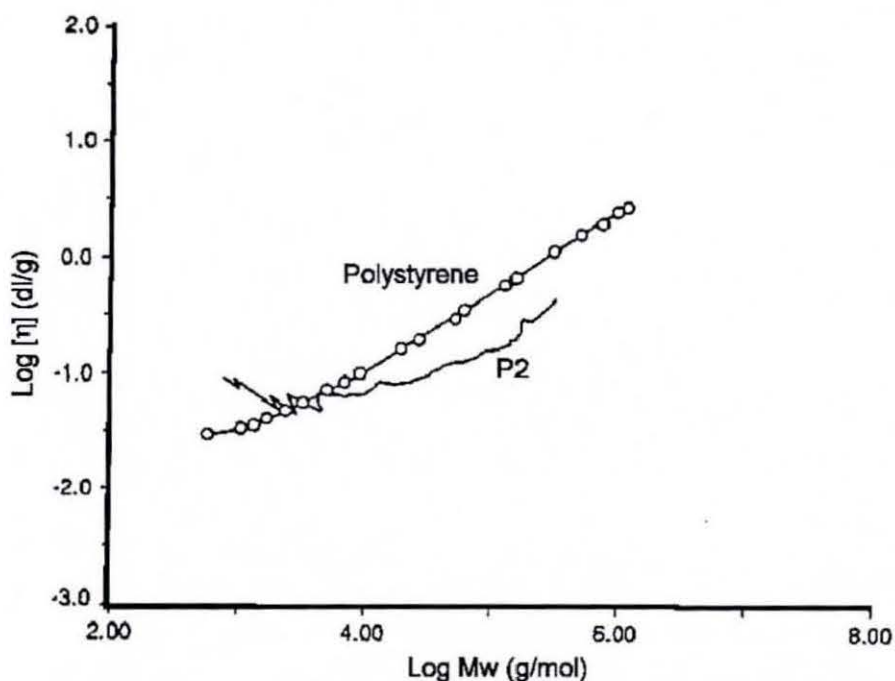
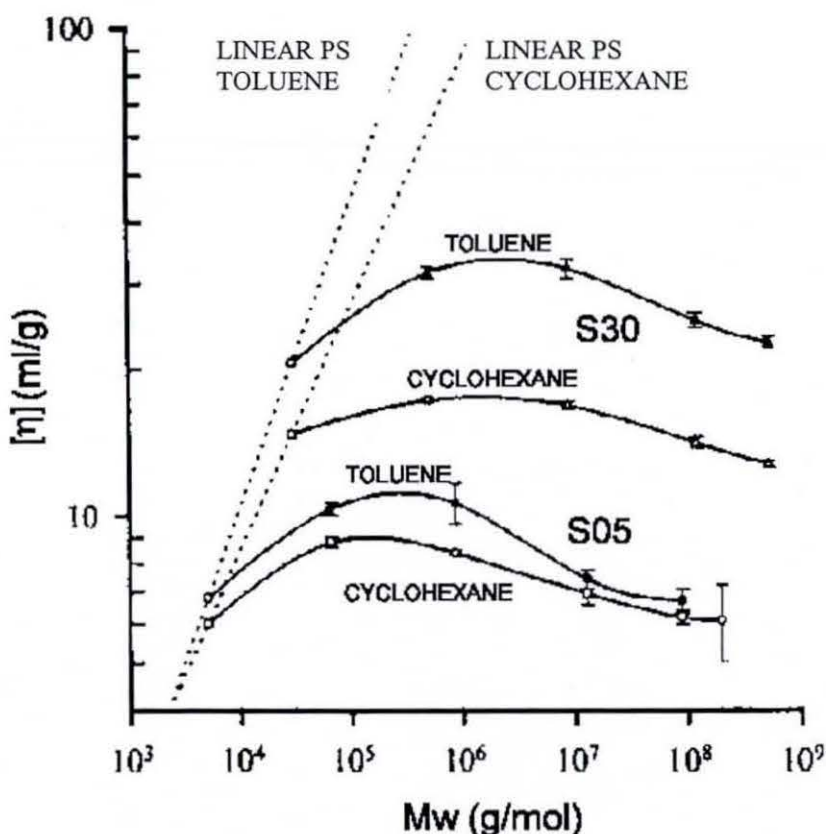


Figure 2-12 M-H plot for a linear PS and the hyperbranched polyester P2.

Arborescent PS molecules were shown to exhibit hard sphere behaviour in solution.<sup>120</sup> The successive grafting reactions produced a dense, rigid core with high segmental density, surrounded by a more diffuse, penetrable layer added in the last grafting reaction. Two series of polymers were prepared. Both series had a PS core polymer of 4,800 g/mol with a target branching functionality of 15 branches per backbone. The S05 series had branch chains of 5,000 g/mol and the S30 series had branch chains of 30,000 g/mol. The results are illustrated in Figure 2-13.



**Figure 2-13 Intrinsic viscosity vs molar mass plotted for two arborescent PS polymers S05 and S30 of successive generations in cyclohexane at 307.5K and toluene at 298K (Linear PS included).**

The left-most point for linear PS has a molar mass of 5 or 30 kg/mol and is followed by the corresponding arborescent polymers of generations G=0, G=1, etc. All curves were relatively flat, which suggested intrinsic viscosity was quite insensitive to the molar mass of the polymers. The intrinsic viscosity of samples in the upper generations was comparable to or even slightly lower than that of the linear polymers, even though their molar mass was up to 40,000 times larger than linear PS. This contrasted with the

behaviour of linear polymers with a slope of 0.50 in cyclohexane or 0.65 in toluene. Globular macromolecules should have an intrinsic viscosity independent of molar mass, as long as the ratio of mass to hydrodynamic volume (the hydrodynamic density) remains constant. Based on the results presented, arborescent polymers behaved like hard spheres. A more careful examination of the data revealed small variations in intrinsic viscosity within each series. The variations observed were clearly outside of the error limits on the individual measurements, and the trends were similar for the two series of polymers. Variations in intrinsic viscosity were relatively minor within each series of arborescent polymers. The size of the branches had a more noticeable effect. The dependence of intrinsic viscosity on solvent quality was also markedly different in the two series of arborescent polymers. Since intrinsic viscosity is inversely proportional to density, an increase in intrinsic viscosity for a polymer sample implies further expansion of the molecules. The change in the S05 series from cyclohexane to toluene was relatively small. The S30 polymers, on the other hand, exhibited considerable expansion from a poor solvent to a good solvent, since their structure was much less crowded and rigid than the S05 polymers.

### 3 EXPERIMENTAL

#### 3.1 List of Chemicals with Abbreviations

Acetone supplied by Carless Solvents - SLR grade.

$\alpha,\alpha'$ -Azobis(isobutyronitrile) (AIBN) supplied by Fluka, recrystallised twice from methanol.

Benzyl Bromide (BzBr) supplied by Aldrich - 99+ %.

Benzyl Chloride (BzBr) supplied by Aldrich - 99+ %.

Benzyl Methacrylate (BzMA) supplied by Aldrich, containing hydroquinone monomethyl ether as stabiliser – 98+ %.

Benzyl Thioglycolic Acid (BzTGA) supplied by Aldrich – 99+ %.

Butan-2-one (MEK) supplied by Aldrich – 99+ %.

Butyl Acetate (BuAc) supplied by Aldrich – 99+ %.

Chloroform (CDCl<sub>3</sub>) supplied by Fischer – GPC grade.

Chloroform-d (CDCl<sub>3</sub>) supplied by Aldrich with 1% v/v tetramethyl silane (TMS) - 99.8 atom %.

Dichloromethane (DCM) supplied by Carless solvents - SLR grade.

Dodecyl Mercaptan (DDM) supplied by Aldrich.

Ethyl Acetate (EtAc) supplied by Carless Solvents - SLR grade.

n-Hexane supplied by Fisher - SLR Grade.

2-Hydroxyethyl Methacrylate (HEMA) supplied by Aldrich, containing hydroquinone monomethyl ether as stabiliser – 97 %.

Inhibitor Remover Column (IRC) Packing supplied by Aldrich (for removal of hydroquinone stabiliser in MMA, BzMA and HEMA monomers).

Methanol (MeOH) supplied by Carless Solvents - SLR grade.

Methyl Methacrylate (MMA) supplied by Aldrich, containing hydroquinone monomethyl ether as stabiliser – 99 %.

Mono-ethyl Hydroquinone (MEHQ) supplied by Aldrich.

para-Toluene Sulphonic Acid Hydrate (p-TSA) supplied by Aldrich, and dried in an oven before use to remove water – 99 %.

Pentaerythritol Tetrakis(3-mercaptopropionate) (PETM) supplied by Aldrich.

PMMA Standards for SEC calibration supplied by Polymer Laboratories Ltd.

Thioglycolic Acid (TGA) supplied by Aldrich – 97 %.

Tetrahydrofuran (THF) supplied by Fisher Scientific UK - stabilised GPC grade.

Toluene supplied by Carless Solvents - SLR grade.

Triethylamine supplied by Aldrich, and dried over sodium wire before use - 99+ %.

Chemicals were used as supplied unless stated. The inhibitor was removed from monomers.

### **3.2 Monomer Destabilisation and Storage**

Monomers were destabilised using a column packed with inhibitor remover. A 30cm column was packed with inhibitor remover to a depth of about 10cm with a small quantity of glass wool in the bottom to prevent the particulate remover escaping. The monomer was collected in a conical flask and stored at 253K before use. The spent column packing was washed with acetone and allowed to dry in a fume cupboard before disposal.

### **3.3 Development and Preparation of PCTA**

#### **3.3.1 Synthesis of MMA**

##### **3.3.1.1 Absence of CTA**

Destabilised MMA and ethyl acetate were added to a three-neck round-bottomed flask equipped with a condenser and dry nitrogen flow. The solution was stirred with a magnetic flea whilst dry nitrogen was bubbled through the solution for 15 minutes to remove oxygen. The flow rate was reduced to a slow purge before addition of the initiator and maintained throughout the polymerisation. A solution of AIBN in ethyl acetate was added to the flask. The flask was heated for 1 hour at 353K in a thermostated oil bath.

The product was isolated by addition to a five-fold excess of distilled water. The polymer was allowed to precipitate with stirring. The precipitated polymer was isolated and dissolved in hot acetone. The solution was precipitated in water by dropwise addition. The particulate polymer was filtered and then dried in a vacuum oven at 323K before weighing. Characterisation of the polymers were by SEC.

##### **3.3.1.2 Presence of CTA**

Polymers prepared in the presence of DDM were synthesised and purified as in Section 3.3.1.1 except DDM was added to the monomer and solvent before initiation.

### **3.3.2 Synthesis of MMA-co-HEMA Copolymers**

Destabilised MMA and HEMA were added to a three-neck round-bottomed flask equipped with a condenser and dry nitrogen flow. Ethyl acetate was added to the flask. DDM was added if a reduction in the final molar mass was required. The solution was stirred with a magnetic flea whilst dry nitrogen was bubbled through the solution for 15 minutes to remove oxygen. The flow rate was reduced to a slow purge before addition of the initiator and maintained throughout the polymerisation. A solution of AIBN in ethyl acetate was added to the flask. The flask was heated for 1 hour at 353K in a thermostated oil bath.

The copolymer was isolated by addition to a five-fold excess of distilled water. The polymer was allowed to precipitate with stirring. Inclusion of a chain transfer agent increased the time for precipitation. The precipitated polymer was isolated and redissolved in hot acetone. The solution was precipitated in water by dropwise addition. The colourless, particulate polymer was filtered and then dried in a vacuum oven at 323K before weighing. Characterisation of the copolymers was by SEC and proton NMR spectroscopy.

### **3.3.3 Synthesis of BzMA-co-HEMA Copolymers**

BzMA-co-HEMA copolymers were prepared as in Section 3.3.2 except BzMA was substituted for MMA. The precipitated copolymers were very tacky, especially the low molar mass copolymers, and tended to adhere to the vessels. Characterisation of the copolymers was by SEC and proton NMR spectroscopy.

### 3.3.4 Functionalisation of Copolymers

#### 3.3.4.1 Esterification Method Provided by ICI Acrylics

In a 500ml round bottomed flask with nitrogen supply and reflux condenser, butyl acetate (200 g) and HEMA-based copolymer (20 g) were added with stirring. When the copolymer had dissolved, p-TSA (0.59 g) and TGA (2.88 g) were added. The flask was heated at 413K for 6 hours under a nitrogen atmosphere, then allowed to cool before precipitation in hexane (~1200g). The product was isolated by filtration, then dissolved in acetone before precipitation in hexane.

#### 3.3.4.2 Developed Method for Esterification

A three-neck round-bottomed flask was equipped with a Dean-Stark apparatus and a nitrogen inlet. Toluene was added to the trap in the Dean-Stark apparatus and a condenser fitted.

In a typical esterification, toluene (120 g) and p-TSA (0.1 g,  $6.06 \times 10^{-4}$  mol) were added to the flask. A magnetic flea was added and the solution was heated to 353K in a thermostated oil bath to aid dissolution of the catalyst (and copolymer). Dry nitrogen was bubbled through the solution to remove any dissolved oxygen. Dry copolymer (10 g) was added and allowed to dissolve with stirring in the hot toluene. When the copolymer had dissolved the first aliquot of TGA was added. The number of aliquots was dependent on the functionality of the copolymer. For lower functional copolymers 2 aliquots were used and for higher functional copolymers three aliquots were used. The aliquots were added after hour intervals. The total TGA concentration for low and high functional copolymers was 0.012 mol and 0.018 mol respectively. The solution was heated for 4 hours at 353K then allowed to cool under nitrogen.

The insoluble material produced in the esterification reaction was removed by filtration. The quantity of insoluble material was higher with higher functional copolymers (typically <5 % wt). The clear esterification solution was precipitated in a five-fold excess

of nitrogen-purged hexane. The filtrate was isolated and dissolved in acetone and re-precipitated in hexane dropwise. The product was a colourless powder. The PCTA was dried under vacuum in a nitrogen-purged oven at room temperature. The product was stored under nitrogen at 253K prior to use to minimise atmospheric oxidation and disulphide formation. Characterisation was by proton NMR spectroscopy. The PCTA had a distinctive odour, most noticeable when enclosed in a sample tube for a few days.

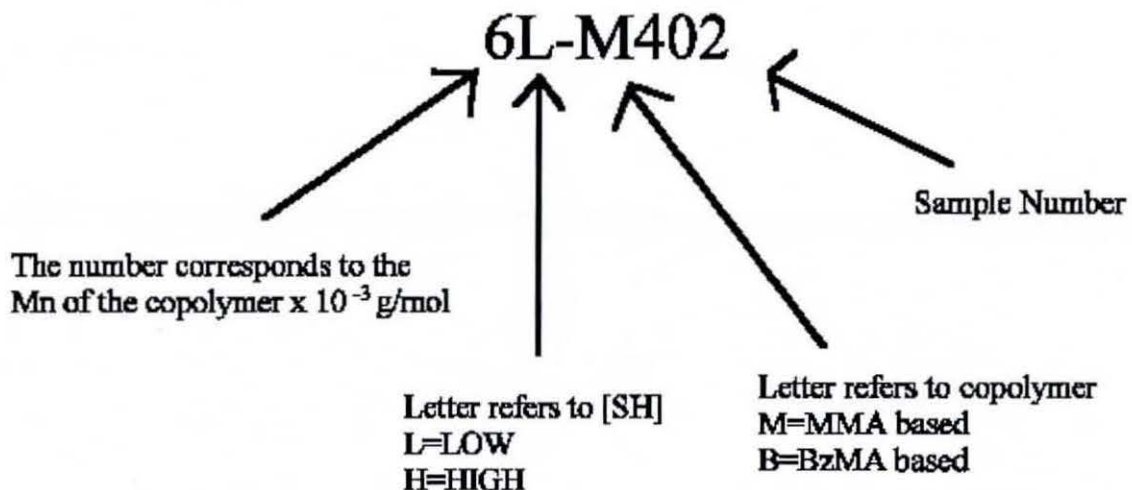
PCTA prepared from both MMA-co-HEMA and BzMA-co-HEMA copolymers were synthesised using the same method. PCTA was characterised by SEC before it was realised that it interacted with the columns. It was postulated that the PCTA may have reacted in the SEC system to form disulphide linked molecules.

### **3.3.5 Analysis of Residual SH Functionality**

The concentration of SH was determined by the reaction of a PCTA dissolved in THF with benzyl bromide (2 molar equivalent) and triethylamine (2 molar equivalent) under a nitrogen atmosphere. The solution was stirred for 16 hours at room temperature and then filtered through glass filter paper to remove the precipitated amine salt. The solution was precipitated in hexane, filtered, then washed with water before drying in a vacuum oven at 323K. The dry product was characterised by proton NMR spectroscopy.

### 3.4 Nomenclature of PCTA Samples

The code given to a PCTA contains information about the PCTA. The explanation of the code is given below.



## 3.5 Synthesis of Branched/Reference Polymers

### 3.5.1 Preparation with PETM

Destabilised MMA and toluene were added to a 25ml two-necked round-bottomed flask equipped with a condenser, nitrogen supply and magnetic flea. The required concentration of PETM was added. The flask was stirred and purged with nitrogen for 15 minutes before the addition of AIBN in toluene. The flask was placed in a thermostated oil bath at 333K or 353K for 24 hours. A nitrogen atmosphere was maintained throughout the polymerisation.

The polymer solution was precipitated in a five-fold excess of non-solvent (methanol or hexane) and isolated via filtration. The polymer was re-dissolved in acetone before re-precipitation in the non-solvent. The filtrate was dried in a vacuum oven at 293K before weighing. The polymer was characterised via SEC.

### 3.5.2 Preparation with PCTA

Destabilised MMA and toluene were added to a 25ml two-necked round bottomed flask equipped with a condenser, nitrogen supply and magnetic flea. PCTA was added and allowed to dissolve to yield a clear solution. The flask was stirred and purged with nitrogen for 15 minutes before the addition of AIBN in toluene. The flask was placed in a thermostated oil bath at 353K for 16 hours. A nitrogen atmosphere was maintained throughout the polymerisation. The mixture became turbid and substantially increased in viscosity within the first hour.

When the polymerisation was complete, acetone (10ml) was added to the flask to aid in the dissolution of the viscous polymer. The flask was stoppered and shaken. The polymer solution was precipitated in a ten-fold volume of hexane. The flask was washed with acetone and shaken before being added to the hexane. The polymer was isolated by filtration before being dissolved in acetone and then precipitated dropwise in hexane. The

recovered product was dried in a vacuum oven at 323K before weighing. The polymer was characterised by a combination of SEC techniques.

The total mass of the polymerisation system was fixed. A lower concentration of toluene was used in samples prepared with an increased concentration of PCTA.

### **3.5.3 Reference Samples**

Samples were prepared in the presence linear PMMA, substituted for PCTA of similar molar mass, under identical conditions for that specific sample. The preparation and purification were identical to Section 3.5.2.

### **3.5.4 Conversion Reactions with PCTA**

Conversion reactions were performed on PCTA systems. The samples were prepared as in Section 3.5.2. At the set polymerisation time the flask was removed from the oil bath and quenched in ice before a solution of MEHQ in acetone (10ml 5% wt) was added to the polymerisation mixture. The flask was shaken vigorously for 30 minutes before purification by the procedure outlined in Section 3.5.2.

### **3.5.5 Solubility Experiments**

PCTA and solvent were placed in a clean sample tube and stoppered. The tube was shaken gently and the progress of dissolution monitored visually. The tubes were left for 24 hours before a final judgement was made on solubility in the solvent system.

## 3.6 Characterisation Techniques

### 3.6.1 Nuclear Magnetic Resonance (NMR) Spectroscopy

Proton NMR spectroscopy was performed on a Bruker 250MHz spectrometer linked to a PC running WinNMR software for data analysis. Samples were dissolved in deuterated chloroform (16.6 mg/ml) containing TMS in a NMR tube and stoppered. Samples were scanned 128 times. A delay time of 1 second was incorporated between each scan so that the nuclei within the polymer molecules were allowed sufficient time to relax back to the ground state.

Integrals from a NMR spectrum were used to determine the composition of copolymers and their derivatives. The calculations are included in Section 4.

### 3.6.2 Size Exclusion Chromatography (SEC)

SEC was performed on linear polymers, copolymers and branched polymers. *SEC studies on PCTA indicated polymer adsorption with damage to the columns. It was decided not to run PCTA through the columns.* Three SEC techniques were utilised for polymer characterisation:

- SEC with RI – (characterisation of linear polymers / copolymers / branched polymers).
- SEC with UV/RI – (characterisation of BzMA-based copolymers / branched polymers).
- SEC with LS/VISC/RI – (characterisation of branched / reference polymers).

Each technique will be described below.

#### 3.6.2.1 SEC with RI Detector

##### 3.6.2.1.1 Apparatus

The apparatus and materials used to perform molar mass determination are detailed below.

- SEC grade stabilised THF solvent (degassed using an ultrasonic bath).
- Knauer HPLC pump 64 with a filter in the solvent reservoir.
- Rheodyne 7125 six-port injection valve with 50 µl injection loop.
- 5cm Mixed-gel guard column.
- 2 x 30cm Mixed-gel B, 10 µm particle size columns, packed with cross-linked PS beads (supplied by Polymer Laboratories Ltd.).
- Knauer RI detector.
- Data capture unit and PC running Calibre Software (Polymer Laboratories Ltd).
- PMMA Standards (Polymer Laboratories Ltd).

The apparatus was connected with the minimum quantity of narrow bore stainless steel tube. The apparatus was located on a bench at room temperature. The flow rate was set to 1.0 ml/min (checked on a regular basis using a flow rate meter connected in series with the pump).

The output from the detector was collected by a data capture unit (DCU) that was linked to a PC. Polymer Laboratories' Calibre software was used to handle and analyse the molar mass data.

### **3.6.2.1.2 Molar Mass Determination and Calibration**

The columns were calibrated with a set of 10 monodisperse PMMA standards. The calibration was carried out by injecting a series of PMMA solutions in THF (1 mg/ml) with 10 $\mu$ l of dry toluene added as reference. The solutions of standards were not filtered and were allowed to dissolve overnight before injection. The peak molar masses ( $M_p$ ) were inputted and the computer software generated a linear regression plot of  $\log M_p$  vs peak elution time. A typical calibration plot is illustrated in Figure 3-1.

Samples for characterisation were dissolved in THF (2 mg/ml) and allowed to equilibrate overnight. The solutions were filtered using Whatman microfibre glass filter paper and dry toluene was added as a flow marker reference before injection. The baseline was set manually for the detector profile before the software calculated the average molar masses. The values for  $M_n$ ,  $M_w$ ,  $M_p$  and polydispersity ( $M_w/M_n$ ) of the samples were determined.

#### PL PMMA Calibrants – Peak molar mass (g/mol)

1,577,000	28,900
660,000	13,000
364,900	5,720
128,000	2,400
69,000	1,020

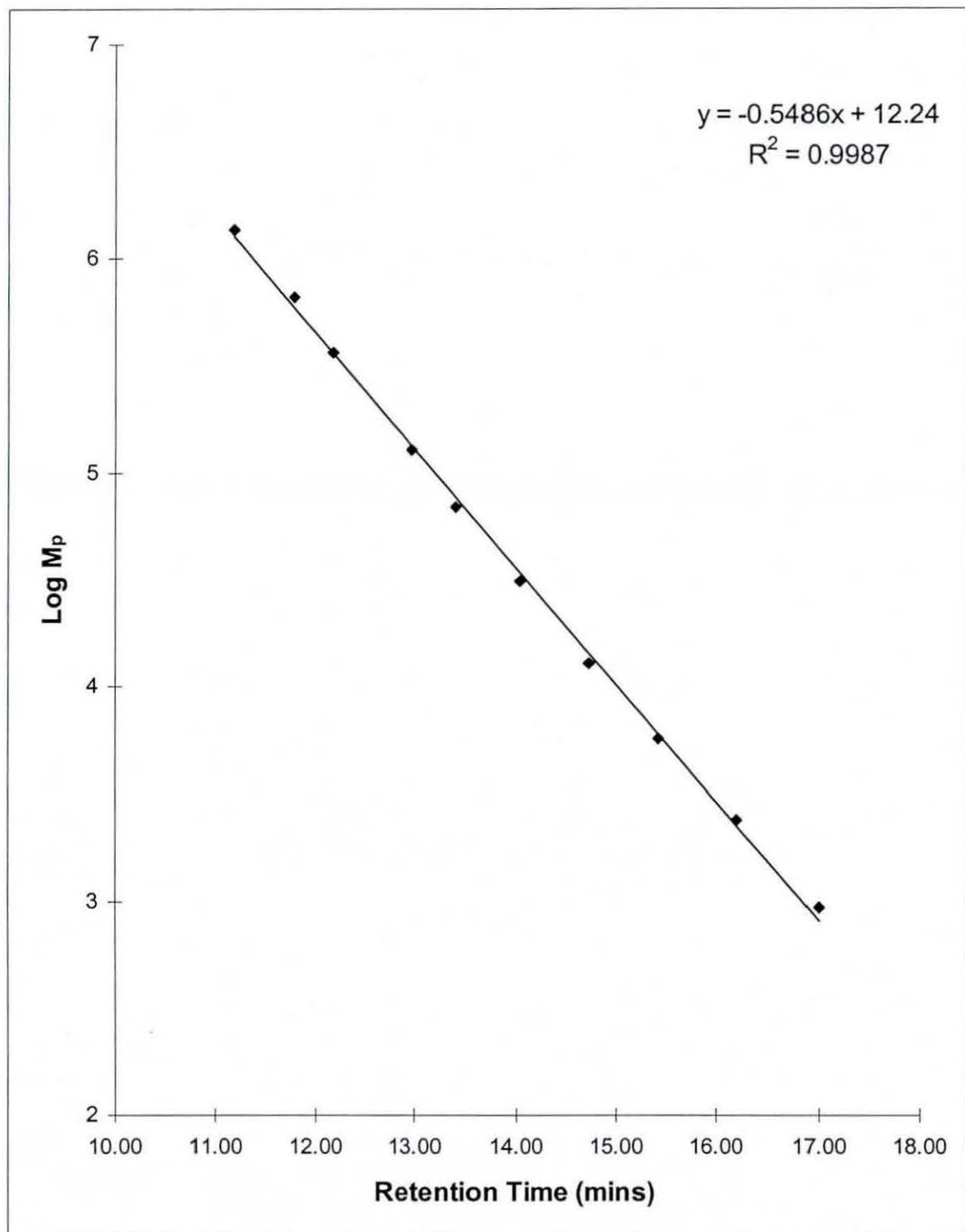


**Figure 3-1** A SEC calibration curve obtained for narrow polydispersity linear PMMA standards.

### 3.6.2.2 SEC with UV / RI Detectors

#### 3.6.2.2.1 Apparatus

The same equipment was used, as in Section 3.6.2.1.1, except a UV detector was included in series between the column output and the RI detector.

- Polymer Laboratories GBC-LC1200.

The excitation wavelength was set to 254nm, which corresponded to the  $\epsilon_{\max}$  for an aromatic chromophore.

#### 3.6.2.2.2 Characterisation

The average molar mass of a sample was not calculated when the system was configured for dual detectors because of software restrictions; hence molar mass calibration was not required. Samples for characterisation were dissolved in THF (2 mg/ml) and allowed to equilibrate overnight. The solutions were filtered using Whatman microfiber glass filter paper and dry toluene was added. Toluene was added as a flow marker reference so the inter-detector delay could be calculated between the detectors.

The baseline was set manually for both detector profiles before the software calculated the inter-detector delay from the toluene flow marker peak from each detector.

### 3.6.2.3 SEC with LS / RI / VISC Detectors (TDSEC)

#### 3.6.2.3.1 Apparatus

The apparatus located at ICI Acrylics was as follows:

- Solvent reservoir.
- Gilson Dilutor 401.
- Erma Optical Works degasser ERC 3310.
- Gilson 231 sample injector.
- Gynotek 300 pump.
- 1 x 60cm PSS linear SDVB 10  $\mu\text{m}$  bead column with a 0.5  $\mu\text{m}$  prefilter for the column.
- Viscotek RALLS (Right-angled laser light scatter) detector 670nm.
- Viscotek combined RI / Differential Capillary Viscometer detectors.

The detectors were configured as illustrated in Figure 3-2 with a split eluent stream to the RI and the viscosity detectors.

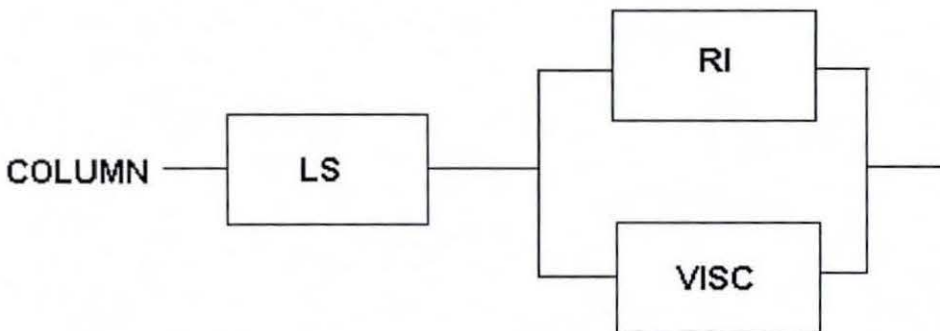


**Figure 3-2 Detector configuration for TDSEC.**

The system was a general-purpose set-up for acrylic polymers. The flow rate was set at 1.0 ml/min and checked regularly. THF was used in series one and chloroform in series two.

The output from the detectors was collected by a data capture unit (DCU) that was linked to a PC. Viscotek multi-detector software was used to handle and analyse the molar mass data.

### **3.6.2.3.2 Set-up**

A monodisperse PS standard was injected to calculate the offset for each detector and the dispersion factor. The peak dispersion for each detector was different. The peak at the lowest retention time was the LS detector, RI detector and VISC detector respectively. The peak retention time from each detector for the monodisperse standard was the after alignment.

The system parameters were set using the Viscotek software. The mass constant was calculated from knowledge of the sample concentration, the volume injected, the flow rate and the  $dn/dc$  value for the polymer-solvent system. These parameters were used to calculate the RI index area that was converted into a constant. The LS cell constant was determined using the same narrow standard. The  $dn/dc$  was inputted (0.062 MMA) together with the average molar mass for the standard. The response from the detector from these two factors led to an area that was used to calculate the constant. Threshold limits were set to collect the data against the noise from the detectors (front 15% and tail 25%). Finally, a well-characterised broad standard was injected and the molar mass data compared.

### **3.6.2.3.3 Sample Preparation.**

A sample of branched polymer was accurately weighed into a labelled glass tube with a screw top lid. The sample was diluted with solvent to a specific concentration (10-15 mg/ml) using the auto-sampler set in solvent dispense mode. The sample was allowed to dissolve for several hours before being transferred to vials.

## 4 RESULTS

### 4.1 Preparation of PMMA

MMA was polymerised under various conditions to obtain an understanding into the control of molar mass before any copolymerisation reactions were performed. The target value  $M_n$  was 10 kg/mol.

#### 4.1.1 Preparation without CTA

The concentration of MMA and AIBN were varied to control the molar mass. The results are illustrated in Table 4-1. A decrease in the initial concentration of MMA reduced the molar mass slightly, whilst an increase the concentration of AIBN decreased the molar mass. The target molar mass of 10 kg/mol was not obtained.

**Table 4-1 Data for PMMA prepared under different reaction conditions.**

Sample	[MMA] (% wt)	[AIBN] (% wt)	$M_w$ (g/mol)	$M_n$ (g/mol)	D	Conv. (%)
JHH92	30	0.30	61,600	30,500	2.02	28
JHH95	40	0.40	65,800	30,000	2.19	26
JHH94	20	0.40	37,600	17,700	2.11	17
JHH99	30	0.60	38,300	17,300	2.21	25
JHH100	40	0.80	43,500	19,900	2.17	35

## 4.1.2 Preparation with CTA

Mono-functional DDM was used to control the molar mass of the copolymer whilst maintaining a moderate conversion to polymer. DDM was substituted for TGA because it contained no pendant functionality, which was suspected to participate in the esterification step used to prepare PCTA. A series of PMMA polymers was prepared in the presence of DDM. The molar mass results are included in Table 4-2.

**Table 4-2 Data for PMMA polymers prepared in the presence of DDM.**

Sample	[MMA] (% wt)	[AIBN] (% wt)	[DDM] (% wt)	M <sub>w</sub> (g/mol)	M <sub>n</sub> (g/mol)	D	Conv (%)
JHH95	40	0.40	0.00	43,400	19,800	2.19	36
JHH96	40	0.40	0.04	33,600	14,500	2.32	38
JHH97	40	0.40	0.08	20,500	9,500	2.16	30
JHH98	40	0.40	0.16	12,700	5,600	2.26	34

Inclusion of DDM at a fixed concentration of MMA and AIBN reduced the molar mass of the final polymer, even when present in low concentration. The range of molar mass obtainable was increased with the utilisation of DDM in the polymerisation, which had important implications on the molar mass control of the polymeric backbone used to prepare a PCTA.

### 4.1.2.1 Calculation of Chain Transfer Constant

The chain transfer constant for a CTA in a radical polymerisation can be calculated from the molar mass data. In the polymerisation of MMA with ethyl acetate at 353K, C<sub>M</sub>, C<sub>I</sub>, C<sub>S</sub> and C<sub>P</sub> values are in the order of 10<sup>-4</sup> or less.<sup>10</sup> These values are negligible compared with the chain transfer constant of an added modifier. The chain transfer equation in the presence of a modifier can be simplified to:

$$\frac{1}{DP} = \frac{1}{DP_0} + C_X \frac{[X]}{[M]}$$

**Eqn 4-1**

where  $DP_0$  is the degree of polymerisation in the absence of a CTA. Data from Table 4-2 can be utilised to plot  $(1/ DP)$  vs  $([DDM] / [MMA])$ . The slope of this line will yield the chain transfer constant. Values of  $M_n$  were used to calculate results for DP. A plot for samples prepared with 40% wt MMA is included in Figure 4-1.

**Table 4-3 Data used to calculate the chain transfer constant of DDM.**

Sample	DP	1/DP	[DDM] (mmol)	[MMA] (mmol)	[DDM]/[MMA]
JHH95	198	0.0051	-	40	0.0000
JHH96	145	0.0069	0.23	40	0.0058
JHH97	95	0.0105	0.46	40	0.0115
JHH98	56	0.0179	0.92	40	0.0230

The value for  $C_{DDM}$  was calculated to be 0.57 at 353K. A value for  $C_{DDM}$  of 0.42 has been reported with MMA at 333K.<sup>121</sup> The experimental value appears slightly high compared to values quoted in the literature.

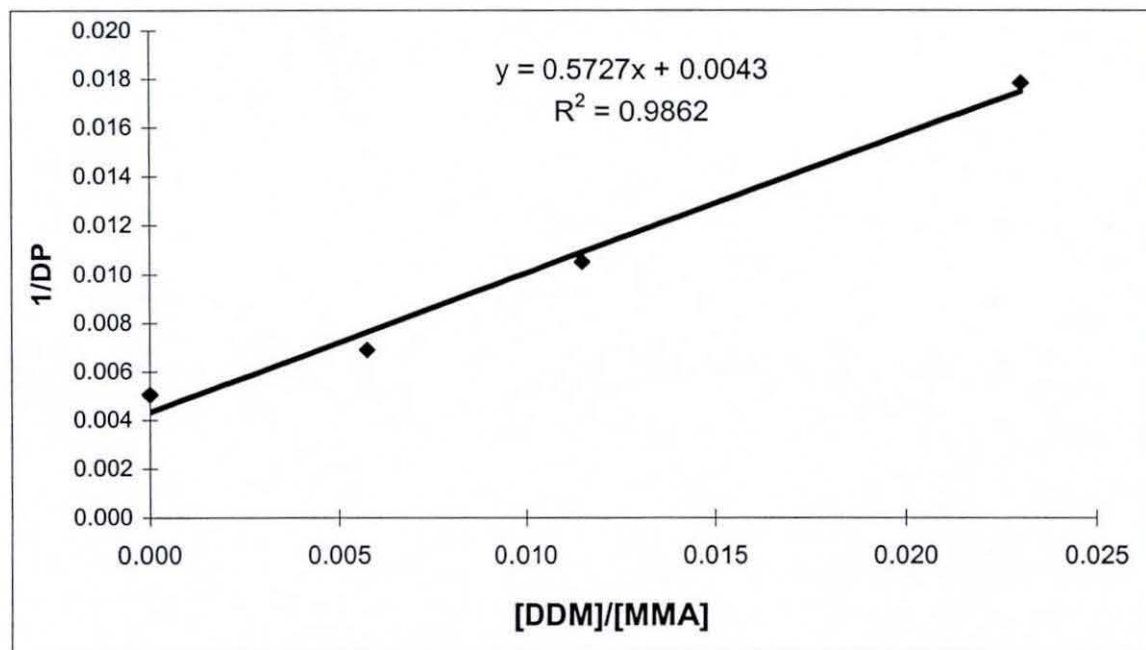


**Figure 4-1 A plot to determine the chain transfer constant of DDM in MMA at 353K.**

## 4.2 Statistical Copolymers

### 4.2.1 MMA-co-HEMA Copolymers

MMA-co-HEMA copolymers were prepared as the precursors to PCTA. The functionality on the backbone was controlled by the initial mole fraction of the comonomers in the feed. A series of copolymer samples prepared with a variation in the mole fractions of comonomers is illustrated in Table 4-4. The compositions were determined by proton NMR spectroscopy. The samples were prepared in the absence of a CTA with a total concentration of comonomers equal to 10% wt. The conversion to copolymer was less than 25%.

**Table 4-4 Summary of the monomer feed mole fractions and final mole copolymer composition.**

Sample	Feed Mole Fraction		Final Mole Fraction		Conv (%)
	MMA	HEMA	MMA	HEMA	
JHH49	0.96	0.04	0.97	0.03	19
JHH50	0.92	0.08	0.94	0.06	22
JHH51	0.88	0.12	0.91	0.09	19
JHH81	0.84	0.16	0.87	0.13	21
JHH82	0.80	0.20	0.84	0.16	24

[comonomer]=10% wt

An increase in the HEMA mole fraction in the comonomer feed increased the composition in the final copolymer, which increased the number of OH groups on the backbone.

MMA-co-HEMA copolymers were prepared in the molar mass range 5 - 20 kg/mol. The addition of DDM was necessary when the molar mass was required to be less than 20 kg/mol. The molar mass data for three copolymers prepared with a decreasing concentration of DDM at fixed monomer feed fractions is included in Table 4-5. The molar mass of the copolymer decreased as the concentration of DDM increased.

**Table 4-5 Effect of the concentration of DDM on molar mass.**

Sample	Mole Feed Fraction		[DDM] (% wt)	$M_w$ (g/mol)	$M_n$ (g/mol)	D	Conv (%)
	MMA	HEMA					
JHH208	0.94	0.06	1.60	9,500	5,600	1.70	43
JHH209	0.94	0.06	0.80	17,100	10,000	1.70	48
JHH222	0.94	0.06	0	38,600	19,800	1.95	46

[Comonomer]= 40% wt, [AIBN]= 0.6% wt

The SEC profiles of the MMA-co-HEMA copolymers are included in Figure 4-2. An increase in retention time of the copolymer was observed in the presence of DDM.

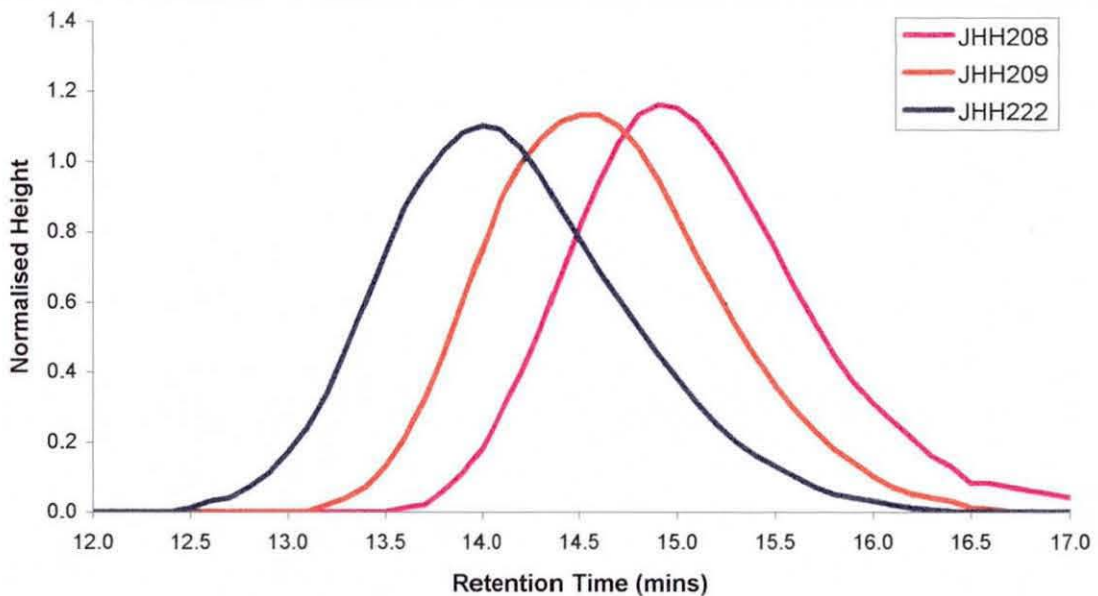


**Figure 4-2 Effect of [DDM] on molar mass in SEC of MMA-co-HEMA copolymers.**

A proton NMR spectrum of the MMA-co-HEMA copolymer JHH209 is shown in Figure 4-3. The assignments of the proton shifts are included in Table 4-6. The labelling of the protons in Structure 4-1 corresponds to the assignments in Figure 4-3. Below  $\delta=2.00$  ppm, the spectrum was dominated by shifts associated with the methacrylate backbone. The methylene protons in the HEMA unit were located at  $\delta=3.85$  ppm (shift **e**) and  $\delta=4.12$  ppm (shift **d**). Their environments are non-equivalent; hence they resonated in different fields of the spectrum. The shift at  $\delta=3.60$  ppm (shift **c**) was assigned to the methyl ester group in the MMA unit.

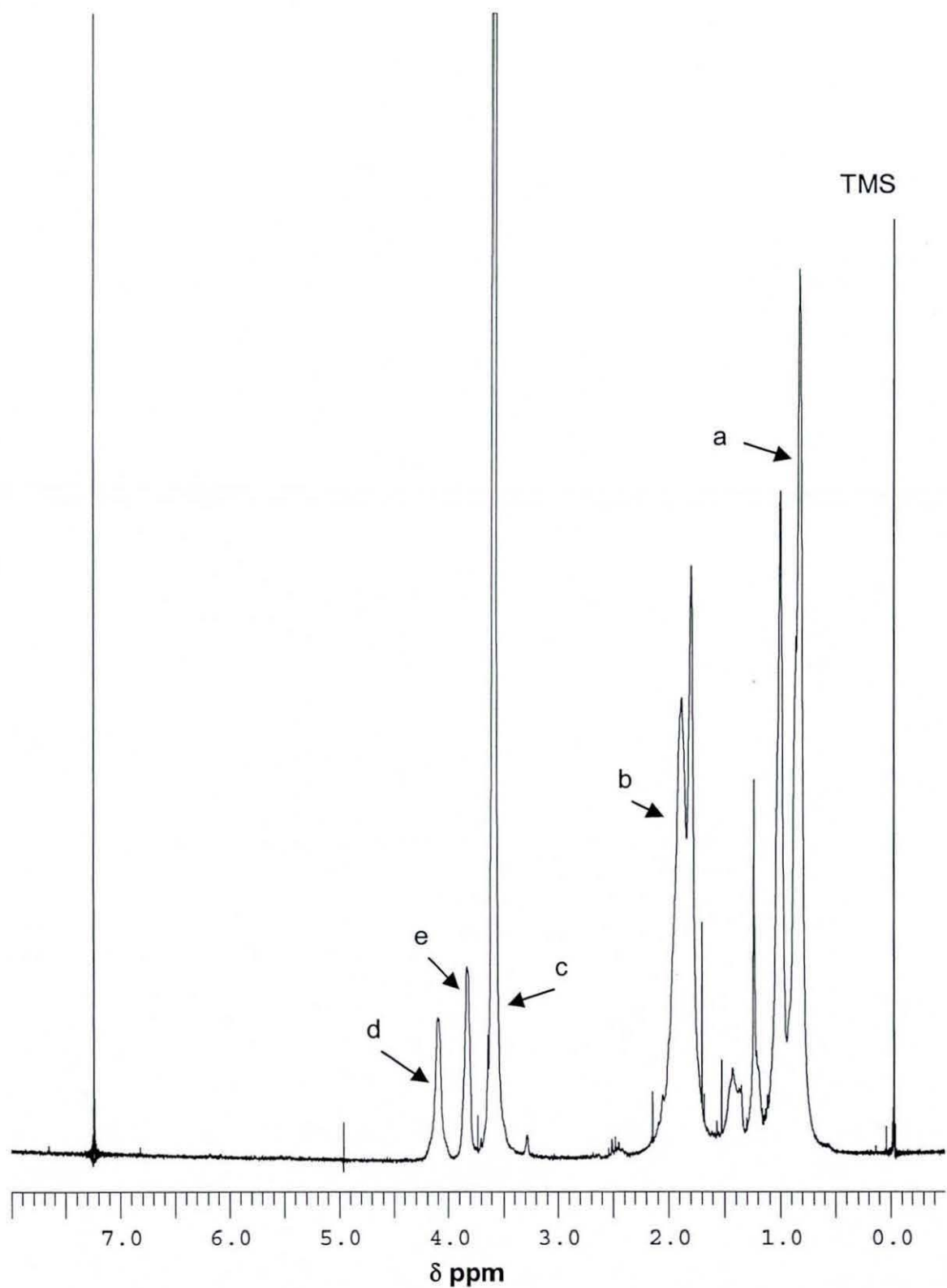


Figure 4-3 A proton NMR spectrum of the MMA-co-HEMA copolymer JHH209.

Structure 4-1 A representation of the structure of a MMA-co-HEMA copolymer.

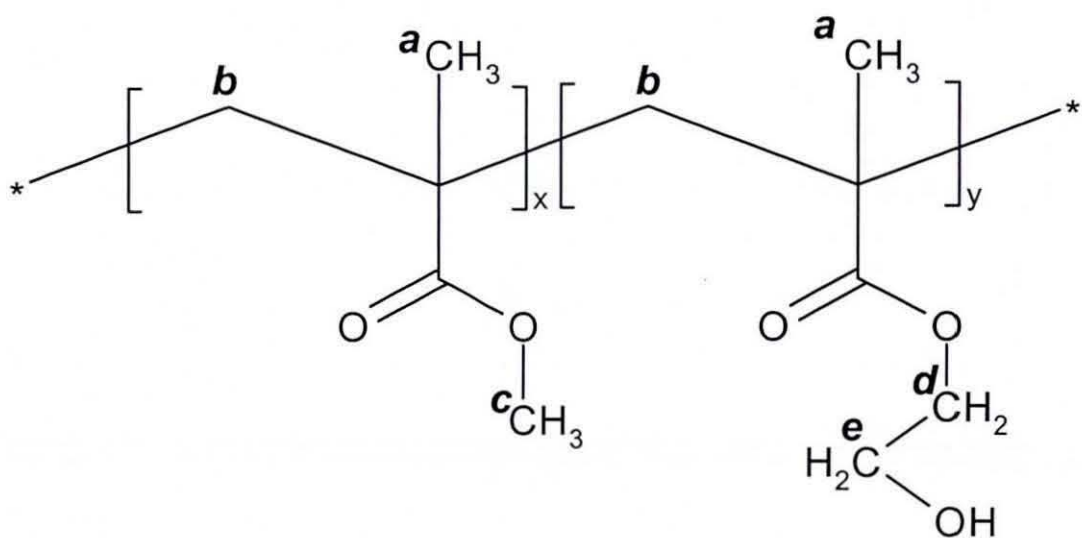


Table 4-6 The proton NMR shift assignments for a MMA-co-HEMA copolymer.

CHEMICAL SHIFT $\delta$ / ppm	ASSIGNMENT	CORRESPONDING LABEL
0.82 – 1.26	$\alpha$ -CH <sub>3</sub>	<i>a</i>
1.80 – 2.02	Backbone -CH <sub>2</sub>	<i>b</i>
3.60	MMA unit ester -CH <sub>3</sub>	<i>c</i>
3.85	HEMA unit -CH <sub>2</sub> (Adjacent -OH)	<i>e</i>
4.12	HEMA unit -CH <sub>2</sub> (Adjacent ether)	<i>d</i>

#### 4.2.1.1 Determination of HEMA Concentration and Functionality

The concentration of HEMA in a MMA-co-HEMA copolymer was calculated from the ratio of integrals of specific shifts in the proton NMR spectrum. The integral of the methyl group (shift **c**) on the MMA ester unit was compared against either methylene groups (shift **d** or **e**) on the HEMA ester unit. These groups had a non-equivalent number of protons and the integral for a single proton must be accounted for. The monomer units in the copolymer had different molar masses (MMA=100 g/mol and HEMA=130 g/mol).

$$[\text{HEMA}] = \frac{(H_d / 2) \times 130}{(H_c / 3) \times 100 + (H_d / 2) \times 130}$$

**Eqn 4-2**

The average number of OH groups per copolymer chain was calculated using the value of  $M_n$  of the copolymer determined from SEC.

$$\text{Average OH} = \frac{M_n}{(H_c / 3) \times 100 + (H_d / 2) \times 130}$$

**Eqn 4-3**

#### 4.2.1.2 Estimation of Reactivity Ratios

Kelen and Tudos developed a method to determine the monomer reactivity ratios in a copolymerisation.<sup>29</sup> The authors reviewed other methods to determine the monomer reactivity ratios. The method developed by the authors is outlined in Section 2.2.2.1/p23.

The experimental data obtained for MMA-co-HEMA copolymers (Table 4-4) was utilised to obtain the monomer reactivity ratios for MMA and HEMA at 353K. The results are plotted graphically in Figure 4-4 and the results from the calculations are included in Table 4-7. Thus, a plot of  $\sigma$  against  $\xi$  produced a straight, which was extrapolated to  $\xi = 0$  to give  $-r_2/\beta$  and extrapolated to  $\xi = 1$  to give  $r_1$  (both as intercepts). The equation obtained for the line of best fit ( $R^2=1$ ) was:

$$\sigma = 1.3149\xi - 0.0668$$

Eqn 4-4

Therefore, the values obtained for the monomer reactivity ratios are:

$$r_{MMA} = 1.31 \quad r_{HEMA} = 0.49$$

The value obtained for MMA suggested the MMA radical preferred to add to its own monomer rather than HEMA. The value obtained for HEMA suggested the HEMA radical preferred to add MMA rather than HEMA. The predicted copolymer structure from monomer reactivity theory indicated an alternating copolymer was produced. The method is only accurate when the conversion is lower. These values give a indication of the possible behaviour.

Monomer reactivity ratios for the copolymerisation of MMA and HEMA have been reported ( $r_{MMA}=0.192$  /  $r_{HEMA}=0.81$ <sup>28</sup> and  $r_{MMA}=0.75$  /  $r_{HEMA}=1.50$ <sup>122</sup>). The values reported were performed under different experimental conditions and used different methods to determine the monomer reactivity ratios.

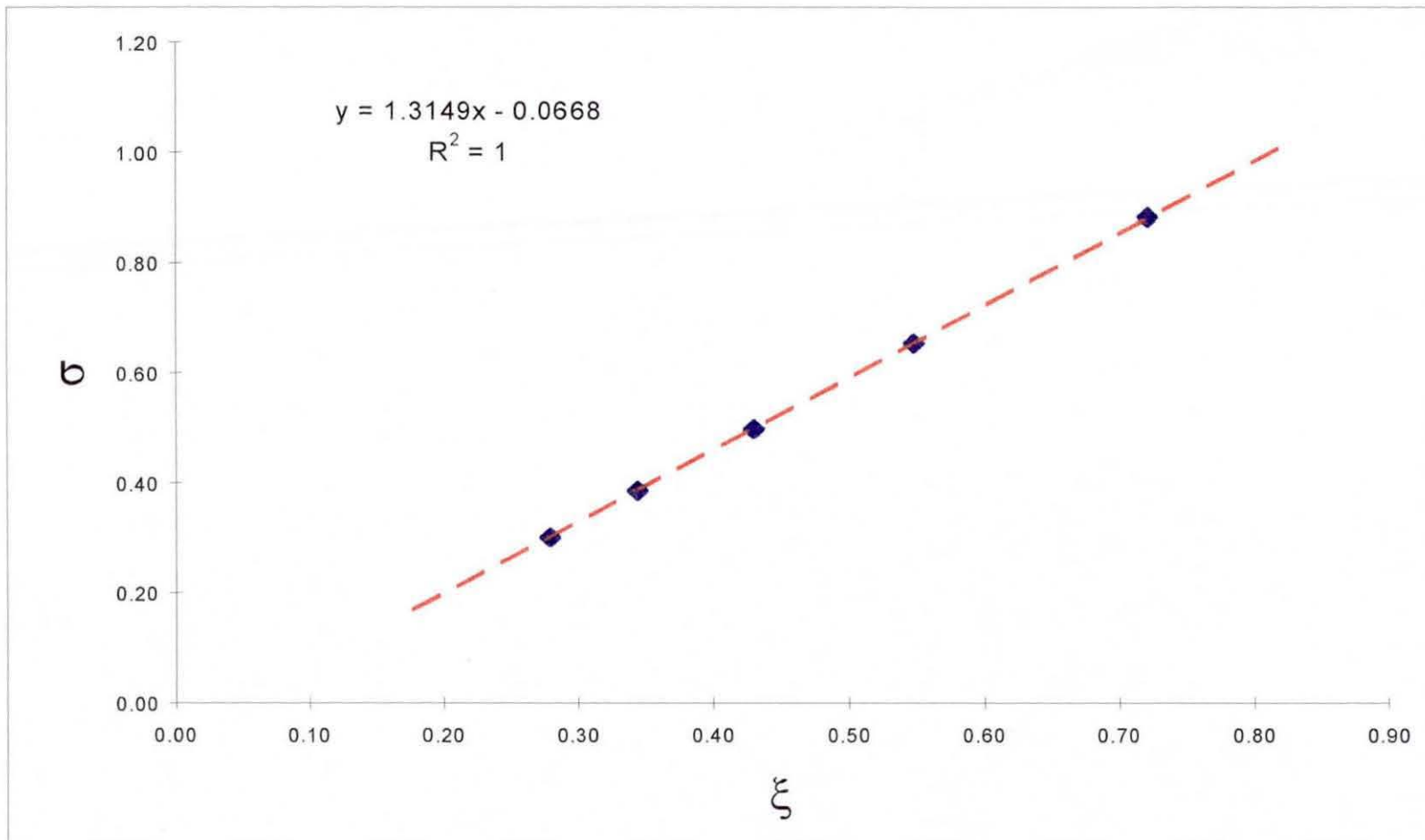


Figure 4-4 A plot to determine  $r_1$  and  $r_2$  using the Kelen-Tudos method.

**Table 4-7 Copolymer data and results from the calculations using the Kelen-Tudos method to determine  $r_1$  and  $r_2$ .**

Sample	M <sub>1</sub> MMA	M <sub>2</sub> HEMA	dM <sub>1</sub> MMA	dM <sub>2</sub> HEMA	x	y	G	F <sub>KT</sub>	σ	ξ
JHH49	0.96	0.04	0.97	0.03	24.70	31.20	23.91	19.55	0.88	0.72
JHH50	0.92	0.08	0.94	0.06	11.70	14.95	10.92	9.16	0.65	0.55
JHH51	0.88	0.12	0.91	0.09	7.37	9.53	6.59	5.69	0.50	0.43
JHH81	0.84	0.16	0.87	0.13	5.20	6.83	4.44	3.96	0.39	0.34
JHH82	0.80	0.20	0.84	0.16	3.90	5.20	3.15	2.93	0.30	0.28

$\beta = 7.56$  (from JHH82 and JHH49)

#### 4.2.2 BzMA-co-HEMA Copolymers

BzMA was utilised as an alternative backbone comonomer to MMA as it contained a UV chromophore. A chromophore in the PCTA allowed the PCTA in the branched polymer to be observed with SEC-UV. BzMA-co-HEMA copolymers were synthesised in the molar mass range 5 - 20 kg/mol. Table 4-8 contains molar mass data for two copolymers prepared in the presence of DDM at fixed monomer feed fractions. Inclusion of DDM decreased the molar mass significantly.

**Table 4-8 The effect of [DDM] on molar mass of BzMA-co-HEMA copolymers.**

Sample	Mole Fraction HEMA		[DDM] (%wt)	$M_w$ (g/mol)	$M_n$ (g/mol)	D
	Feed	Final				
JHH249	0.13	0.13	0	37,300	16,000	2.34
JHH288	0.13	0.12	4.00	9,600	5,200	1.85

[Comonomer]=40% wt

A chromatogram of the BzMA-co-HEMA copolymer JHH249 obtained by SEC-UV is included in Figure 4-5. When the interdetector delay had been adjusted, the retention times from both the UV and RI detectors corresponded, which suggested a uniform distribution of BzMA throughout the MMD.

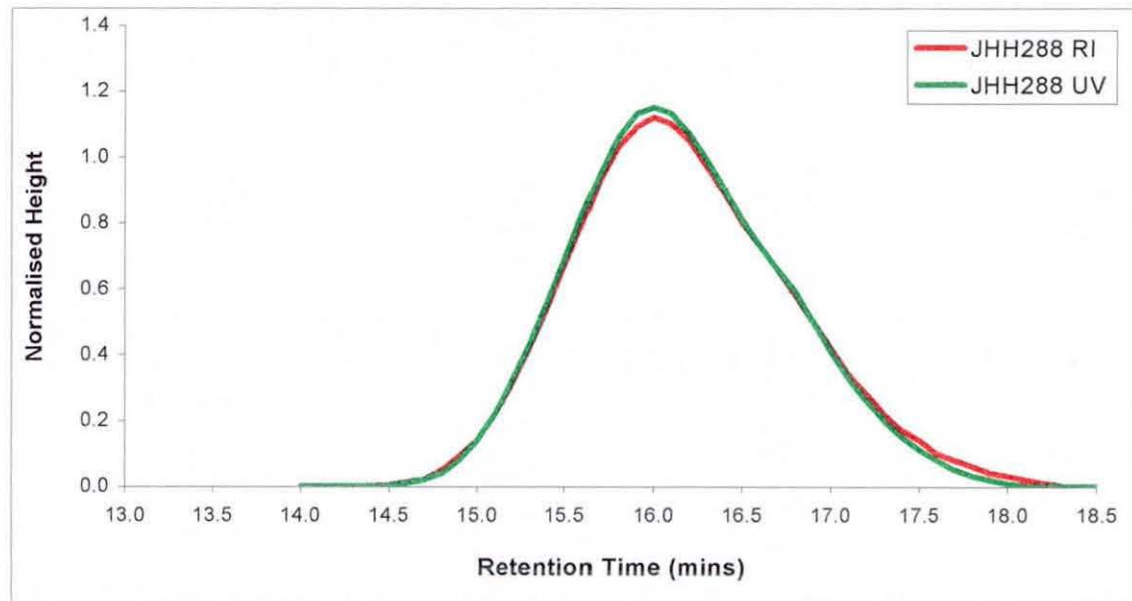


**Figure 4-5 A dual detector SEC profile of BzMA-co-HEMA copolymer JHH249.**

A proton NMR spectrum of the BzMA-co-HEMA copolymer JHH249 is shown in Figure 4-6. The assignments of proton shifts are included in Table 4-9 and correspond to those in Structure 4-2. The methacrylate backbone dominated the region below  $\delta=2.00$  ppm. The chemical shifts at  $\delta=3.75$  ppm (shift *t*) and  $\delta=4.05$  ppm (shift *s*) were assigned to methylene protons in the HEMA unit. The shift *f* at  $\delta=4.95$  ppm was assigned to the benzyl methylene. Chemical shifts above  $\delta=7.00$  ppm were assigned to the aromatic protons.

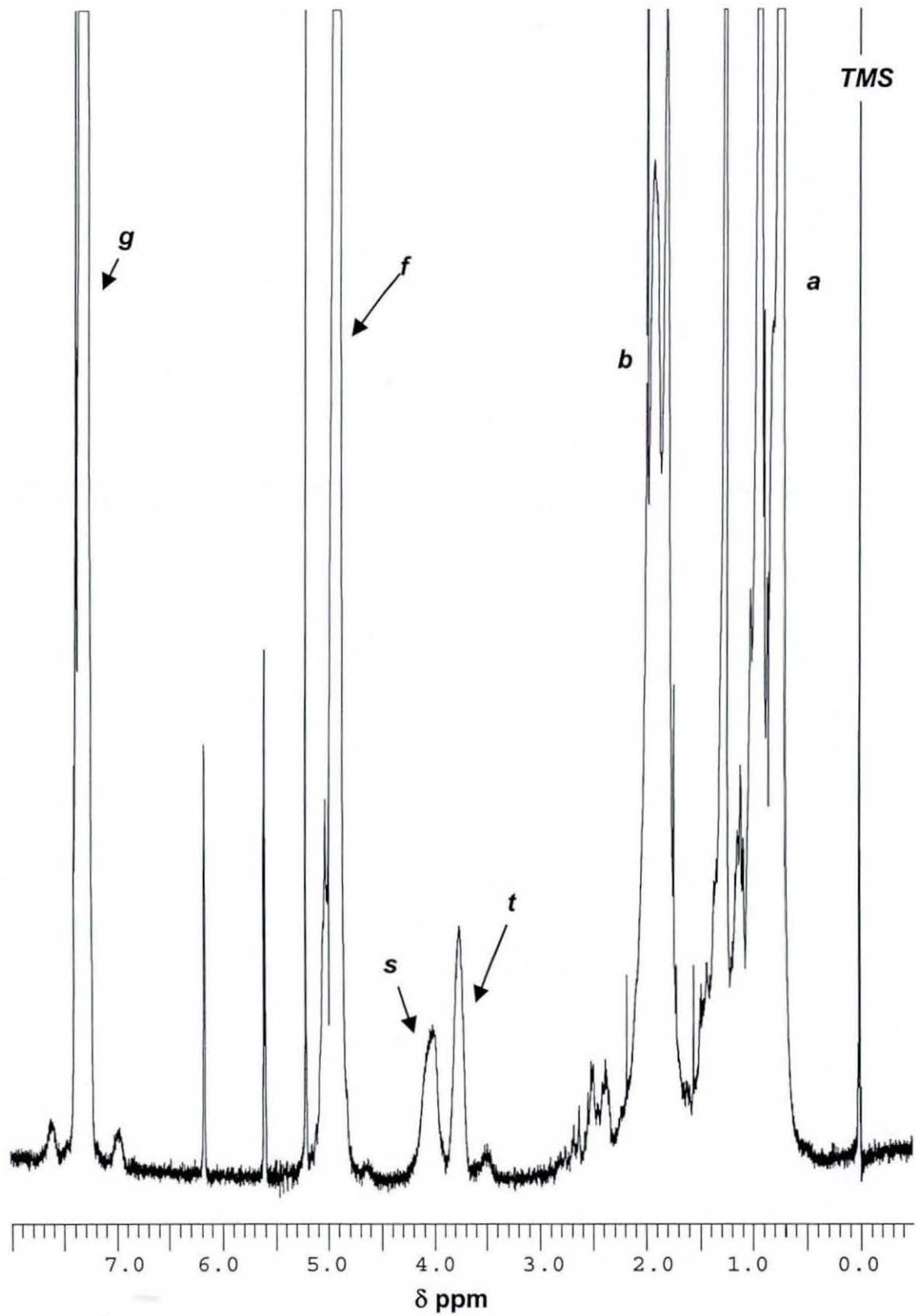


Figure 4-6 A proton NMR spectrum of the BzMA-co-HEMA copolymer JHH249.

Structure 4-2 A representation of a BzMA-co-HEMA copolymer structure.

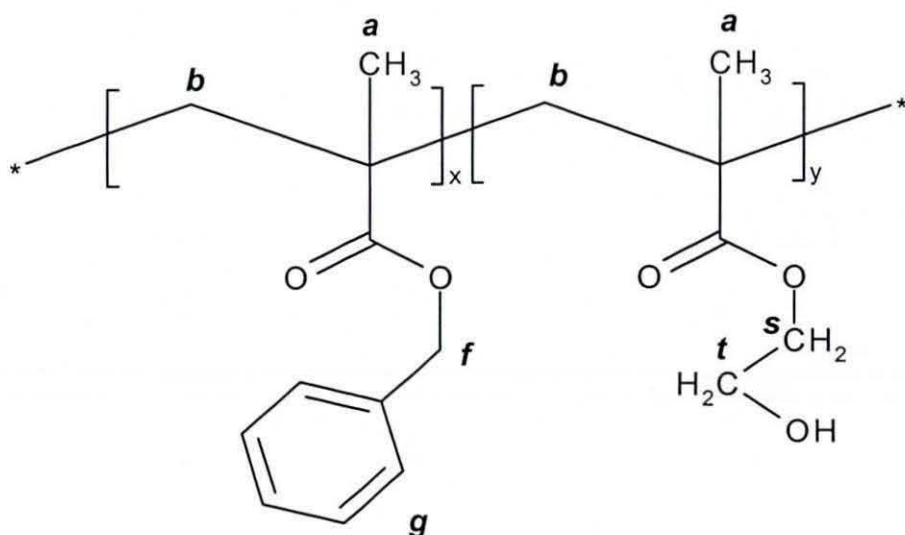


Table 4-9 The proton NMR shift assignments for a BzMA-co-HEMA copolymer.

CHEMICAL SHIFT $\delta$ / ppm	ASSIGNMENT	CORRESPONDING LABEL
0.82 – 1.26	$\alpha$ -CH <sub>3</sub>	<i>a</i>
1.80 – 2.02	Backbone -CH <sub>2</sub>	<i>b</i>
3.75	HEMA unit-CH <sub>2</sub> (Adjacent -OH)	<i>t</i>
4.05	HEMA unit-CH <sub>2</sub> (Adjacent ether)	<i>s</i>
4.95	BzMA unit-CH <sub>2</sub> (Benzyl)	<i>f</i>
7.27	BzMA Aromatic (5H)	<i>g</i>

#### 4.2.2.1 Determination of HEMA Concentration and Functionality

##### 4.2.2.1.1 Proton NMR Spectroscopy

The concentration of HEMA in a BzMA-co-HEMA copolymer was calculated from the ratio of integrals of specific shifts in a proton NMR spectrum. The integral of the benzyl methylene group (shift *f*) was compared against either HEMA methylene units (shift *s* or *t*). The integrals can be used directly as both shifts had equivalent proton numbers. The monomer units in the copolymer had different molar masses which must be accounted for (BzMA=176 g/mol and HEMA=130 g/mol).

$$[\text{HEMA}] = \frac{H_S \times 130}{(H_f \times 176) + (H_S \times 130)}$$

**Eqn 4-5**

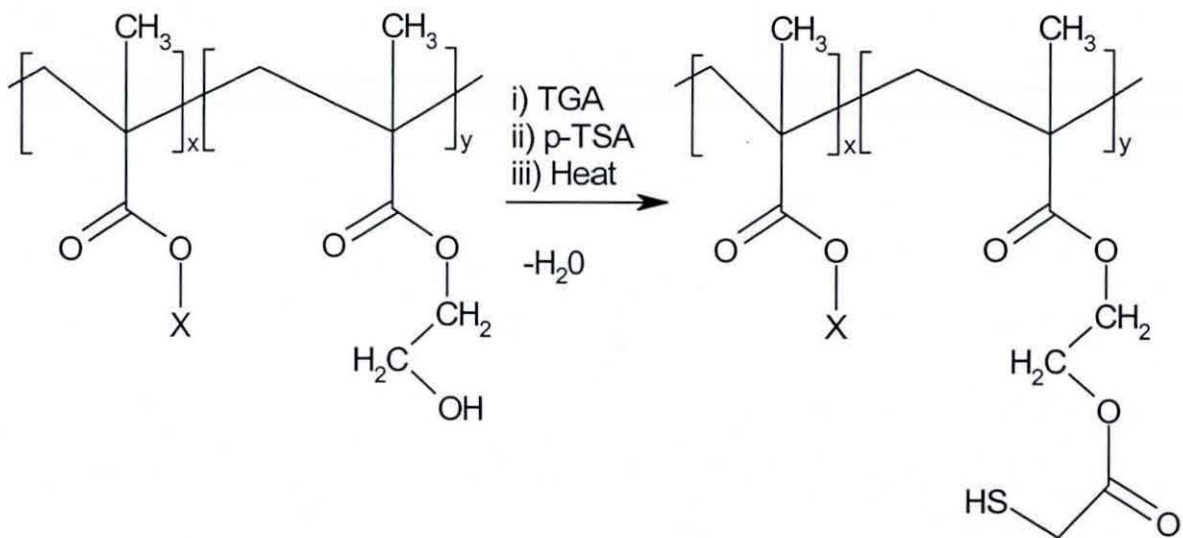
The average number of OH groups per copolymer chain was calculated using the value of  $M_n$  of the copolymer determined by SEC.

$$\text{Average OH} = \frac{M_n}{(H_f \times 176) + (H_S \times 130)}$$

**Eqn 4-6**

### 4.3 Preparation of PCTA

The functionalisation of MMA-co-HEMA and BzMA-co-HEMA copolymers was performed via an acid-catalysed esterification reaction. An OH group on the HEMA unit reacted with a carboxylic acid group on TGA to produce an ester linkage with the loss of a water molecule. The reaction is outlined in Scheme 4-1. Both copolymers were prepared under the same conditions.



**Scheme 4-1** The acid-catalysed esterification reaction of HEMA-based copolymers with TGA (where X= CH<sub>3</sub> or benzyl).

## 4.3.1 Method Development of Functionalisation Reaction

### 4.3.1.1 Initial Investigations

A method was provided by ICI Acrylics (see Section 3.3.4.1) for the functionalisation of OH-containing copolymer via an esterification reaction. The method involved refluxing a copolymer for 6 hours at 393K in butyl acetate with TGA and p-TSA present. Reactions performed under these conditions yielded colourless powders. Proton NMR spectroscopy of the product indicated that no incorporation of TGA had occurred. However, the methylene groups *d* and *e* in the HEMA unit moved downfield (shift *d* from  $\delta$ =4.12 to  $\delta$ =4.17 and shift *e* from  $\delta$ =3.85 to  $\delta$ =4.28 ppm). A series of reactions was performed to investigate why TGA incorporation was unsuccessful and what caused the downfield shift observed in the proton NMR spectrum. The reaction conditions were investigated by eliminating each component in the esterification reaction to observe the effect on the copolymer.

The results from proton NMR spectroscopy indicated that the acid catalyst was responsible for the downfield shift in methylene groups *d* and *e* – termed the ‘acid-effect’. It was suspected that the acid-catalysed OH groups reacted with the ester solvent rather than TGA; the acetate reacted onto the OH groups in a trans-esterification reaction. A MMA-co-HEMA copolymer was esterified with butyl acetate, purified, then esterified with toluene. The aim of this experiment was to confirm that butyl acetate was reacting onto the OH in the HEMA units. The proton NMR spectrum of the copolymer esterified in butyl acetate exhibited the characteristic ‘acid-effect’ shift in the HEMA methylene protons *d* and *e*. The NMR spectrum indicated partial TGA incorporation had occurred on the HEMA units unaffected by the esterification in butyl acetate after further esterification with toluene, which confirmed the theory that solvent reacted with the OH functionality.

The solvent for the esterification reaction was changed to toluene. Proton NMR spectroscopy results indicated that TGA incorporated onto the HEMA units. The products of the reaction were colourless powders that possessed a strong odour. The individual components of the polymerisation were investigated to observe their effects. The results are summarised in Table 4-10.

**Table 4-10 Investigation into the esterification reaction with toluene.**

Sample	TGA	p-TSA	Proton NMR Spectrum Comments	Conversion
JHH35	✓	✓	TGA incorporated on backbone	80%
JHH39	✓	✗	Partial TGA incorporation	<5%
JHH45	✗	✓	Slight downfield shift in HEMA shift <i>e</i>	5%

The acid catalyst was very important. In the absence of an acid catalyst, the reaction proceeded very slowly and to a low conversion. Previously reported methods used no catalyst and achieved high conversion.<sup>11,13</sup> Attempts to duplicate these reactions in the absence of a catalyst proved unsuccessful. Esterification in the presence of a catalyst yielded high conversion (>80%).

#### 4.3.1.2 PCTA Insolubility and Implications

The occurrence of insoluble/microgel PCTA became more frequent when the mass fraction of HEMA in the copolymer increased above 0.15. In the extreme an insoluble product resulted. Attempts to dissolve these subsequent products in THF, acetone and DCM yielded swollen networks, which indicated the presence of cross-links. The cause of PCTA insolubility was investigated. The reactivity of mercaptan groups is well known, even at ambient temperatures.<sup>123</sup> Disulphide bonds are produced when SH is oxidised by atmospheric oxygen. It was postulated that during the esterification reaction the mercaptan groups reacted to form disulphide linkages that led to a network structure.

Disulphide formation was investigated using benzyl TGA (structure inset in Figure 4-7). The benzyl group eliminated any side reactions associated with free SH. A MMA-co-HEMA copolymer (0.24 mass fraction HEMA - JHH155) was esterified in toluene to a conversion above 80% (JHH212) yielding a soluble product. A similar reaction with TGA as the esterifying acid produced an insoluble product. The proton NMR spectrum of JHH212 is included in Figure 4-7 and the interpretation corresponds to Table 4-13/p112. A similar spectrum was obtained in the benzylation reaction of PCTA to estimate the free SH concentration. The spectrum indicated the presence of benzyl TGA with the appearance of aromatic protons and a methylene shift at  $\delta=3.85$  ppm and at  $\delta=3.15$  ppm.

A downfield shift in the HEMA methylene was further evidence for incorporation. The shifts associated with the HEMA unit methylene groups appeared broadened. The benzyl groups in benzyl TGA can be removed to yield free mercaptan groups in a one step procedure using liquid ammonia and sodium.<sup>124</sup> The solubility of JHH212 indicated the involvement of SH in the formation of a network product.

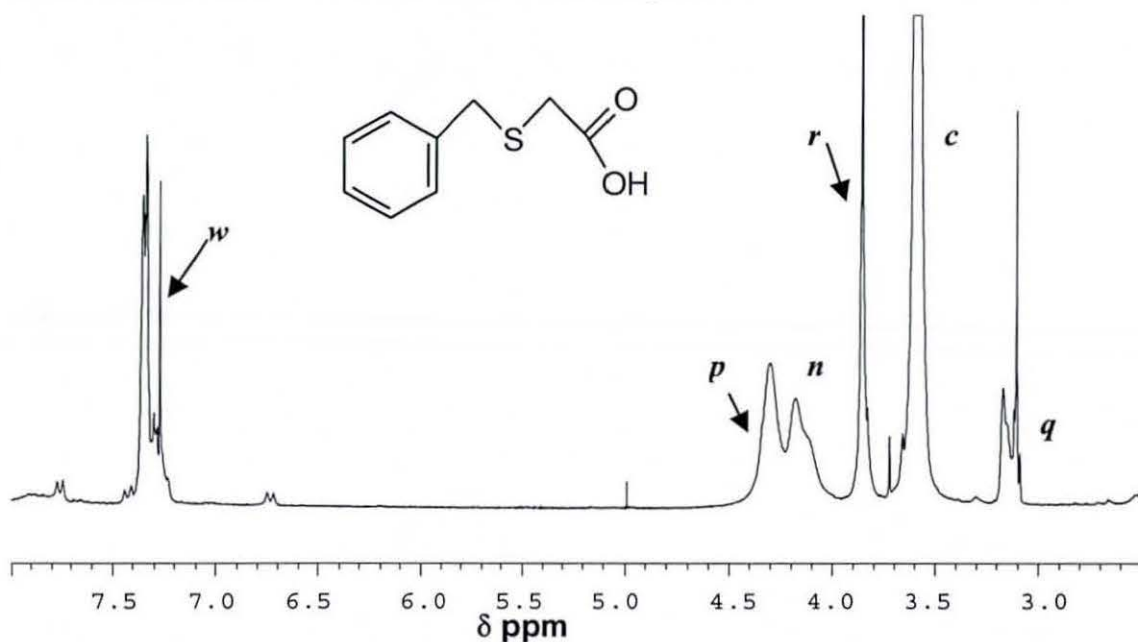


**Figure 4-7** A proton NMR of JHH212 esterified in toluene with benzyl TGA (inset).

A proton NMR spectrum of a swollen, insoluble PCTA in  $\text{CDCl}_3$  indicated high conversion to esterified HEMA. Subsequent benzylation of these swollen products to determine the concentration of free SH indicated a high concentration of SH functionality was still present. This followed with the conclusion of Yamaguchi et al.<sup>110</sup> that the disulphide concentration was low in the cross-linked polymers but high enough to produce insolubility problems.

A small concentration of insoluble product (<5% wt) was present in all the esterification reaction mixtures. The cooled esterification mixture was slightly cloudy and typically contained small insoluble particles. Filtration of this mixture yielded a clear solution free of insoluble material. The concentration of insoluble product was dependent on the functionality of the PCTA precursor.

The observed insoluble material and turbid esterification solutions indicated disulphide formation present in all the esterification reactions. SEC was performed on the PCTA before it was realised that the PCTA might be damaging the gel columns. The SEC profiles of the copolymer JHH53 and the corresponding PCTA 10L-M55 are included in Figure 4-8. The molar mass data is also reported.<sup>i</sup>

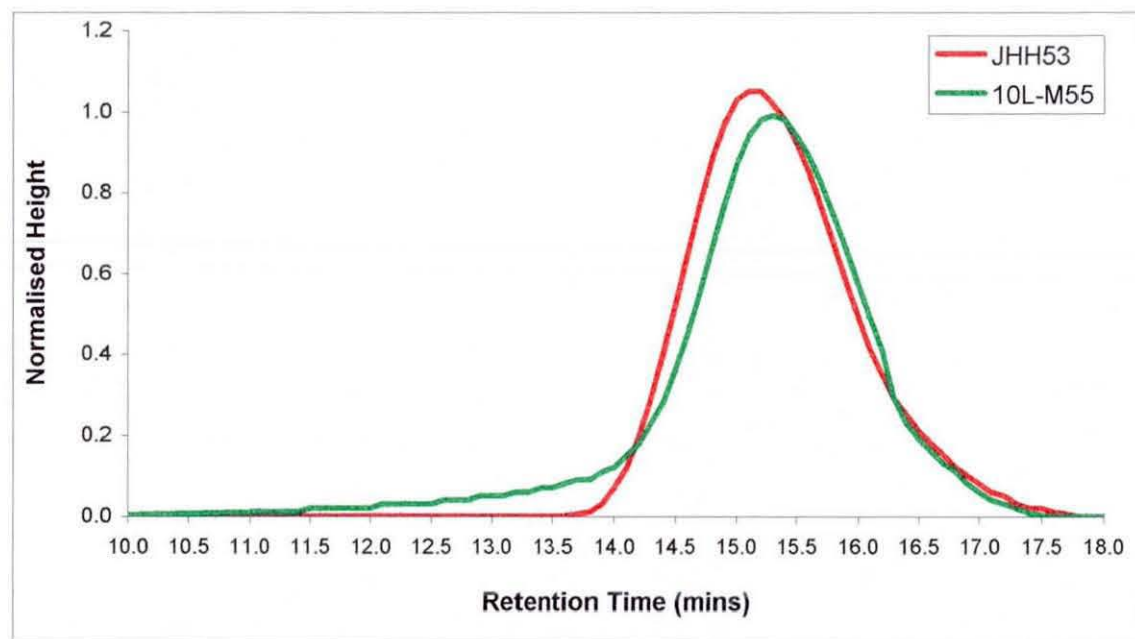


**Figure 4-8 The SEC profiles of a copolymer JHH53 and PCTA 10L-M55.**

A characteristic high molar mass front was observed on the peak with all PCTA samples characterised by SEC. The high molar mass portion was probably microgel. It was postulated that PCTA cross-linked on the column through oxidation and accumulated over a period of time.

i	$M_w$ (g/mol)	$M_n$ (g/mol)	D	Conversion
JHH53	18,500	9,700	1.91	-
10L-M55*	82,600	10,600	7.82	89%

\* apparent molar mass data reported.

### 4.3.1.3 Reaction Parameters

A reproducible method for esterification was required. The strategy was to minimise the reactivity of a mercaptan group in order to reduce the concentration of partial/total insoluble material. A compromise between conversion and product solubility was necessary.

#### 4.3.1.3.1 Copolymer Phase Separation

The copolymer became less soluble with toluene as the mass fraction of HEMA increased above 0.15. The copolymer/toluene solution was hazy, and in the extreme case, swollen copolymer was present. Another solvent was sought for the esterification reaction; butan-2-one (MEK) was investigated. Incorporation of TGA with MEK was low (~20% conversion) in comparison to those reactions with toluene (~80% conversion) when esterified over 16 hours. Mixtures of toluene and MEK (up to 30% wt MEK) increased the solubility of the copolymer but resulted in much lower conversions (35% conversion with 30% wt MEK). As the fraction of MEK increased the conversion to product decreased.

The solubility of the copolymers was improved by a reduction in the molar mass from 20 kg/mol to 5 kg/mol. This improved the solubility compared with a higher molar mass copolymer of equivalent functionality.

#### 4.3.1.3.2 Esterification Temperature

Esterification reactions were initially performed at temperatures exceeding 383K to boil off any water produced in the esterification reaction, which favoured product formation through the equilibrium reaction. The esterification temperature was reduced to 353K to reduce the reactivity of the SH groups. Conversions of around 80% were still obtained with all copolymers.

#### 4.3.1.3.3 Esterification Reaction Time

The aim was to minimise exposure of SH at elevated temperature to avoid disulphide formation. A series of conversion reactions was carried out at 353K using the copolymer JHH209 (Table 4-11).

**Table 4-11 Conversion of MMA-co-HEMA copolymer to PCTA.**

Sample	Reaction Time (hours)	Conversion (%)
13L-M277	2	~ 60
13L-M278	4	~ 80
13L-M279	16	~ 85

The proton NMR data indicated that 4 hours appeared to be the optimum time for esterification.

#### 4.3.1.3.4 Sequential Addition of TGA

The concentration of TGA in an esterification reaction was proportional to the concentration of HEMA in the copolymer. To reduce the initial concentration of free SH in the reaction mixture, TGA was added sequentially. Sequential addition of the TGA reduced the occurrence and quantity of insoluble PCTA.

### 4.3.2 Characterisation of MMA-co-HEMA PCTA

Proton NMR spectroscopy was the primary method utilised for the characterisation of PCTA. Expanded views of the proton NMR spectra for a copolymer and a PCTA are included in Figure 4-9a and Figure 4-9b. Assigned chemical shifts are reported in Table 4-12 and correspond to those in Structure 4-3. The movement and appearance of shifts can be clearly observed.

TGA has two active proton groups: a methylene group at  $\delta=3.35$  ppm (shift *k*) and a mercaptan group at  $\delta=2.00$  ppm (shift *m*). Evidence of TGA incorporation in the copolymer was given by the appearance of these shifts in the PCTA spectrum. The shift associated with a mercaptan group was usually obscured by the copolymer backbone.

A downfield shift in the methylene protons in the HEMA unit was observed when TGA had reacted on. The methylene in HEMA (shift *e*) moved downfield to shift *j* because of the deshielding nature of TGA. The methylene *d* also shifted slightly downfield to shift *h*.

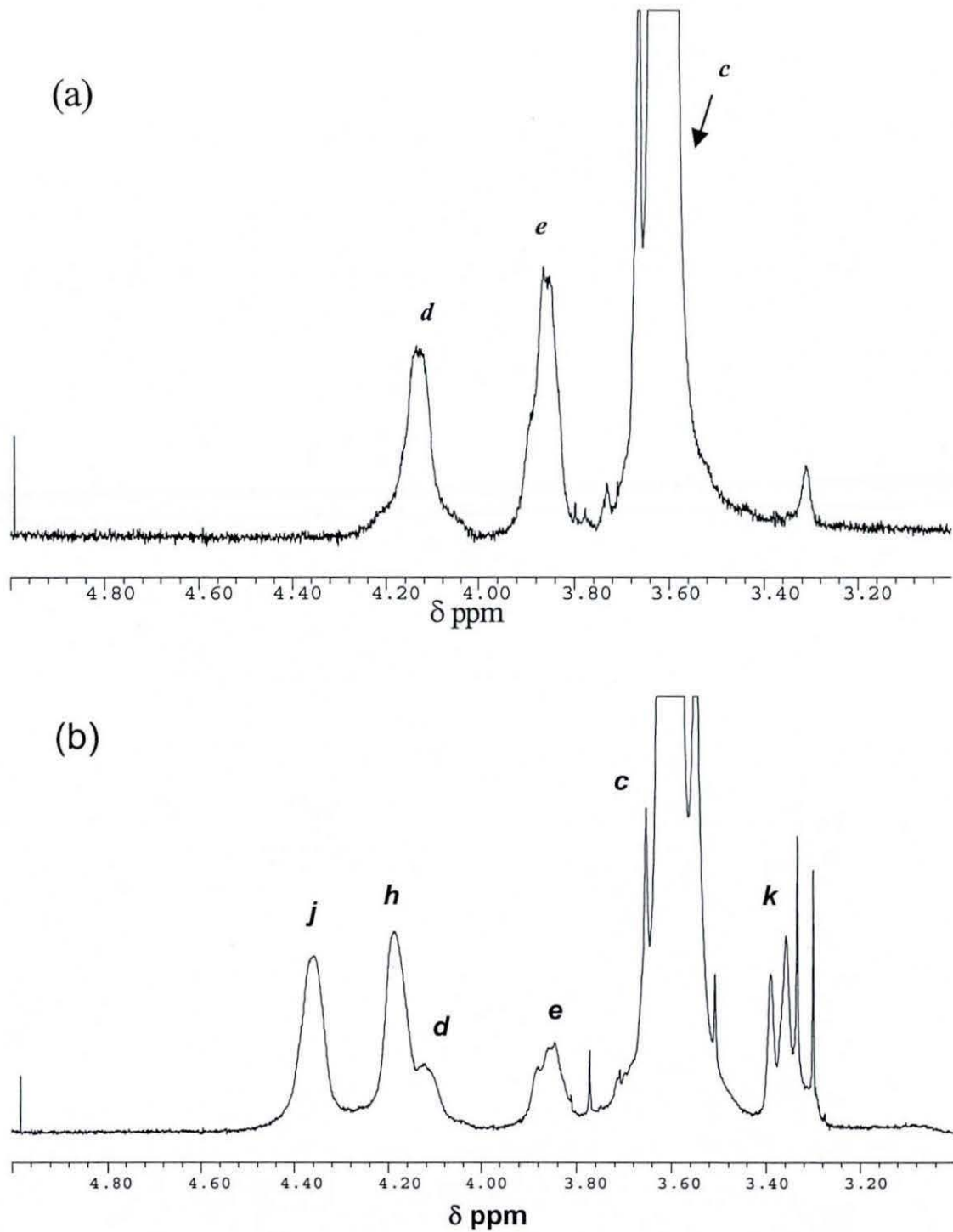


**Figure 4-9** The proton NMR spectra of (a) starting MMA-co-HEMA copolymer JHH208 and (b) PCTA 6L-M215 showing the changes in chemical shifts with TGA incorporation.

**Structure 4-3 A structural representation of a MMA-co-HEMA PCTA.**

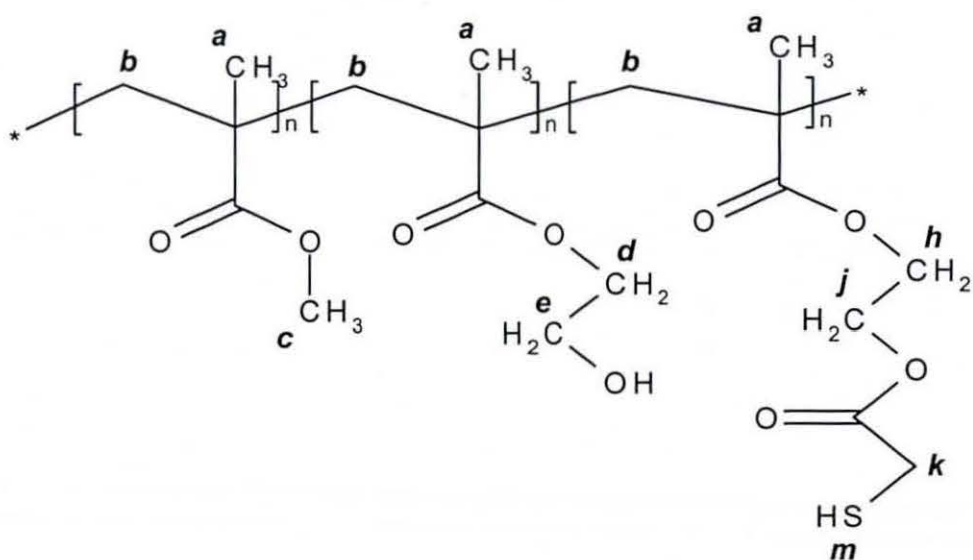


**Table 4-12 The proton NMR shift assignments for a MMA-co-HEMA PCTA.**

CHEMICAL SHIFT $\delta$ / ppm	ASSIGNMENT	CORRESPONDING LABEL
0.82 – 1.26	$\alpha$ -CH <sub>3</sub>	<b>a</b>
1.80 – 2.02	Backbone -CH <sub>2</sub>	<b>b</b>
3.35	TGA -CH <sub>2</sub> (Adjacent -SH)	<b>k</b>
3.60	MMA unit ester -CH <sub>3</sub>	<b>c</b>
3.85	HEMA unit -CH <sub>2</sub> UNREACTED	<b>e</b>
4.12	HEMA unit -CH <sub>2</sub> UNREACTED	<b>d</b>
4.17	HEMA unit -CH <sub>2</sub> REACTED	<b>h</b>
4.36	HEMA unit -CH <sub>2</sub> REACTED	<b>j</b>

#### 4.3.2.1 Conversion of Copolymer to PCTA

The conversion of OH groups in the esterification reaction was calculated from the integrals of the methylene groups in a HEMA unit. Using shift *e* at  $\delta=3.85$  ppm as the reference for unreacted HEMA bearing OH introduced inaccuracies, as there is a spin-spin coupling shift from the methyl ester in MMA (shift *c*). Therefore, shift *j* (reacted HEMA only) was used against shift *h+d* (mix of reacted and unreacted HEMA) to determine the extent of the reaction.

$$\text{Converted HEMA \%} = \frac{H_j}{H_{h+d}} \times 100$$

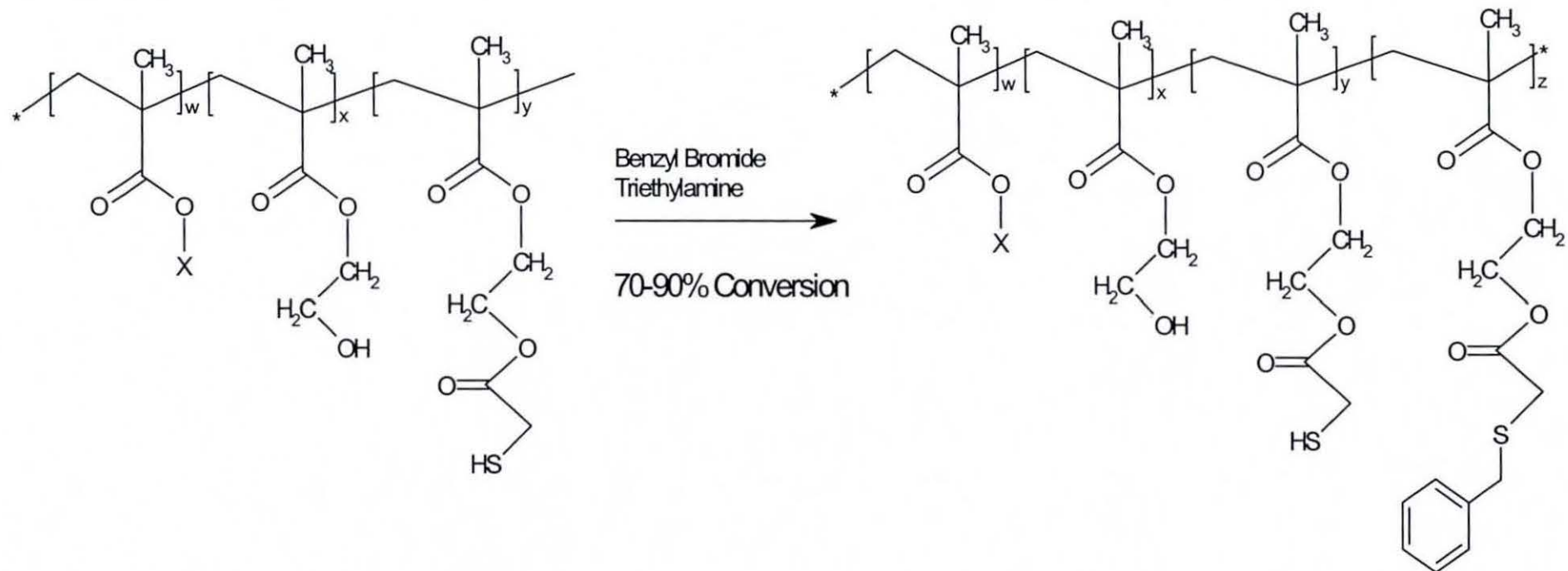
Eqn 4-7

#### 4.3.2.2 Estimation of SH Concentration in PCTA

A method was sought to quantify the concentration of free SH in a PCTA (assuming disulphide formation was inevitable). Mercaptan groups are protected in organic synthesis by benzylation with a benzyl halide in the presence of a base.<sup>123</sup> The product of the reaction is a benzyl-protected mercaptan. Aromatic functional groups have distinctive chemical shifts in proton NMR spectroscopy and are active chromophores in the UV region, making them desirable groups to utilise. The benzylation reaction is represented in Scheme 4-2.

Benzyl chloride was utilised initially as the aromatic halide but the reaction proceeded slowly and to a very low conversion. Benzyl bromide was used as it is more reactive than the chloride derivative. The reaction conversion was increased further with the addition of TEA as it removed HBr by-product, driving the equilibrium over to product. The TEA/HBr complex was insoluble in THF and precipitated out of solution.

Scheme 4-2 The representation of a reaction of a PCTA with benzyl bromide and triethylamine (where X=CH<sub>3</sub> or benzyl).



The expanded views of the proton NMR spectra of a PCTA and corresponding benzylated PCTA are included in Figure 4-10a and Figure 4-10b respectively. The structure and assigned shifts are included in Structure 4-4 and Table 4-13. Benzylation of the PCTA broadened the chemical shift of the methylene protons in a HEMA unit and shifted them upfield. The broadening effect was probably associated with the number of mixed species in the region (benzylated/free SH/disulphide species). A benzyl methylene (shift *r*) that had reacted with a sulphur had the same chemical shift ( $\delta$ =3.85 ppm) as a methylene in the HEMA unit in the original copolymer (shift *d*). The chemical shift associated with a TGA methylene (shift *k*) on the backbone moved upfield with the addition of a benzyl group (to shift *q*). The appearance of aromatic protons (shift *w*) was further evidence of benzylation.

The extent of the benzylation reaction ranged from 70-90%. However, it seemed unlikely that up to 30% of the SH groups were present as disulphide bonds producing cross-links. Intra-molecular disulphide formation was one theory for the reduced concentration of SH.

Attempts to benzylate a MMA-co-HEMA copolymer using the above method yielded no benzylated copolymer, which suggested the benzylation reaction was selective with SH groups only.

A PMMA sample prepared in the presence of a PCTA was benzylated to identify if any free SH groups were present post-polymerisation. The results were inconclusive due to the low concentration of SH present in the systems.

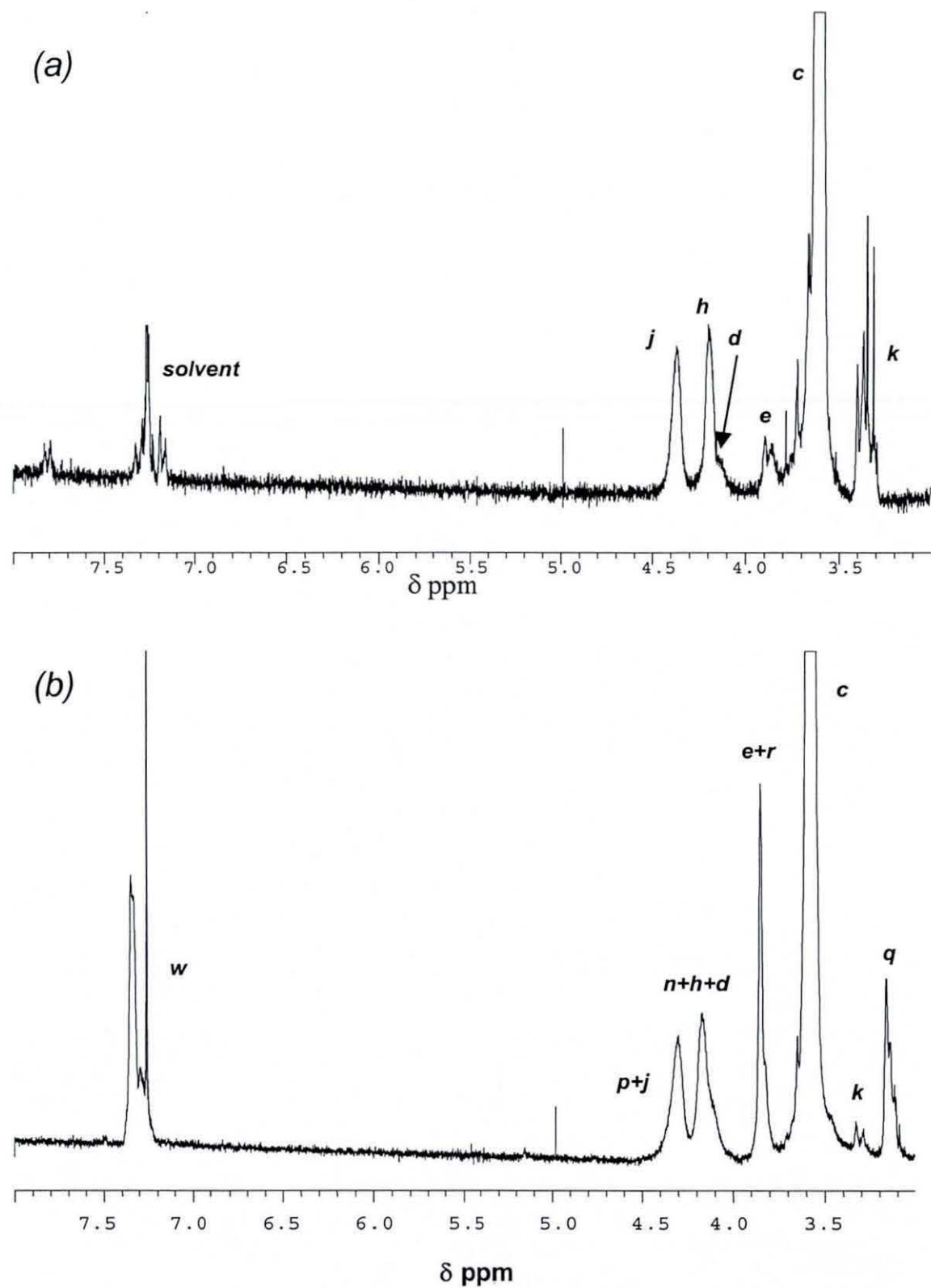


**Figure 4-10** The proton NMR spectra of (a) a PCTA and (b) the corresponding benzylated PCTA.

**Structure 4-4** The structural representation of a benzylated PCTA with shift assignments.

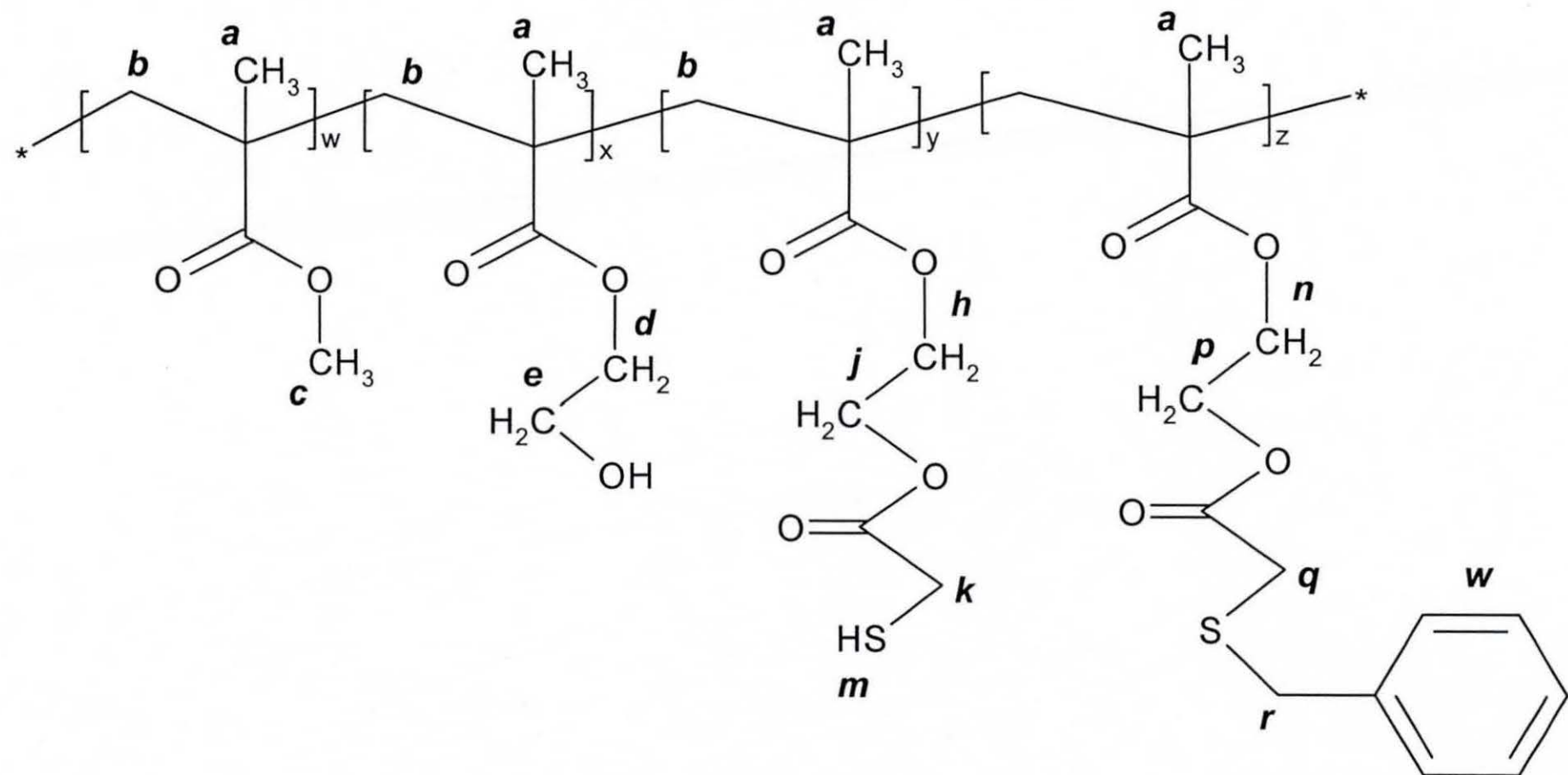


**Table 4-13 The proton NMR shift assignments for a benzylated PCTA.**

CHEMICAL SHIFT $\delta$ / ppm	ASSIGNMENT	CORRESPONDING LABEL
0.82 – 1.26	$\alpha$ -CH <sub>3</sub>	<i>a</i>
1.80 – 2.02	Backbone -CH <sub>2</sub>	<i>b</i>
3.12	TGA –CH <sub>2</sub> IN BENZYL-PCTA	<i>q</i>
3.35	TGA –CH <sub>2</sub> IN PCTA	<i>k</i>
3.60	MMA unit ester –CH <sub>3</sub>	<i>c</i>
3.85	HEMA unit-CH <sub>2</sub> UNREACTED BENZYL –CH <sub>2</sub> REACTED	<i>e</i> <i>r</i>
~4.17	HEMA unit -CH <sub>2</sub> UNREACTED	<i>d</i>
BROAD	HEMA unit –CH <sub>2</sub> REACTED	<i>h</i>
	HEMA unit –CH <sub>2</sub> BENZYLATED	<i>n</i>
4.32	HEMA unit -CH <sub>2</sub> BENZYLATED	<i>p+j</i>
BROAD	(and HEMA unit -CH <sub>2</sub> REACTED)	
4.36	HEMA unit -CH <sub>2</sub> REACTED	<i>j</i>
7.00	Aromatic benzyl	<i>w</i>

#### 4.3.2.3 Calculation of SH Concentration in PCTA

A benzyl methylene (shift  $r$ ) reacted to a sulphur had the same chemical shift as the methylene in the HEMA unit in the original copolymer (shift  $e$ ). The concentration of unreacted HEMA in a PCTA was calculated and deducted from the integral of shift  $e+r$  to determine the concentration of free SH.

The concentration of unreacted HEMA at  $\delta=3.85$  ppm (shift  $e$ ) is equivalent to Eqn 4-8.

$$H_e \approx (H_{n+h+d} - H_{p+j})$$

**Eqn 4-8**

The integral at  $\delta=3.85$  ppm in a benzylated PCTA due to benzylation only (shift  $r$ ) and not residual unreacted HEMA is:

$$H_r = (H_{3.85} - H_e)$$

**Eqn 4-9**

The percentage of free SH is then (Eqn 4-10).

$$Free [SH] = \left( \frac{H_r}{H_{p+j}} \right) \times 100$$

**Eqn 4-10**

### 4.3.3 Characterisation of BzMA-co-HEMA PCTA

Proton NMR spectroscopy was used to characterise PCTA prepared from BzMA-co-HEMA copolymer. An expanded view of the spectra for a BzMA-co-HEMA copolymer and the corresponding PCTA highlight the region of incorporation of TGA on the polymeric backbone (Figure 4-11a and Figure 4-11b respectively). The assignments correspond to those in Structure 4-5 and Table 4-14.

The methylene (shift *t*) in the HEMA unit shifted downfield to shift *v* when the TGA had reacted on. Traces of unreacted HEMA from the precursor were observed in the spectrum of the PCTA (shift *t* and obscured shift *u*). The methylene *s* in the HEMA unit moved downfield slightly when TGA had incorporated. The shifts remained broad because of the various chemical environments. The appearance of shift *k*, which corresponded to the methylene in TGA, was further evidence of incorporation.

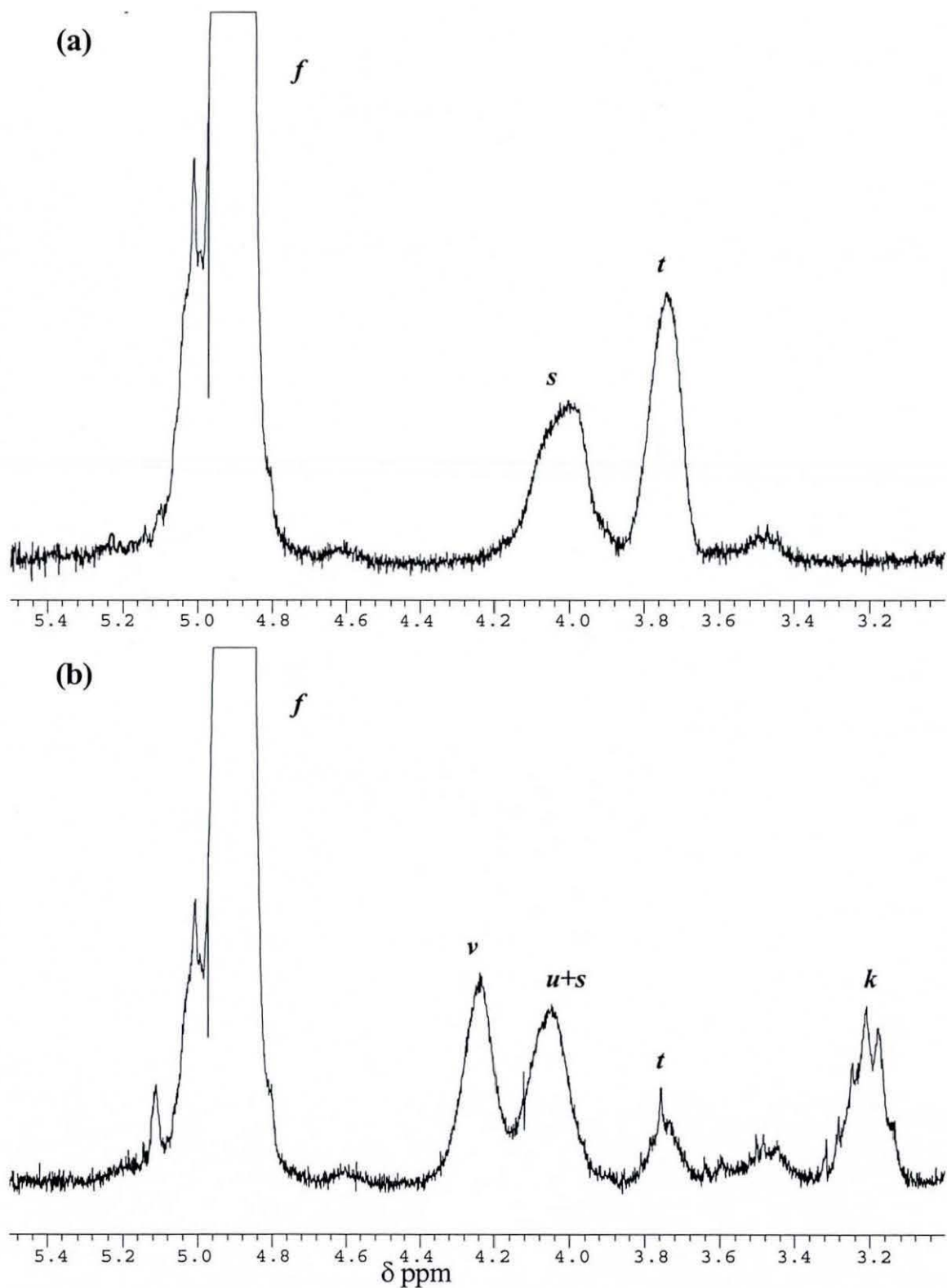


**Figure 4-11** The proton NMR spectra of (a) the BzMA-co-HEMA copolymer JHH311 and (b) corresponding PCTA 5L-B349.

Structure 4-5 A structural representation of a BzMA-co-HEMA PCTA.

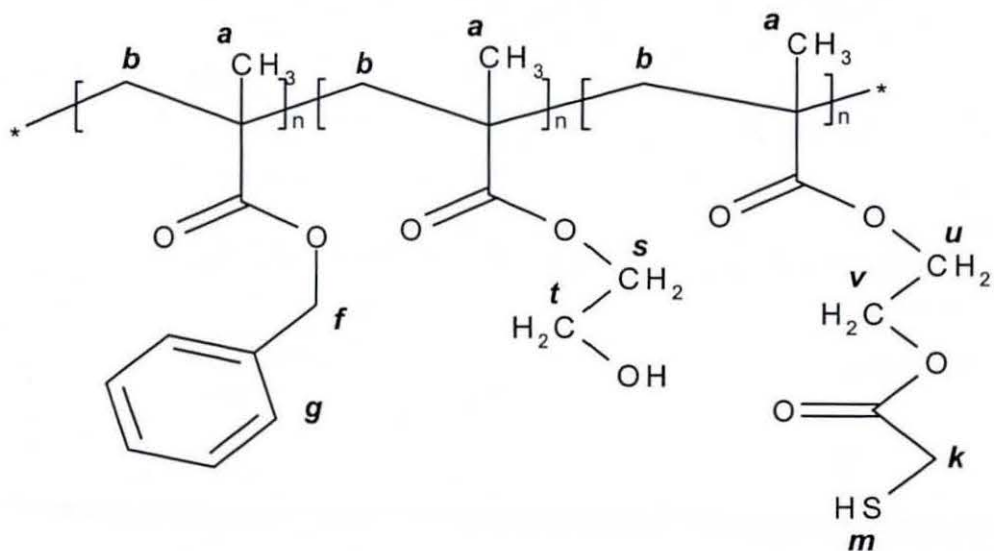


Table 4-14 The proton NMR spectroscopy assignments for BzMA-co-HEMA PCTA.

CHEMICAL SHIFT $\delta$ / ppm	ASSIGNMENT	CORRESPONDING LABEL
0.82 – 1.26	$\alpha$ -CH <sub>3</sub>	<i>a</i>
1.80 – 2.02	Backbone -CH <sub>2</sub>	<i>b</i>
3.20	TGA -CH <sub>2</sub> (Adjacent -SH)	<i>k</i>
3.75	HEMA unit -CH <sub>2</sub> UNREACTED	<i>t</i>
4.03	HEMA unit -CH <sub>2</sub> UNREACTED	<i>s</i>
4.05	HEMA unit -CH <sub>2</sub> <b>REACTED</b>	<i>u</i>
4.28	HEMA unit -CH <sub>2</sub> <b>REACTED</b>	<i>v</i>
4.90	BzMA - CH <sub>2</sub> BENZYL	<i>f</i>
~7.30	BzMA –AROMATIC 5H	<i>g</i>

#### 4.3.3.1 Conversion of Copolymer to PCTA

The methylene integral in TGA was utilised to estimate the conversion of OH groups in the esterification reaction. Integrals from the HEMA unit were not utilised to calculate the conversion because shift *v* partially overlapped with shift *u+s*. Hence, in order to estimate the conversion, an integral value for a methylene unit in HEMA was required. This was achieved by adding up all the integrals associated with the two methylene units in HEMA and dividing by two. The integral of TGA was then divided by this value. The concentration of reacted material was calculated as a percentage.

$$\text{Reacted HEMA \%} = \frac{H_k}{(H_v + H_{u+s} + H_t) \div 2} \times 100$$

Eqn 4-11

#### 4.3.3.2 Estimation of SH Concentration in PCTA

The concentration of SH was determined by a similar procedure as outlined in Section 4.3.2.2. Expanded views of the spectra for the PCTA 5L-B349 and the corresponding benzylated PCTA are included in Figure 4-12a and Figure 4-12b. The assignments correspond to those in Structure 4-6 and Table 4-15. The benzylated product still contained traces of TEA/Br complex, which corresponded to a shift at  $\delta=3.15$  ppm. The salt complex had an identical shift to TGA. The appearance of shift *r* indicated that the benzylation reaction had occurred. Methylenes *k* in TGA shifted upfield to shift *q* with the addition of a benzyl group. The broad peak was associated to the mixed environment of methylene groups *k* and *q*.

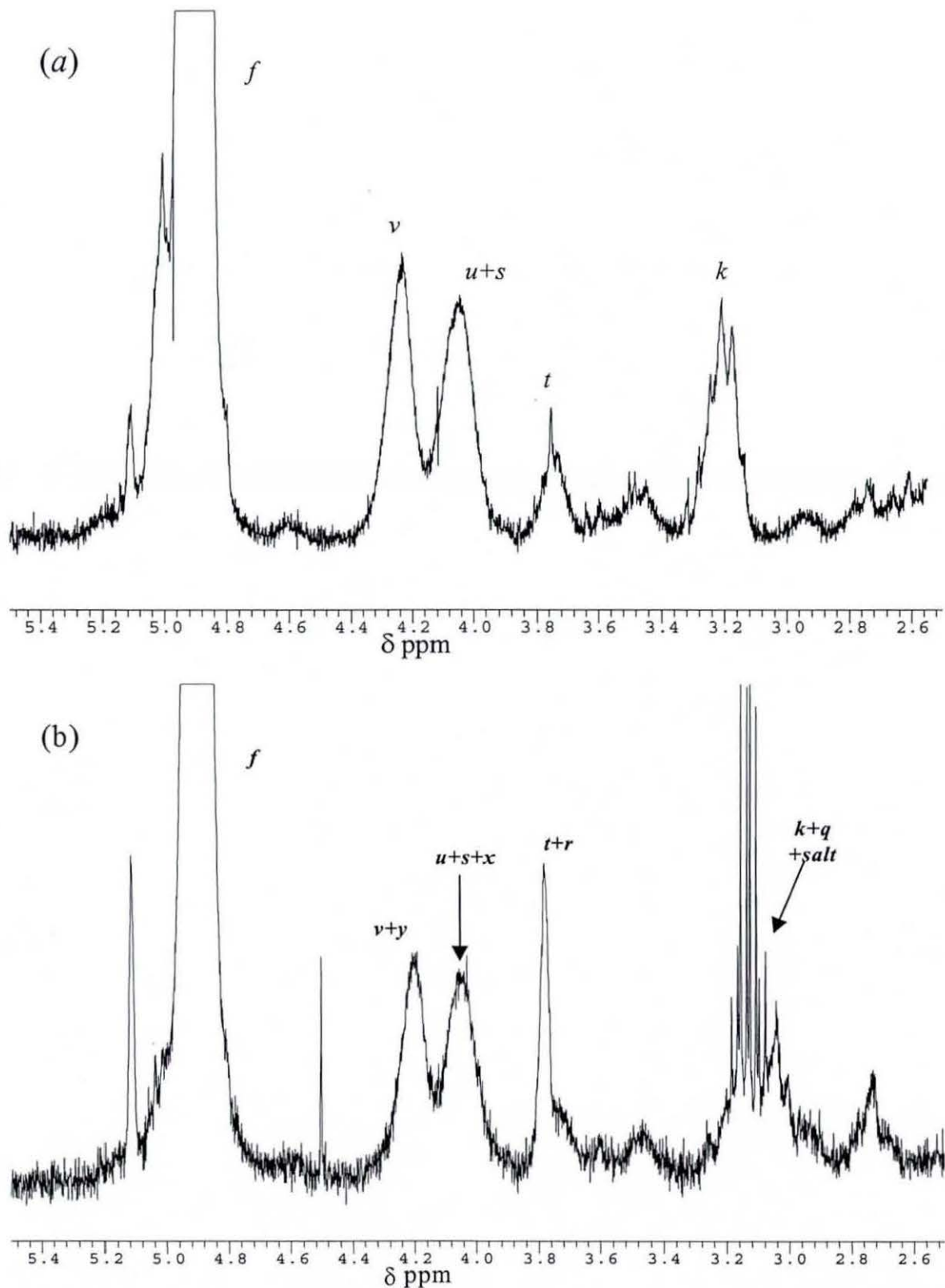


**Figure 4-12** The proton NMR spectra of (a) a BzMA-co-HEMA PCTA 5L-B349 and (b) a corresponding benzylated PCTA indicating the appearance of benzyl methylene (shift *r*).

Structure 4-6 A structural representation of a benzylated BzMA-co-HEMA PCTA with NMR assignments.

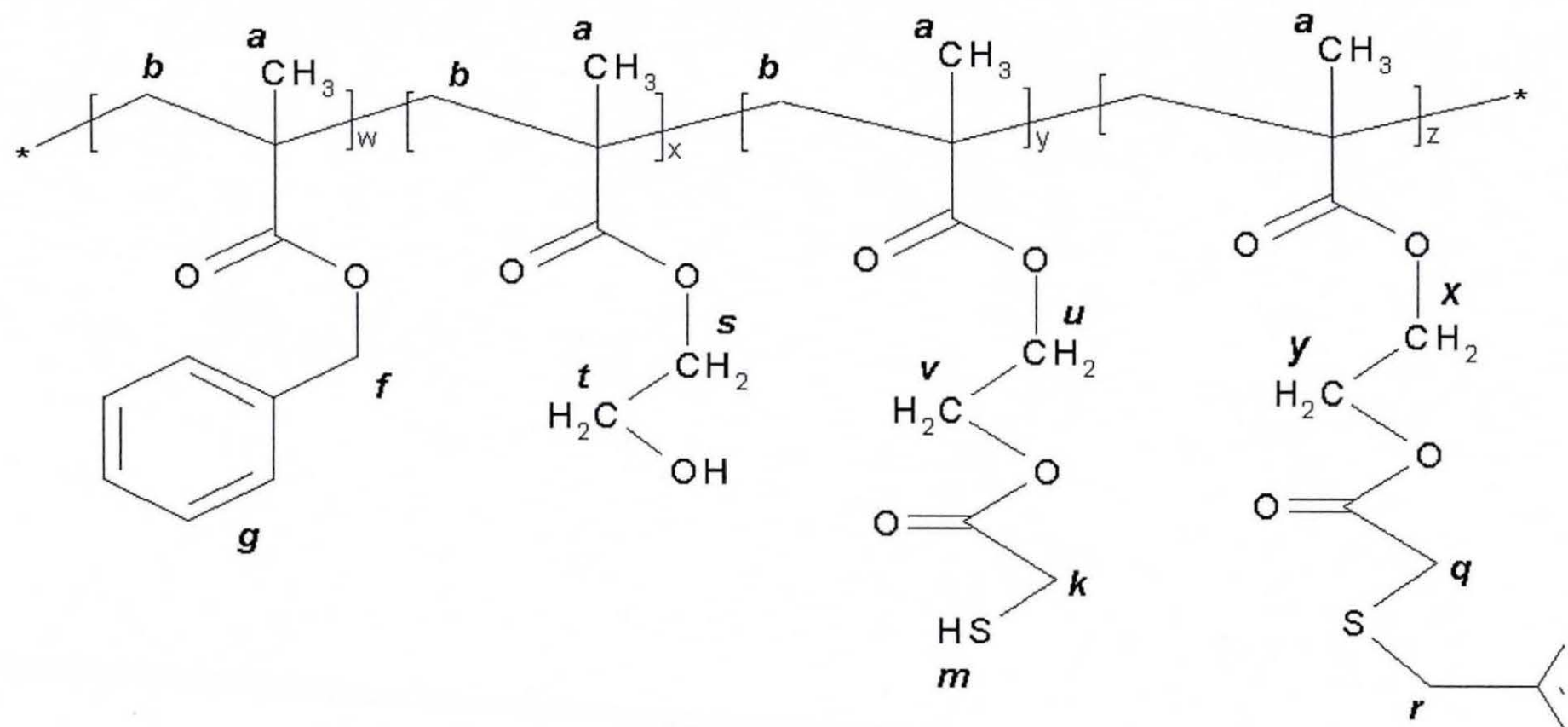


**Table 4-15 The proton NMR shift assignments for a benzylated BzMA-co-HEMA PCTA.**

CHEMICAL SHIFT $\delta$ / ppm	ASSIGNMENT	CORRESPONDING LABEL
0.82 – 1.26	$\alpha$ -CH <sub>3</sub>	<i>a</i>
1.80 – 2.02	Backbone -CH <sub>2</sub>	<i>b</i>
3.10	TGA –CH <sub>2</sub> IN BENZYL-PCTA	<i>q</i>
~3.15	TRIETHYLAMINE SALT SHIFT	-
3.20	TGA –CH <sub>2</sub> IN PCTA	<i>k</i>
3.75	HEMA unit -CH <sub>2</sub> UNREACTED	<i>t</i>
3.80	Benzyl methylene – BzBr REACTED	<i>r</i>
4.03	HEMA unit -CH <sub>2</sub> UNREACTED	<i>s</i>
	HEMA unit -CH <sub>2</sub> REACTED	<i>u</i>
	HEMA unit -CH <sub>2</sub> BENZYLATED	
4.28	HEMA unit -CH <sub>2</sub> REACTED	<i>v</i>
	HEMA unit -CH <sub>2</sub> BENZYLATED	<i>y</i>
4.90	BzMA - CH <sub>2</sub> BENZYL	<i>f</i>
~7.30	BzMA –AROMATIC 5H ON BACKBONE & BENZYL	<i>g+w</i>

#### 4.3.3.3 Calculation of SH Concentration in PCTA

A benzyl methylene (shift  $r$ ) that had reacted with sulphur had a similar chemical shift to a methylene in the HEMA unit in the original copolymer (shift  $t$ ). The integral of the methylene in an unreacted HEMA unit in a PCTA (shift  $t$ ) was deducted from the integral of shift  $t+r$  to calculate the concentration of free SH (shift  $r$ ). The integral at  $\delta=3.80$  ppm in the benzylated PCTA (shift  $r$ ) due to benzylation only (and not residual unreacted HEMA) is:

$$H_r = (H_{t+r} - H_t)$$

**Eqn 4-12**

The percentage of free SH is then given by:

$$Free [SH] = \frac{H_r}{H_{v+y}} \times 100$$

**Eqn 4-13**

## 4.4 Copolymer and PCTA Summary Tables

**Table 4-16 Summary table of MMA-co-HEMA copolymers utilised in branching investigations.**

Copolymer	[DDM] (% wt)	Initial HEMA Fraction		Final HEMA Fraction		M <sub>w</sub> (g/mol)	M <sub>n</sub> (g/mol)	D	Av. no of OH groups per chain
		Mass	Mole	Mass	Mole				
JHH144	1.60	0.08	0.06	0.09	0.07	9,800	5,500	1.77	3.7
JHH147	0.30	0.08	0.06	0.10	0.08	26,200	16,400	1.60	12.1
JHH148	0.30	0.15	0.12	0.17	0.14	27,500	15,500	1.77	20.6
JHH155	1.60	0.25	0.20	0.24	0.20	9,600	5,400	1.76	10.0
JHH208	1.60	0.08	0.06	0.09	0.07	9,500	5,600	1.70	3.8
JHH209	0.80	0.08	0.06	0.09	0.07	17,100	12,900	1.70	9.1
JHH222	-	0.08	0.06	0.09	0.07	38,600	19,800	1.95	14.3
JHH405	1.60	0.15	0.12	0.17	0.14	10,300	5,800	1.77	7.6

**Table 4-17 Summary table of BzMA-co-HEMA copolymers utilised in branching investigations.**

Copolymer	[DDM] (% wt)	Initial HEMA Fraction		Final HEMA Fraction		M <sub>w</sub> (g/mol)	M <sub>n</sub> (g/mol)	D	Av. No of OH groups per chain
		Mass	Mole	Mass	Mole				
JHH249	-	0.10	0.13	0.09	0.12	37,400	16,000	2.34	11.5
JHH311	1.60	0.80	0.84	0.07	0.09	9,000	4,700	1.92	2.6

**Table 4-18 Summary table of MMA-co-HEMA PCTA utilised in branching investigations.**

PCTA	Based on Copolymer	Copolymer $M_n$ (g/mol)	Esterification Conversion (%)	Free SH (Benzylation)	Fraction of Free SH		Av. no of SH groups per chain
					Mass	Mole	
6L-M215	JHH208	5,600	85	83	0.06	0.05	2.7
13L-M227	JHH209	12,900	86	81	0.06	0.05	6.3
20L-M223	JHH222	19,800	88	86	0.07	0.06	10.8
20L-M293	JHH222	19,800	75	74	0.05	0.04	7.9
6L-M402	JHH144	5,500	93	81	0.07	0.05	2.8
16L-M403	JHH147	16,400	80	79	0.06	0.05	7.6
6H-M426	JHH405	5,800	79	84	0.11	0.09	5.0
16H-M427	JHH148	15,500	82	85	0.12	0.10	14.4

**Table 4-19 Summary table of BzMA-co-HEMA PCTA utilised in branching investigations.**

PCTA	Based on Copolymer	Copolymer $M_n$ (g/mol)	Esterification Conversion (%)	Free SH (Benzylation)	Fraction of Free SH		Av. no of SH groups per chain
					Mass	Mole	
16L-B250	JHH249	16,000	82	77	0.06	0.08	7.2
5L-B326	JHH311	4,700	82	69	0.04	0.05	1.5
5L-B349	JHH311	4,700	70	72	0.04	0.05	1.3

**PCTA CODE:** First number = copolymer  $M_n \times 10^{-3}$  gmol<sup>-1</sup> / [SH] is L=low or H=high / copolymer composition M=MMA or B=BzMA.

## 4.5 Branching Investigations with PETM

PETM has been utilised as a tetra-functional CTA in the radical polymerisation of MMA to prepare star polymers.<sup>53,54,55,57</sup> PMMA samples were prepared and characterised using SEC in the absence of a mass detector and the results are detailed in Table 4-20. There was a considerable reduction in the molar mass and polydispersity when PETM was incorporated in a polymerisation (JHH159-JHH162). The molar mass and polydispersity decreased as the concentration of PETM increased. The effect appeared to plateau at a limiting concentration of PETM. The polymerisation conversion was low compared with the reported results under similar conditions.<sup>54,55</sup>

**Table 4-20 Samples prepared at 333K (non-solvent is methanol).**

Sample	[MMA] (%wt)	[AIBN] (%wt)	[PETM] (%wt)	M <sub>w</sub> (g/mol)	M <sub>n</sub> (g/mol)	D	Conv (%)
JHH159	23.6	0.14	0.00	103,000	57,700	1.78	60
JHH161*	23.6	0.14	0.38	41,500	27,200	1.52	44
JHH160*	23.6	0.14	0.46	27,900	19,600	1.42	55
JHH162*	23.6	0.14	0.58	28,800	20,300	1.41	55
JHH163	40.0	0.40	0.00	97,300	54,500	1.78	53
JHH164*	40.0	0.40	0.80	23,500	17,700	1.33	54

\* apparent molar mass data reported.

At a high concentration of MMA and PETM a polydispersity of 1.33 was obtained but the conversion to polymer was still low. The presence of PETM in the polymerisation can be clearly observed in the SEC profiles of JHH163 and JHH164 included in Figure 4-13.

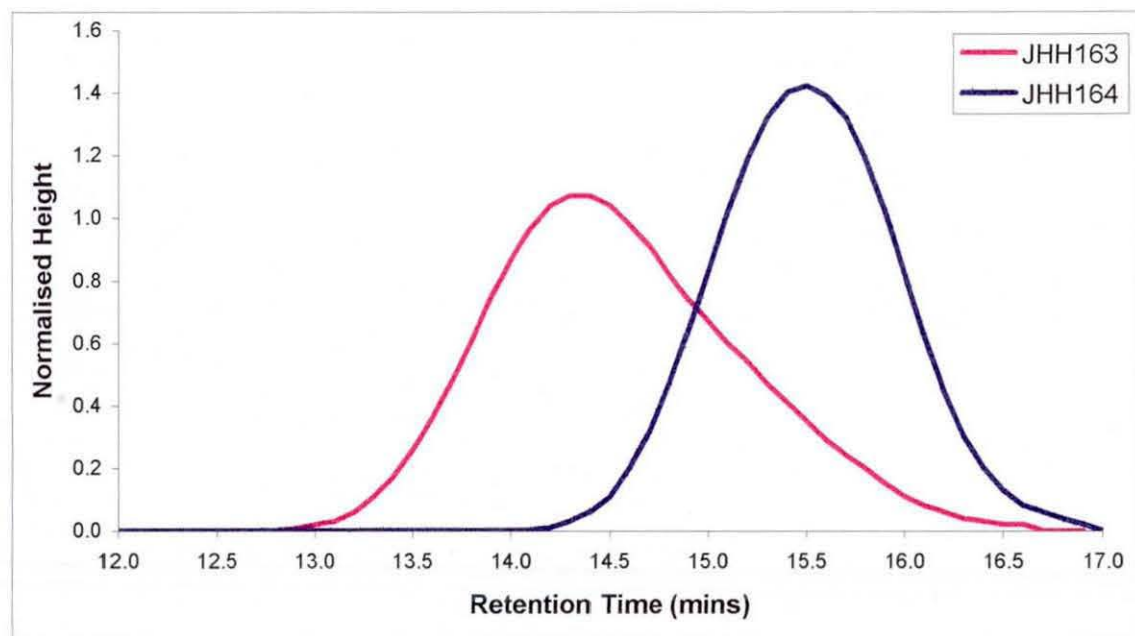


**Figure 4-13 The SEC profiles for JHH163 prepared in the absence of PETM and JHH164 prepared in the presence of PETM.**

Attempts were made to increase the conversion of the polymerisation by an increase in the polymerisation temperature. The results are included in Table 4-21.

**Table 4-21 PMMA prepared at 353K with PETM (non-solvent methanol).**

Sample	[MMA] (%wt)	[PETM] (%wt)	M <sub>w</sub> (g/mol)	M <sub>n</sub> (g/mol)	D	Conv (%)
JHH170	40	0	93,300	54,800	1.70	80
JHH171*	40	0.40	42,000	26,200	1.60	79
JHH172	40	0.80	39,100	24,800	1.58	74
JHH173*	40	1.20	25,500	18,000	1.41	66

[AIBN]=0.40 %wt. \* apparent molar mass data reported.

Conversion in the presence of a low concentration of PETM decreased as the concentration of PETM increased. The MMD of the polymers broadened at 353K compared with those prepared at 333K.

Low molar mass PMMA is known to be soluble in methanol.<sup>125</sup> It was suspected that maximum conversions were obtained but the low molar mass PMMA was being removed in the non-solvent. The non-solvent was changed from methanol to hexane. The results for samples precipitated in hexane are included in Table 4-22.

**Table 4-22 PMMA prepared at 353K with of PETM (non-solvent hexane).**

Sample	[MMA] (%wt)	[PETM] (%wt)	M <sub>w</sub> (g/mol)	M <sub>n</sub> (g/mol)	D	Conv. (%)
JHH200	40	0.00	43,300	23,200	1.87	93
JHH201*	40	0.40	35,000	18,600	1.88	98
JHH202*	40	0.80	22,300	13,000	1.73	95
JHH203*	40	1.20	16,600	9,800	1.70	94

[AIBN]=0.40% wt.

\* apparent molar mass data reported.

Within experimental error the conversions reached maximum conversion, which suggested that methanol selectively removed low molar mass PMMA. Recovery of the polymer with hexane decreased the average molar mass and increased the polydispersity of the final PMMA.

## 4.6 Branching Investigations with PCTA

All PCTA details are located in Table 4-18/p123 and Table 4-19/p123

### 4.6.1 Initial Investigations with MMA-co-HEMA PCTA

The polymerisation of MMA was performed under various conditions in the presence of a PCTA to understand how a PCTA interacted, if at all, in a polymerisation. The influence of a PCTA in the polymerisation of MMA on the SEC profiles is included in Figure 4-14. JHH228 was prepared in the presence of the PCTA 13L-M227 and JHH211 was prepared in the presence of the linear PMMA JHH85 under identical reaction conditions. JHH85 was a linear PMMA of similar molar mass to the PCTA and is included in the figure to illustrate the influence of the PCTA. The molar mass data for the samples is also included.<sup>ii</sup> The inclusion of a PCTA in the polymerisation broadened the MMD and reduced the molar mass slightly compared against JHH211 prepared in the presence of the linear polymer. It was suspected that the high molar mass material was predominantly branched polymer, which resulted from chain transfer reactions with the PCTA. JHH211 had a distinctive sloping tail in the SEC profile that was attributed to the added linear polymer. A branched polymer has a smaller hydrodynamic volume than a linear polymer of an equivalent molar mass, hence, the molar mass data in the absence of a mass detector may be inaccurate (assuming branching is present in the samples prepared in the presence of a PCTA).

ii	PCTA	Mw (g/mol)	Mn (g/mol)	D
JHH228*	13L-M227	48,300	16,600	2.90
JHH211	-	57,400	24,800	2.31
JHH85	-	13,800	8,200	1.69

\* apparent molar mass data reported.

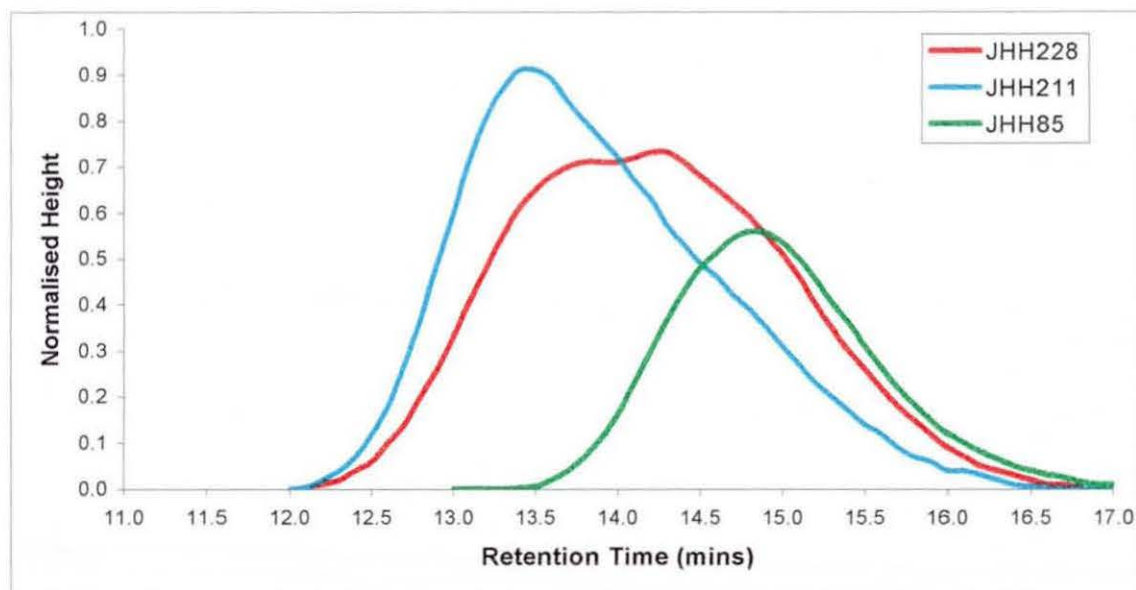


**Figure 4-14** The effect of PCTA on the molar mass (JHH228) against a sample prepared in the presence of linear PMMA (JHH211).

PMMA samples were prepared to explore various reaction parameters and to observe their effects on the MMD. A series of samples was prepared in the presence of a PCTA of varying molar mass but with a similar concentration of SH. The molar mass data for samples prepared is included in Table 4-23.

**Table 4-23** The molar mass data for samples prepared in the presence of a PCTA of increasing backbone molar mass at fixed PCTA concentration.

Sample	Copolymer $M_n$ (g/mol)	PCTA	$M_w$ (g/mol)	$M_n$ (g/mol)	D
JHH225*	5,500	6L-M215	32,700	14,300	2.28
JHH228*	12,800	13L-M227	48,300	16,600	2.90
JHH229*	19,800	20L-M223	121,000	23,500	5.15

[MMA]=40% wt, [PCTA]=8% wt, [AIBN]=0.4% wt.

\* apparent molar mass data reported.

An increase in the molar mass of the PCTA increased the molar mass of the resultant polymer and broadened the MMD. The MMD became less uniform as the molar mass of the PCTA increased; JHH229 was bimodal.

## 4.6.2 Investigations with BzMA-co-HEMA PCTA

The SEC data of PMMA samples prepared in the presence of a PCTA indicated a change in the MMD compared with a PMMA prepared in the presence of a linear PMMA. The observations suggested branching was the probable cause of the molar mass change but more evidence of incorporation was required. The UV-active chromophore in a BzMA-co-HEMA PCTA was utilised to confirm the modification of a PCTA in the polymerisation. SEC-UV was utilised to observe the retention time of the PCTA chromophore in the PMMA samples. A shift in the PCTA chromophore retention time indicated that the PCTA had been modified.

### 4.6.2.1 Reaction Variables

A series of experiments was performed to observe the effect of reaction variables on the retention time of the chromophore. Two PCTA were utilised: PCTA 5L-B326 and PCTA 16L-B250. Both had a similar concentration of SH.

JHH331 and JHH332 were prepared in the presence of PCTA 5L-B326 at two concentration levels. The results are included in Table 4-24. JHH311 was the copolymer precursor for PCTA 5L-B326, which could not be used as a reference material because of the suspected column damage analysing PCTA (see Section 3.6.2). An increase in concentration of PCTA 5L-B326 had no significant effects on the molar mass.

**Table 4-24 Molar mass data for samples prepared in the presence of PCTA 5L-B326.**

Sample	[5L-B326] (% wt)	M <sub>w</sub> (g/mol)	M <sub>n</sub> (g/mol)	D
JHH311	-	9,800	5,100	1.92
JHH331*	4	52,300	20,000	2.62
JHH332*	12	48,900	22,700	2.16

[MMA]=40% wt, [AIBN]=0.4% wt.

\* apparent molar mass data reported.

The chromatogram obtained from SEC-UV for JHH332 and JHH311 is included in Figure 4-15. JHH311 is included as a reference position for the chromophore of the unmodified PCTA. The responses from both the RI detector and the UV detector are included. The retention times from both detectors for the copolymer JHH311 were similar as expected. Comparison of the UV chromophore positions for JHH332 and JHH311 indicated that the PCTA had increased in molar mass. If the PCTA had remained unmodified the chromophore position would have remained unchanged in JHH332. The modification to molar mass was suspected to be branched polymer.

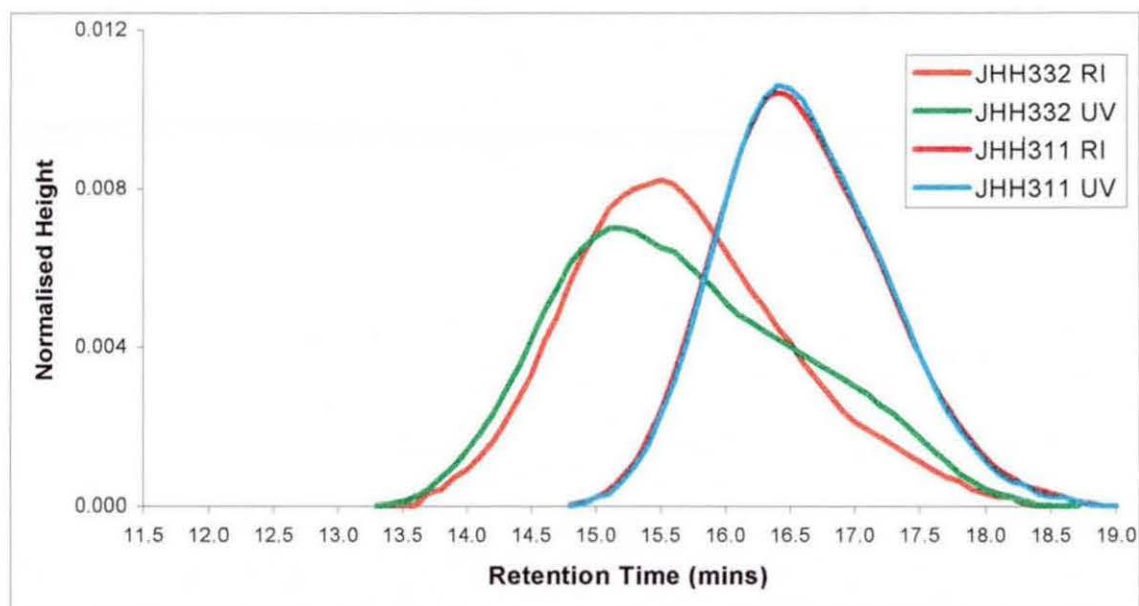


**Figure 4-15 The SEC-UV profiles for JHH332 and JHH311.**

JHH261 and JHH262 were prepared at two concentration levels with PCTA 16L-B250. The results are included in Table 4-25. JHH249 was the precursor of PCTA 16L-B250.

**Table 4-25 The molar mass data for samples prepared in the presence of PCTA 16L-B250.**

Sample	[16L-B250] (% wt)	$M_w$ (g/mol)	$M_n$ (g/mol)	D
JHH249	-	37,400	16,000	2.34
JHH261*	4	120,400	29,500	4.08
JHH262*	12	242,500	21,000	11.52

[MMA]=40% wt, [AIBN]=0.4% wt

\* apparent molar mass data reported.

An increase in the concentration of PCTA 16L-B250 increased the molar mass significantly and broadened the MMD of the resultant polymers. The chromatograms obtained from SEC-UV for JHH261 and JHH262 are included in Figure 4-16. JHH249 was the precursor copolymer for PCTA 16L-B250 and is included as a reference for the chromophore of the unmodified PCTA. The retention times from both the RI detector and the UV detector for the copolymer are the identical.

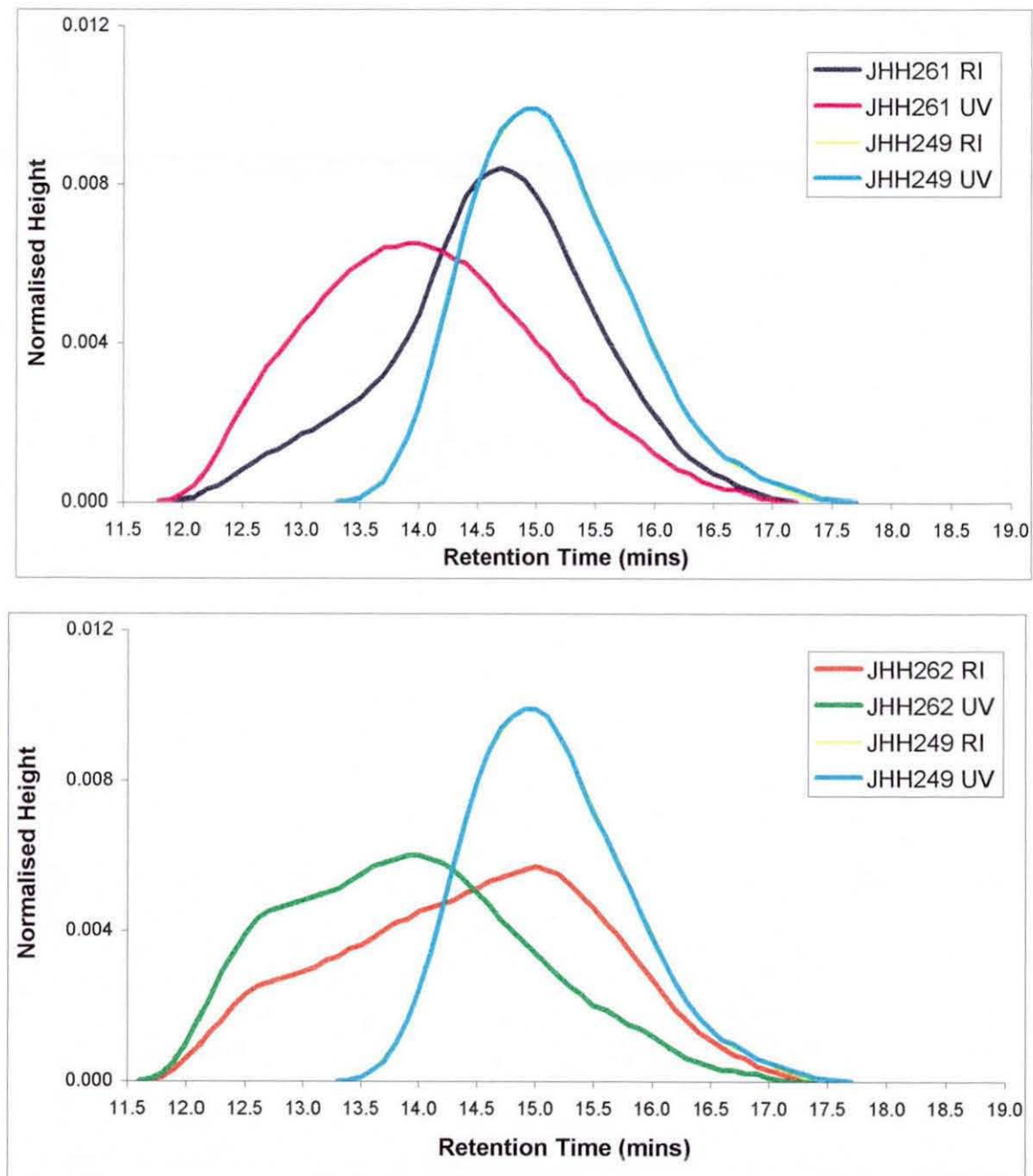


**Figure 4-16 The SEC-UV profiles for JHH261 and JHH262. JHH249 is included for reference as the precursor for PCTA 16L-B250.**

Inspection of the SEC chromatograms yielded interesting information about the effect of a PCTA in a polymerisation. The RI response for JHH261 had a distinct sloping shoulder at high molar mass that corresponded to the position of the chromophore, which suggested the PCTA had been modified. The relatively low UV response at lower molar mass suggested the presence of predominantly linear material, unreacted PCTA or PCTA with a low level of branching.

JHH262 had a large UV response that corresponded with high molar mass material. The low molar mass section of the distribution was predominantly linear polymer with a low response from the PCTA chromophore. A change in the concentration of PCTA 16L-B250 had significant effects on the position and distribution of PCTA in the polymer. A higher concentration of PCTA 16L-B250 increased the molar mass and MMD of the final polymer. Utilisation of a high molar mass PCTA produced a polymer of higher molar mass than its equivalent low molar mass PCTA at an equivalent concentration of SH.

#### 4.6.2.2 Phase Separation of PCTA

The polymerisation of MMA in the presence of a PCTA produced a turbid polymerisation mixture, even before the initiator had been added. The solubility characteristics of two PCTA samples of different molar mass with four solvents were investigated. The results obtained are summarised in Table 4-26. The solubility was assessed visually and graded from 1 to 5 (5 being readily soluble). The concentration of PCTA represented the limit utilised in these studies. The low molar mass PCTA 6L-M215 was slightly more soluble with a given solvent than its higher molar mass counterpart PCTA 20L-M223.

**Table 4-26 Summary of solubility results of PCTA in various solvents.**

PCTA	[PCTA] (%wt)	Visual Assessment of Solubility			
		Toluene	THF	MEK	EtAc
6L-M215	12	3/5	5/5	5/5	2/5
20L-M223	12	2/5	4/5	5/5	2/5

With both toluene and ethyl acetate, fine particulate material settled to the bottom of the tube when left for 24 hours, leaving a clear solution. When the tube was agitated the particles became suspended and the solution became cloudy.

The polymerisation mixture of MMA and PCTA in MEK was heterogeneous; however, PCTA at an equivalent concentration was readily soluble in both MEK and THF. This indicated that MMA was responsible for the solution heterogeneity. Indeed, a MEK/MMA mixture produced a turbid solution, which suggested PCTA was not completely soluble in its own monomer. The solubility of PCTA in certain solvents suggested that high molar mass coupled PCTA molecules were present in the PCTA. The reactivity of SH groups with oxygen to yield disulphide is well known.<sup>123,126</sup>

The PCTA purification method was modified to include a filtration step that removed the high molar mass material. The polymerisation mixture containing PCTA, toluene and MMA was homogeneous with the inclusion of a filtration step.

#### **4.6.2.3 Phase Separation during Polymerisation with PCTA**

The onset of partial phase separation in the polymerisation mixture was observed 45-60 minutes into the polymerisation. The phase-separated material was probably coupled PCTA or highly branched PMMA. Phase separation using other PCTA-based systems had been observed previously.<sup>13</sup> The influence of the phase-separated component was investigated by preparing two PMMA samples under identical conditions and filtering one of them post-polymerisation. Both solutions were initially homogeneous and both polymerisation mixtures were turbid on completion. JHH314 was filtered to yield a clear solution before the final precipitation step. Both JHH314 and JHH315 were characterised using TDSEC. The data obtained from TDSEC is located in Table 4-28/p138 and Figure 4-18. The filtration step yielded a polymer marginally lower in branching. The data is discussed in Section 5.4.3.

Both samples were subjected to solubility tests in THF. The filtered JHH314 produced a less turbid solution but still contained phase separated material (suspected to be microgel).

## 4.7 Characterisation of Samples by TDSEC

TDSEC was utilised to confirm the presence and level of branching in PMMA samples prepared in the presence of a PCTA. Samples were characterised in two series on two separate visits. *The mobile phase was THF in the first series and chloroform in second series.*

Samples characterised in the first series were used to obtain an understanding of how branching was influenced by specific variables. A comprehensive matrix of further samples was developed and characterised in the second series to explore the reaction variables in more detail. The variables investigated were:

- PCTA concentration.
- Molar mass of PCTA.
- Functionality of PCTA.
- MMA concentration.
- AIBN concentration.

The branching data is discussed in **Section 5**.

### Note: Calculation of the concentration of free SH

The value for the free concentration of SH quoted in the TDSEC data tables was calculated based on a PCTA mass in a 10g polymerisation. The mass fraction of free SH was used to calculate the free SH concentration. A molar mass of 205 g/mol was used for a HEMA unit with TGA reacted on. i.e. JHH225 prepared in the presence of the PCTA [6L-M215]=8% wt.

Mass fraction of free SH in PCTA 6L-M215 determined from proton NMR data is 0.062. In a 10g polymerisation there will be 0.8g of PCTA. Therefore, the mass of free SH is  $0.8g \times 0.062 = 0.0496g$  and the concentration in moles is then  $0.0496g / 205 \text{ g/mol} = 0.242 \text{ mmol}$  (value quoted).

## 4.7.1 Series ONE

### 4.7.1.1 Linear Samples

Linear polymers were characterised with branched samples to assess the effect of a PCTA on solution properties. The molar mass and branching data for a selected number of linear samples are included in Table 4-27. The solution properties of the linear PMMA samples corresponded with expected values for linear PMMA in THF at 298K ( $\alpha=0.72$  and  $\log K = -4.13$ ).<sup>127</sup> The MMD and M-H plots for the linear samples are included with the branched samples for comparison.

**Table 4-27 Summary of data for linear polymers.**

Sample	Temp (K)	[MMA] (% wt)	[AIBN] (% wt)	M <sub>w</sub> (g/mol)	M <sub>n</sub> (g/mol)	D	g'	<i>a</i>	Log K
JHH200	353	40	0.40	46,200	24,500	1.89	0.98	0.71	-4.05
JHH239	333	40	0.64	149,900	84,600	1.77	0.95	0.75	-4.27

#### 4.7.1.2 Samples Prepared with MMA-co-HEMA PCTA

Numerical data obtained for samples prepared in the presence of various MMA-co-HEMA PCTA are included in Table 4-28. The corresponding MMD, M-H and  $g'$  plots are illustrated in Figure 4-17/p139 and Figure 4-18/p140.

JHH225, JHH228 and JHH229 explored the effect of a PCTA molar mass. JHH314 (filtered) and JHH315 investigated the implication of filtering a sample post-polymerisation.

**Table 4-28 Samples prepared in the presence of a MMA-co-HEMA PCTA.**

Sample	PCTA	Free [SH] <sup>a</sup> (mmol)	[MMA] (% wt)	[PCTA] (% wt)	[AIBN] (% wt)	M <sub>w</sub> (g/mol)	M <sub>n</sub> (g/mol)	D	g'	<i>a</i>	Log K
JHH225	6L-M215	0.24	40	8	0.40	36,600	16,900	2.17	0.82	0.60	-3.61
JHH228	13L-M227	0.25	40	8	0.40	74,400	23,000	3.23	0.72	0.51	-3.22
JHH229	20L-M223	0.28	40	8	0.40	393,100	26,800	14.67	0.66	0.41	-2.77
JHH314 <sup>b</sup>	20L-M293	0.26	40	10	0.40	352,200	31,600	11.15	0.65	0.44	-2.88
JHH315	20L-M293	0.26	40	10	0.40	470,800	29,500	15.96	0.69	0.42	-2.78

<sup>a</sup> Concentration of free SH based on a 10g polymerisation.

<sup>b</sup> JHH314 filtered post-polymerisation.

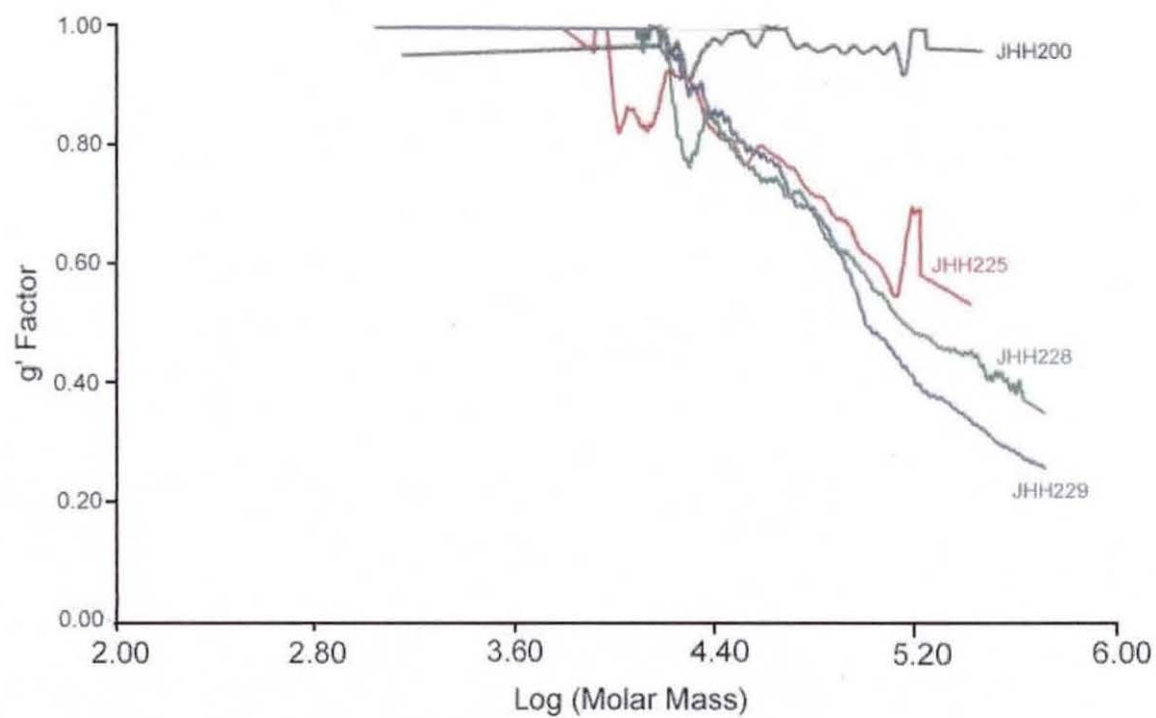
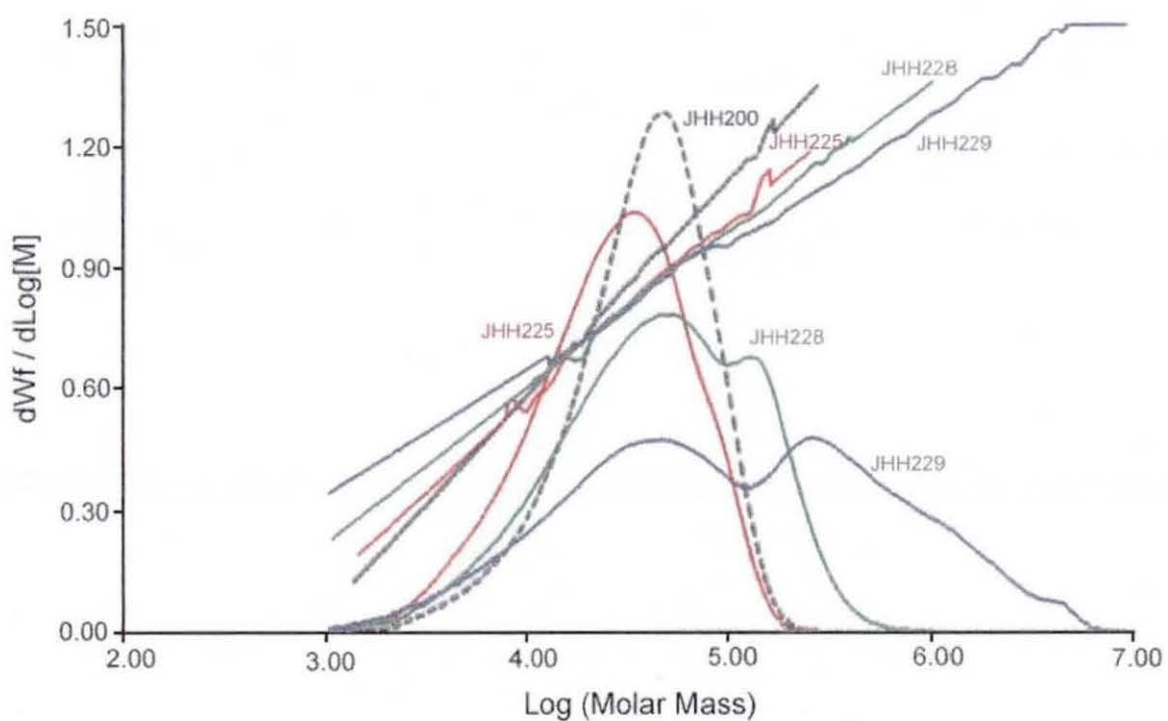


Figure 4-17 The MMD, M-H and  $g'$  plots for JHH225, JHH228 and JHH229.

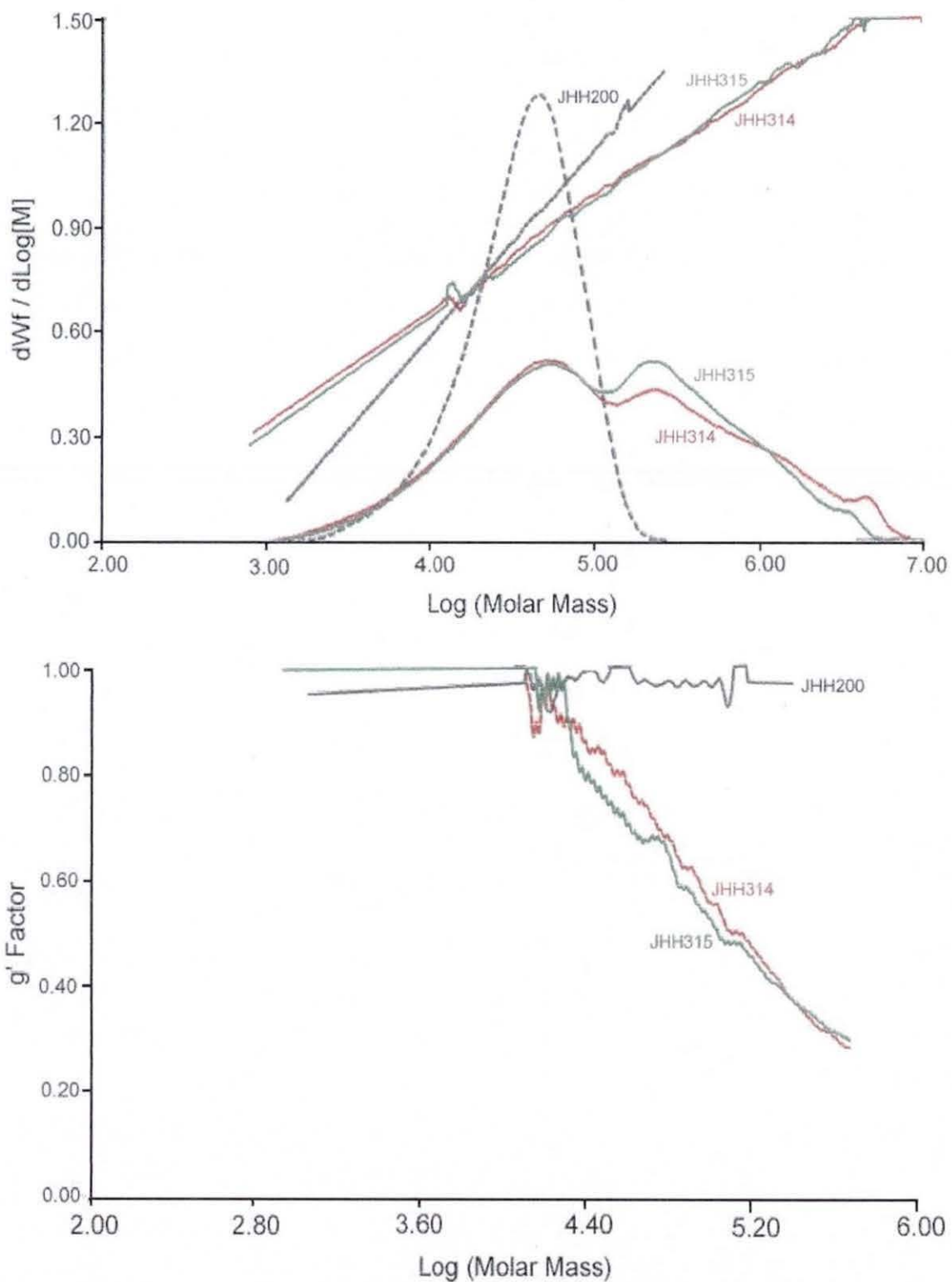


Figure 4-18 The MMD, M-H and  $g'$  plots for JHH314 and JHH315.

#### 4.7.1.3 Samples Prepared with BzMA-co-HEMA PCTA

Numerical data obtained for samples prepared in the presence of a BzMA-co-HEMA PCTA are included in Table 4-29. The corresponding MMD, M-H and  $g'$  plots are illustrated in Figure 4-19/p143.

**Table 4-29 Samples prepared in the presence of a BzMA-co-HEMA PCTA.**

Sample	PCTA	Free [SH] <sup>a</sup> (mmol)	[MMA] (% wt)	[PCTA] (% wt)	[AIBN] (% wt)	M <sub>w</sub> (g/mol)	M <sub>n</sub> (g/mol)	D	g'	<i>a</i>	Log K
JHH331	5L-B326	0.08	40	4	0.40	65,100	26,200	2.48	0.83	0.59	-3.53
JHH332	5L-B326	0.20	40	10	0.40	66,800	23,100	2.89	0.72	0.51	-3.22

<sup>a</sup> Concentration of free SH based on a 10g polymerisation.

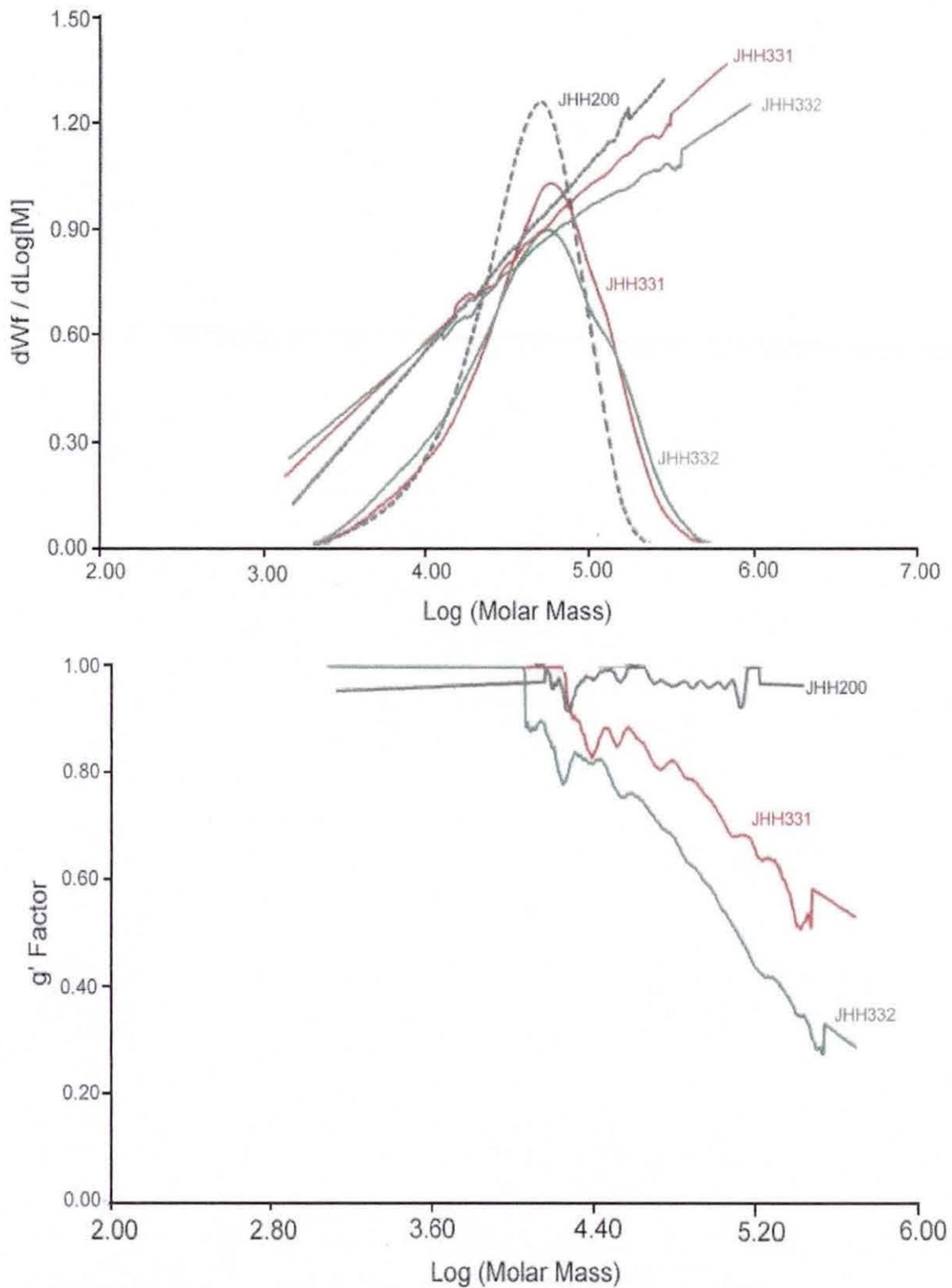


Figure 4-19 The MMD, M-H and  $g'$  plots for JHH331 and JHH332.

## 4.7.2 Series TWO

### 4.7.2.1 Linear/Reference Samples

A series of reference polymers was prepared under identical conditions to the branched samples except a linear PMMA was substituted for a PCTA. The effect associated with the inclusion of PCTA was studied. The molar mass and branching data are included in Table 4-30. The linear samples covered the molar mass range of typical branched samples (6 to 55 kg/mol). The branching parameter  $g'$  was close to unity and the M-H exponent  $a$  and constant Log K were similar to reported values for linear PMMA in chloroform ( $a=0.79$  and Log K = -4.22).<sup>128</sup> The MMD and M-H plots for the linear standard and reference samples are illustrated in Figure 4-20. The linear relationship between the intrinsic viscosity and the molar mass was consistent throughout the molar mass range of standard linear and reference polymers.

Polydisperse linear standard samples were included in the characterisation runs to check the quality of the data.

**Table 4-30 The preparation and characterisation data of linear/reference PMMA.**

Sample	PMMA M <sub>n</sub> <sup>a</sup> (g/mol)	[MMA] (% wt)	[PMMA] (% wt)	[AIBN] (% wt)	M <sub>w</sub> (g/mol)	M <sub>n</sub> (g/mol)	D	g'	$\alpha$	Log K
19_120k2	-	VISCOTEK STANDARD			115,700	55,300	2.09	1.00	0.75	-4.07
JHH200	-	40	-	0.40	40,700	17,300	2.35	1.00	0.78	-4.21
JHH457	6,300	40	12	2.40	12,200	5,900	2.06	0.99	0.73	-4.00
JHH456	6,300	40	12	0.60	26,000	11,300	2.30	0.99	0.76	-4.12
JHH458	17,900	40	6	0.60	40,600	18,900	2.15	0.98	0.75	-4.11

<sup>a</sup> Linear PMMA of similar molar mass and polydispersity to corresponding PCTA.

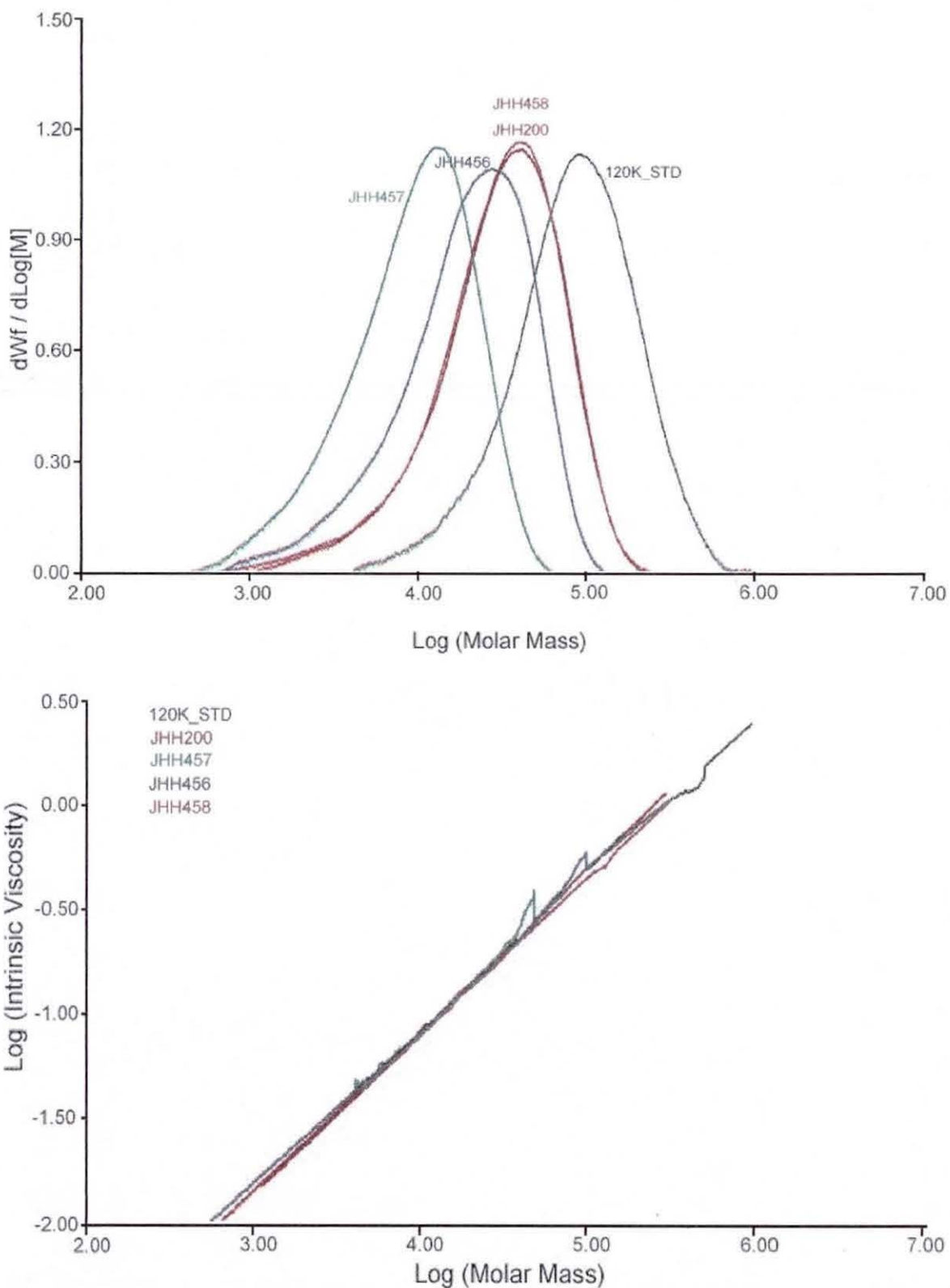


Figure 4-20 The MMD and M-H plot for the linear reference samples.

#### 4.7.2.2 Samples Prepared with MMA-co-HEMA PCTA

Numerical data obtained for samples prepared in the presence of MMA-co-HEMA PCTA is included in Table 4-31/p148, Table 4-32/p151, Table 4-33/p155 and Table 4-34/p159. The corresponding MMD, M-H and  $g'$  plots follow each table.

Conversion reactions were performed with a selected number of samples. The results are included in Table 4-35/p163.

Table 4-31 Samples prepared in the presence of a 6 kg/mol PCTA at [PCTA]=6% wt

Sample	PCTA	Free [SH] <sup>a</sup> (mmol)	[MMA] (% wt)	[AIBN] (% wt)	M <sub>w</sub> (g/mol)	M <sub>n</sub> (g/mol)	D	g'	<i>a</i>	Log K
JHH440	6H-M426	0.33	20	0.30	28,800	6,400	4.49	0.62	0.44	-2.87
JHH441	6H-M426	0.33	20	1.20	24,700	6,800	3.62	0.69	0.49	-3.07
JHH428	6H-M426	0.33	40	0.30	63,000	15,100	4.17	0.87	0.61	-3.50
JHH429	6H-M426	0.33	40	1.20	32,100	6,300	5.03	0.85	0.56	-3.31

[PCTA]=6% wt

<sup>a</sup> Concentration of free SH based on a 10g polymerisation.

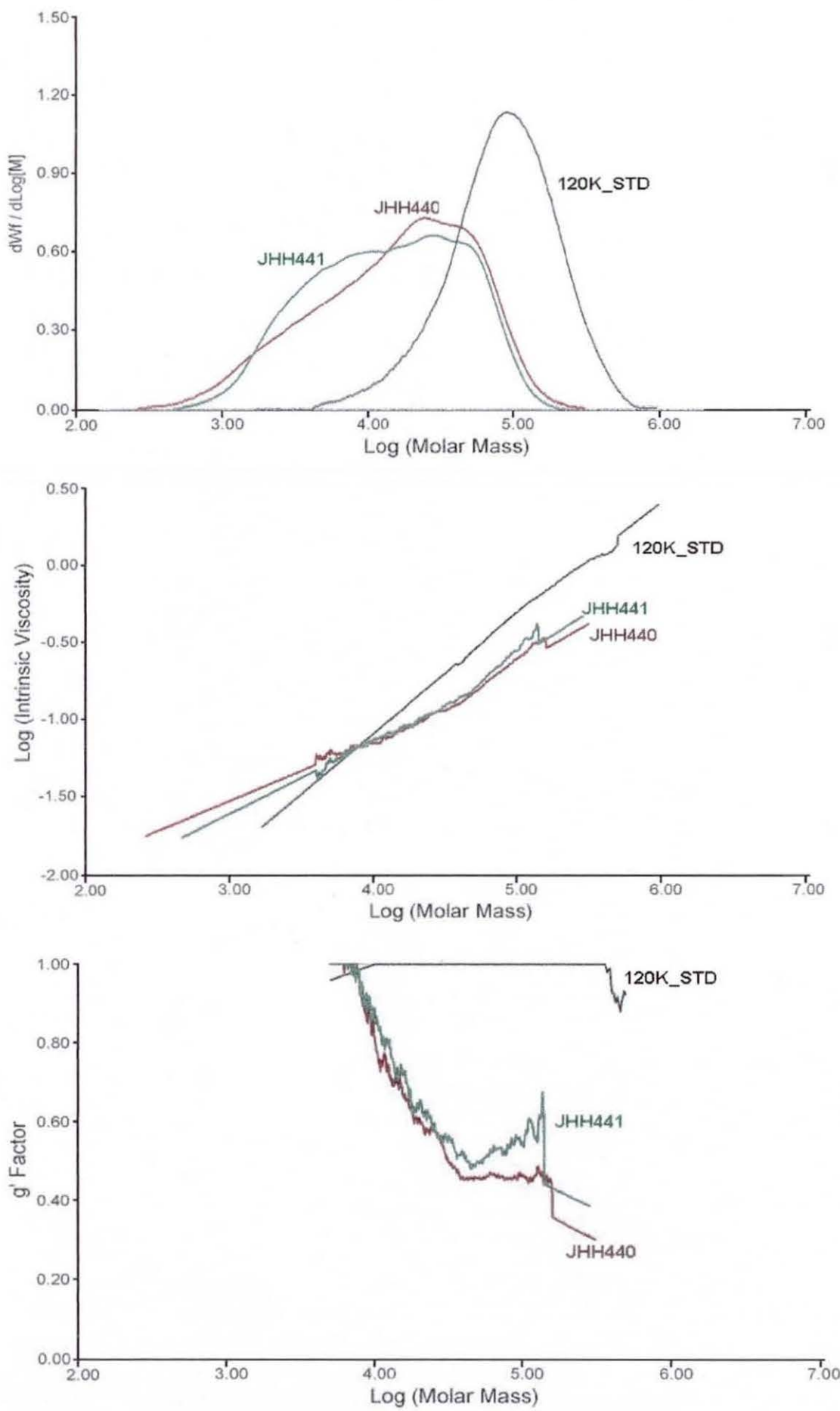


Figure 4-21 The MMD, M-H and  $g'$  plots of JHH440 and JHH441.

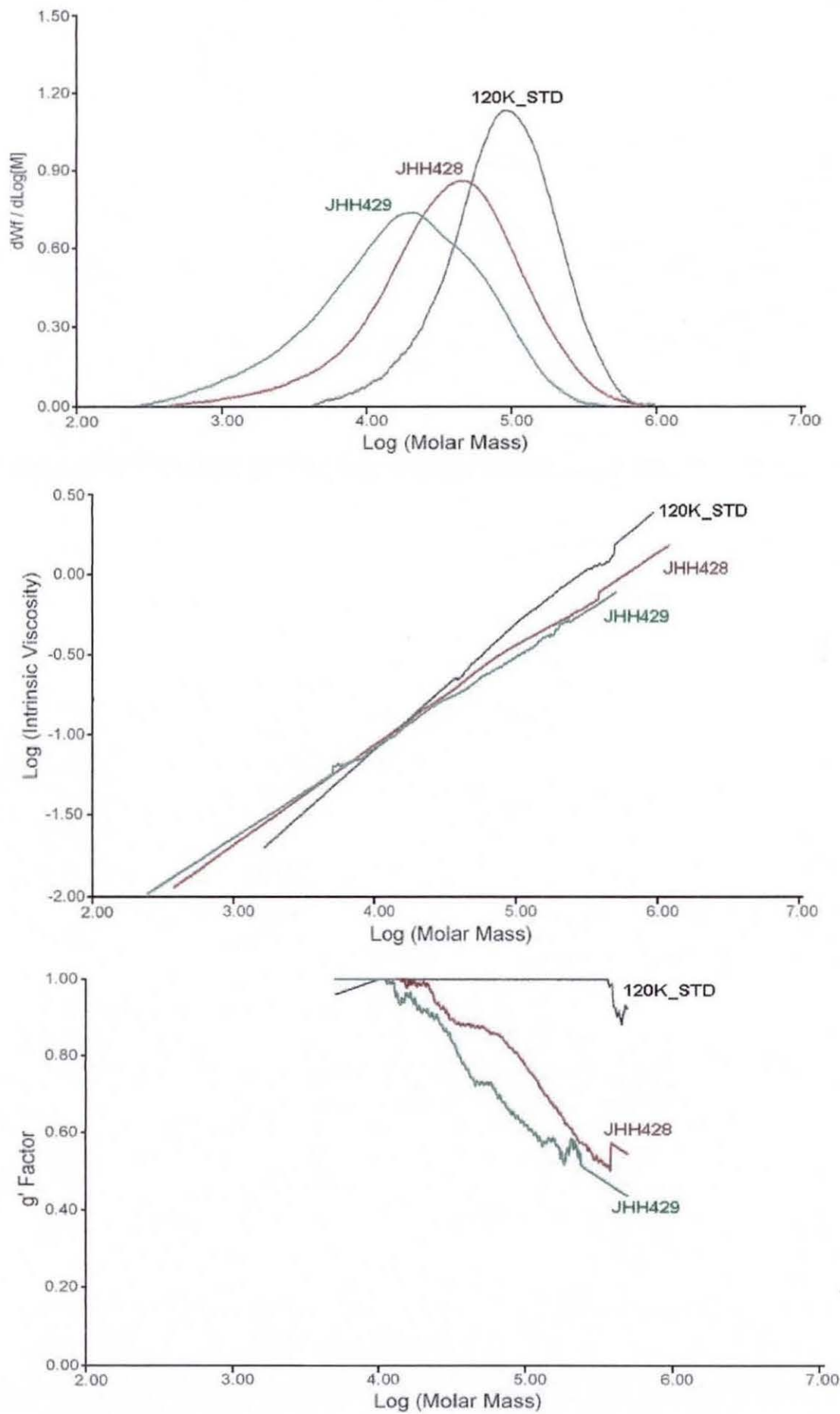


Figure 4-22 The MMD, M-H and  $g'$  plots of JHH428 and JHH429.

**Table 4-32 Samples prepared in the presence of a 6 kg/mol PCTA at [PCTA]=12% wt**

Sample	PCTA	Free [SH] <sup>a</sup> (mmol)	[MMA] (% wt)	[AIBN] (% wt)	M <sub>w</sub> (g/mol)	M <sub>n</sub> (g/mol)	D	g'	<i>a</i>	Log K
JHH462	6L-M402	0.38	40	0.30	18,700	7,700	2.44	0.69	0.64	-3.75
JHH408	6L-M402	0.38	40	0.60	18,800	9,100	2.08	0.68	0.62	-3.66
JHH409	6L-M402	0.38	40	2.40	14,400	4,000	3.59	0.81	0.45	-2.87
JHH442	6H-M426	0.66	20	0.60	32,700	10,500	3.11	0.65	0.54	-3.29
JHH443	6H-M426	0.66	20	2.40	22,600	3,100	7.41	0.66	0.37	-2.58
JHH463	6H-M426	0.66	40	0.30	52,400	7,400	7.11	0.67	0.43	-2.76
JHH430	6H-M426	0.66	40	0.60	44,900	10,900	4.12	0.63	0.55	-3.33
JHH431	6H-M426	0.66	40	2.40	25,600	3,090	8.28	0.69	0.36	-2.50

[PCTA]=12% wt

<sup>a</sup> Concentration of free SH based on a 10g polymerisation.

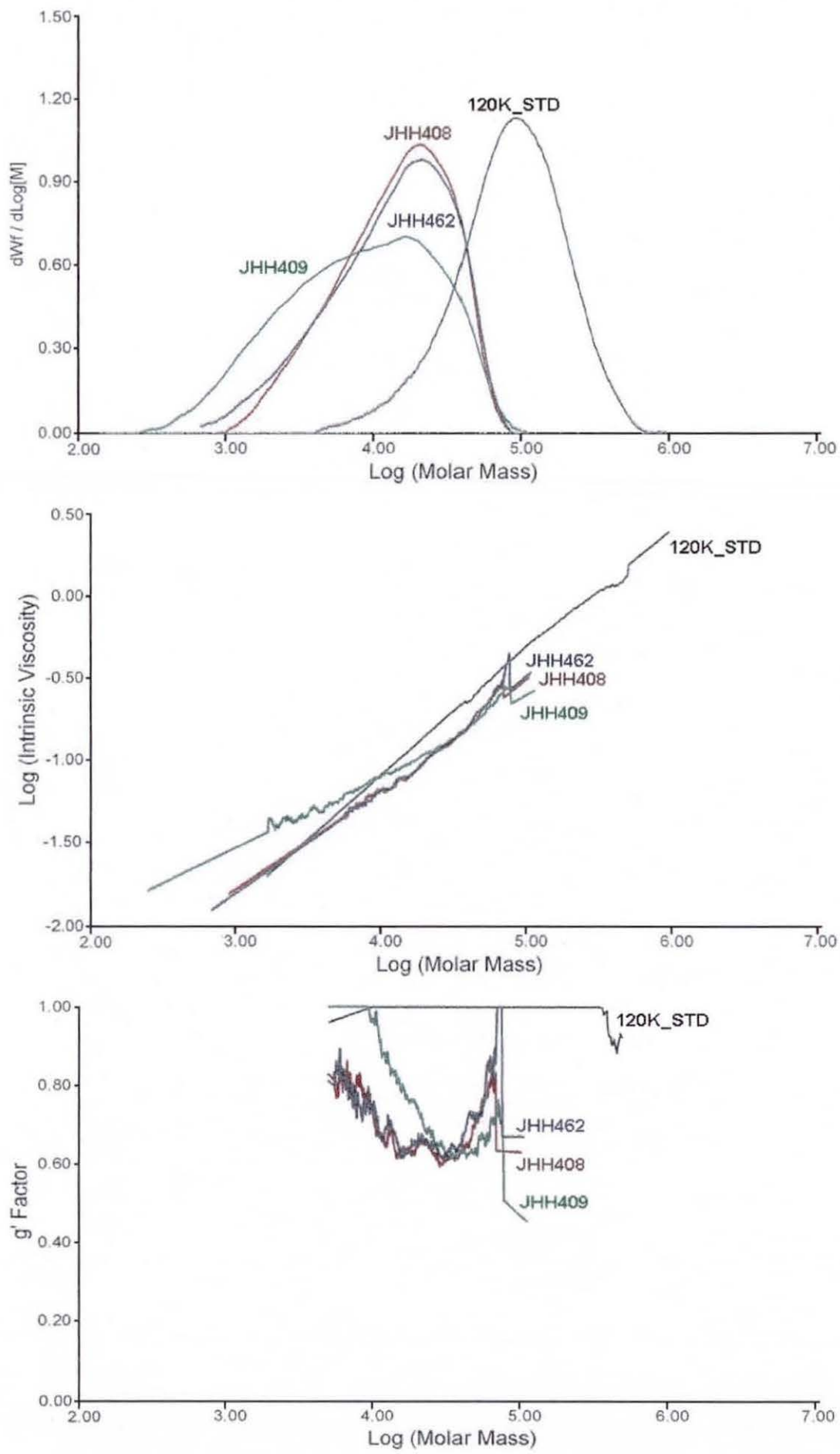


Figure 4-23 The MMD, M-H and  $g'$  plots of JHH462, JHH408 and JHH409.

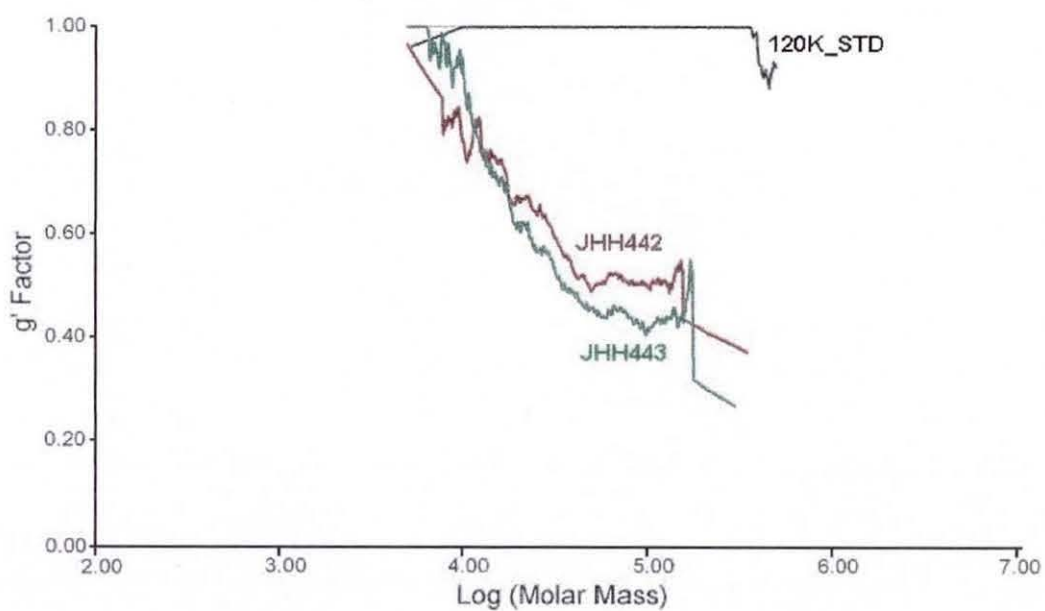
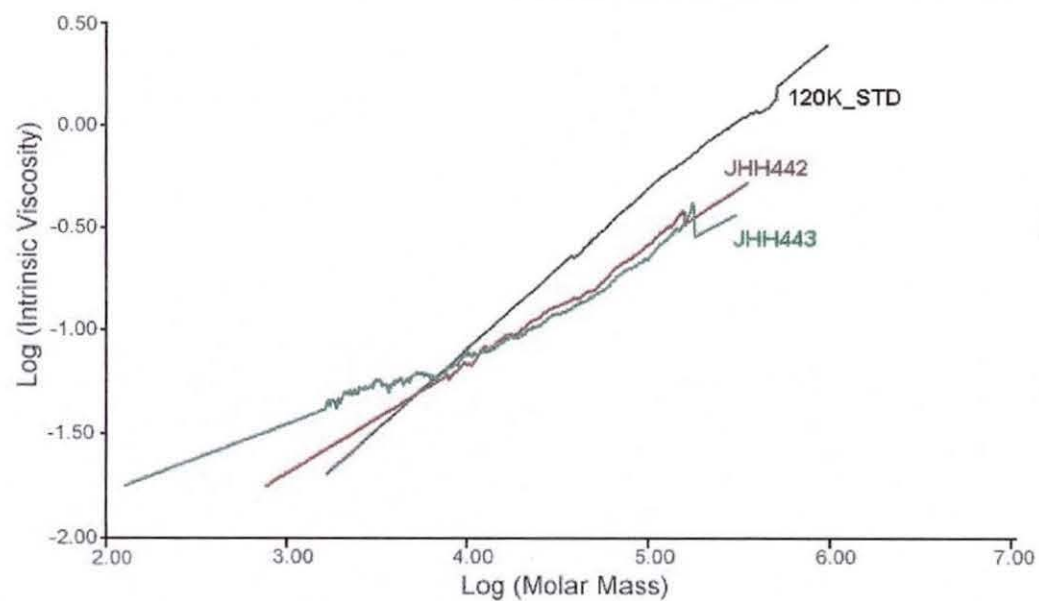
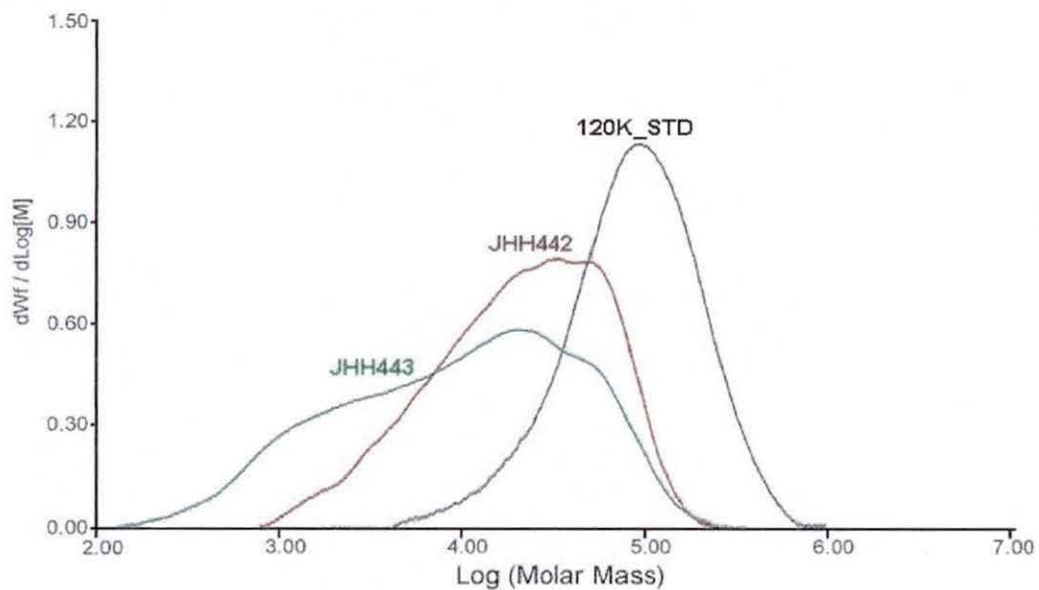


Figure 4-24 The MMD, M-H and  $g'$  plots of JHH442 and JHH443.

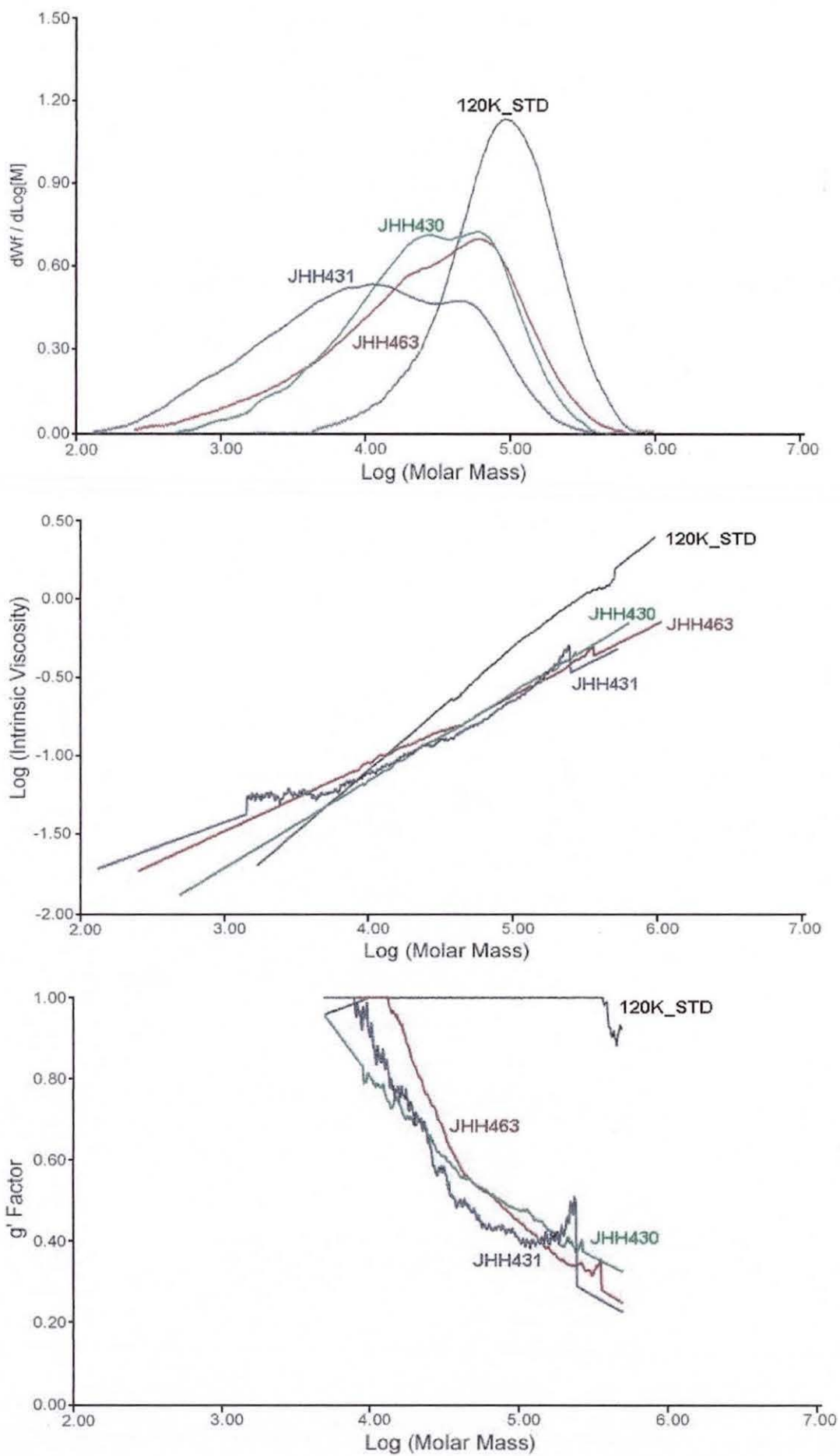


Figure 4-25 The MMD, M-H and  $g'$  plots of JHH463, JHH430 and JHH431.

Table 4-33 Samples prepared in the presence of a 16 kg/mol PCTA at [PCTA]=6% wt

Sample	PCTA	Free [SH] <sup>a</sup> (mmol)	[MMA] (% wt)	[AIBN] (% wt)	M <sub>w</sub> (g/mol)	M <sub>n</sub> (g/mol)	D	g'	<i>a</i>	Log K
JHH410	16L-M403	0.18	40	0.30	91,400	11,400	8.02	0.71	0.53	-3.16
JHH411	16L-M403	0.18	40	1.20	53,100	6,300	8.47	0.70	0.49	-3.05
JHH436	16H-M427	0.35	20	0.30	63,800	17,000	3.75	0.63	0.53	-3.24
JHH437	16H-M427	0.35	20	1.20	37,900	5,800	6.58	0.74	0.42	-2.76
JHH464	16H-M427	0.35	40	0.15	280,300	50,500	5.55	0.67	0.49	-2.97
JHH432	16H-M427	0.35	40	0.30	135,200	26,100	5.18	0.70	0.52	-3.13
JHH433	16H-M427	0.35	40	1.20	35,600	5,500	6.51	0.78	0.53	-3.21

[PCTA]=6% wt

<sup>a</sup> Concentration of free SH based on a 10g polymerisation.

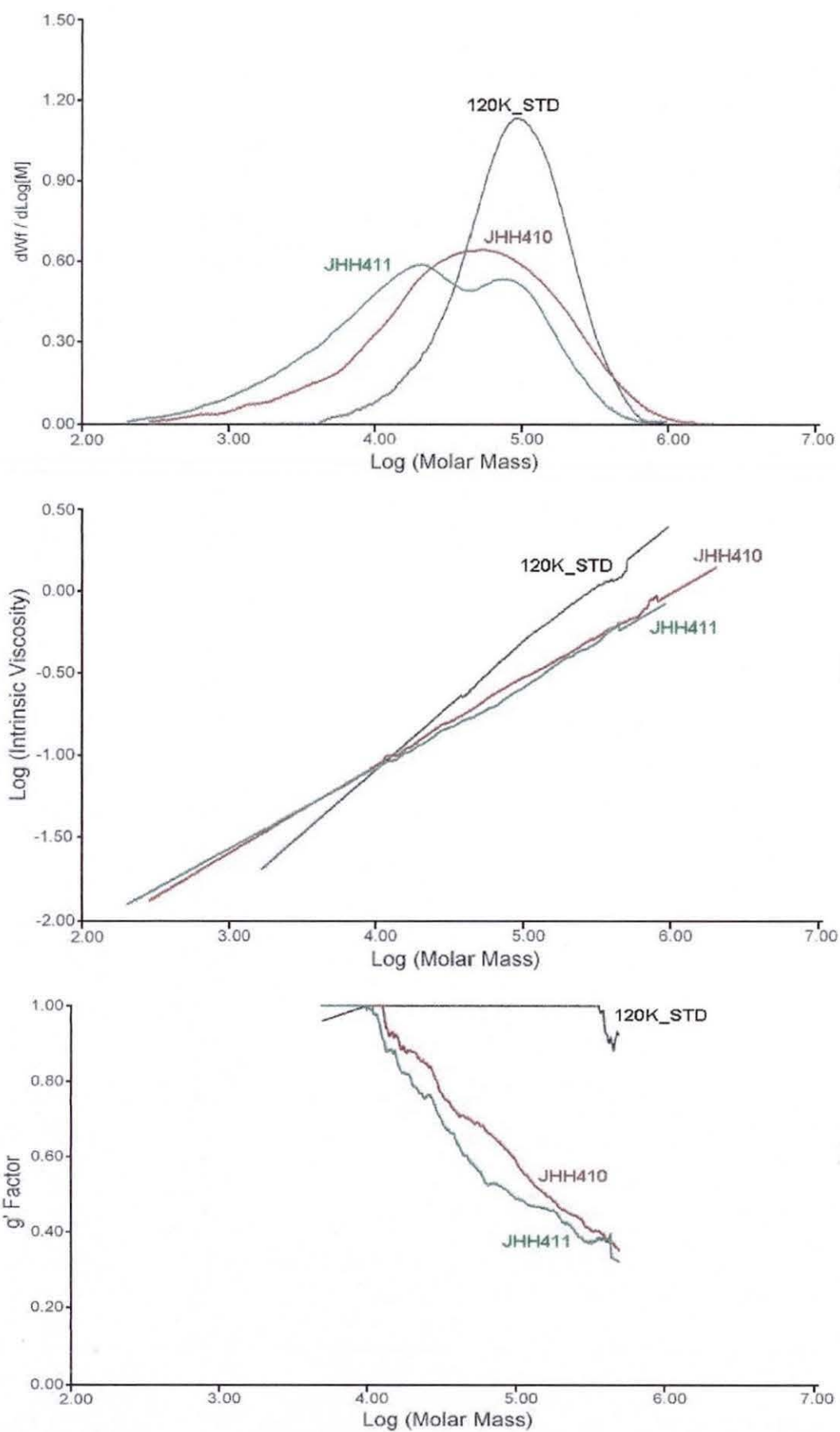


Figure 4-26 The MMD, M-H and  $g'$  plots of JHH410 and JHH411.

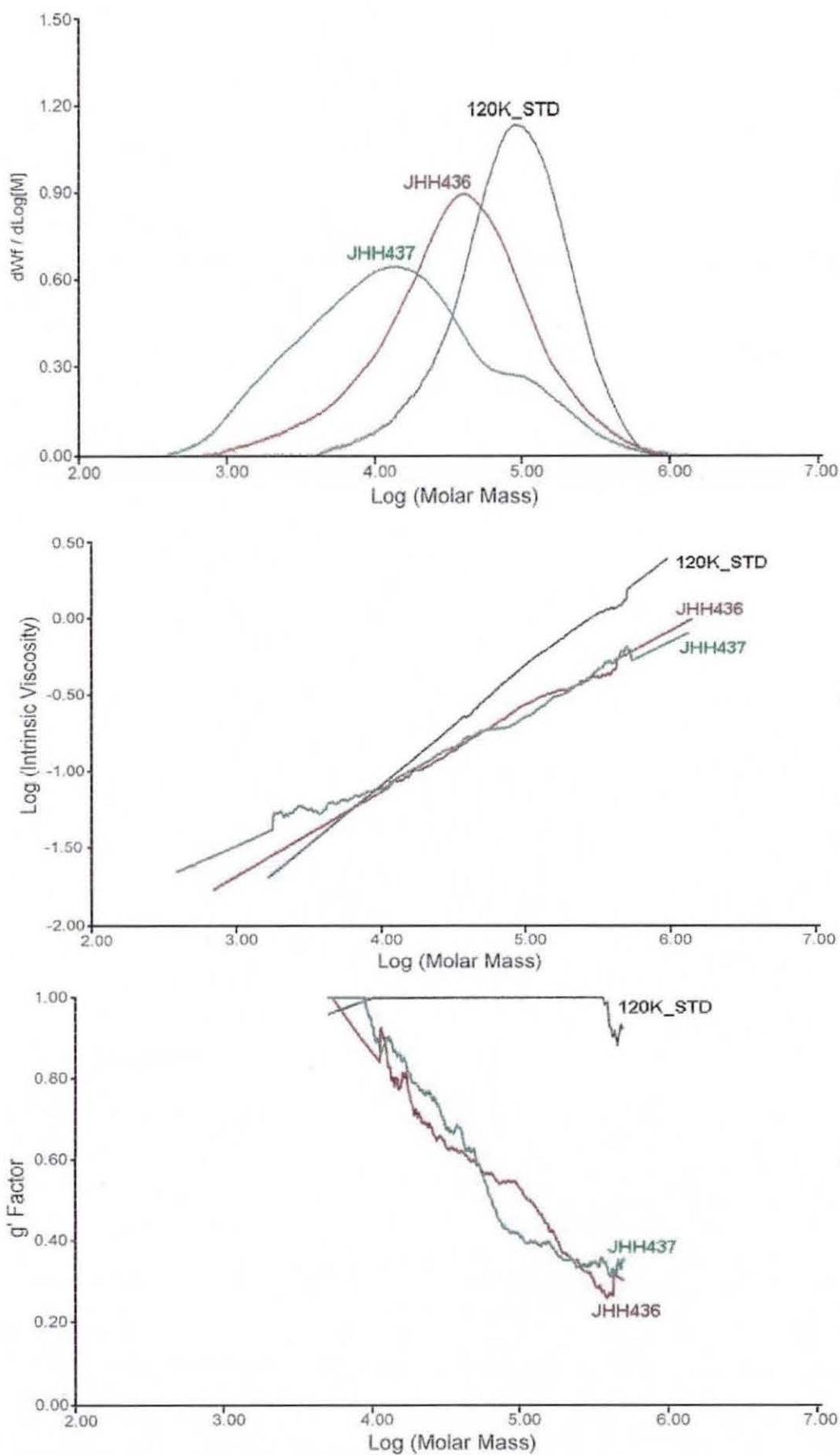


Figure 4-27 The MMD, M-H and  $g'$  plots of JHH436 and JHH437.

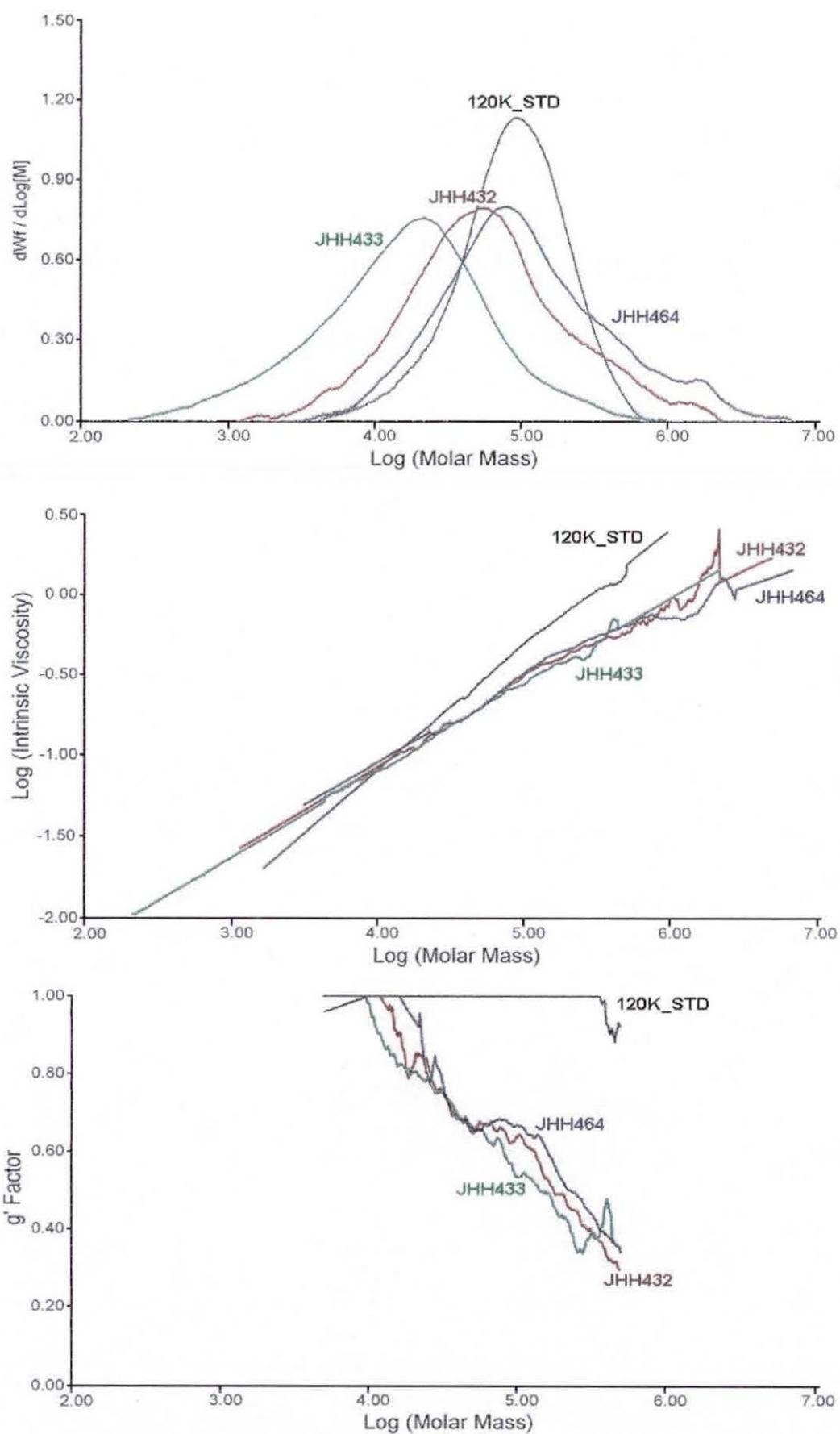


Figure 4-28 The MMD, M-H and  $g'$  plots of JHH464, JHH432 and JHH433.

**Table 4-34 Samples prepared in the presence of a 16 kg/mol PCTA at [PCTA]=12% wt**

Sample	PCTA	Free [SH] <sup>a</sup> (mmol)	[MMA] (% wt)	[AIBN] (% wt)	M <sub>w</sub> (g/mol)	M <sub>n</sub> (g/mol)	D	g'	<i>a</i>	Log K
JHH465	16L-M403	0.36	40	0.30	68,200	4,400	15.50	0.59	0.460	-2.93
JHH412	16L-M403	0.36	40	0.60	57,300	6,000	9.55	0.58	0.47	-3.01
JHH413	16L-M403	0.36	40	2.40	40,900	6,200	6.59	0.58	0.47	-3.04
JHH438	16H-M427	0.70	20	0.60	125,400	6,600	18.91	0.56	0.44	-2.86
JHH439	16H-M427	0.70	20	2.40	159,100	34,800	4.57	0.22	0.61	-3.92
JHH466	16H-M427	0.70	40	0.30	336,400	6,300	53.31	0.75	0.37	-2.41
JHH434	16H-M427	0.70	40	0.60	176,100	9,400	18.85	0.69	0.44	-2.81
JHH435	16H-M427	0.70	40	2.40	79,600	11,100	7.17	0.50	0.51	-3.25

[PCTA]=12% wt

<sup>a</sup> Concentration of free SH based on a 10g polymerisation.

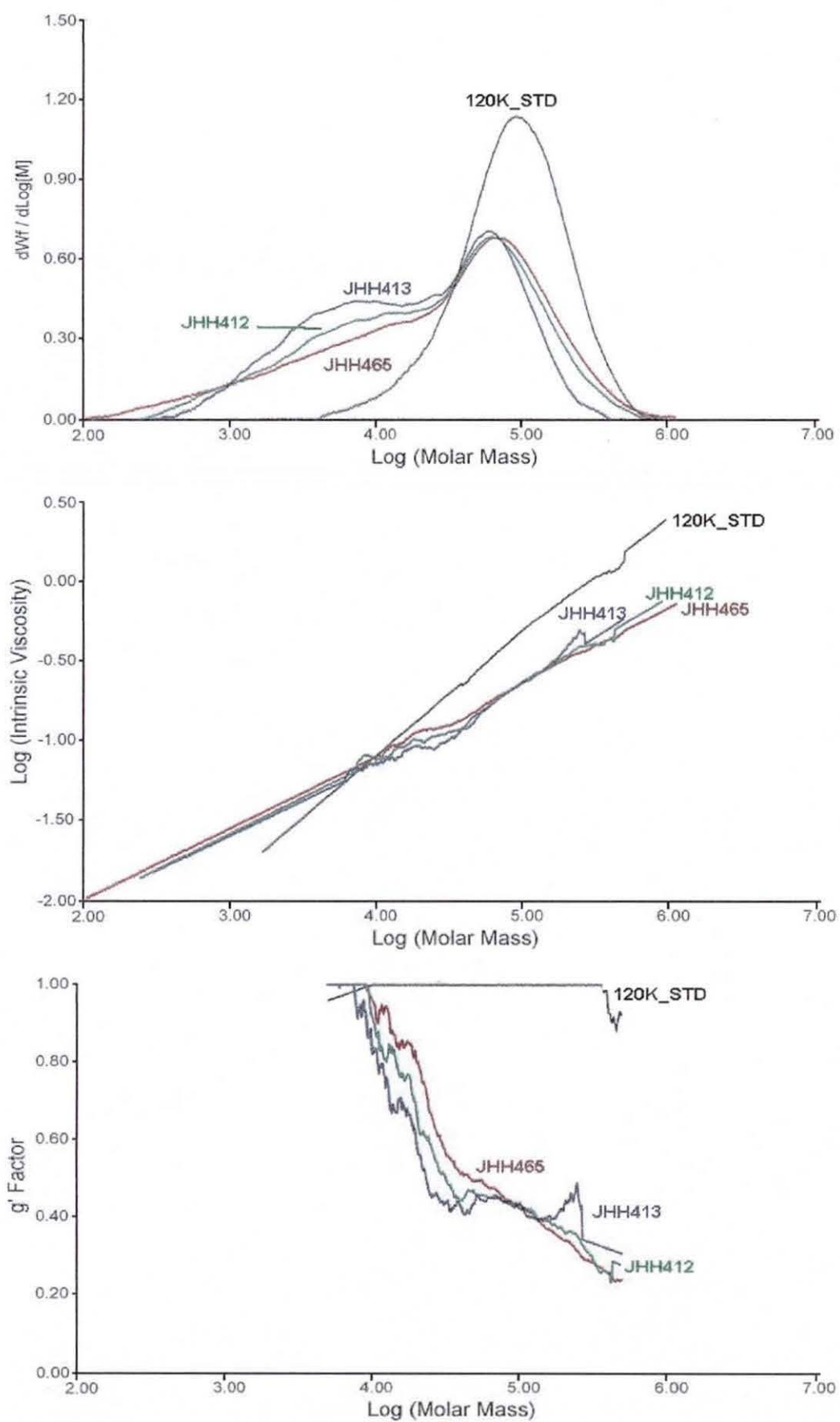


Figure 4-29 The MMD, M-H and  $g'$  plots of JHH465, JHH412 and JHH413.

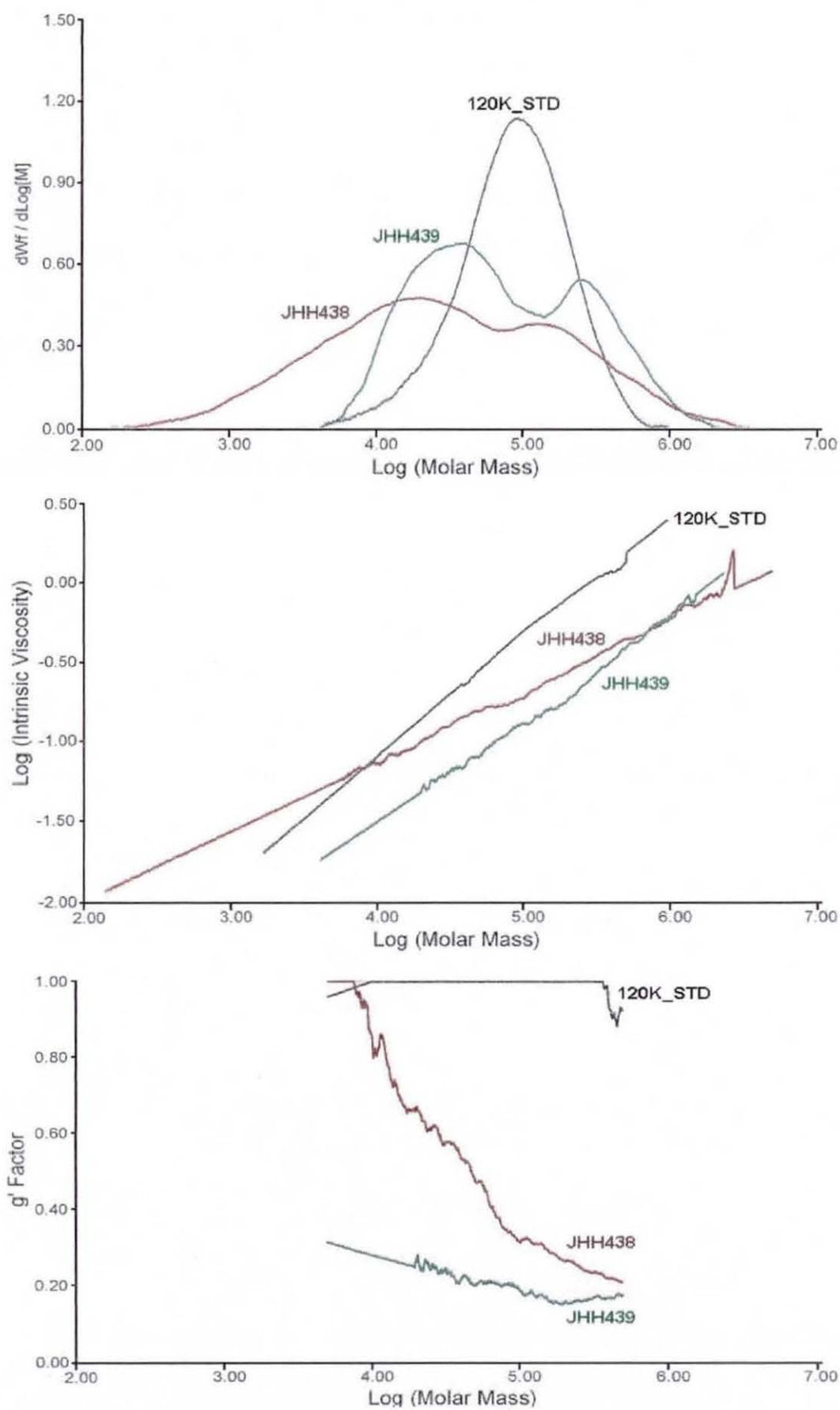


Figure 4-30 The MMD, M-H and  $g'$  plots of JHH438 and JHH439.

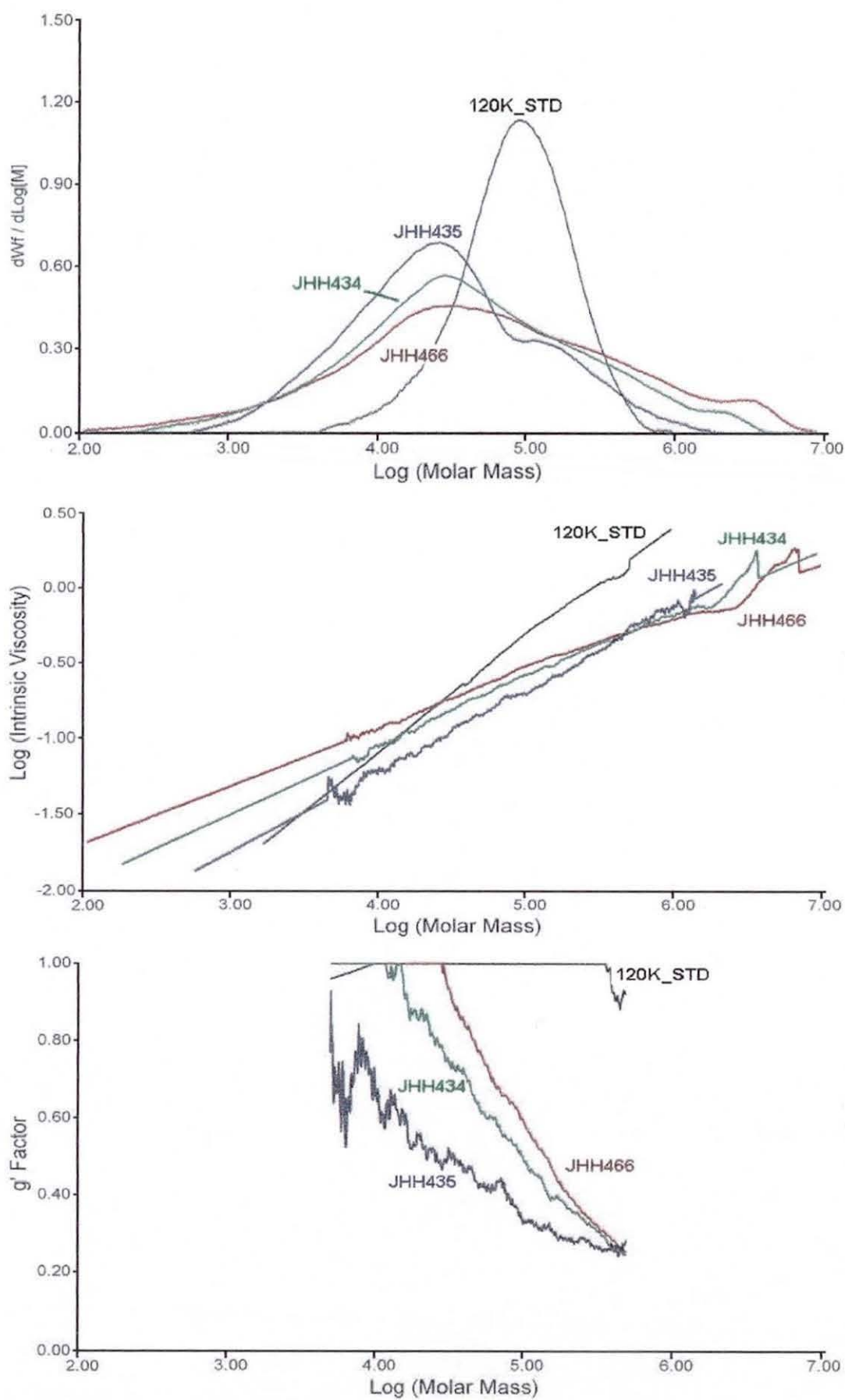


Figure 4-31 The MMD, M-H and  $g'$  plots of JHH466, JHH434 and JHH441.

Table 4-35 Conversion reactions performed with a PCTA at [PCTA]=12% wt

Sample	PCTA	Free [SH] <sup>a</sup> (mmol)	Time (hrs)	Conversion (%)	[AIBN] (% wt)	M <sub>w</sub> (g/mol)	M <sub>n</sub> (g/mol)	D	g'	<i>a</i>	Log K
JHH430	6H-M426	0.66	16	100	0.60	44,900	10,900	4.12	0.63	0.55	-3.33
JHH450	6H-M426	0.66	2	87	0.60	35,200	9,300	3.77	0.67	0.46	-2.94
JHH452	6H-M426	0.66	1	60	0.60	27,700	9,200	3.02	0.71	0.57	-3.44
JHH434	16H-M427	0.70	16	100	0.60	176,100	9,300	18.85	0.69	0.44	-2.81
JHH446	16H-M427	0.70	2	64	0.60	153,400	15,400	9.96	0.64	0.47	-2.96
JHH448	16H-M427	0.70	1	42	0.60	89,100	42,100	2.12	0.41	0.71	-4.17
JHH435	16H-M427	0.702	16	100	2.40	79,600	11,100	7.17	0.497	0.512	-3.251
JHH449	16H-M427	0.702	1	77	2.40	78,100	10,000	7.85	0.639	0.465	-2.980

[MMA]=40% wt and [PCTA]=12% wt.

<sup>a</sup> Concentration of free SH based on a 10g polymerisation.

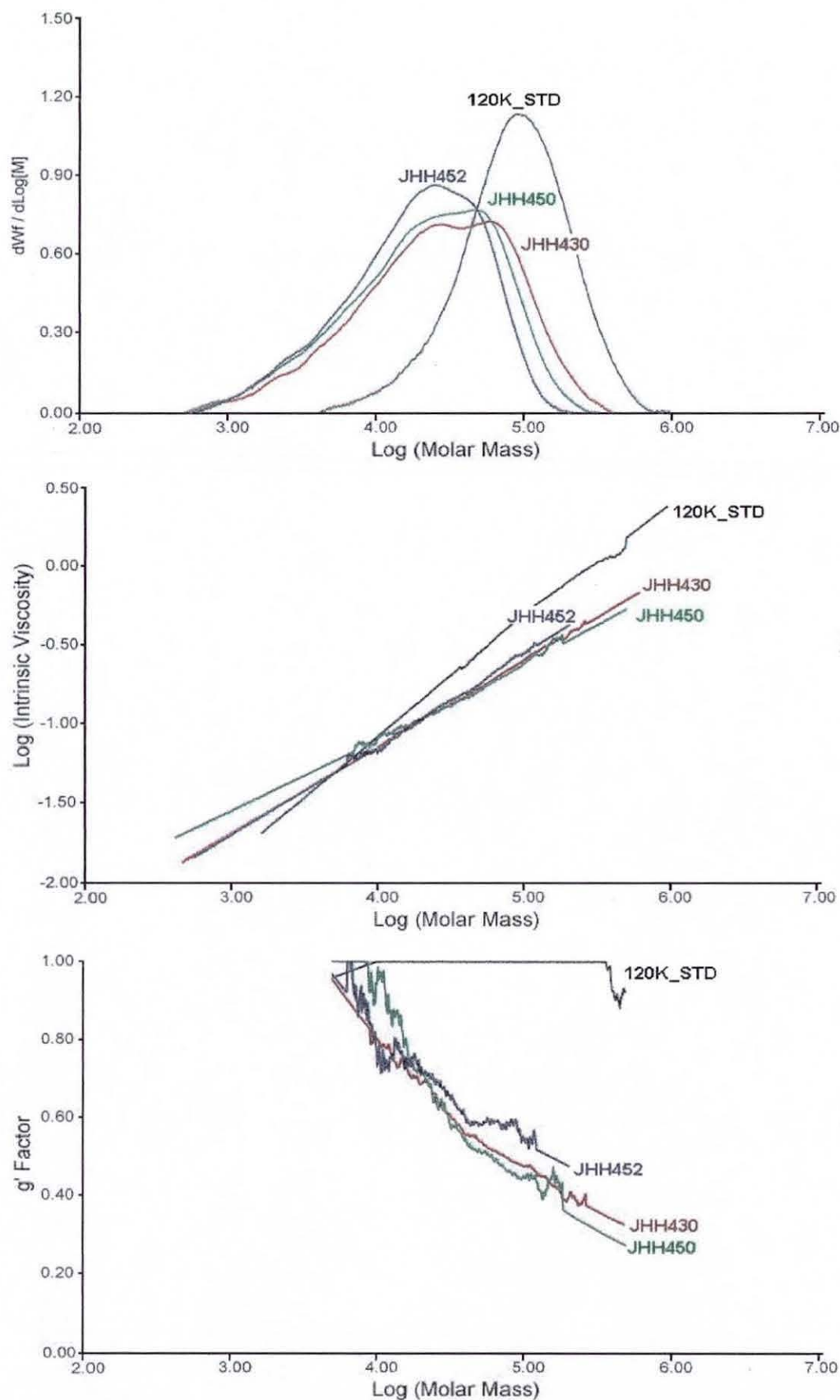


Figure 4-32 The MMD, M-H and  $g'$  plots of JHH430, JHH452 and JHH450.

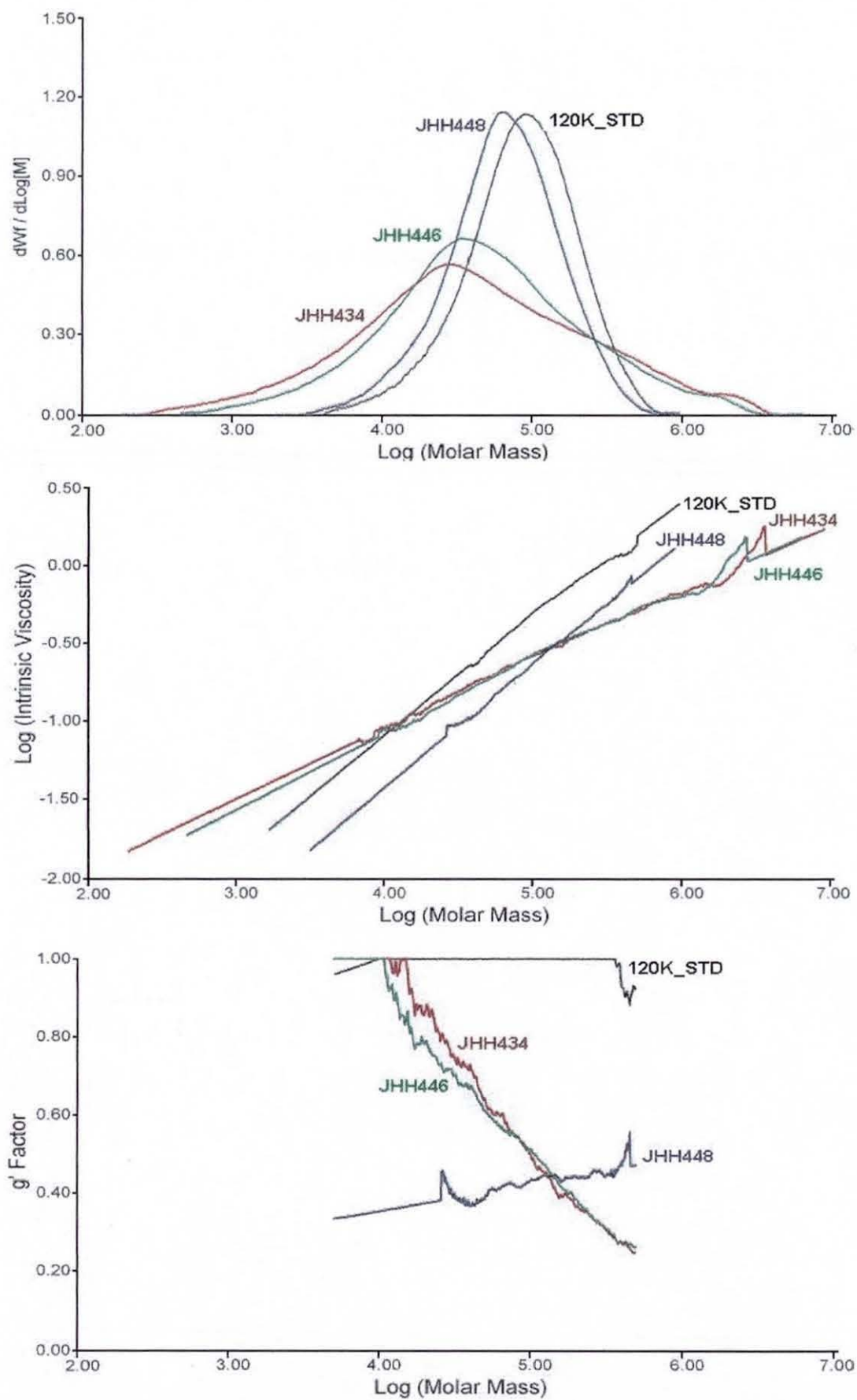


Figure 4-33 The MMD, M-H and  $g'$  plots of JHH434, JHH448 and JHH446.

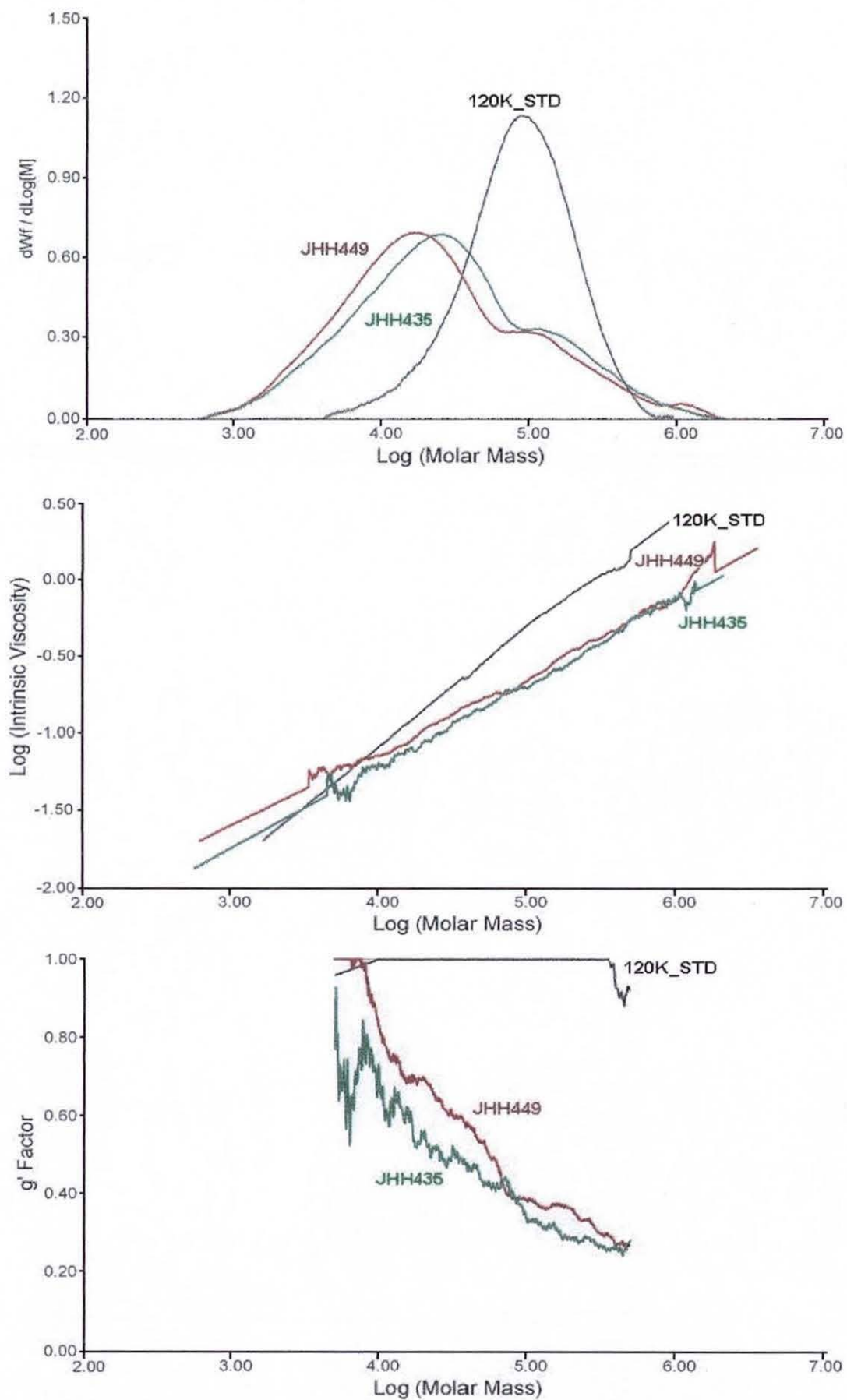


Figure 4-34 The MMD, M-H and  $g'$  plots of JHH435 and JHH449.

## 5 DISCUSSION OF BRANCHING

### 5.1 Role of PCTA

#### 5.1.1 Activation

The abstraction of a hydrogen atom from a SH group on a PCTA produces a thio radical. The abstraction can occur through the following mechanisms:

- Direct abstraction by an initiator fragment.
- Abstraction by an active chain radical, where the active chain may be a linear polymer or another branch chain on a polymeric backbone.

The newly formed thio radical on a PCTA can be envisaged as a potential branch point, which can propagate with monomer to produce a branch chain. The branch chain can terminate to yield a discrete molecule containing one PCTA molecule or combine with another active PCTA species.

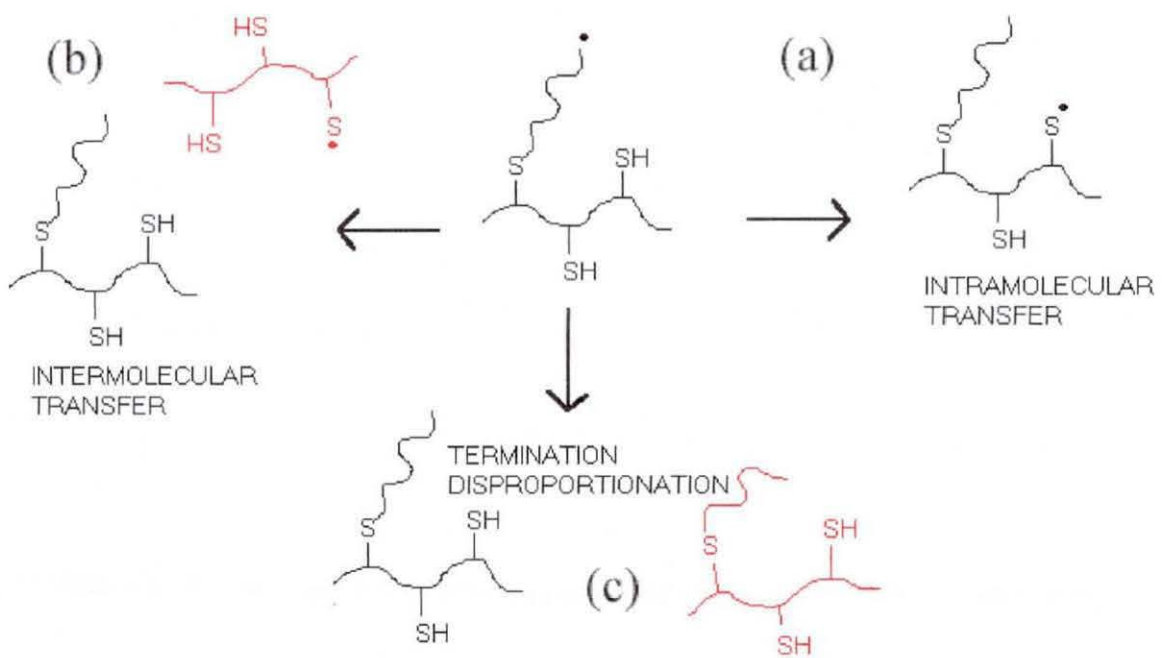
## 5.1.2 Branched Polymer Formation Containing Single PCTA Molecules

The proposed mechanisms for the preparation of a branched molecule containing one PCTA molecule are detailed below. The active branch chain can terminate by the following mechanisms:

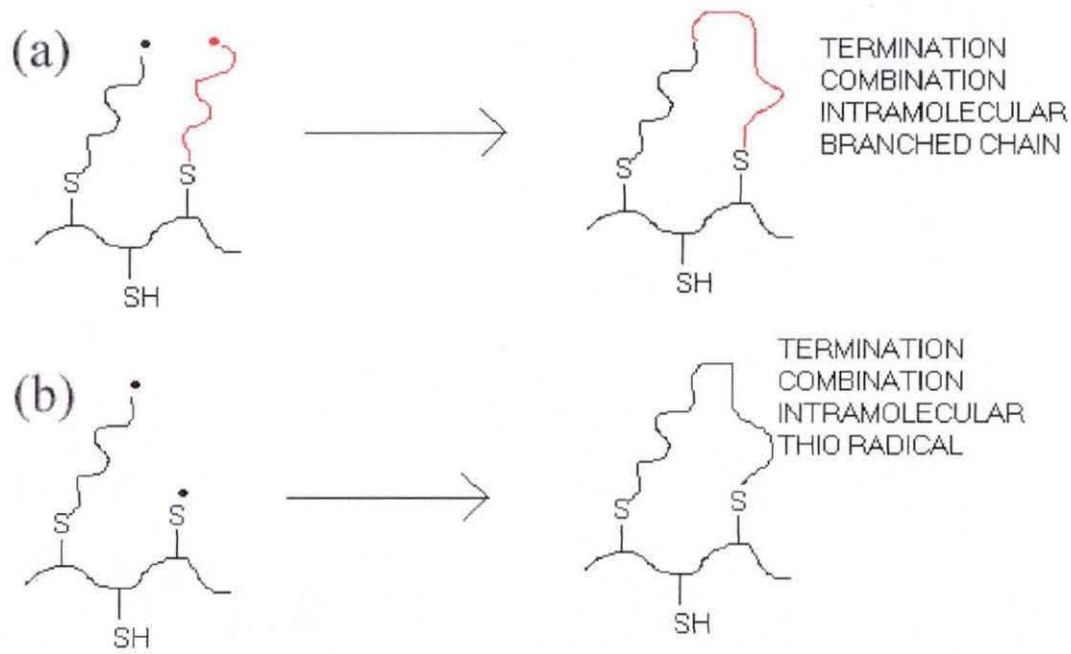
- Intramolecular chain transfer with a SH group on the same PCTA molecule to produce an inactive branch chain and an active radical site on the same PCTA molecule (Figure 5-1a).
- Intermolecular chain transfer with a SH group on another PCTA molecule to produce an inactive branch chain and an active site on another PCTA molecule (Figure 5-1b).
- Intramolecular bimolecular termination via disproportionation of two active branch chains on the same PCTA molecule to produce two inactive branch chains.
- Intermolecular bimolecular termination via disproportionation of two active branch chains on different PCTA molecules to produce one inactive branch chain on each PCTA molecule (Figure 5-1c).
- Bimolecular termination via disproportionation of an active branch chain with a linear chain to produce one inactive branch chain and one inactive linear chain.

- Intramolecular bimolecular termination via combination of two active branch chains to yield a loop configuration (Figure 5-2a).
- Intramolecular bimolecular termination via combination of an active branch chain with a thio radical to yield a loop configuration (Figure 5-2b).
- Intermolecular bimolecular termination via combination of an active branch chain with a linear chain to yield an inactive extended branch chain.



**Figure 5-1** Formation of a discrete polymer molecule via disproportionation and chain transfer.



**Figure 5-2** Formation of discrete molecule via bimolecular termination combination.

### 5.1.3 Branched Polymer Formation Containing Coupled PCTA Molecules

Coupled PCTA molecules potentially have important consequences on the final molar mass of the polymer. For example, two PCTA molecules having molar mass of 16 kg/mol coupled together could potentially contain over 20 SH sites capable of branch chain formation. The implications of disulphide coupling on the polymerisation may be minimised, as it has been demonstrated that disulphide groups are active chain transfer agents.<sup>17</sup>

#### 5.1.3.1 Coupling during Preparation of PCTA

The formation of coupled PCTA molecules during the esterification reaction and in storage was inevitable as oxidation of SH groups to disulphide is well known (Figure 5-3). A PCTA with a high concentration of SH was expected to increase the occurrence of coupling because of a higher probability of disulphide formation. Solubility experiments and the heterogeneous polymerisation mixture indicated the presence of coupled PCTA molecules.

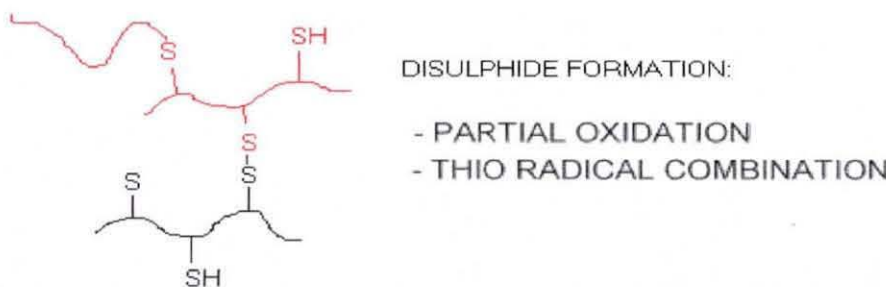


**Figure 5-3 Disulphide formation through oxidation or combination.**

Yamaguchi et al.<sup>110</sup> polymerised a functional monomer bearing a silyl-protected mercaptan. The protected polymer was soluble in THF, chloroform and benzene. When a deprotection step was performed an insoluble network was produced. The cause of insolubility was postulated to be partial oxidative cross-linking of the SH groups. Raman spectroscopy performed on the insoluble polymer indicated the concentration of S-S must be very low as the band arising from S-S stretching could not be detected.

### 5.1.3.2 Combination Reactions

Coupling of PCTA molecules within a polymerisation may occur by bimolecular termination combination of branch radicals. MMA is known to terminate predominantly by bimolecular disproportionation, especially at elevated temperatures, but termination via combination is also a feature.<sup>99,100</sup> The following mechanisms may be active:

- Intermolecular bimolecular termination combination of two active branch chains on two different PCTA molecules (Figure 5-4a).
- Intermolecular bimolecular termination via combination of a branch chain and a thio radical on two different PCTA molecules (Figure 5-4b).
- Combination of two thio radicals yielding a disulphide bond.

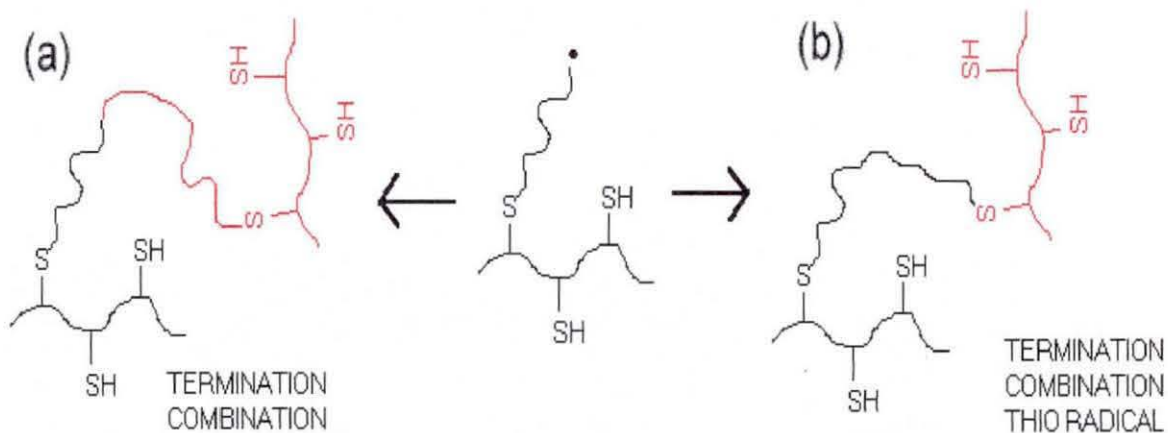


**Figure 5-4 Representation of mechanisms for coupling of PCTA molecules through combination.**

### 5.1.3.3 Branching through Terminal Unsaturation

Zhu and Hamielec studied gel formation in a radical polymerisation via chain transfer and terminal branching.<sup>129</sup> Chain transfer reactions with MMA can be neglected relative to the activity of the transfer activity of SH groups. Terminal double bond formation is via termination disproportionation. A chain terminated by disproportionation may yield an unsaturated double bond. If the terminal bond is reactive, radical propagation through this unsaturated bond can connect two molecules.

## 5.2 Characterisation of Branched Polymers

### 5.2.1 Molar Mass Determination

The SEC-UV data indicated that the PCTA was predominantly in the high molar mass region of the MMD corresponding to branched polymer. The molar mass data of the samples characterised using conventional SEC and SEC-UV is not absolute because branching causes a reduction in hydrodynamic size. The benefits of using TDSEC to determine molar mass are exemplified in Table 5-1. JHH200 and JHH239 are linear PMMA samples and JHH225, JHH228 and JHH229 are branched polymer samples (details Table 4-28/page138 and Figure 4-17/page139).

**Table 5-1 Comparison of molar mass data from conventional SEC and TDSEC.**

Sample	Conventional SEC			TDSEC		
	M <sub>w</sub> (g/mol)	M <sub>n</sub> (g/mol)	D	M <sub>w</sub> (g/mol)	M <sub>n</sub> (g/mol)	D
JHH200	43,300	23,200	1.87	46,200	24,500	1.89
JHH239	137,900	74,100	1.86	149,900	84,600	1.77
JHH225	32,700	14,300	2.28	36,600	16,900	2.17
JHH228	48,300	16,600	2.90	74,400	23,000	3.23
JHH229	121,000	23,500	5.15	393,100	26,800	14.67

The molar mass data for linear polymer samples from both techniques were similar, which demonstrated confidence in both SEC and TDSEC for linear chains. Comparison of the molar mass data for branched polymer samples revealed an increase in the deviation of molar mass between the two techniques as the molar mass of the samples increased. The M<sub>w</sub> and polydispersity for JHH229 was far higher than that measured by conventional SEC. SEC calibrated with linear PMMA will generate low M<sub>n</sub> and M<sub>w</sub> values for branched samples.

## 5.2.2 Solution Behaviour

The fractionation mechanism of SEC was an inherent advantage of utilising TDSEC to characterise a statistically branched sample. This had obvious advantages over traditional methods of solution viscometry measurements using a viscometer; especially when characterising statistically branched polymers that covered a broad MMD.

Numerical data for branching was based on the overall solution properties of the sample; however, examination of the graphical data revealed interesting features about the solution behaviour. For example, JHH464 (Figure 4-28/p158) exhibited a distinct change in the relationship between intrinsic viscosity and molar mass at  $\sim 125$  kg/mol, reflected in a change in the slope in the M-H plot. This change was not reflected in the numerical data. Branching data was not recorded at low molar mass (ca.  $< 10$  kg/mol) therefore the numerical data maybe misleading without correlation to the graphical raw data.

### 5.3 Prediction of Branched Polymer Molar Mass

The molar mass of a polymer prepared in the presence of a CTA was estimated using Eqn 4-1/p82, where chain transfer to solvent, monomer, initiator and polymer was negligible compared with the added agent.

From a knowledge of the degree of polymerisation in the absence of chain transfer (with a linear polymeric product), the concentrations of SH and MMA and the chain transfer constant, the average degree of polymerisation was determined. The calculation estimated the average chain length of a linear chain. This value for a linear chain was utilised to estimate the molar mass of branched polymer, assuming the molar mass of a linear chain was equivalent to a branch chain (tethered to a PCTA molecule). If the average number of SH groups per PCTA was known, then the average molar mass of the branched molecule could be calculated.

JHH408 (Table 4-32/p151) was selected because it had a relatively narrow polydispersity (2.08). The fixed variables for the calculation are summarised below. The value of  $M_n$  for the reference sample prepared in the absence of PCTA (JHH456 – Table 4-30/p145) was 11,300 g/mol.

$DP_0$ (absence of CTA) = 113	$PCTA$ unit molar mass = 205 g/mol
$PCTA$ MOLAR MASS = 6 kg/mol	$MMA$ unit molar mass = 100 g/mol
Av. SH group per PCTA = 2.80	[SH] = 0.285 mmol
	[MMA] = 0.030 mol

Table 5-2 contains the estimated  $M_n$  values based on two variables:

- the chain transfer constant (~0.60 for a mono-functional SH).
- the percentage of reacted SH groups on a PCTA backbone leading to the formation of a branch chain (branch chain molar mass was assumed to be equivalent to the linear chain molar mass in the presence of a CTA).

**Table 5-2 Predicted molar mass data for JHH408 with a variable chain transfer constant and extent of branching.**

C <sub>tr</sub>	Av. Arm M <sub>n</sub> (g/mol)	M <sub>n</sub> at Various SH Group Conversions (g/mol)			
		100%	75%	50%	25%
1	5,400	20,700	16,900	13,100	9,300
0.6	6,900	24,700	19,900	15,100	10,300
0.2	9,300	31,500	25,000	18,500	12,000

The experimental data for JHH408: M<sub>w</sub> 18,800 g/mol, M<sub>n</sub> 9,060 g/mol and D 2.08.

The predicted molar mass results for JHH408 suggested a transfer constant of 1 and a low number of branch chains per PCTA molecule. However, the experimental molar mass data included linear polymer that reduced the overall average molar mass values.

Prediction work was carried out with JHH435 (Table 4-34/p159) prepared in the presence of PCTA 16H-M427. The sample had a relatively broad MMD of 7.17. The value of M<sub>n</sub> for the reference sample prepared in the absence of PCTA (JHH458 – Table 4-30/p145) was 18,900 g/mol.

$$\begin{array}{llll}
 DP_0 \text{ (absence of CTA)} = 189 & \text{PCTA unit molar mass} = 205 \text{ g/mol} \\
 \text{PCTA MOLAR MASS} = 15.5 \text{ kg/mol} & \text{MMA unit molar mass} = 100 \text{ g/mol} \\
 \text{Av. SH group per PCTA} = 14.4 & [\text{SH}] = 0.529 \text{ mmol} \\
 & [\text{MMA}] = 0.030 \text{ mol}
 \end{array}$$

Table 5-3 contains the estimated molar mass estimations based on two variables:

- the chain transfer constant (~0.60 for mono-functional SH).
- the percentage of reacted SH groups on the PCTA backbone leading to the formation of a branch chain (branch chain molar mass is assumed to be equivalent to the linear chain molar mass in the presence of a CTA).

**Table 5-3 Predicted molar mass data for JHH435 with a variable chain transfer constant and extent of branching.**

$C_{tr}$	Av. Arm Mass (g/mol)	M <sub>n</sub> at Various SH Group Conversions (g/mol)			
		100%	75%	50%	25%
1	4,400	78,300	62,600	46,900	31,200
0.6	6,300	106,200	83,500	60,800	38,200
0.2	11,300	178,800	138,000	97,100	56,300

The experimental data for JHH435: M<sub>w</sub> 79,600 g/mol, M<sub>n</sub> 11,100 g/mol and D 7.17.

The estimated results for the molar mass of JHH435 were low compared with the experimental value for M<sub>n</sub>. The low molar mass linear material was included in the average molar mass values. The broad MMD indicated the presence of high molar mass polymer in the sample. A transfer constant of around 0.60 would produce a branched polymer molecule in the region of 40 - 60 kg/mol in the absence of PCTA coupling.

This estimation has many errors due to the complex nature of the polymerisation involving PCTA. Complications included coupled PCTA molecules, a polydisperse distribution of molar mass, a variable chain transfer constant as the polymerisation proceeded as well as a mixture of linear polymer and branched polymer in the sample. If the branched polymer could be extracted and characterised then the average chain transfer constant and extent of branching could be estimated with greater accuracy.

## 5.4 Implications of Utilising PCTA

### 5.4.1 Polymerisation Media and Kinetics

Inclusion of PCTA in a polymerisation reaction increased the viscosity of the polymerisation media. Studies into the homopolymerisation of macromonomers have revealed important information concerning the viscosity of the polymerisation media.<sup>26,27</sup> The gel effect was demonstrated to appear from the beginning of the polymerisation reaction because of the high viscosity of the polymerisation media. The rate constants  $k_p$  and  $k_t$  of macromonomers were reduced compared to those of corresponding small monomers due to the diffusion control effect as a result of the viscous polymerisation media.

It was postulated that some PCTA-based systems (notably 16 kg/mol PCTA) behaved more like poly(macromonomer) systems than conventional monomer systems. Complications in polymerisation kinetics were suspected to operate within the restricted diffusion environment of the viscous polymerisation media. It was suspected that access to transfer sites and termination reactions were reduced at high conversion as a consequence of high local segment density. Chain transfer and termination reactions are diffusion controlled; hence branch chain length potentially increased in polydispersity as the polymerisation proceeded because of exhausted/restricted transfer sites and restricted termination reactions. Initiator efficiency has also been observed to decrease considerably in a restricted diffusion environment, reducing the rate of polymerisation.<sup>26,27</sup>

## 5.4.2 Nature of PCTA

Samples prepared in the presence of PCTA were not model systems. Deviations in the relationship between the intrinsic viscosity and the molar mass of branched polymers and linear polymers were related to the size of the molecule in solution (related to its structure). Structural changes and the influence on intrinsic viscosity across the MMD of a branched polymer were a consequence of:

- A PCTA was not a discrete molecule but had a MMD and a functionality distribution; hence, in the absence of PCTA coupling there were still large PCTA molecules present as a consequence of polydispersity.
- The branch chain length and frequency were polydisperse. Branch chain length and distribution were important in determining the overall dimensions of a molecule.
- Coupled PCTA molecules (through oxidation and termination via combination) potentially produced highly branched, high molar mass macromolecules.
- Linear polymer was present in all samples as a consequence of the chain transfer mechanism. The presence of linear polymer did not permit the total characterisation of a branched polymer, which was a problem at lower molar mass where the linear polymer was predominant.
- The concentration of SH was finite. As the polymerisation reaction proceeded the availability of transfer sites diminished.
- The inclusion of PCTA potentially interfered with the polymerisation kinetics by increasing the viscosity of the polymerisation media.

### 5.4.3 PCTA Partial Phase Separation

Partial phase separation occurred within 45 minutes of initiation. A turbid MMA/PCTA/toluene polymerisation mixture indicated partial phase separation, probably attributed to high molar mass microgel.

The implications of this material on intrinsic viscosity were studied by preparing 2 samples under identical conditions and filtering one sample post-polymerisation. JHH314 was filtered during the washing stage and produced a clear solution before the final precipitation. JHH314 and JHH315 were characterised by TDSEC and the results are reported in Table 4-28/p138 and summarised below.<sup>iii</sup> A solution of JHH314 at a concentration of 40% wt in THF still produced a turbid solution, which suggested the phase-separated material was microgel. Comparison of the data for JHH314 and JHH315 indicated that filtration reduced the molar mass and polydispersity of the polymer. The branching data appeared relatively unaffected. Phase separation of PCTA was postulated to reduce the effective concentration of SH groups in the system, and so increase the concentration of linear polymer.<sup>13</sup> TDSEC data indicated that filtration removed the high molar mass polymer.

### 5.4.4 Concentration of Free SH

The benzylation reaction performed on PCTA to determine the concentration of free SH typically yielded a value of 70-90%. A reduction in the concentration of free SH was attributed to disulphide bonds through oxidation. Intermolecular disulphide bonds yielded a network structure and increased PCTA insolubility. Intramolecular disulphide bonds reduced the concentration of free SH with no adverse effect on solubility.

---

<sup>iii</sup>

	PCTA	Mw (g/mol)	Mn (g/mol)	D	$g'$	$\alpha$	Log K
JHH314	20L-M293	352,200	31,600	11.15	0.65	0.44	-2.88
JHH315	20L-M293	470,800	29,500	15.96	0.69	0.42	-2.78

## 5.5 Branched Polymer Formation with PCTA

A series of conversion reactions was performed at [PCTA]=12% wt. Conversion data was utilised to obtain information about branched polymer formation as the polymerisation progressed. The conversion data indicated that conversion was dependent on the concentration of AIBN and the molar mass of PCTA. Inspection of the TDSEC data revealed that the two PCTA systems (6 kg/mol and 16 kg/mol) behaved differently and are discussed separately. **All conversion data is located in Table 4-35/p163.**

### 5.5.1 Conversion with 6 kg/mol PCTA

Conversion reactions were only performed with PCTA 6H-M426 (Figure 4-32/p164). Conversion increased with time at [AIBN]=0.60% wt for samples prepared in the presence of 6H-M426.<sup>iv</sup> The conversion rate decreased between 1 and 2 hrs. As conversion increased the molar mass increased and MMD broadened. This was attributed to an increased branch chain length and branch chain frequency as conversion increased. The level of branching was the same in each conversion sample at a similar molar mass.

Full conversion was obtained after 1 hour at [AIBN]=2.40% wt. JHH431 had a lower molar mass and higher level of branching than the series prepared with [AIBN]=0.60% wt. Conversion was expected to be higher at an equivalent time because of an increased concentration of radicals.

It was postulated that the polymerisation in the presence of 6 kg/mol PCTA produced discrete branched molecules. Conversion data followed with the expected trend in molar mass and MMD; the polymerisation was postulated to commence without any serious restrictions to diffusion processes.

---

iv	PCTA	Conv (%)	Time (hr)	Mw (g/mol)	Mn (g/mol)	D	g'	$\alpha$	Log K
JHH430	6H-M426	100	16	44,900	10,900	4.12	0.63	0.55	-3.33
JHH450	6H-M426	87	2	35,200	9,300	3.77	0.67	0.46	-2.94
JHH452	6H-M426	60	1	27,700	9,200	3.02	0.71	0.57	-3.44

## 5.5.2 Conversion with 16 kg/mol PCTA

Samples prepared at [16H-M427]=12% wt exhibited unusual solution behaviour and MMD compared with other samples.

Conversion increased with time at [AIBN]=0.60% wt for samples prepared in the presence of 16H-M427.<sup>v</sup> The molar mass increased and the MMD broadened significantly with conversion. JHH448 (conversion 42%) exhibited different solution behaviour to both JHH446 and JHH434. The M-H plot for JHH446 and JHH448 is included in Figure 5-5. The slope of the M-H plot for JHH448 was similar to the behaviour observed with a star polymer, which was indicative of a compact structure that increased in hydrodynamic size at a constant rate with an increase in molar mass (see Section 2.6.2.2). The behaviour was consistent in the  $g'$  plot (Figure 4-33/p165).

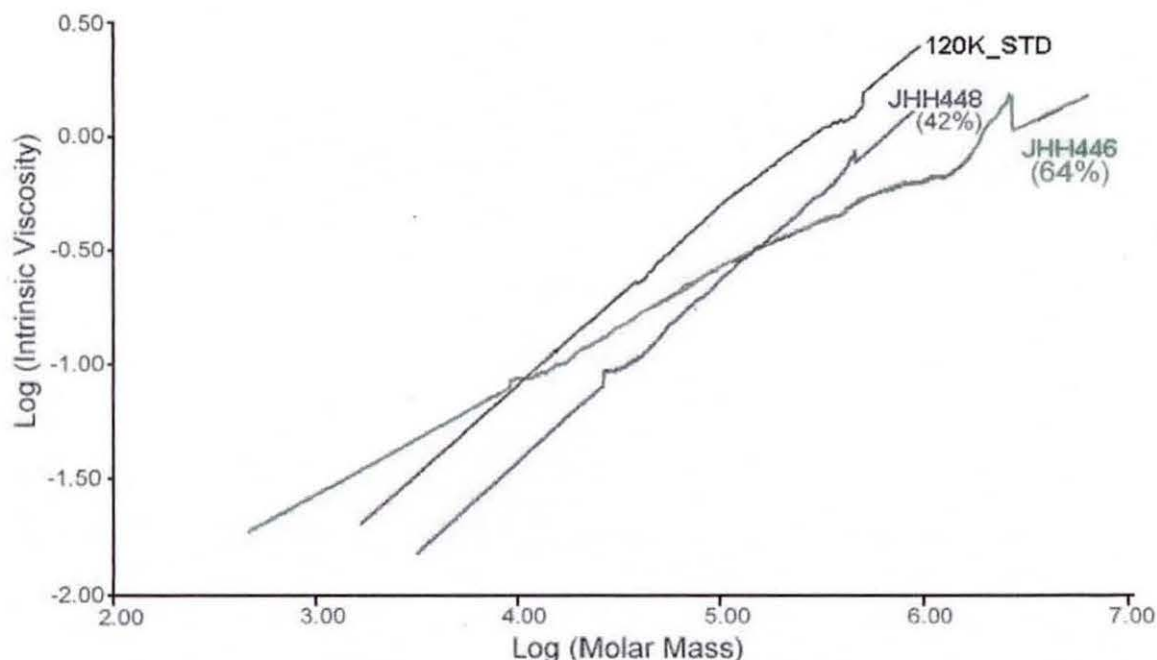


Figure 5-5 M-H plot of JHH448, JHH446 and linear standard (conversion indicated).

v	PCTA	Conv (%)	Time (hr)	Mw (g/mol)	Mn (g/mol)	D	$g'$	$\alpha$	Log K
JHH434	16H-M427	100	16	176,100	9,300	18.85	0.69	0.44	-2.81
JHH446	16H-M427	64	2	153,400	15,400	9.96	0.64	0.47	-2.96
JHH448	16H-M427	42	1	89,100	42,100	2.12	0.41	0.71	-4.17

The MMD for JHH448 was narrow (2.12), which suggested a uniform distribution of molecular sizes. It was postulated that the branched molecules were predominantly discrete molecules with a narrow distribution of branch chain lengths. The branch chain length and branch numbers were limited by the extent of conversion.

JHH446 (conversion 64%) behaved as a statistically branched polymer. The polymer deviated further from linearity as the molar mass increased. The broadened MMD with conversion indicated an increase in the range of molecular sizes. The polydispersity of the branch chain lengths and the distribution of branch chains per molecule were expected to increase with conversion. The concentration of polymer below 10 kg/mol increased considerably with conversion.

The change in intrinsic viscosity between JHH448 and JHH446 was attributed to a structure change as a consequence of branch chain length, number of branch chains and coupling of molecules. An increase in conversion between JHH448 and JHH446 resulted in three changes:

- 1) The concentration of low molar mass branched polymer diminished but the concentration of low molar mass linear polymer increased.
- 2) The level and concentration of high molar mass branched polymer increased.
- 3) The average molar mass increased and the MMD broadened significantly.

It was postulated that below ~42% conversion (JHH448) the active chains in the polymerisation were predominantly branch chains. Between a conversion of 42% and 64% a transition occurred. The molar mass and polydispersity of the polymer increased considerably with an extra 22% monomer conversion. The experimental observations for the transition from star-type behaviour to statistical behaviour might have been attributed to:

- 1) An increase in the concentration of coupled branched PCTA molecules. The low molar mass branched polymer present as predominantly discrete molecules in JHH448 became coupled through bimolecular combination reactions. This reduced the

concentration of low molar mass branched polymer and increased the concentration of high molar mass branched polymer (extending the molar mass).

- 2) An increase in the molar mass of the branched polymer molecules through increased conversion (branch chain length and number per molecule increased) that shifted the branched polymer distribution to higher molar mass. The concentration of SH groups diminished as the polymerisation proceeded. This increased the branch chain length as a consequence of the reduction in the probability of a transfer reaction.
- 3) An increase in the concentration of linear material at low molar mass was attributed to a reduction in accessibility/diminished transfer sites. If transfer reactions were reduced the linear polymer molar mass would increase before encountering a transfer site. An increased concentration of linear polymer will reduce the influence of branched polymer on the intrinsic viscosity.

In a restricted diffusion environment, the rate of transfer reactions and termination reactions will be reduced. Propagating branched molecules will continue to grow in size. If access to transfer sites was reduced, the concentration of linear polymer would increase and propagating branch chains would attain higher molar mass. A small concentration of coupled molecules will increase the molar mass and branching density considerably. JHH434 (100% conversion) had a higher concentration of low molar mass linear polymer than JHH446, probably as a consequence of diminished/restricted accessibility to SH groups.

The extent of conversion increased with time at  $[AIBN]=2.40\%$  wt (1hour – 77% and 2hours – 100 %). The molar mass, MMD and branching levels between JHH435 and JHH449 remained unchanged with conversion (Table 4-35/p163). Both were highly branched polymers. An increase in the concentration of AIBN increased the rate of conversion of monomer to polymer and reduced the overall molar mass and MMD of the final polymer.

## 5.6 Reaction Variables

### 5.6.1 Concentration of MMA

#### 5.6.1.1 PCTA 6H-M426

An increase in the concentration of MMA at a fixed concentration of AIBN increased the molar mass of the branched polymer. Examples are included in Table 4-31/p148 and illustrated by JHH428 and JHH440.<sup>vi</sup> An increase in the concentration of monomer increased the chain length at a fixed concentration of initiator. This was consistent with the expected behaviour for the kinetic chain length in a radical polymerisation of small monomers (Eqn 2-19).

The data indicated an increase in branching at a lower concentration of MMA at [6H-M426]=6% wt (JHH440). A reduction in observed branching levels at a high concentration of MMA was attributed to an increase in the concentration of linear polymer, which reduced the influence of branched polymer on intrinsic viscosity. An increase in the concentration of MMA at [6H-M426]=12% wt had no effect on branching. No trend was apparent.

---

vi	[6H-M426] (%wt)	[MMA] (%wt)	Mw (g/mol)	Mn (g/mol)	D	g'	a	Log K
JHH440	6	20	28,800	6,400	4.49	0.62	0.44	-2.87
JHH428	6	40	63,000	15,100	4.17	0.87	0.61	-3.50

### 5.6.1.2 PCTA 16H-M427

An increase in the concentration of MMA in the presence of PCTA [16H-M427]=6% wt at [AIBN]=0.30% wt increased the molar mass of the polymer (JHH436 vs JHH432 - Table 4-33/p155). The branching parameters remained relatively unaffected. An increase in the concentration of MMA at [AIBN]=1.20% wt had a minimal effect on the molar mass of the polymer. There was a slight decrease in branching levels, possibly attributed to an increase in the concentration of linear polymer.

An increase in the concentration of MMA in the presence of PCTA [16H-M427]=12% wt at [AIBN]=0.60% increased the molar mass of the polymer (JHH438 vs JHH434 - Table 4-34/p159). The MMD of both polymers were broad. Both samples exhibited high levels of branching. JHH434 had a lower intrinsic viscosity at a comparable molar mass. The MMD indicated JHH438 had a higher concentration of polymer below ~10 kg/mol which was not measured in the branching data.

An increase in the concentration of MMA at [AIBN]=2.40% wt had a dramatic consequence on the intrinsic viscosity between JHH439 and JHH435 (Table 4-34/p159).<sup>vii</sup> The M-H and  $g'$  plots indicated a large deviation from linear behaviour as the molar mass increased (Figure 4-30/p161). JHH439 exhibited star-type behaviour, indicative of highly branched and compact molecules (JHH439 is discussed in Section 5.6.2). JHH439 had a higher molar mass and lower polydispersity than JHH435. Comparison of the MMD and M-H plots for JHH439 and JHH435 indicated that an increase in the concentration of MMA increased the concentration of linear polymer. It was postulated that the structure of the branched molecules in both systems maybe similar, but the presence of a high concentration of linear polymer reduced the influence of branched polymer on intrinsic viscosity in JHH435.

vii	PCTA	[MMA] (% wt)	[AIBN] (% wt)	Mw (g/mol)	Mn (g/mol)	D	$g'$	$\alpha$	Log K
JHH439	16H-M427	20	2.40	159,100	34,800	4.57	0.22	0.61	-3.92
JHH435	16H-M427	40	2.40	79,600	11,100	7.17	0.50	0.51	-3.25

## 5.6.2 Concentration of AIBN

The concentration of AIBN determined the concentration of radicals able to initiate monomer and, in the presence of PCTA, abstract hydrogen directly to produce a thio radical. At a low concentration of AIBN the number of termination and transfer reactions are lower. The chain length of linear and branch chains will be longer relative to the chain lengths at a higher concentration of initiator under similar conditions. The concentration of linear polymer was expected to increase as a result of a higher concentration of radicals. The concentration of linear polymer below 10 kg/mol generally increased as the concentration of AIBN increased (excluding 16 kg/mol PCTA systems at [PCTA]=12% wt). Samples prepared in the presence of a lower concentration of AIBN generally yielded polymers of higher molar mass (JHH464 vs JHH433 - Table 4-33/p155).<sup>viii</sup>

Spurious solution behaviour was observed with an increase in the concentration of AIBN at [16H-M427]=12% in the series JHH438 and JHH439 (Table 4-34/p159).<sup>ix</sup> The M-H plot is included in Figure 5-6. JHH438 was prepared at [AIBN]=0.60% wt. The polymer was highly branched at high molar mass and the MMD was broad, which indicated a large array of molecular sizes. The resultant polymer exhibited solution properties of a statistically branched polymer. An increase in the deviation from linearity at high molar mass suggested the branched molecules increased in density.

JHH439 exhibited an intrinsic viscosity profile similar to JHH448 (discussed in Section 5.5.2). JHH439 had a high molar mass and moderate MMD. The M-H plot was representative of the intrinsic viscosity of a star-type polymer. The bimodal distribution was not reflected in the M-H plot; there was a change in gradient at ~250 kg/mol (marked on the plot). The large deviation from linearity, even at low molar mass, indicated a low concentration of linear polymer. The data suggested JHH439 was a highly branched

viii	[16H-M427] %wt	[AIBN] %wt	Mw (g/mol)	Mn (g/mol)	D	g'	a	Log K
JHH464	6	0.15	280,300	50,500	5.55	0.67	0.49	-2.97
JHH433	6	1.20	35,600	5,500	6.51	0.78	0.53	-3.21
ix	[16H-M427] %wt	[AIBN] %wt	Mw (g/mol)	Mn (g/mol)	D	g'	a	Log K
JHH438	12	0.60	125,400	6,600	18.91	0.56	0.44	-2.86
JHH439	12	2.40	159,100	34,800	4.57	0.22	0.61	-3.92

polymer across the MMD with a low concentration of linear polymer. The branch chain length polydispersity per molecule was relatively narrow.

The properties of JHH439 were explained by the experimental conditions. A high concentration of AIBN increased the number of propagating centres and potentially increased direct hydrogen abstraction from the SH groups (that led to a low linear polymer concentration). The high number of propagating centres combined with a high concentration of SH increased the frequency of chain transfer reactions. The low concentration of MMA limited the concentration of polymer in the system, which minimised complications attributed to a highly viscous polymerisation media.

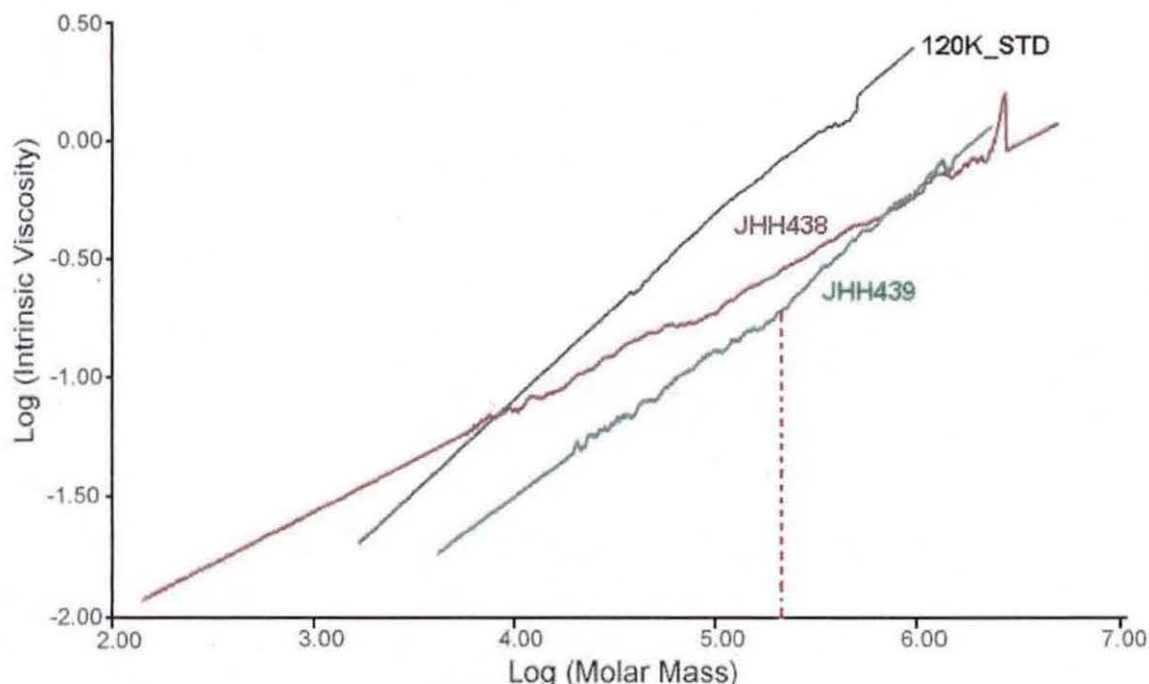


**Figure 5-6** The M-H plot of JHH438, JHH439 and a linear PS standard.

## 5.7 PCTA Variables

### 5.7.1 Molar Mass of PCTA

For a specified concentration of SH there was a higher number of SH groups on the backbone as the molar mass of the backbone increased but the number of molecules decreased. Figure 5-7 is a representation of the effect of the backbone molar mass on branching at a fixed concentration of SH.

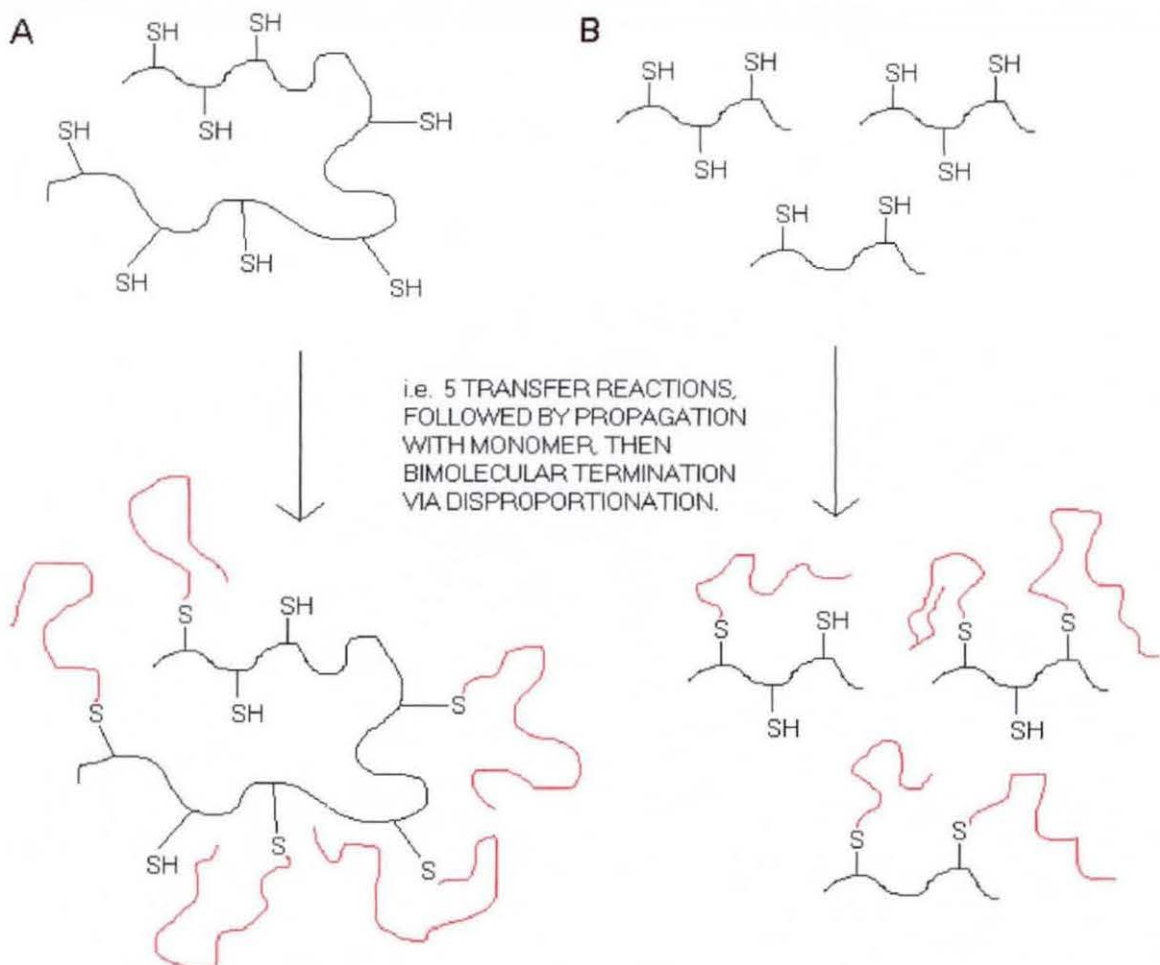


Figure 5-7 A representation of (A) the effect of a high molar mass PCTA on polymer molecule size and (B) a low molar mass PCTA of comparable SH functionality.

It was postulated that at a fixed concentration of SH the 16 kg/mol PCTA produced polymer molecules of higher molar mass than 6 kg/mol PCTA because of the increased number of SH groups per PCTA molecule.

JHH430 and JHH434 (Table 4-32/p151 and Table 4-34/p159 respectively) were prepared under identical conditions except the PCTA used had different molar masses.<sup>x</sup> JHH430 was prepared in the presence of PCTA 6H-M426 and JHH434 was prepared in the presence of PCTA 16H-M427. Both had a similar concentration of SH. The high molar mass PCTA produced a higher molar mass polymer with a broader MMD. Other examples include JHH225 / JHH228 / JHH229 - Table 4-28/p138)

---

x	PCTA	Mw (g/mol)	Mn (g/mol)	D	$g'$	$a$	Log K
JHH430	6H-M426	44,900	10,900	4.12	0.63	0.55	-3.33
JHH434	16H-M427	176,100	9,300	18.85	0.69	0.44	-2.81

## 5.7.2 Influence of PCTA Concentration at Fixed SH Concentration

The concentration of PCTA determined the concentration of SH in a polymerisation system when the number of SH groups on a PCTA was fixed. An increase in the concentration of SH at a fixed concentration of initiator in the polymerisation of small monomers with mono-functional CTA reduces the chain length of the polymer as a result of more frequent transfer reactions. Therefore, an increase in the concentration of SH groups might be expected to reduce the branch chain length but increase the number of branch chains on a PCTA molecule. A representation of an increase in the concentration of PCTA and the effect of that increase on branch chain length is included in Figure 5-8.

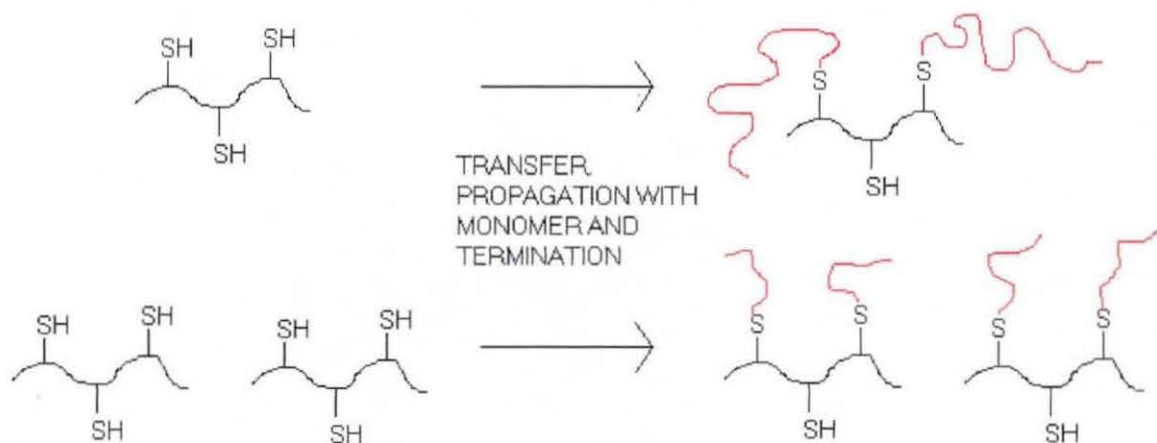


**Figure 5-8 The effect of a two-fold increase in the concentration of a PCTA – reduction in branch chain length but an increase in the number of branch chains.**

An increase in the concentration of PCTA was expected to increase the concentration of branched polymer molecules and increase the concentration of linear polymer.

### 5.7.2.1 PCTA 6H-M426

[6H-M426]=6% wt to 12% wt at fixed [SH] and [AIBN]

JHH428 had a higher molar mass and narrower MMD than JHH463 (Table 4-31/p148 and Table 4-32/p151).<sup>xii</sup> The MMD of JHH463 indicated an increase in the concentration of low molar mass polymer that accounted for increased polydispersity (not included in numerical branching data). A decrease in the values of  $g'$  and  $a$  indicated that an increase in the concentration of PCTA 6H-M426 yielded a polymer with a higher concentration of branched molecules.

### 5.7.2.2 PCTA 16L-M403

[16L-M403]=6% wt to 12% wt at fixed [SH] and [AIBN]

A comparison of molar mass data for JHH410 and JHH465 revealed that a two-fold increase in the concentration of PCTA 16L-M403 reduced the molar mass but broadened the MMD (Table 4-33/p155 and Table 4-34/p159).<sup>xiii</sup> The broad MMD with JHH465 was a consequence of a high concentration of low molar mass polymer (Figure 4-29/p160). The branching parameters decreased as the concentration of PCTA 16L-M403 increased, which suggested a high concentration of branching in the polymer. A higher concentration of PCTA produced more branched polymer molecules. Both the  $g'$  and M-H plots indicated high levels of branching across the MMD. Inspection of the graphical data for JHH465 indicated that branching was not recorded below 10 kg/mol, where a proportion of the polymer was situated.

xi	[6H-M426] (%wt)	Mw (g/mol)	Mn (g/mol)	D	$g'$	$a$	Log K
JHH428	6	63,000	15,100	4.17	0.87	0.613	-3.503
JHH463	12	52,400	7,400	7.11	0.67	0.427	-2.758

xii	[16L-M403] (%wt)	Mw (g/mol)	Mn (g/mol)	D	$g'$	$a$	Log K
JHH410	6	91,400	11,400	8.02	0.71	0.53	-3.16
JHH465	12	68,200	4,400	15.50	0.59	0.46	-2.93

### 5.7.2.3 PCTA 16H-M427

[16H-M427]=6% wt to 12% wt at fixed [SH] and [AIBN]

A comparison of molar mass data for JHH432 and JHH466 revealed that a two-fold increase in the concentration of 16H-M427 increased both the molar mass and broadened the MMD considerably (Table 4-33/p155 and Table 4-34/p159).<sup>xiii</sup> A polydispersity of 53 in JHH466 indicated a very large distribution of molecular sizes. Inspection of the M-H plot revealed a change in the relationship between intrinsic viscosity and molar mass as the molar mass increased (Figure 4-31/p162). At a molar mass  $\sim 10^6$  g/mol the exponent  $a$  was estimated to be less than 0.20.

### 5.7.2.4 Summary

The probability of a PCTA molecule bearing a branch chain increased at a high concentration of PCTA. A 16 kg/mol PCTA molecule with a high concentration of SH will increase in size considerably relative to a 6 kg/mol PCTA. The broad MMD observed with a 16 kg/mol PCTA suggested that a high molar mass PCTA had a greater impact on the intrinsic viscosity of the resultant polymer.

---

xiii	[16L-M403] (%wt)	Mw (g/mol)	Mn (g/mol)	D	$g'$	$a$	Log K
JHH432	6	135,200	26,100	5.18	0.69	0.52	-3.13
JHH466	12	336,400	6,300	53.31	0.75	0.37	-2.41

### 5.7.3 Influence of SH Concentration in PCTA

#### 5.7.3.1 Influence of SH Concentration at Fixed PCTA Molar Mass and PCTA Concentration

An increase in the concentration of SH at a fixed concentration of initiator was expected to reduce the chain length of the polymer because of more frequent transfer reactions. Moares et al.<sup>11</sup> demonstrated in EVA-based PCTA systems that an increase in the concentration of SH at a fixed concentration of AIBN reduced the molar mass of the grafted and linear polymer. Figure 5-9 is a representation of an increase in the concentration of SH on a PCTA backbone at a fixed PCTA molar mass. An increase in the concentration of SH on a PCTA was expected to reduce the branch chain length but increase the number of branch chains on the PCTA molecule as a result of more frequent transfer reactions (the density of branching will increase).

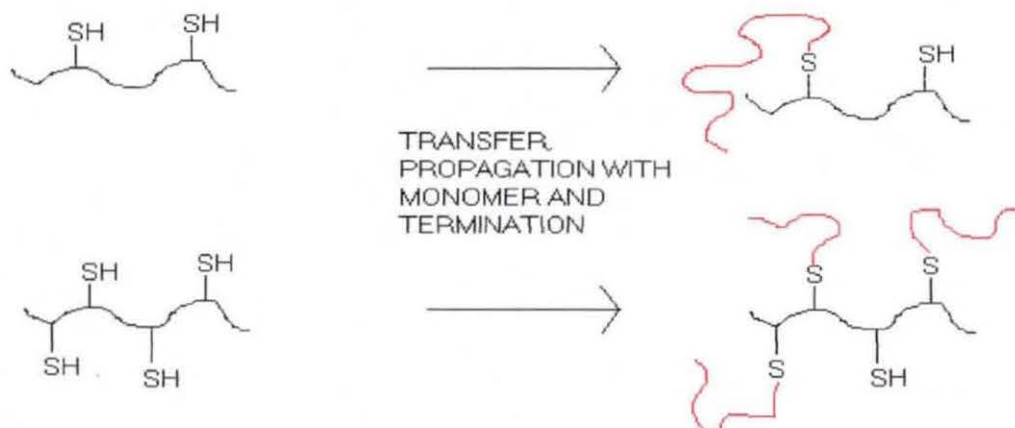


**Figure 5-9** A representation of the effect on branching of increased [SH] on the PCTA backbone at fixed PCTA molar mass.

Samples prepared in the presence of a 6 kg/mol PCTA and a 16 kg/mol PCTA followed the predicted trend. An increase in the concentration of SH increased the molar mass, broadened the MMD (increased concentration of low molar mass polymer) and increased the levels of branching (i.e. JHH465 vs JHH466 - Table 4-34/p159).

### 5.7.3.2 Distribution of SH on PCTA

The contribution of a PCTA on the solution viscosity of the polymerisation media and the distribution of SH groups was studied when the concentration of SH groups in two systems was fixed. The SH groups in one system were distributed on two PCTA molecules and the SH groups in the other system were distributed on one PCTA molecule. The effect of branch density and the concentration of branched polymer on the intrinsic viscosity was studied.

A system with a PCTA of high concentration SH at [PCTA]=6% wt was compared against a system containing a PCTA of low concentration SH at [PCTA]=12% wt. The first system was expected to produce a polymer molecule with a high branch density but a low concentration of branched polymer (Figure 5-10(a)). The second system was expected to produce a high concentration of branched polymer with a lower branch density (Figure 5-10(b)). The concept applied to all PCTA molar masses.

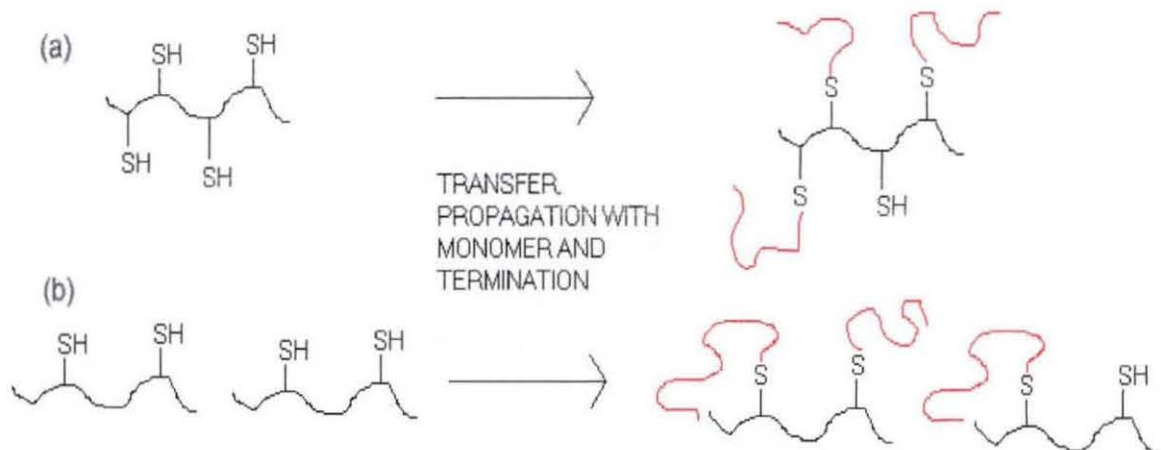


**Figure 5-10** A representation of the effect of increased SH distribution on (a) one molecule and (b) two molecules.

### 5.7.3.2.1 PCTA 6H-M426 vs PCTA 6L-M402

[6H-M426]=6% wt vs [6L-M402]=12% wt

The molar mass data for JHH428 and JHH462 indicated an increase in the molar mass as the PCTA functionality increased (Table 4-31/p148 and Table 4-32/p151).<sup>xiv</sup> The MMD for JHH428 was broader as a result of a higher concentration of polymer <10 kg/mol. It was postulated that in JHH428 the branched molecules had a higher branch density than in JHH462 but their concentration was lower. Evidence of highly branched polymer at high molar mass was observed in the M-H and  $g'$  plots of JHH428 (Figure 4-22/p150). An increased deviation from linearity in the slope of the M-H plot (that corresponded to a molar mass ~80 kg/mol) indicated the presence of molecules of a different structure. The slope of the  $g'$  plot also changed at a similar molar mass. JHH462 contained a higher concentration of branched molecules with a lower density of branching. The M-H plot for this sample indicated branching was present at low molar mass (Figure 4-23/p152). High molar mass polymer was not produced because of the limited number of branch chains per PCTA molecule. PCTA coupling was minimal.

xiv	PCTA	PCTA (%wt)	Mw (g/mol)	Mn (g/mol)	D	$g'$	$a$	Log K
JHH428	6H-M426	6	63,000	15,100	4.17	0.87	0.61	-3.50
JHH462	6L-M402	12	18,700	7,600	2.44	0.69	0.64	-3.75

### 5.7.3.2.2 PCTA 16H-M427 vs PCTA 16L-M403

[16H-M427]=6% wt vs [16L-M403]=12% wt

JHH432 had a higher molar mass and lower polydispersity than JHH465 (Table 4-33/p155 and Table 4-34/p159).<sup>xv</sup> With a 16 kg/mol PCTA there was a larger range of molecule sizes due to the increased number of SH groups on the PCTA.

Evidence of highly branched polymer at high molar mass was observed in the M-H plot of JHH432 (Figure 5-11). An obvious change in the slope of the M-H plot (which corresponded to a molar mass ~130 kg/mol) indicated a transition in structure at high molar mass. The transition in structure indicated species of a highly branched nature. The branched molecules were presumed to have a high branch density. The  $g'$  profile revealed similar information about the presence of branched polymer (Figure 4-28/p158).

JHH465 possessed a high concentration of branched molecules. The branch density was predicted to be lower than JHH432. The deviation from linearity in the M-H plot indicated branching was prevalent at low-moderate molar mass. The  $g'$  profile suggested high levels of branching at low molar mass, which lowered as the molar mass increased (Figure 4-29/p160). High molar mass polymer with high branching was not produced because of the limited number of branch chains per PCTA molecule. The high concentration of polymer below 10 kg/mol was attributed to reduced accessibility of transfer sites. The intrinsic viscosity was lower in JHH465 than in JHH432 at a comparable molar mass.

---

xv	PCTA	PCTA (%wt)	Mw (g/mol)	Mn (g/mol)	D	$g'$	$\alpha$	Log K
JHH432	16H-M427	6	135,200	26,100	5.18	0.69	0.52	-3.13
JHH465	16L-M403	12	68,200	4,400	15.50	0.59	0.46	-2.93

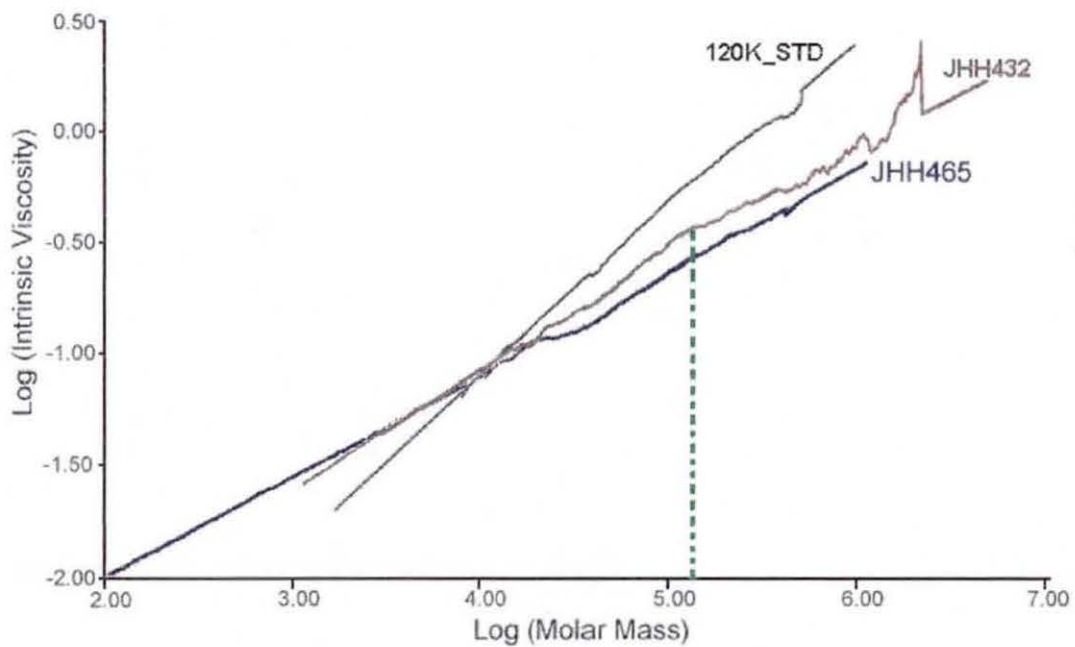


**Figure 5-11 The M-H plot of JHH432, JHH465 and a linear PMMA standard.**

The results indicated a high molar mass branched polymer was produced in the presence of a low concentration of highly functional PCTA. A low-moderate molar mass polymer was produced in the presence of a higher concentration of low functional PCTA.

### 5.7.3.3 Influence of SH Concentration and PCTA Molar Mass

#### 5.7.3.3.1 PCTA 6H-M426 vs PCTA 16L-M403

The effect of PCTA functionality and PCTA molar mass were studied to determine which factors were more influential on intrinsic viscosity. Samples prepared with the high functional PCTA 6H-M426 were compared against samples prepared with the low functional PCTA 16L-M403 at a fixed concentration of PCTA. In a polymerisation with PCTA 6H-M426 there were an average of 1.9 more SH groups than with PCTA 16L-M403. Figure 5-12 is a representation of the comparison.

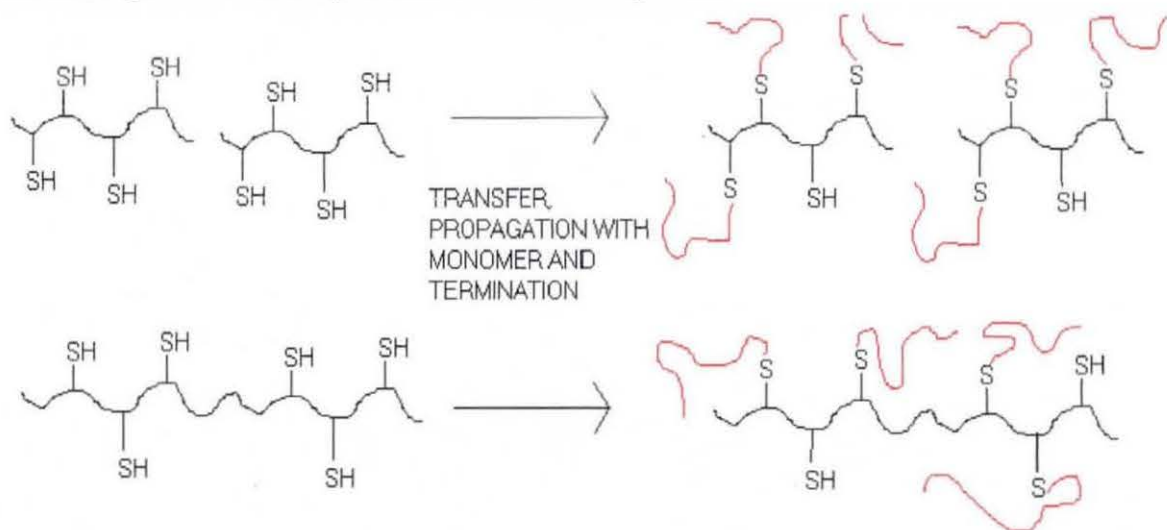


**Figure 5-12** A representation of the high functional PCTA 6H-M426 against a low functional PCTA 16L-M403 at fixed [MMA], [AIBN] and [PCTA].

JHH428 / JHH429 prepared in the presence of PCTA 6H-M426 (Table 4-31/p148) were compared against JHH410 / JHH411 prepared in the presence of PCTA 16L-M403 (Table 4-33/p155) at [PCTA]=6% wt.<sup>xvi</sup> JHH410 and JHH411 exhibited higher molar mass, increased polydispersity and higher levels of branching than their respective equivalents JHH428 and JHH429. This was attributed to an increased number of SH

xvi	PCTA	AIBN (%wt)	Mw (g/mol)	Mn (g/mol)	D	$g'$	$\alpha$	Log K
JHH429	6H-M426	1.20	32,100	6,400	5.03	0.85	0.56	-3.31
JHH411	16L-M403	1.20	53,100	6,300	8.48	0.70	0.49	-3.05

groups attached to the same PCTA molecule. The lower concentration of SH increased the branch chain length. Similar trends in molar mass, polydispersity and branching levels were observed for samples prepared at [PCTA]=12% wt (JHH462 / JHH408 / JHH409 Table 4-32/p151 vs JHH465 / JHH412 / JHH413 respectively Table 4-34/p159).

The experimental data suggested that a high molar mass PCTA with a low concentration of SH was more influential on intrinsic viscosity than a low molar mass PCTA with an increased concentration of SH.

### 5.7.3.3.2 PCTA 16H-M427 vs PCTA 6L-M402

The reverse scenario was studied with the high functional PCTA 16H-M427 against the low functional PCTA 6L-M402 at a fixed concentration of PCTA. Figure 5-13 is a representation of the comparison. It was estimated that for every SH group in the polymerisation with the low functional 6 kg/mol PCTA, there was an equivalent of 2.0 SH groups in the polymerisation with the 16 kg/mol PCTA.

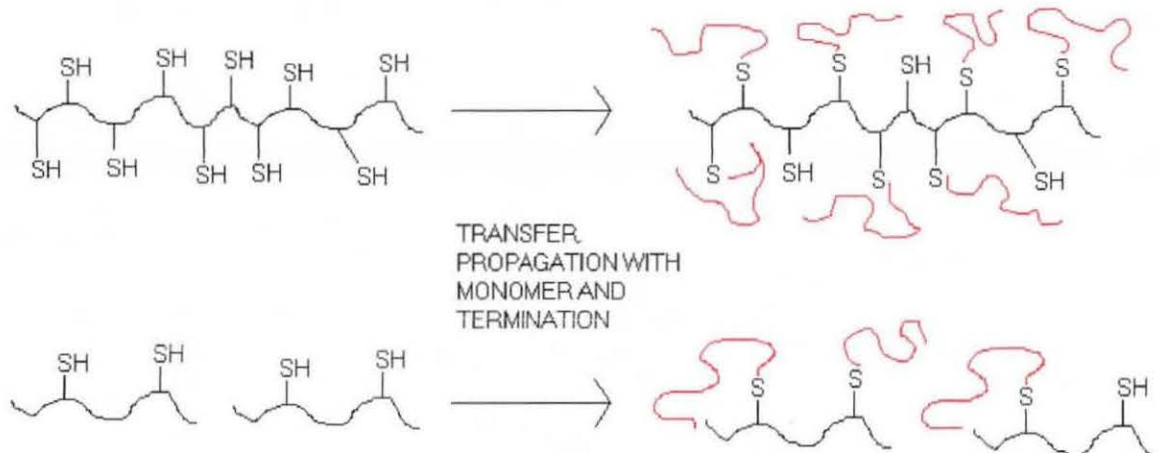


**Figure 5-13 A representation of the high functional PCTA 16H-M427 against the low functional PCTA 6L-M402 at fixed [MMA], [AIBN] and [PCTA].**

Samples prepared at [PCTA]=12% wt in the presence of PCTA 16H-M427 exhibited higher molar mass, broader MMD and higher branching levels, which extended to higher molar mass (JHH466/ JHH434/ JHH435 Table 4-34/p159 vs JHH462/ JHH408/ JHH409 Table 4-32/p151 respectively).<sup>xvii</sup> The high molar mass and broad MMD were expected as a result of the high number of transfer groups attached to the 16 kg/mol molecule.

The observations suggested that a high molar mass PCTA combined with a high concentration of SH produced highly branched polymers with high molar mass.

xvii	PCTA	AIBN (%wt)	Mw (g/mol)	Mn (g/mol)	D	$g'$	$a$	Log K
JHH435	16H-M427	2.40	79,600	11,100	7.17	0.50	0.51	-3.25
JHH409	6L-M402	2.40	14,400	4,000	3.59	0.81	0.45	-2.87

## 6 SUMMARY AND CONCLUSIONS

- Statistical copolymers of MMA-co-HEMA and BzMA-co-HEMA were prepared with control of composition and molar mass.
- A method was successfully developed for the preparation and characterisation of PCTA based on an acid-catalysed esterification of a HEMA-based copolymer with thioglycolic acid.
- PCTA with various concentrations of SH and molar mass was successfully prepared and characterised.
- Disulphide formation was the probable cause for partial phase separation observed in the synthesis of PCTA via atmospheric oxidation of the SH groups.
- Modification of a PCTA in the polymerisation of MMA was demonstrated by a BzMA-co-HEMA-based PCTA using SEC coupled with a UV detector. A decrease in the retention time of the PCTA chromophore post-polymerisation indicated the PCTA had increased in molar mass (through branching).
- SEC coupled with LS, VISC and RI detectors was successfully utilised to characterise samples prepared in the presence of a PCTA. The molar mass data for linear polymers characterised using conventional SEC were in good agreement with data obtained using TDSEC.
- Branched PMMA was successfully prepared in a one-step radical polymerisation in the presence of both MMA-co-HEMA-based PCTA and BzMA-co-HEMA-based PCTA. The following conclusions were made:
  - Conversion had important effects on the solution behaviour of the resultant polymer. The molar mass generally increased and the MMD broadened as

conversion increased. A transition between two types of solution behaviour was observed.

- Polymers prepared in the presence of a high molar mass PCTA generally had a higher molar mass, broader MMD and increased levels of branching compared with polymers prepared in the presence of a low molar mass PCTA under identical conditions.
- An increase in the concentration of PCTA broadened the MMD and increased the level of branching. The effect was magnified in polymers prepared in the presence of a high molar mass PCTA.
- An increase in the concentration of SH on the PCTA increased the polymer molar mass, broadened the MMD and increased the level of branching when all other parameters were fixed.
- A high concentration of low density branched polymer had a greater influence on solution viscosity than a low concentration of high density branched polymer at a comparable molar mass. However, the resultant polymer had a lower molar mass.
- A high molar mass PCTA with a low branch density had a greater effect on intrinsic viscosity than a low molar mass PCTA with a high branch density at a fixed branched polymer concentration.
- It was suspected that polymers prepared with 16 kg/mol PCTA at [PCTA]=12% wt were more susceptible to complications as a consequence of increased viscous polymerisation media.

• The results indicated that the molar mass of the PCTA and the concentration of SH on a PCTA were the most important parameters that determined the level of branching and molar mass of the resultant polymer.

## 7 PROPOSALS FOR FURTHER WORK

- Functionalise the copolymer with a different esterifying acid to increase the distance of the SH group from the polymeric backbone.
- Prepare a PCTA with a disulphide bond instead of a SH group to observe the effect of disulphide in a radical polymerisation.
- Synthesise a PCTA with a molar mass above 25 kg/mol to observe the effects on branching. Look at low and high concentrations of SH.
- Perform polymerisations in the presence of PCTA at lower polymerisation temperatures to increase bimolecular termination via combination and reduce the rate of propagation.
- Perform polymerisations in the presence of PCTA with different solvents to minimise partial phase separation.
- Attempt to extract branched polymer from linear polymer. Use methanol as a non-solvent to extract any low molar mass PMMA and increase the concentration of branched polymer.
- Prepare a series of polymers with a low concentration of monomer to duplicate and understand the star-type behaviour.
- Perform conversion work at 5 or 6 levels to understand how the PCTA interacts and how branching is effected with conversion. Attempt conversion work at various concentrations of monomer.
- Characterise branched samples prepared using BzMA-co-HEMA PCTA with multi-detection SEC incorporating LS / UV detectors to observe the position of the chromophore across the MMD to understand how the PCTA interacts in the polymerisation.

- Reduce the SEC flow rate from 1.0 ml/min to 0.1 - 0.5 ml/min to improve the resolution of the high molar mass branched polymer.
- Fractionate a polydisperse sample to obtain high molar mass branched polymer only.
- Determine the physical properties of branched polymer prepared utilising PCTA i.e. thermal and coating characteristics.

## 8 REFERENCES

---

<sup>1</sup> Buchard, W.: *Adv. Polym. Sci.*, 143, 112, **1999**.

<sup>2</sup> Tobita, H.: *Macromolecules* 30, 1685, **1997**.

<sup>3</sup> Zimm, B. H. and Stockmayer, W. H.: *J. Chem. Phys.*, 17, 1301, **1949**.

<sup>4</sup> Grest, G. S., Fetter, L. J., Huang J. S. and Richter, D.: *Adv. Chem. Phys.*, 94, 67, **1996**.

<sup>5</sup> Tomalia D. A.: *Adv. Materials*, 6, 529, **1994**.

<sup>6</sup> Service, R. F.: *Science*, 267, 458, **1995**.

<sup>7</sup> Houtz, R. C. and Adkins, H.: *J. Am. Chem. Soc.*, 55, 1609, **1933**.

<sup>8</sup> Flory, P. J.: *J. Am. Chem. Soc.*, 59, 241, **1937**.

<sup>9</sup> Mayo, F. R.: *J. Am. Chem. Soc.*, 65, 2324, **1943**.

<sup>10</sup> Brandrup, A. and Immergut E.H. (Ed): in *Polymer Handbook*, 4<sup>th</sup> Edition, Wiley, Chichester, **1999**.

<sup>11</sup> Moares, M. A .R., Moreira, A. C .F., Barbosa, R. V. and Soares, B. G.: *Macromolecules*, 29, 416, **1996**.

<sup>12</sup> Fox, T. G., Gluckman, M. S., Gornick F., Graham, R. K. and Gratch, S.: *J. Polymer Sci.*, 37, 397, **1959**.

<sup>13</sup> Gluckman, M. S., Kampf, M. J., O'Brien, J. L., Fox, T. G. and Graham, R. K.: *J. Polymer Sci.*, 37, 411, **1959**.

<sup>14</sup> Dawkins, J. V., Houseman, J. H. and Slark, A. T.: *Abs. Papers Am. Chem. Soc.*, 218, 443-POLY, **1999**. (see **Appendix**)

<sup>15</sup> Flory, P. J.: *Principles of Polymer Chemistry*, Ithaca, Cornell Univ. Press, **1953**.

<sup>16</sup> Tsukahara, Y., Nakanishi, Y., Yamahita, Y., Ohtani, H., Nakashima, Y., Luo, Y. F., Ando, T. and Tsuge, S.: *Macromolecules*, 24, 2493, **1991**.

<sup>17</sup> Murthy, K. S., Ganesh, K. and Kishore, K.: *Polymer*, 37, 5541, **1996**.

<sup>18</sup> Madruga, E. L. and Malfeito, J. J.: *Eur. Polymer J.*, 28, 863, **1992**.

<sup>19</sup> Bamford C. H. and Tipper, C. F. H.: *Comprehensive Chemical Kinetic - Chapter 1*, Elsevier Scientific, Amsterdam, **1976**.

<sup>20</sup> Szesztay, M., Foldes-Berezsnich, T. and Tudos, F.: *Int. J. Polym. Anal. & Charact.*, 3, 381, **1997**.

<sup>21</sup> Zammit, M. D., Davis, T. P., Haddleton, D. M. and Suddaby, K. G.: *Macromolecules*, 30, 1915, **1997**.

---

<sup>22</sup> Norrish, R. G. W. and Smith, R. R.: *Nature (London)*, 150, 336, **1942**.

<sup>23</sup> Tromsdorff, E., Kohle, H. and Lagally, P.: *Makromol. Chem.*, 1, 169, **1947**

<sup>24</sup> O'Neil, G. A., Wisnudel, M. B. and Torkelson, J. M.: *Macromolecules*, 29, 7477, **1996**.

<sup>25</sup> O'Neil, G. A. and Torkelson, J. M.: *Macromolecules*, 32, 411, **1999**.

<sup>26</sup> Tsukahara, M. K., Mizuno, K., Segawa, A. and Yamashita, Y.: *Macromolecules*, 22, 1546, **1989**.

<sup>27</sup> Tsukahara, M. K., Tsutsumi, K., Yamashita, Y and Shimada, S.: *Macromolecules*, 23, 5201, **1990**.

<sup>28</sup> Varma, I. K. and Patnaik, S.: *Euro. Polym. J.*, 12, 259, **1976**.

<sup>29</sup> Kelen, T. and Tudos, F.: *J. Macromol. Sci.- Chem.*, A9, 1, **1975**.

<sup>30</sup> Rosen, S. L.: *Fundamental Principles of Polymeric Materials*, Wiley-Interscience, New York, **1993**.

<sup>31</sup> Bohdanecky, M. and Netopilik, M.: *Polymer*, 36, 3377, **1995**.

<sup>32</sup> Zimm, B. H. and Kilb, R. W.: *J. Polym. Sci.*, 37, 19, **1959**.

<sup>33</sup> Berry, G. C.: *J. Polym. Sci: Part A: Polym. Chem.*, 9, 687, **1971**.

<sup>34</sup> Roovers, J. and Toporowski, P. M.: *Macromolecules*, 14, 1174, **1981**.

<sup>35</sup> Jackson, C., Frater, D. J. and Mays, J. W.: *J. Polym. Sci: Part B: Polym. Phys.*, 33, 2159, **1995**.

<sup>36</sup> Hunt B. J. and Holding S. R.: *Size Exclusion Chromatography*, Blackie, Glasgow and London, **1989**.

<sup>37</sup> Ouano, A. C., Horne, D. L. and Gregges, A. R.: *J. Polym. Sci: Part A: Polym. Chem.*, 12, 307, **1974**.

<sup>38</sup> Haney, M. A.: *Amer. Lab.*, 17, 41, **1985**.

<sup>39</sup> Jackson, C. and Yau, W. G.: in *Chromatographic Characterization of Polymers – Hyphenated and Multidimensional Techniques*, ed. Provder, T., Barth, H. G. and Urban, M. W., American Chemical Society, Series 247, 69, **1995**.

<sup>40</sup> Jackson, C. and Yau, W. G.: *J. Chromat.*, 645, 209, **1993**.

<sup>41</sup> Jackson, C.: *J. Chromat.*, 662, 1, **1994**.

<sup>42</sup> Jackson, C. and Barth, H.G.: in *Chromatographic Characterization of Polymers – Hyphenated and Multidimensional Techniques*, ed. Provder, T., Barth, H. G. and Urban, M. W., American Chemical Society, Series 247, 59, **1995**.

<sup>43</sup> Mourey, T. H., Miller, S. M. and Balke, S. T.: *J. Liq. Chromat.*, 13, 435, **1990**.

---

<sup>44</sup> Pispas, S., Avgeropoulos, A., Hadjichristidis, N. and Roovers, J.: *J. Polym. Sci: Part B: Polym. Phys.*, **37**, 1329, **1999**.

<sup>45</sup> Hadjichristidis, N., Pispas, S., Pitsikalis, M., Iatrou, H. and Vlahos, C.: *Adv. Polym. Sci.*, **142**, 71, **1999**.

<sup>46</sup> Charleux, B. and Faust, R.: *Adv. Polym. Sci.*, **142**, 1, **1999**.

<sup>47</sup> Ito, K. and Kawaguchi, S.: *Adv. Polym. Sci.*, **142**, 130, **1999**.

<sup>48</sup> Shohi, H., Sawamoto, M. and Higashimura, T.: *Macromolecules*, **24**, 4926, **1991**.

<sup>49</sup> Zhu, Z., Rider, J., Yang, C. Y., Gilmartin, M. E. and Wnek, G. E.: *Macromolecules*, **25**, 7330, **1992**.

<sup>50</sup> Maier, S., Sunder, A., Frey, H. and Mulhaupt, R.: *Macromol. Rapid Com.*, **21**, 226, **2000**.

<sup>51</sup> Ullisch, B. and Burchard, W.: *Makromol. Chem.*, **178**, 1403, **1977**.

<sup>52</sup> Ullisch, B. and Burchard, W.: *Makromol. Chem.*, **178**, 1427, **1977**.

<sup>53</sup> Yuan, C. M., Silvestro, G. D. and Farina, M.: *Macromol. Theory Simul.*, **3**, 193, **1994**.

<sup>54</sup> Yuan, C. M. and Farina, M.: *Macromol. Theory Simul.*, **3**, 203, **1994**.

<sup>55</sup> Yuan, C. M. and Silvestro, G. D.: *Macromol. Chem. Phys.*, **196**, 2905, **1995**.

<sup>56</sup> O' Brien, J. L. and Gornick, F.: *J. Am. Chem. Soc.*, **77**, 4757, **1955**.

<sup>57</sup> Tobita, H., Mima, T., Okada, A., Mori, J. and Tanabe, T.: *Macromolecules*, **37**, 1267, **1999**.

<sup>58</sup> Tobita, H.: *Macromolecules*, **29**, 693, **1996**.

<sup>59</sup> Simms, J. A. and Spinnelli, H. J.: *J. Coat. Technol.*, **59**, 125, **1987**.

<sup>60</sup> Simms, J. A.: *J. Rubber Chem. Technol.*, **64**, 139, **1991**.

<sup>61</sup> Eschwey, H. and Burchard, W.: *Polymer*, **16**, 180, **1975**.

<sup>62</sup> Charleux, B. and Faust, R.: *Adv. Polym. Sci.*, **142**, 2, **1999**.

<sup>63</sup> Efstratiadis, V., Tselikas, G., Hadjichristidis, N., Li, J., Yunan, W. and Mays, J. W.: *Polym. Intl.*, **33**, 174, **1994**.

<sup>64</sup> Zhang, X., Xia, J. H. and Matyjaszewski, K.: *Macromolecules*, **33**, 2340, **2000**.

<sup>65</sup> Fetter, L. J. and Morton, M.: *Macromolecules*, **7**, 552, **1974**.

<sup>66</sup> Eschwey, H., Hallensleben, M. L. and Burchard, W.: *Die Makromol. Chemie*, **173**, 235, **1973**.

<sup>67</sup> Okay, O. and Funke, W.: *Macromolecules*, **23**, 2623, **1990**.

<sup>68</sup> Quirk, R. P., Lee, B. and Schock, L. E., *Makromol. Chem.: Macromol. Symp.*, **53**, 201, **1992**.

---

<sup>69</sup> Quirk, R. P., Yoo, T. and Lee, B.: *Macromol. Sci.: Pure Appl. Chem.*, A31, 911, **1994**.

<sup>70</sup> Frater, D. J., Mays, J. W. and Jackson, C.: *J. Polym. Sci: Part B: Polym. Phys.*, 35, 141, **1997**.

<sup>71</sup> Roovers, J. E. L. and Bywater, S.: *Macromolecules*, 5, 385, **1972**.

<sup>72</sup> Roovers, J. E. L. and Bywater, S.: *Macromolecules*, 7, 443, **1974**.

<sup>73</sup> Toporowski, P. M. and Roovers, J. E. L.: *J. Polym. Sci: Part A: Polym Chem.*, 24, 3009, **1986**.

<sup>74</sup> Zhou, L., Hadjichristidis, N., Fetters, L. J. and Roovers, J. E. L.: *J. Rubber Chem. Technol.*, 65, 303, **1992**.

<sup>75</sup> Roovers, J., Zhou, L., Toporowski, P. M., van der Zwan, M., Iatrou, H. and Hadjichristidis, N.: *Macromolecules*, 26, 4324, **1993**.

<sup>76</sup> Roovers, J., Toporowski, P. M. and Martin, J.: *Macromolecules*, 22, 1897, **1989**.

<sup>77</sup> Tsukahara, Y., Kohjiya, S., Tsutsumi, K. and Okamoto, Y.: *Macromolecules*, 27, 1662, **1994**.

<sup>78</sup> Ito, K., Tomi, Y. and Kawaguchi, S.: *Macromolecules*, 25, 1534, **1992**.

<sup>79</sup> Jenkins, A. D.: *Makromol. Chem.: Macromol. Symp.*, 53, 267, **1992**.

<sup>80</sup> Chen, G-F. and Jones, F. N.: *Macromolecules*, 24, 2151, **1991**.

<sup>81</sup> Radke, W., Roos, S., Stein, H. M. and Muller, A. H. E.: *Macromol. Symp.*, 101, 19, **1996**.

<sup>82</sup> Yokota, K., Hirabayashi, T. and Inai, Y.: *Polym. J.*, 26, 105, **1994**.

<sup>83</sup> Ito, K.: *Prog. Polym. Sci.*, 23, 581, **1998**.

<sup>84</sup> Tung, L. H., Hu, A. T., McKinley, S. V. and Paul, A. M., *J. Polym. Sci: Part A: Polym. Chem.*, 19, 2027, **1981**.

<sup>85</sup> Tung, L. H.: *J. Polym. Sci.: Part A: Polym Chem.*, 19, 3209, **1981**.

<sup>86</sup> Tobita, H.: *Macromolecules*, 30, 1693, **1997**.

<sup>87</sup> Roovers, J.: *Polymer*, 20, 843, **1979**.

<sup>88</sup> Varshney, S. K., Hautekeer, J. P., Fayt, R., Jerome, R. and Teysee, P.: *Macromolecules*, 23, 2618, **1990**.

<sup>89</sup> Quirk, R. P., Yin, J., Guo, S. H., Hu, X. W., Summers, G., Kim, J., Zhu, L. F., Ma, J. J., Takizawa, T. and Lynch, T.: *Rubber Chem. Technol.*, 64, 648, **1991**.

<sup>90</sup> Hseih, H. L. and Quirk, R. P.: *Anionic Polymerisation : Principles and Practical Applications*, Marcel Dekker Inc., New York, **1996**.

---

<sup>91</sup> Fargere, T., Abdennadher, M., Delmas, M. and Boutevin, B.: *J. Polym. Sci: Part A: Polym. Chem.*, 32, 1377, **1994**.

<sup>92</sup> Akutsu, F., Inoki, M., Takahagi, A., Kasashima, Y. and Naruchi, K.: *Macromol. Chem.*, 197, 3675, **1996**.

<sup>93</sup> Jenkins, A. D., Tsartolia, E. and Walton, D. R. M.: *Makromol. Chem.*, 191, 2501, **1990**.

<sup>94</sup> Greber, G. and Tolle, J.: *Makromol. Chem.*, 52, 208, **1962**.

<sup>95</sup> Lutz, P., Beinert, G. and Rempp, P., *Makromol. Chem.*, 183, 2787, **1982**.

<sup>96</sup> Morin, B. P., Breusova, I. P. and Rogovin, Z. A.: *Adv. Polym. Sci.*, 42, 139, **1982**.

<sup>97</sup> Smets, G. and Claesen, M.: *J. Polym. Sci.*, 8, 289, **1952**.

<sup>98</sup> Wheeler, O. L., Ernst, S. L. and Crozier, R. N.: *J. Polym. Sci.*, 8, 409, **1952**.

<sup>99</sup> Britton, D., Heatley, F. and Lovell, P. A.: *Macromolecules*, 31, 2828, **1998**.

<sup>100</sup> Ahmad, N. M., Heatley, F. and Lovell, P. A., *Macromolecules*, 31, 2822, **1998**.

<sup>101</sup> Roedel, M.: *J. Am. Chem. Soc.*, 75, 6110, **1953**.

<sup>102</sup> Ravel, H., Singh, Y. P., Mehta, M. H. and Devi, S.: *Polym. Int.*, 29, 261, **1992**.

<sup>103</sup> Huang, N. J. and Sundberg, D.: *J. Polym. Sci.: Part A: Polym. Chem.*, 33, 2533, **1995**.

<sup>104</sup> Huang, N. J. and Sundberg, D., *J. Polym. Sci.: Part A: Polym. Chem.*, 33, 2551, **1995**.

<sup>105</sup> Huang, N. J. and Sundberg, D., *J. Polym. Sci.: Part A: Polym. Chem.*, 33, 2571, **1995**.

<sup>106</sup> Huang, N. J. and Sundberg, D., *J. Polym. Sci.: Part A: Polym. Chem.*, 33, 2587, **1995**.

<sup>107</sup> Barbosa, R. V., Soares, B. G. and Gomes, A. S.: *J. Appl. Polym. Sci.*, 47, 1411, **1993**.

<sup>108</sup> Kihara, N., Kanno, C. and Fukutomi H., *J. Polym. Sci.: Part A: Polym. Chem.*, 35, 1443, **1997**.

<sup>109</sup> Trollsas, M., Hawker, C. J., Hedrick, J. L., Carrot, G. and Hilborn, J.: *Macromolecules*, 31, 5960, **1998**.

<sup>110</sup> Yamaguchi, K., Kato, T., Hirao, A. and Nakahama, S.: *Makromol. Chem.: Rapid Comm.*, 8, 203, **1987**.

<sup>111</sup> Yokota, K., Hirabayashi, T. and Inai, Y.: *Polym. J.*, 26, 105, **1994**.

<sup>112</sup> Kurata, M., Abe, M. and Iwama, M.: *Polym. J.*, 3, 729, **1972**.

<sup>113</sup> Degoulet, C., Nicolai, T., Durand, D. and Busnel, J. P.: *Macromolecules*, 28, 6819, **1995**.

<sup>114</sup> Hult, A., Johanson, M. and Malmstrom, E.: *Adv. Polym. Sci.*, 143, 1, **1999**.

<sup>115</sup> Kim, Y. H.: *J. Polym. Sci: Part A: Polym. Chem.*, 36, 1685, **1998**.

<sup>116</sup> Turner, S. R., Voit, B. I. and Mourey, T. H.: *Macromolecules*, 26, 4617, **1993**.

---

<sup>117</sup> Turner, S. R., Walter, F., Voit, B. I. and Mourey, T. H.: *Macromolecules*, 27, 1611, 1994.

<sup>118</sup> Yang, G., Jikei, M. and Kakimoto, M.: *Macromolecules*, 32, 2215, 1999.

<sup>119</sup> Hempenius, M. A., Michelberger, W. and Moller, M.: *Macromolecules*, 30, 5602, 1997.

<sup>120</sup> Gauthier, M., Wenguang, L. and Tichagwa, L.: *Polymer*, 38, 6363, 1997.

<sup>121</sup> Jahanzad, F., Kazemi, M., Sajjadi, S. and Afshar-Taromi, F.: *Polymer*, 34, 3542, 1993.

<sup>122</sup> Fink, J. K.: *Makromol. Chem.* 182, 2105, 1981.

<sup>123</sup> Patai, S.: *The Chemistry of the Thiol Group: Part 1*, Wiley-Interscience, London, 1974.

<sup>124</sup> Patai, S.: *The Chemistry of the Thiol Group: Part 2*, Wiley-Interscience, London, 1974.

<sup>125</sup> Fox, T. G., Kinsinger, J. B., Mason, H. F. and Schnele, E. M.: *Polymer*, 3, 71, 1962.

<sup>126</sup> Tohyama, M., Hirao, A., Nakahama, S. and Takenaka, K.: *Macromol. Chem. Phys.*, 197, 3135, 1996.

<sup>127</sup> Gruibisic, Z., Rempp, P. and Benoit, H.: *J. Polym. Sci.: Part B: Polym. Phys.*, 5, 753, 1967.

<sup>128</sup> Cantow, H. J., Pouget, J. and Wippler, C.: *Makromol. Chem.*, 14, 110, 1954.

<sup>129</sup> Zhu, S. and Hamielec A. E.: *J. Polym. Sci.: Part B: Polymer Physics*, 32, 929, 1994.

---

## BACKGROUND TEXT

Billmeyer Jr, F. W.: Textbook of Polymer Science, 3<sup>rd</sup> Edition, Wiley-Interscience, 1984.

Mijs, W. J.: New Methods of Polymer Synthesis, Plenum Press, New York, 1992.

Hseih, H. L. and Quirk, R. P.: Anionic Polymerisation : Principles and Practical Applications, Marcel Dekker Inc., New York, 1996.

Cowie, J. M. G.: Polymers : Chemistry and Physics of Modern Materials, 2<sup>nd</sup> Edition, Blackie and Sons Ltd., 1991.

Yau, W. W., Kirkland, J. J. and Bly, D. D.: Modern Size Exclusion Liquid Chromatography: Practice of Gel Permeation and Gel Filtration Chromatography, Wiley-Interscience, New York, 1979.

Mori, S. and Barth, H. G.: Size Exclusion Chromatography, Springer, Berlin/New York, 1999.

## APPENDIX

## BRANCHING IN METHYL METHACRYLATE POLYMERISATIONS INCORPORATING A POLYMERIC CHAIN TRANSFER AGENT

John V. Dawkins<sup>a</sup>, Jon H. Houseman<sup>a</sup> and Andrew T. Stark<sup>b</sup>.

(a) Department of Chemistry, Loughborough University, Loughborough, LE11 3TU. England. (b) ICI Acrylics, Wilton Centre, Middlesbrough, TS90 8JE. England.

### Introduction

It is well known that mercaptans have a high chain transfer constant with a variety of monomers. Tri- and tetra-functional mercaptans have been used to prepare star polymers.<sup>1,2</sup> An extension of this idea is to use a multifunctional mercaptan based on a polymeric backbone. This allows the potential to introduce many mercaptan groups and reduce any steric effects that might be encountered with a small, multifunctional molecule. Soares et al<sup>3</sup> used a functionalised poly(ethylene-co-vinyl acetate) backbone as the polymeric chain transfer agent (PCTA) to synthesise poly(ethylene-co-vinyl acetate-g-methyl methacrylate); however, the SH groups on the backbone suffered from poor accessibility due to natural coiling of the backbone. Fox et al<sup>4</sup> used a poly(methyl methacrylate-co-glycidal methacrylate) (MMA-co-GMA) based PCTA to produce poly(MMA-co-GMA-g-styrene) and poly(MMA-co-GMA-g-IMA), but they were not subjected to detailed characterisation of branching. This paper centres on the preparation of branched PMMA using poly(MMA-co-2-hydroxy ethyl methacrylate)-based PCTA. The SH groups are located away from the backbone to minimise any steric effects. The influence of the PCTA is explored using triple detector size exclusion chromatography (TDSEC).

### Experimental

**Materials.** Methyl methacrylate (MMA), benzyl methacrylate (BZMA) and 2-hydroxy ethyl methacrylate (HEMA) were supplied by Aldrich. The monomers were de-stabilised before use with an inhibitor remover (Aldrich) and stored in a sealed flask at -20°C. Azoisobutyronitrile (AIBN) from Lancaster was re-crystallised from ethanol twice. Mercaptoacetic acid (MAA) from Lancaster, dodecyl mercaptan (DDM) and benzyl bromide (BZBr) from Aldrich were stored at 20°C. Para-toluene sulphonic acid (p-TSA) from Aldrich was kept anhydrous. All other solvents and chemicals were used as supplied.

**Synthesis of HEMA-co-MMA and HEMA-co-BZMA polymers.** In a three-necked flask equipped with a condenser and dry nitrogen flow, ethyl acetate (50 g) was dissolved in a mixture of monomers (10 g, MMA/HEMA or BZMA/HEMA in determined mole fractions). A predetermined amount of DDM was added if control of the final molecular weight was required. The solution was stirred whilst being purged with nitrogen. A solution of AIBN in ethyl acetate (0.4 g, 0.0024 mol AIBN in 0 g ethyl acetate) was added. The flask was heated for 1 hour at 80°C in a oil bath. On completion the mixture was precipitated in a large excess of water, the product isolated by filtration and dissolved in acetone, before re-precipitation in water. The copolymer was filtered and dried. Copolymers made using MMA and HEMA were white powders, those made with BZMA and HEMA were tacky and white. Characterisation of the polymers was by SEC and <sup>1</sup>H NMR.

**Preparation of Polymeric Chain Transfer Agent (PCTA).** Functionalisation of the copolymer was performed by an acid-catalysed esterification. In a three-necked flask equipped with a Dean-Stark apparatus and dry nitrogen flow, p-TSA (0.1 g, 6.06 x 10<sup>-4</sup> mol) was dissolved in 120 g of toluene with stirring at 80°C in a constant temperature oil bath. Dry copolymer (10 g, 7.69 x 10<sup>-3</sup> mol HEMA) was added and allowed to dissolve, then MAA (1.1 g, 0.012 mol) was added to the mixture under nitrogen. The solution was heated for 5 hours at 80°C, then allowed to cool whilst maintaining a nitrogen flow. The solution was filtered and precipitated into a five-fold excess of hexane. The product was filtered, dissolved in acetone and precipitated in hexane, before drying under vacuum. The product was stored under nitrogen at -20°C prior to use to avoid oxidation and disulphide formation. Characterisation was by <sup>1</sup>H NMR.

**Analysis of Residual SH Functionality.** Mercaptan content was determined by reacting a sample of PCTA dissolved in THF with BZBr (molar equivalent) and triethyl amine (2 molar equivalent) under nitrogen. The solution was stirred for 16 hours at room temperature then filtered to remove the precipitated amine salt. The solution was precipitated in hexane, filtered, then washed with water before drying.

**Radical Polymerisation of MMA with PCTA.** The preparation of branched PMMA was carried out in a three-necked flask equipped with a condenser and nitrogen inlet. Predetermined concentrations of PCTA, MMA, and AIBN were dissolved in toluene to make a total system weight of 10 g. The reaction was stirred at 80°C for 24 hours to achieve maximum conversion. The reaction mixture was diluted with acetone before precipitation in hexane. The product was re-dissolved in acetone and precipitated, then filtered before drying. Characterisation was by a combination of SEC techniques.

**Instrumentation.** <sup>1</sup>H NMR spectra were obtained with a Bruker AC-250 spectrometer operating in the FT mode. Size exclusion chromatography (SEC) was used to determine the weight average (M<sub>w</sub>), the number average (M<sub>n</sub>) and the polydispersity (D = M<sub>w</sub>/M<sub>n</sub>) of the polymers. A dual detector system comprising of a UV-detector and differential refractometer with 2x30 cm mixed B gel columns (Polymer Laboratories), was used to characterise the copolymer/UV-active branched samples. The solvent was tetrahydrofuran with a flow rate of 1 ml/min. The retention times were calibrated against monodisperse PMMA standards. The triple detector SEC with light scattering, differential viscometer and RI detectors was used to characterise the branched PMMA samples.

### Results and Discussion

**PCTA.** A series of copolymers was prepared with HEMA and MMA or HEMA and BZMA. Results are summarised in Table 1. Copolymers synthesised in the presence of DDM produced lower molecular weights. If BZMA was used in the copolymerisation, a UV-active chromophore was introduced in the PCTA backbone. Samples JH292 and JH290 have similar average molecular weight but different functionality. Samples JH250 and JH326 have similar residual SH functionality but different average molecular weight, resulting in a variation in the number of SH groups per molecule. The SH functionality of the MMA prepared samples cannot be compared directly with the BZMA samples, as the monomers are of different molar mass.

Table 1. Characterisation of PCTA Samples.

PCTA	AVERAGE MW <sup>a</sup>			MOLE FRACTION <sup>b</sup>			RESIDUAL SH <sup>d</sup>	AV. SH / CHAIN <sup>e</sup>
	Mw	Mn	D	MMA	HEMA	M-HEMA <sup>c</sup>		
JH292	9792	5627	1.74	0.944	0.023	0.033	0.020	1.5
JH290	9980	5584	1.79	0.884	0.028	0.088	0.054	4
BZMA								
JH250	37377	15989	2.33	0.899	0.008	0.093	0.052	8
JH326	9066	4734	1.92	0.923	0.002	0.075	0.044	2

<sup>a</sup> - Average molecular weight obtained by SEC of the copolymer (not the PCTA). SEC of the PCTA is not advised due to interaction of SH with the column packing.

<sup>b</sup> - Obtained from the ratio of integrals in <sup>1</sup>H NMR.

<sup>c</sup> - M-HEMA refers to a HEMA unit which has been successfully esterified with MAA.

<sup>d</sup> - Residual SH mole fraction; obtained from <sup>1</sup>H NMR by reaction of PCTA with BZBr.

<sup>e</sup> - Estimation of the maximum number of average SH groups per chain obtained from the weight fraction and average molecular weight of the chain.

Difficulties arise in the esterification step when the HEMA concentration in the copolymer rises above 15% w/w; insoluble PCTA is formed. It is postulated that the SH groups on the modified backbone form disulphide linkages. When MAA is replaced by benzyl mercaptoacetic acid, removing the free SH, copolymers with 30% w/w HEMA can be esterified successfully. It is expected that some disulphide bonds will be present in the PCTA. In order to minimise this reaction, lower esterification time and temperature were used than previously reported<sup>3,4</sup> in combination with an acid catalyst. However, disulphide bonds have been shown<sup>5</sup> to display chain transfer properties in radical polymerisations.

In Figure 1 a series of NMR spectra is displayed for a UV-active copolymer, its corresponding PCTA (JH326 - see Table 1), and JH326 reacted with BZBr. There is an upfield shift in the methylene

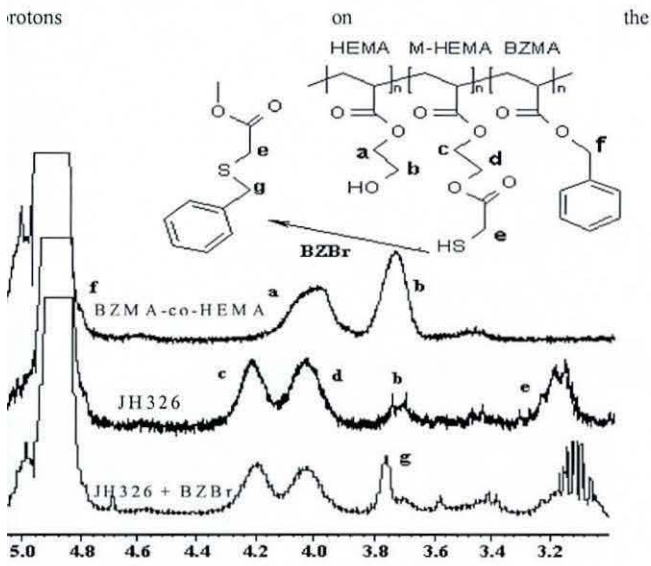


Figure 1.  $^1\text{H}$  NMR spectra (from top to bottom): BZMA-co-HEMA copolymer, JH326 PCTA, and PCTA reacted with BZBr.

HEMA unit as the MAA is incorporated (shifts **b**, s, 2H,  $\delta$  3.75 ppm and **a**, s, 2H,  $\delta$  4.03 ppm to **c**, s, 2H,  $\delta$  4.25 ppm and **d**, s, 2H,  $\delta$  4.05 ppm respectively), as well as the appearance of the methylene protons on MAA **e**, d, 2H,  $\delta$  3.15 ppm). The shift associated with SH at  $\delta$  2.00 ppm is obscured by the backbone. Shift **f** at  $\delta$  4.90 ppm is the methylene group in the BZMA adjacent to the aromatic ring. The BZBr-reacted PCTA has a shift **g** at  $\delta$  3.85 ppm that is assigned to the methylene attached to the sulphur and aromatic ring. The molar concentration of SH can be calculated from this integral. The shift at  $\delta$  3.15 ppm is a mixture of MAA and the triethylamine-bromide salt formed as a by-product in the enylation reaction.

**Branched PMMA.** A selection of branched PMMA samples was characterised utilising TDSEC. The results are included in Table 2. Branching is measured by the changes in the relationship between hydrodynamic volume and molecular weight as a branched molecule is smaller than a linear molecule of the same molecular weight. The Mark-Louwink (M-H) equation ( $[\eta] = KM^a$ ) defines the relationship between intrinsic viscosity,  $[\eta]$ , and molecular weight, M, by two constants, K and  $a$ . The reduction of intrinsic viscosity between a branched molecule and a linear molecule of the same molecular weight is given by the parameter  $g' = [\eta]_{\text{branch}}/[\eta]_{\text{linear}}$ .

Table 2. Summary of TDSEC Results for Branched Samples.

SAMPLE	PCTA	[PCTA] % w/w	AVERAGE MW			M-H		$g'$
			Mw	Mn	D	a	Log K	
JH200	-	-	46200	24500	1.89	0.709	-4.051	0.975
JH239	-	-	149900	84600	1.77	0.749	-4.265	0.946
JH303	JH292	12	44500	19000	2.34	0.487	-3.127	0.775
JH297	JH290	12	54500	8360	6.52	0.331	-2.454	0.707
JH331	JH326	4	65100	26200	2.48	0.586	-3.529	0.831
JH261	JH250	4	312100	29100	10.7	0.390	-2.642	0.695

$[\text{MMA}] = 40.0\% \text{ w/w}$ ,  $[\text{AIBN}] = 0.4\% \text{ w/w}$ ,  $[\text{Toluene}] = 47.6\% \text{ w/w}$  with JH303/JH297 and 55.6% w/w with JH331/JH261.

The linear samples JH200 and JH239 are consistent with reported M-H values for linear PMMA in THF.<sup>6</sup> The presence of PCTA as a profound effect on the solution behaviour compared to linear PMMA. The increasing SH concentration on the PCTA is illustrated in the M-H plots for JH303 and JH297 shown in Figure 2. Both branched PMMA samples deviate from the linear plot, with the greatest deviation occurring at higher molecular weights. The data suggests JH297 prepared with the PCTA high in SH concentration is more branched than JH303 prepared with the PCTA lower in SH concentration. The  $g'$  values are consistent with this trend. It is envisaged that at high conversion, branched PMMA may contain more than one PCTA per chain, and in particular for a PCTA

with a high concentration of SH groups, very polydisperse PMMA may be produced as shown by JH297.

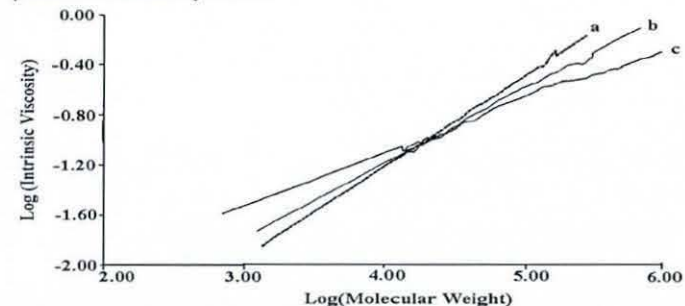


Figure 2. M-H plot of: (a) Linear PMMA JH200, (b) JH303 (JH292: Mn=5627 / SH=0.020), (c) JH297 (JH290: Mn=5584 / SH=0.054), showing the effect of SH concentration on the PCTA.

JH331 and JH261 were synthesised from two PCTA samples having different molecular weights. The total number of SH groups in the polymerisation will be comparable but their distribution will be different, there will be 3 times more SH groups on the higher molecular weight PCTA. The data in Table 2 and the M-H plot in Figure 3 indicate a large difference in solution behaviour. The high molecular weight PCTA increases the viscosity of the initial polymerisation mixture, which alters the kinetics of the polymerisation by making the propagation and termination steps predominantly diffusion controlled. High conversion leads to high molecular weight polymer that is highly branched; probably containing several linked PCTA molecules. This effect is exaggerated when the concentration of high molecular weight PCTA is increased.

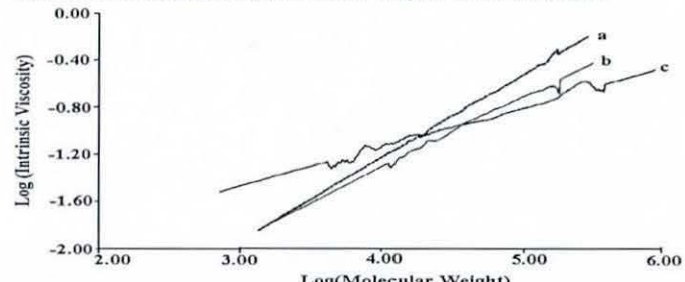


Figure 3. M-H plot of: (a) Linear PMMA JH200, (b) JH326 (JH331: Mn=4734 / SH=0.044), (c) JH261 (JH250: Mn=15989 / SH=0.052), showing the effect of PCTA molecular weight.

## Conclusions

Incorporation of a PCTA in a MMA radical polymerisation produces a branched PMMA. Changing the molecular weight and concentration of SH on the PCTA has dramatic effects on the solution behaviour of the final PMMA.

## Acknowledgements

The authors thank Alan Titterton at ICI Acrylics for aid in characterisation of the branched samples and the EPSRC and ICI Acrylics for funding.

- (1) Yuan, C.M.; Di Silvestro, G. *Macromol. Chem. Phys.* **1995**, 196, 2905.
- (2) Ullisch, B.; Burchard, W. *Makromol. Chem.* **1997**, 178, 1427.
- (3) Moraes, M.A.R.; Moreira, A.C.F.; Barbosa, R.V.; Soares, B.G. *Macromolecules* **1996**, 29, 416.
- (4) Fox, T.G.; Gluckman, M.S.; Gornick, R.K.; Gratch, S. *J. Polymer Sci.* **1959**, 37, 397.
- (5) Shanmugananda Murty, K.; Ganesh, K.; Kishore, K. *Polymer* **1996**, 37, 5541.

<sup>6</sup> THF reference



